

AGARD-AR-245

AGARD-AR-245

AD-A226 378

# AGARD

ADVISORY GROUP FOR AEROSPACE RESEARCH & DEVELOPMENT

7 RUE ANCELLE 92200 NEUILLY SUR SEINE FRANCE

AGARD ADVISORY REPORT No.245

## Recommended Practices for Measurement of Gas Path Pressures and Temperatures for Performance Assessment of Aircraft Turbine Engines and Components

(Les Méthodes Recommandées pour la Mesure de la  
Pression et de la Température de la Veine Gazeuse en  
Vue de l'Evaluation des Performances des Turbines  
Aéronautiques et de leurs Composants)

NORTH ATLANTIC TREATY ORGANIZATION



DISTRIBUTION STATEMENT A

Approved for public release;  
Distribution Unlimited

DISTRIBUTION AND AVAILABILITY  
ON BACK COVER

90 09 10 275

DTIC  
ELECTE  
SEP 11 1990  
S B D

AGARD-AR-245

①

NORTH ATLANTIC TREATY ORGANIZATION  
ADVISORY GROUP FOR AEROSPACE RESEARCH AND DEVELOPMENT  
(ORGANISATION DU TRAITE DE L'ATLANTIQUE NORD)

AGARD Advisory Report No. 245

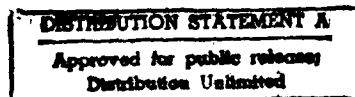
**Recommended Practices for Measurement of Gas Path  
Pressures and Temperatures for Performance  
Assessment of Aircraft Turbine Engines  
and Components**

(Les Méthodes Recommandées pour la Mesure de la Pression et de la Température  
de la Veine Gazeuse en Vue de l'Evaluation des Performances des Turbines Aéronautiques  
et de leurs Composants)

Edited by

H.I.H. Saravanamuttoo

Report of the Propulsion and Energetics Panel Working Group 19



DTIC  
ELECTE  
SEP 11 1980  
S B D

This Advisory Report was prepared at the request of the  
Propulsion and Energetics Panel of AGARD.

90 09 10 2.5

# The Mission of AGARD

According to its Charter, the mission of AGARD is to bring together the leading personalities of the NATO nations in the fields of science and technology relating to aerospace for the following purposes:

- Recommending effective ways for the member nations to use their research and development capabilities for the common benefit of the NATO community;
- Providing scientific and technical advice and assistance to the Military Committee in the field of aerospace research and development (with particular regard to its military application);
- Continuously stimulating advances in the aerospace sciences relevant to strengthening the common defence posture;
- Improving the co-operation among member nations in aerospace research and development;
- Exchange of scientific and technical information;
- Providing assistance to member nations for the purpose of increasing their scientific and technical potential;
- Rendering scientific and technical assistance, as requested, to other NATO bodies and to member nations in connection with research and development problems in the aerospace field.

The highest authority within AGARD is the National Delegates Board consisting of officially appointed senior representatives from each member nation. The mission of AGARD is carried out through the Panels which are composed of experts appointed by the National Delegates, the Consultant and Exchange Programme and the Aerospace Applications Studies Programme. The results of AGARD work are reported to the member nations and the NATO Authorities through the AGARD series of publications of which this is one.

Participation in AGARD activities is by invitation only and is normally limited to citizens of the NATO nations.

This document represents the views and opinions of the contributors and does not necessarily represent the views and opinions of the organisations they represent.

Published June 1990

Copyright © AGARD 1990  
All Rights Reserved

ISBN 92-835-0499-2



Set and printed by Specialised Printing Services Limited  
40 Chigwell Lane, Loughton, Essex IG10 3TZ

## Recent Publications of the Propulsion and Energetics Panel

### CONFERENCE PROCEEDINGS (CP)

**Problems in Bearings and Lubrication**  
AGARD CP 323, August 1982

**Engine Handling**  
AGARD CP 324, February 1983

**Viscous Effects in Turbomachines**  
AGARD CP 351, September 1983

**Auxiliary Power Systems**  
AGARD CP 352, September 1983

**Combustion Problems in Turbine Engines**  
AGARD CP 353, January 1984

**Hazard Studies for Solid Propellant Rocket Motors**  
AGARD CP 367, September 1984

**Engine Cyclic Durability by Analysis and Testing**  
AGARD CP 368, September 1984

**Gears and Power Transmission Systems for Helicopters and Turboprops**  
AGARD CP 369, January 1985

**Heat Transfer and Cooling in Gas Turbines**  
AGARD CP 390, September 1985

**Smokeless Propellants**  
AGARD CP 391, January 1986

**Interior Ballistics of Guns**  
AGARD CP 392, January 1986

**Advanced Instrumentation for Aero Engine Components**  
AGARD CP 399, November 1986

**Engine Response to Distorted Inflow Conditions**  
AGARD CP 400, March 1987

**Transonic and Supersonic Phenomena in Turbomachines**  
AGARD CP 401, March 1987

**Advanced Technology for Aero Engine Components**  
AGARD CP 421, September 1987

**Combustion and Fuels in Gas Turbine Engines**  
AGARD CP 422, June 1988

**Engine Condition Monitoring — Technology and Experience**  
AGARD CP 448, October 1988

**Application of Advanced Material for Turbomachinery and Rocket Propulsion**  
AGARD CP 449, March 1989

**Combustion Instabilities in Liquid-Fuelled Propulsion Systems**  
AGARD CP 450, April 1989

**Aircraft Fire Safety**  
AGARD CP 467, October 1989

**Unsteady Aerodynamic Phenomena in Turbomachines**  
AGARD CP 468, February 1990

**Secondary Flows in Turbomachines**  
AGARD CP 469, February 1990



<b>Accession For</b>	
NTIS GRA&I	<input checked="" type="checkbox"/>
DTIC TAB	<input type="checkbox"/>
Unannounced	<input type="checkbox"/>
Justification	
By	
Distribution/	
Availability Codes	
Dist	Avail and/or Special
A-1	

#### **ADVISORY REPORTS (AR)**

**Through Flow Calculations in Axial Turbomachines** (*Results of Working Group 12*)

AGARD AR 175, October 1981

**Alternative Jet Engine Fuels** (*Results of Working Group 13*)

AGARD AR 181, Vol.1 and Vol.2, July 1982

**Suitable Averaging Techniques in Non-Uniform Internal Flows** (*Results of Working Group 14*)

AGARD AR 182 (in English and French), June/August 1983

**Producibility and Cost Studies of Aviation Kerosines** (*Results of Working Group 16*)

AGARD AR 227, June 1985

**Performance of Rocket Motors with Metallized Propellants** (*Results of Working Group 17*)

AGARD AR 230, September 1986

**Recommended Practices for Measurement of Gas Path Pressures and Temperatures for Performance Assessment of Aircraft Turbine Engines and Components** (*Results of Working Group 19*)

AGARD AR 245, June 1990

**The Uniform Engine Test Programme** (*Results of Working Group 15*)

AGARD AR 248, February 1990

**Test Cases for Computation of Internal Flows in Aero Engine Components** (*Results of Working Group 18*)

AGARD AR 275, July 1990

#### **LECTURE SERIES (LS)**

**Operation and Performance Measurement of Engines in Sea Level Test Facilities**

AGARD LS 132, April 1984

**Ramjet and Ramrocket Propulsion Systems for Missiles**

AGARD LS 136, September 1984

**3-D Computation Techniques Applied to Internal Flows in Propulsion Systems**

AGARD LS 140, June 1985

**Engine Airframe Integration for Rotorcraft**

AGARD LS 148, June 1986

**Design Methods Used in Solid Rocket Motors**

AGARD LS 150, April 1987

AGARD LS 150 (Revised), April 1988

**Blading Design for Axial Turbomachines**

AGARD LS 167, June 1989

**Comparative Engine Performance Measurements**

AGARD LS 169, May 1990

#### **AGARDOGRAPHS (AG)**

**Rocket Altitude Test Facility Register**

AGARD AG 297, March 1987

**Manual for Aeroelasticity in Turbomachines**

AGARD AG 298/1, March 1987

AGARD AG 298/2, June 1988

**Measurement Uncertainty within the Uniform Engine Test Programme**

AGARD AG 307, May 1989

#### **AGARD REPORTS (R)**

**Application of Modified Loss and Deviation Correlations to Transonic Axial Compressors**

AGARD R 745, November 1987

**Rotorcraft Drivetrain Life Safety and Reliability**

AGARD R 775, June 1990

## Summary

This document presents recommended practices for the instrumentation of aviation turbine components undergoing development in rigs and engines. The document should be of interest to engineers concerned with all aspects of the performance testing of engines and components. These engineers may include specialists in widely diverse areas such as instrumentation or aerodynamics, or those more concerned with technical management including programme managers and project engineers.

It is recognized that manufacturing and research organizations throughout the world have developed their own design practices for the application and evaluation of instrumentation and this will continue in the future. Although based on the same fundamental principles, these practices can vary significantly between different organizations, leading to confusion and misunderstandings between the customers, contract agencies and research and development organizations. The recent trend towards multi-company and multi-national engine projects increases the likelihood of problems of reconciling different practices. By reference to these recommended practices, confidence will be generated through a common understanding of the techniques used, enhancing the quality of the data obtained.

In order to keep the document to a reasonable length, it is necessary to limit the types of measurement to be considered. Other AGARD documents have considered overall performance and this document will be restricted to the measurement of temperature and pressure throughout the gas path. In particular, only steady state measurement of temperature and pressure will be considered, taken while the component or engine is running in an equilibrium state. The recommended practices described address individual components and parameters, and the problems associated with interpreting the information obtained in terms of spatial and temporal resolution. The major problem of measurement uncertainty (error evaluation) will be dealt with at some length. Typical installations and the impact on overall performance calculations are illustrated through two examples on components of an aircraft turbine engine.

## Sommaire

Ce document expose les méthodes recommandées pour l'instrumentation des composants de turbines aéronautiques en cours de développement soit au banc soit sur les moteurs. Il devrait intéresser tout ingénieur impliqué dans les mesures de performance des moteurs et de leurs composants. Ces ingénieurs pourraient inclure des spécialistes dans des domaines divers tels que l'instrumentation ou l'aérodynamique, aussi bien que des chefs de projet ou d'ingénieurs de projet, plutôt concernés par les aspects de gestion technique.

Il est de fait que les industriels et les organismes de recherche dans le monde entier ont développé leurs propres méthodes pour l'application et l'évaluation de l'instrumentation, et cette tendance se confirmera pour l'avenir. Quoique basées sur les mêmes principes, ces méthodes peuvent varier de façon sensible entre les différents organismes, ce qui peut prêter à confusion et aux malentendus entre les utilisateurs, les contractants et les organismes de recherche et développement. La tendance récente vers des projets de construction de moteurs en consortium multi-société ou multinational ne fait qu'accroître les difficultés qui risquent d'être rencontrées en ce qui concerne l'harmonisation de ces différentes méthodes. Par contre, l'adoption de procédures normalisées créerait un climat de confiance, grâce à une meilleure compréhension mutuelle des techniques utilisées qui en résulterait, tout en mettant en valeur la qualité des données obtenues.

Il a été nécessaire de limiter les types de mesures à considérer, pour que le volume de ce document garde des proportions raisonnables. Le sujet des performances globales ayant été traité par d'autres documents AGARD le présent rapport se limitera à la mesure des températures et des pressions le long de la veine gazeuse. En particulier, seules des mesures instantanées de température et de pression seront considérées, soit sur le composant soit sur moteur fonctionnant en régime établi. Les pratiques recommandées dans ce rapport s'appliquent à des composants et à des paramètres singuliers et aux problèmes associés au dépouillement des données obtenues en termes de la résolution spatio-temporelle.

Le problème majeur de l'incertitude sur les mesures (évaluation de l'erreur) sera examiné en détail. L'impact des installations type sur le calcul des performances globales sont illustrées par deux cas, qui concernent tous les deux des composants de turbines aéronautiques.

## Working Group 19 Members

Mr A.H.A. Halfacre  
Senior Technical Consultant — Instrumentation  
Pratt & Whitney Canada Inc.  
1000 Marie Victorin Blvd.  
Longueuil, Quebec J4G 1A1  
Canada

Prof. Herbert I.H. Saravanamuttoo  
Chairman, Mechanical and Aeronautical Engineering  
Carleton University  
Ottawa, Ontario K1S 5B6  
Canada

Mr Gilbert Ballarin  
Direction Technique  
SNECMA  
Centre d'Essais de Villaroche  
77550 Moissy Cramayel  
France

M. Ing. Arm. Philippe Castellani  
Centre d'Essais de Propulseurs  
Saclay  
91406 Orsay  
France

Dr-Ing. Hanns Lichtfuss  
Hauptabteilungsleiter EW  
Motoren und Turbinen Union GmbH  
Dachauerstrasse 665  
8000 München 50  
Federal Republic of Germany

Dipl-Ing. Klaus Novack  
EVRI  
Motoren und Turbinen Union GmbH  
Postfach 50 60 40  
8000 München 50  
Federal Republic of Germany

Professor Ronald S. Fletcher  
Pro Vice Chancellor  
Cranfield Institute of Technology  
Cranfield, Bedford MK43 0AL  
United Kingdom

Mr A.R. Osborn  
Royal Aircraft Establishment  
Pyestock  
Farnborough, Hants GU14 0LS  
United Kingdom

Mr Noel Seyb  
Aerodynamics Department  
Rolls Royce plc  
PO Box 3  
Filton, Bristol BS12 7QE  
United Kingdom

Mr W. Gilbert Alwang  
Pratt & Whitney Engineering Div.  
400 Main Street  
East Hartford, Connecticut 06118  
United States

Mr R.D. De Rose  
Air Force Wright Aeronautical Laboratories/POTX  
Wright Patterson Air Force Base  
Ohio 45433  
United States

Mr Paul R. Griffiths  
General Electric Company  
1 Neumann Way  
Cincinnati, Ohio 45215  
United States

Mr Robert E. Smith, Jr  
Vice President and Chief Scientist  
Sverdrup Technology Inc AEDC Div.  
Arnold Air Force Station  
Tennessee 37389  
United States

Mr Donald W. Stephenson  
Garrett Turbine Engine Company  
PO Box 5217  
Phoenix, Arizona 85010  
United States

Dr Arthur J. Wennerstrom  
Air Force Wright Aeronautical Laboratories/POTX  
Wright Patterson Air Force Base  
Ohio 45433  
United States

### PEP PANEL EXECUTIVE

Mr G. Gruber (GE)

AGARD-OTAN  
7, rue Ancelle  
92200 Neuilly sur Seine  
France

From USA and Canada  
AGARD-NATO  
Attn: PEP Executive  
APO New York 09777

Tel: (1)4738 5790 Telex: 610176F  
Telefax: (1)4738 5799

# Contents

	Page
<b>Recent Publications of PEP</b>	iii
<b>Summary/Sommaire</b>	v
<b>Working Group 19 Membership</b>	vi
<b>Nomenclature</b>	ix
<b>Glossary</b>	xi
<b>Acronyms</b>	xvi
<b>1. Introduction</b>	<b>1</b>
1.1 Objective	1
1.2 Scope	1
1.3 How to Use	1
<b>2. General Requirements for Engine and Component Rig Testing</b>	<b>3</b>
2.1 Introduction	3
2.2 General Considerations for Pressure & Temperature Measurement	4
2.3 Measurement Identification Codes	5
2.4 Test Cell Environment	11
2.5 Intake	17
2.6 Compressors, Fans & Associated Ducts	18
2.7 Combustion Chamber	21
2.8 Turbines and Associated Ducting	25
2.9 Afterburner	28
2.10 Propelling Nozzle	29
2.11 Component Testing in Engines	33
<b>3. Uncertainty Analysis</b>	<b>35</b>
3.1 Introduction	35
3.2 Overview of Concepts and Definitions	36
3.3 Estimating Uncertainty Prior to Testing	40
3.4 Post-Test Evaluation of Uncertainty	41
3.5 Combining Pre-Test and Post-Test Results	41
<b>4. Spatial Sampling, Probe Arrays and Data Editing</b>	<b>42</b>
4.1 Introduction	42
4.2 Averaging Considerations	42
4.3 Profile Considerations	42
4.4 Component Versus Engine Test Considerations	44
4.5 Instrumentation Editing	45
<b>5. Pressure Measurement</b>	<b>47</b>
5.1 Definition of the System	47
5.2 Pressure Probe Design	51
5.3 Recommended Practices	62
5.4 Pressure Measurement Uncertainty Analysis	73
<b>6. Temperature Measurement</b>	<b>77</b>
6.1 Definition of System	77
6.2 Temperature Probe Design	81
6.3 Recommended Practices	89
6.4 Temperature Measurement Uncertainty Analysis	99

	<b>Page</b>
<b>7. Special Factors in Small Engines</b>	<b>103</b>
7.1 Introduction	103
7.2 Blockage Effects	103
7.3 Instrumentation Scaling	103
7.4 Inlet Distortion Testing	104
7.5 Use of Traversing Probes	104
<b>8. Specimen Cases</b>	<b>106</b>
8.1 Exhaust Nozzle Calibration	106
8.2 Compressor Efficiency Measurement	122
<b>9. References</b>	<b>138</b>

# Nomenclature

The nomenclature listed below applies to the text of documents and is used herein. The list is based on International Standard ISO 31 with additional definitions derived from SAE ARP 755 where applicable. Instrument lines to which identification tags are to be attached are treated as a special case (See Section 2.3) requiring cross referencing to drawings of the test sections.

## Fundamental Parameters

	<i>Recommended Definition</i>
$a$	Acceleration
$a$	Velocity of Sound
$A$	Area, Geometric
$A_H$	Bleed Area
$A_E$	Entry Area
ALT	Altitude
$B$	Uncertainty Bias
$b$	Elemental Bias
$C$	Celsius
$C$	Coefficient or Constant
$c_p$	Specific Heat at Constant Pressure
$C_F$	Nozzle Thrust Coefficient
$C_w$	Nozzle Flow Coefficient
$D$	Diameter
$D_n$	Diameter of nth arc/circle
$e$	Clearance
$F$	Force, Thrust
$FD$	Drag
$g$	Acceleration due to gravity
$h$	Height
$h$	Specific Enthalpy
$H$	Stagnation Enthalpy
$k$	Conductivity
$k_G$	Coefficient of Thermal Conductivity in a Gas
$k_S$	Coefficient of Thermal Conductivity in a Solid
$K$	Kelvin
$L$	Length
$m$	Mass
$M, Ma$	Mach Number
$M_\infty$	Mach Number in Free Stream
$M_j$	Mach Number at junction, e.g. thermocouple
$N$	Rotation Speed
$Nu$	Nusselt Number
$P$	Pressure
$P_{AMB}$	Ambient Pressure
$P_S$	Static Pressure
$P_T$	Total Pressure
$q$	Velocity Dynamic Head
$Q$	Heat, Quantity of heat
$r$	Radius
$r$	Recovery Factor (Thermocouple Probes)
$R$	Gas Constant
$R$	Ratio
$R$	Recovery Ratio (Thermocouple Probes)
$Re$	Reynolds Number
$RH$	Relative Humidity
$s$	Elemental Precision Index
$S$	Uncertainty Precision Index
$S$	Measured Static Pressure Identification
$t$	Time
$T$	Temperature
$T_j$	Thermocouple Junction Temperature
$T_s$	Static Temperature

$T_T$	Total Temperature
TAS	True Air Speed
$t_{0.5}$	Statistical Coefficient
U	Uncertainty of Measurements
v	Velocity
V	Volume
w	Weight
W	Mass Flow Rate
X	Measured Delta Pressure Identification
X	Individual Parameter Reading
Y	Error
$Y_C$	Catalytic Error
$Y_K$	Conduction Error
$Y_R$	Radiation Error
$Y_V$	Velocity Error
$\alpha, \beta, \gamma$	Angle
$\xi$	Damping Ratio
$\delta$	Delta (pressure/std SLS pressure)
$\rho$	Density
$\eta_{isen}$	Efficiency Isentropic
$\eta_{poly}$	Efficiency Polytropic
$\omega$	Frequency
$\Phi$	Heat Transfer Rate
$\gamma$	Ratio of Specific Heats
$\theta$	Theta (temperature/Std SLS temperature)
$\mu$	Viscosity
—	Average, e.g. $\bar{P}$ = average P value of P
	Ideal value, e.g. $h^*$ , $T^*$ , etc.

The following general descriptive symbols can be used to modify a Fundamental Parameter and should be appended as a subscript of the basic symbols e.g.  $T_{AMB}$  Ambient Temperature,  $P_T$  Total Pressure,  $P_s$  Static Pressure, etc.

#### Descriptive Symbols

	<i>Recommended Definition</i>
AMB	Ambient
AV	Average
DIST	Distortion
E	Effective
N	Net
R	Referred (corrected)
REL	Relative
SL	Sea Level
STD	Standard
S	Static
SW	Swirl
TIP	Tip
T	Total

The following are descriptors for rotor speeds.

	<i>Recommended Definition</i>
$N_H$	High pressure compressor/turbine
$N_I$	Intermediate pressure compressor/turbine
$N_L$	Low pressure compressor/turbine
$N_F$	Fan (Note: If the fan is on a common shaft with a low pressure compressor then $N_F$ is to be used in preference to $N_L$ ).
$N_{PT}$	Power Turbine
$N_p$	Power shaft/propeller

## Glossary

Accuracy	The closeness or agreement between a measured value and a standard or true value; uncertainty as used herein, is the maximum inaccuracy or error that may reasonably be expected (see measurement error).
Average Value	The arithmetic mean of N readings. The average value is calculated as: $\bar{X} = \text{average value} = \frac{\sum_{i=1}^N X_i}{N}$
Bias (B)	The difference between the average of all possible measured values and the true value. The systematic error or fixed error which characterizes every member of a set of measurements.
Blockage	The ratio of the frontal area of a probe or a set of probes at a given station to the total flow area at that station.
Blockage Effects	General term referring both to measurement errors and real component performance effects caused by probe blockage.
Blockage Factor	Ratio of the change in gas velocity near a probe to the velocity that would be present without the probe inserted.
Calibration	The process of comparing and correcting the response of an instrument to agree with a standard instrument over the measurement range in specified environment.
Calibration "As-Is"	The results of a calibration performed before any adjustments are made to the calibrated equipment or curve fitting coefficients.
Calibration "On-Line"	Calibration of a measurement system, in situ during the period that data is being taken.
Calibration Drift (Instrument Stability)	When an instrument is recalibrated, this refers to the recording of the difference between the present calibration before adjustment and the previous calibration. It is a measure of the stability of the instrument between successive calibrations.
Calibration Hierarchy	The chain of calibrations which link or trace a measuring instrument to a National Standard Institution.
Calibration Shunt	Feature of some strain gauge diaphragm pressure transducers permitting application of a shunt resistance equivalent to a given pressure signal.
Centres of Equal Area	A method of locating probe elements radially in the span between the hub and the shroud. The cross-sectional flow area is divided into annular segments of equal area. The elements are then located on the radii that further divide these areas into twice the number of equal area.
Confidence Interval	A range within which the true value is expected to lie with a specified confidence (see also Coverage).
Correlation Coefficient	A measure of the linear interdependence between two variables. It varies between -1 and +1 with the intermediate value of zero indicating the absence of correlation. The limiting values indicate perfect negative (inverse) or positive correlation.
Coverage	A property of confidence intervals with the connotation of including or containing within the interval with a specified relative frequency. Ninety-five percent confidence intervals provide 95 percent coverage of the true value. That is, in repeated sampling, when a 95 percent confidence interval is constructed for each sample, over the long run the intervals will contain the true value 95 percent of the time.
Defined Measurement Process	A detailed description of a measurement including: objective, test procedure, elemental measurement systems including calibration hierarchy and methods, and mathematical models.
Degree of Freedom (df)	A sample of N values is said to have N degrees of freedom, and a statistic calculated from it is also said to have N degrees of freedom. But if K functions

of the sample values are held constant, the number of degrees of freedom is reduced by K.

For example, the statistic 
$$\frac{\sum_{i=1}^N (X_i - \bar{X})^2}{N}$$

where  $\bar{X}$  is the sample mean, is said to have  $N - 1$  degrees of freedom. The justification for this is that (a) the sample mean is regarded as fixed or (b) in normal variation, the  $N$  quantities  $(X_i - \bar{X})$  are distributed independently of  $\bar{X}$  and hence may be regarded as  $N - 1$  independent variates or  $N$  variates connected by the linear relation  $\sum (X_i - \bar{X}) = 0$ .

Drag Coefficient	Coefficient used to calculate the aerodynamic drag force imposed on an object immersed in a flow stream.
Elemental Error	The bias and/or precision error associated with a single component or process in a chain of components or processes.
Elemental Measurement System	When several measurands are required in a Defined Measurement Process, the measurement system devoted to each measurand is termed an elemental measurement system.
Estimate	A value calculated from a sample of data as a substitute for an unknown population constant. For example, the sample standard deviation ( $S$ ) is the estimate which describes the population standard deviation ( $\sigma$ ).
Filtering	Elimination of disturbing signals that are super-imposed on the signal of interest.
Fossilized Error, Fossilization	In a calibration hierarchy, error sources considered to be precision (random) error during early steps in the hierarchy should be treated as bias (fixed) error if in the Defined Measurement Process that step is carried out only once and not repetitively.
Intake or Ram Pressure Recovery	The engine intake system efficiency at converting the freestream kinetic energy into total pressure at the inlet plane. (Actual ram total pressure/ideal ram total pressure).
Joint Distribution Function.	A function describing the simultaneous distribution of two variables. The cumulative probability distribution for two variables.
Kiel Head	A shield placed around a total pressure sensor and intended to increase its tolerance to changes in air angle. Includes generic forms of the or the original Kiel head design.  or In the case of a thermocouple, to improve recovery and increase its tolerance to changes in air angle. Includes generic forms of the original Kiel head design.
Laboratory Standard	An instrument which is calibrated periodically at a National Standard Institution. The laboratory standard may also be called an interlaboratory standard.
Map, Performance	One or more curves of a gas turbine component performance parameter or parameters presented as a function of one or more other parameters. For example, compressor pressure ratio is presented as a function of referred compressor inlet flow and referred compressor rotor speed.
Match	Term used to denote the process of causing a gas turbine engine component to operate at a particular point or points on its performance map, usually by the control of one or more operating parameters such as rotor speed, and sizing of the downstream geometry.
Mathematical Model	A mathematical description of a system. It may be a formula, a computer program, or a statistical model.
Measurand	An elemental physical quantity which is the objective of a specific measurement.
Measurement Acquisition	The recording and/or display of information coming from a sensor.
Measurement Channel	Route followed by a signal from a sensor to the recording media.
Measurement Error	The collective term meaning the difference between the true value and the measured value. Includes both bias and precision error — see accuracy and uncertainty. High accuracy implies small measurement error and small uncertainty.
Measurements, Operability	Measurements intended to yield information on transient operating limits.

Measurement, Performance	Measurements intended to yield the steady state performance of a component or engine.
Multiple Measurement	More than a single concurrent measurement of the same parameter.
Multiplexing	The recording of signals from multiple sensor inputs on to a single recording channel.
NBS	National Bureau of Standards. The reference or source of the true value for all measurements in the United States of America.
Nozzle, Coannular	Exhaust system used on a turbofan engine consisting of a separate exhaust nozzle each for the core and bypass streams, with the core nozzle throat being located coplanar with or axially downstream of the fan nozzle throat.
Nozzle, Compound	Exhaust system used on a turbofan engine consisting of an internal coplanar mixing plane for the core and bypass streams and a common final nozzle exit for both core and bypass streams.
Nozzle, Compound, Mixer	Compound nozzle with an internal mixer to promote mixing core and bypass streams in a turbofan engine prior to the common final nozzle exit.
Nozzle, Exhaust	Device for providing a desired match of upstream components of a gas turbine engine and for converting the engine exhaust energy into thrust in an efficient manner.
Nozzle, Exhaust, Convergent	Exhaust nozzle with a converging flow passage between inlet and exit, with the exit being the nozzle throat.
Nozzle, Exhaust, Convergent Divergent	Exhaust nozzle with a converging flow passage between inlet and nozzle throat, followed by a diverging flow passage between nozzle throat and exit.
Outlier	A data point which does not seem consistent with the rest of the data. A "wide" or "rogue" point. Various schemes for rejection of outliers are used.
Parameter	An unknown quantity which may vary over a certain set of values. In statistics, it occurs in expressions defining frequency distributions (population parameters). (Examples: the mean of a normal distribution, the expected value of a Poisson variable.)
Perturbing	The technique used to determine sensitivities of one dependent variable to other independent variables. The value of one independent variable is changed slightly (in increments of 0.1%, for example) and the change in the dependent variable is noted. This is normally done where the partial derivatives are too complex to evaluate.
Precision Error	The random error observed in a set of repeated measurements. This error is the result of a large number of small effects.
Precision Index	The precision index is defined herein as the computed standard deviation of the measurements. $S = \sqrt{\frac{\sum_{i=1}^N (X_i - \bar{X})^2}{N - 1}}$
Pressure, Non-Steady	Pressure varying in time as a consequence of various non-steady phenomena in gas turbine components such as turbulence, rotor blade wakes, unstable boundary layers and mixing.
Pressure, Total, Stagnation, Impact or Pitot	The pressure sensed by a probe which is at rest with respect to the system boundaries and which locally stagnates the fluid isentropically.
Pressure, Dynamic, Kinetic	Pressure equivalent of the directed kinetic energy of the fluid.
Pressure, Static or Stream	Actual pressure in a fluid independent of its state of motion. Pressure that would be measured by a pressure sensor moving with the fluid.
Probe	An assembly containing a single sensor or combination of sensors, such as temperature or pressure sensors. An aerodynamic sensor and its support.
Probe, Cylinder, Banjo, Wedge	Different geometries of pressure sensors designed to measure air angle, static and/or total pressure.
Probe, Pitot	Any of various total pressure sensors.
Probe, Pitot Static	A combination probe used to measure total and static pressure.
Probe, Prandtl	Static pressure sensor designed according to Prandtl such that errors due to support and head effects tend to cancel each other.

Probe, Traversing	A probe capable of being moved in one or more directions through the flow and usually controlled through a remote actuator.
Rake	A probe assembly containing two or more similar sensors or combination of sensors or, an aerodynamic probe consisting of a single support with an array of sensors attached.
Rake, Wake	A rake assembly with sensors aligned and proportionally spaced to best evaluate the wake characteristics from upstream engine components.
Rating Station	Component interface location for use in defining the elements included in the performance of a particular component.
Recovery Factor	Ratio of actual to total thermal energy that will be available from the adiabatic deceleration of the gas stream at the temperature measuring junction.
Response Time	As temperature measuring systems are usually first order systems, therefore, response times can be defined in terms of the time constant. However, since pressure measuring systems are usually second order systems, frequently non-linear and with various degrees of damping, no simple definition of time constant is possible. Benedict (Ref.3-11) defines a recovery time for a fairly general case which is the time for a damped system to attain 98 percent of its final response to step change. For any given system, appropriate definitions of time response should be selected and clearly defined.
Root-Sum-Square (RSS)	<p>The method of combining bias errors and precision errors, e.g.</p> $S = \pm \sqrt{S_1^2 + S_2^2 + S_3^2 + S_4^2 + \dots + S_n^2}$ $B = \pm \sqrt{B_1^2 + B_2^2 + B_3^2 + B_4^2 + \dots + B_n^2}$ <p>Note that in this document, lowercase notation always indicates elemental errors i.e. s and b for elemental precision and bias, and uppercase notation indicates the Root-Sum-Square (RSS) combination of several errors, e.g.</p> $S = \pm \sqrt{s_1^2 + s_2^2 + s_3^2}$ $B = \pm \sqrt{b_1^2 + b_2^2 + b_3^2}$ <p>where:</p> $S_2 = \pm \sqrt{\sum_i s_i}$ $B_2 = \pm \sqrt{\sum_i b_i}$
RTDs	Resistance Temperature Detectors.
Sample Size (N)	The number of repeated observations or measurement used to estimate a given statistic such as $\bar{X}$ or S.
Sampling	Selection, for a given parameter, of an acquisition frequency and a measurement time, dependent on the physical process and the performance of the measurement system.
Sensor	That part of the instrument intended to sense or respond directly to the physical quantity being measured. In a pressure probe, it is the open end of the pitot tube with its Kiel head.
Signal Conditioning	Operations that are necessary to make the sensor signal compatible with the recording devices.
Signal Processing	All the operations on the signal between the output of the sensor and the conversion into engineering units.
Standard Deviation (S)	The most widely used measure of dispersion of a frequency distribution. It is the precision index and is the square root of the variance; S is an estimate of $\sigma$ calculated from a sample of data.
Standard Error of Estimate	<p>The measure of dispersion of the dependent variable (output) about the least-squares line in curve fitting or regression analysis. It is the precision index of the output for any fixed level of the independent variable input. The formula for calculating this is:</p> $S_{y,x} = \sqrt{\frac{\sum_{i=1}^N (Y_{obs} - Y_{cal})^2}{N - K}}$ <p>for a curve fit for N data points in which K constants are estimated for the curve.</p>

## Standard Error of the Mean

An estimate of the scatter in a set of sample means based on a given sample of size  $N$ . The sample standard deviation ( $S$ ) is estimated as:

$$S = \sqrt{\frac{\sum_{i=1}^N (X_i - \bar{X})^2}{N - 1}}$$

Then the standard error of the mean is  $S/\sqrt{N}$ . In the limit, as  $N$  becomes large, the estimated standard error of the mean converges to zero while the standard deviation converges to a fixed non-zero value.

## Statistic

A parameter value based on data.  $\bar{X}$  and  $S$  are statistics. The bias limit, when it is based on judgement and not on data, is not a statistic.

## Statistical Confidence Interval

An interval estimate of a population parameter based on data. The confidence level established the coverage of the interval. That is, a 95 percent confidence interval would cover or include the true value of the parameter 95 percent of the time in repeated sampling.

## Statistical Quality Control Charts

A plot of the results of repeated sampling versus time. The central tendency and upper and lower limits are marked. Points outside the limits and trends and sequences in the points indicate non-random conditions.

## Student's "t" Distribution

The ratio of the difference between the population mean and the sample mean to the sample standard deviation (multiplied by a constant) in samples from a normal population. It is used to set confidence limits for the population mean;  $t_{\alpha/2}$  percent confidence range. It depends on the number of degrees of freedom or sample size. For large sample sizes,  $t_{\alpha/2}$  has a value of  $\approx 2$ . For small sample sizes, it is much greater than 2.

## Switching

Connection by electric or electronic devices of several instrumentation channels to a single amplifier. See also Multiplexing.

## Taylor's Series

A power series to calculate the value of a function at a point in the neighborhood of some reference point. The series expresses the difference or differential between the new point and the reference point in terms of the successive derivatives of the function. Its form is

$$f(x) - f(a) = \sum_{r=1}^{N-1} \frac{(x-a)^r}{r!} f^{(r)}(a) + R_N$$

Where  $f^{(r)}(a)$  denotes the value of the  $r$ th derivative of  $f(x)$  at the reference point  $x = a$ . Commonly, if the series converges, the remainder  $R_N$  is made infinitesimal by selecting an arbitrary number of terms.

## Traceability

The ability to trace the calibration of a measuring device through a chain of calibrations to a National Standards Institution.

## Transducer

A device which converts the measurand into an electrical signal.

## Transfer Standard

A laboratory instrument which is used to calibrate working standards and which is periodically calibrated against the laboratory standard.

## True Value

The reference value defined by a National Standards Institution which is assumed to be the true value of any measured quantity.

## Uncertainty (U)

The error reasonably expected for the defined measurement process. Usually expressed as  $U_{add}$  and  $U_{rss}$  at a specified confidence level.

## UTR Box

Uniform Temperature Reference box.

The 0°C reference junction is replaced by a near ambient temperature junction. The temperature is measured in the box and the acquired measurement is corrected to the accepted temperature scales.

## Variance ( $\sigma^2$ )

A measure of scatter or spread of a distribution. It is estimated by

$$S^2 = \frac{\sum (X_i - \bar{X})^2}{N - 1}$$

from a sample of data. The variance is the square of the standard deviation.

## Wire, Extension

Wire made of the same material as the thermocouple but which may be of a lower grade. For this reason it must be used where temperature gradients are less than 100°C.

## Working Standard

An instrument that is calibrated in a laboratory against an interlaboratory or transfer standard and is used as a standard in calibrating measuring instruments.

## Acronyms

AEDC	Arnold Engineering Development Center (USA)
AIAA	American Institute of Aeronautics and Astronautics
AIR	Aerospace Information Report
ANSI	American National Standards Institute
ARC	Aeronautical Research Council (UK)
ARP	Aerospace Recommended Practice (USA)
ASME	American Society of Mechanical Engineers
ASTM	American Society of Testing and Materials
DIN	Deutsches Institute für Normung (German Standards Institute)
ICRPG	Interagency Chemical Rocket Propulsion Group (USA)
IPTS	International Practical Temperature Scale
ISA	Instrument Society of America
ISO	International Standards Organization
MFCAM	Measurement of Fluid Flow in a Closed Circuit
MIDAP	Ministry/Industry Drag Analysis Panel (UK)
MIT	Massachusetts Institute of Technology
NACA	National Advisory Committee for Aeronautics (USA)
NASA	National Aeronautics and Space Administration (USA)
NBS	National Bureau of Standards (USA)
NFC	Norme Française; Section C (Electricity)
RAE	Royal Aerospace Establishment (UK)
SAE	Society of Automotive Engineers (USA)
SI	Système International (System of units of measurement)
UETP	Uniform Engine Test Program
USAF	United States Airforce

## 1. INTRODUCTION

### 1.1 Objective

The objective of this document is to establish recommended practices for the instrumentation for performance evaluation of aviation gas turbine components undergoing development in rigs and engines.

The intent of this document is to provide a common understanding between manufacturers, research organizations and procurement agencies of the factors affecting performance test data. This will be achieved by providing guidance in establishing the adequacy of instrumentation designs. The use of common terms of reference for the description, application and evaluation of instrumentation is directed at obtaining meaningful and unambiguous values of parameters with an associated estimate of measurement uncertainty.

The application of these recommended practices will ensure confidence in the mutual understanding of the quality and consistency of data obtained in test programs. This should be of particular value in multi-company or multi-national engine programs.

### 1.2 Scope

The scope of this document will be limited to the measurement of the key gas path parameters of pressure and temperature as they relate to component performance. Only steady state measurements are considered, with the component or engine operating in an equilibrium condition.

Instrumentation of gas turbines is a wide ranging subject, covering a range from the minimum required for safe operation to the comprehensive instrumentation of one or more components on a test rig or development engine. Performance may be considered at the overall level where the manufacturer must demonstrate specified levels of thrust and specific fuel consumption while observing limiting values of rotational speed or temperature; this type of testing is required for performance demonstration during the *certification* phases and in a more limited way for the product acceptance tests during the *production* phases. This document is concerned with instrumentation required during the *development* phase, where the development team is largely concerned with isolating, and correcting, deficiencies in engine performance. The extensive investigation carried out by AGARD PEP WG-15 (Ref 1.2-1) has dealt with the overall measurement of thrust, specific fuel consumption and airflow, so these will not be considered in this document.

The measurement requirements for each aerodynamic component of an aviation gas turbine are reviewed and suitable configurations for the distribution of pressure and temperature measurements at the inlet and discharge planes of engines, compressors, combustors, and turbines, afterburners and propelling nozzles are detailed. Consideration is given to averaged and mean flows, uniform and distorted flow conditions, size effects and their impact on the use of fixed rakes and traversing probes.

The testing of complete engines generally requires a minimum of instrumentation to reduce the adverse effects on performance due to probe installations. Rig testing of individual components, however, is aimed at achieving maximum information and hence the instrumentation is much more comprehensive. It is desirable to conserve cross correlation between component rig and full engine testing, and as far as possible the rig test should include

instrumentation that will subsequently be used on the engine. It should be noted that each instrumentation installation introduces its own effect on the flow path data.

The problems of pressure and temperature measurement as related to calibration (including on-line) and probe design are reviewed. Although this document is primarily concerned with steady state measurements, it is important to recognize the effects of dynamic pressure changes such as the pulses experienced behind rows of compressor and turbine blades. This leads to consideration of establishing spatial and temporal sampling effects and the use of probe arrays.

The uncertainty of measurement analysis techniques required to determine the accuracy of measurements is discussed. This includes reference to the calibration of individual components and overall systems and to their impact on overall accuracy tolerances. The impact of using a limited number of probes on the level of confidence in the accuracy of data is considered.

Instrumentation installations are strongly influenced by engine size. The instrumentation of large engines has its own unique problems primarily related to the mechanical integrity of probe structures. In the case of small engines, the small total cross-sectional area of the flow paths and the relatively large blockages caused by probes present specific difficulties that are addressed in a section on special factors in small engines.

The problem areas described are brought together by example in specimen cases. These examples are presented in order to guide the reader through the process of instrumentation design and to illustrate the impact of measurement errors on the overall test data.

### 1.3 How to Use

This document provides guidelines on the application of measurement systems. The text is organized into segments that enable the reader to follow through from basic considerations of pressure and temperature measurement to actual examples as applied to component performance analysis. It will be assumed that the reader will use the definitions in this document when communicating with appropriate organizations on test requirements that reference these recommended practices.

Section 2 addresses the general requirements of engine and component measurement and contains descriptions of basic components and the associated identifier and special requirements that are presented in the rest of the document. This section provides a primer on the special considerations that must be applied when investigating the performance of individual components. Included are representative formulae used for determining the aerodynamic performance of the component which can be used for the evaluation of the impact of errors on measurement accuracy.

The determination of overall accuracy as it relates to national and international standards is described under Uncertainty Analysis (Section 3). This method of determining the accuracy of a measurement, whether it be in absolute or relative terms, applies to all systems and is therefore a keystone of any measurement system design. Statements on the uncertainty analysis determination of errors must be included with any system design.

The flows through engines and components under steady state operating conditions can be far from stable. Gas flow chopped by passing blades, wakes, plus centrifugal flows in axial components add to the problems of establishing average flows. Time delays through components that are not absolutely stable can confuse the data. Added to these problems are measurements that appear to deviate from the others. These problems are considered in Section 4 on Spatial Sampling, Probe Arrays and Data Editing.

The unique problems of temperature and pressure measurement are provided for guidance. By using these Sections (5 & 6) in conjunction with uncertainty analysis and the evaluation of special considerations of spatial and temporal averaging, spatial sampling and data editing, the overall confidence in data accuracy can be established. This

may well determine if the risk factor in performing a test warrants the expense or not.

Small engines with associated small gas path geometries are considered as a special case (Section 7). Here the concern is with the impact of blockage and modifications of the gas flow due to the intrusion of mechanically relatively large probes. The mechanical integrity of the probe is not so much the ruling factor as the mechanical size necessary to ensure confidence in the accuracy of the measurements over a wide operating range from sub-atmospheric to multiple atmospheric pressures.

The foregoing form the ground work for designing and evaluating measurement systems. Section 8 on Specimen Cases works through examples to determine the design requirements and expected accuracies of the various component performances.

## 2. GENERAL REQUIREMENTS FOR ENGINE AND COMPONENT RIG TESTING

### 2.1 Introduction

The determination of the aerodynamic performance of a gas turbine engine component is a very complex process, and as well as the configuration of the instrumentation and "accuracy" of the recordings, there are many other features which will influence the perceived performance of the machine. These other features could include; methods of data reduction (averaging process i.e. mathematical methods and instrumentation system dynamics), environment and procedure under which the tests are carried out, mechanical standard of the machine and the adequacy (meaning and interpretation) of the derived component performance parameters. Although these aspects can have a significant influence on the perceived performance of the component only those items related to the instrumentation system itself and the initial data processing methods will be considered in the following sections of this document. The other aspects will however be mentioned so that the user is made aware of them and can therefore guard against the misinterpretation of the results.

Obviously it would be ideal to do all component testing on an engine since the real environment would be more nearly simulated, but there are many cases where this is neither practical nor cost effective and component testing on an isolated test stand may be more profitable. Furthermore, the instrumentation requirements will be dependent upon the objective of the test programme and thus the instrumentation design and specification could be quite different between pure research rigs and engine validation/development investigations. Research rigs may thus require comprehensive, special and sophisticated instrumentation and the unit tested over a wide range in a well defined environment whereas, on an engine, there will be a strong incentive to have minimum instrumentation which must be robust and present minimum hazard.

On the other hand, development investigations on an isolated test stand represents an intermediate phase where it is preferable that the instrumentation used be similar to that which could be installed in the engine if that is the final destination of the component. This is highly desirable as the use of common instrumentation will reduce the degree of uncertainty in the comparison of rig results with engine measurements. There remains however, the difficult problem of simulating an adequately representative environment on an isolated test stand. It is well known for example, that when a component is tested in this way that its performance may appear different than when operated in series with other components (i.e. in the engine) which force on it an environment influenced by the unique demands and characteristics of those neighbouring components.

In many cases, an absolute value defining the component performance is necessary if the data is to be read across into another environment or compared with data from similar units obtained from tests using different facilities and instrumentation. In this case, considerable additional care must be taken to provide adequate instrumentation and a realistic simulation of the desired environment and to quantify the uncertainty of the results. It is particularly important when deriving component performance from engine tests that a consistent method of averaging measurements at interface planes (between components) is used throughout the engine. Corresponding averaging

methods should also be used for rig tests if the results are to be read across to the engine.

Alternatively, there are certain investigations where it may be sufficient to obtain relative measurements which are limited to defining changes in component performance, when tested on the same facility (or on an engine) using the same instrumentation, following small changes in component configuration. This method of testing can minimise the influence of some of the measurement uncertainties and be achieved using a limited amount of instrumentation. This method of testing is commonly referred to as Back to Back testing.

However, in all cases it is necessary to measure and record all relevant mechanical aspects of the component's configuration which could influence its aerodynamic performance. Items such as leakage path clearances, mechanical tolerances, profile geometry, surface finish etc., fall into this category and it should be noted that many of these can vary with mechanical load, temperature and running hours, and therefore may need to be measured or monitored while running. In many cases the performance of the component will vary with time due to the accumulation of dirt, wear leading to increased leakage flows, minor foreign object damage etc. Therefore for those tests which occupy a large number of test hours it is recommended that, when possible, selected test points be repeated to ascertain whether or not such performance penalties exist.

Thus for each type of test, research or development, and for each component it is possible that a different standard and configuration of instrumentation, test procedures and analysis technique may be required. It will therefore not be possible to recommend a single configuration of instrumentation etc., which would be adequate in all cases.

Although there are many different measurements and parameters required to define the performance, environment and configuration of a component, this document is restricted to measurement of pressure and temperature. The forms of measurement will include total pressure, static pressure (including those on surfaces), differential pressures and total temperature as these measurements form the basis for the assessment of the aerodynamic performance of an engine or component.

Furthermore, this document will be confined to those measurements which can be adequately quantified by a single average or mean value. There are however, in all machines varying degrees of unsteadiness in the flow and three different classifications are often defined: steady state, transient and dynamic.

*Steady state conditions* are those where the machine is running at a nominally fixed operating point and the measurand is essentially constant with time. Even in steady state conditions it must be recognised that there may be substantial unsteadiness due to the presence of rotor passage wakes, turbulence etc., which could significantly influence the performance and calibration characteristics of the probe system itself. Also, the machine under test cannot be held at a precisely constant condition and so over a period of time a sequence of slow variations must be expected. These factors should be considered when assessing the uncertainty of the results.

Included in this concept of steady state conditions is the requirement that the machine should be allowed time to reach equilibrium conditions in terms of stable aerodynamic

and/or structural temperature gradients, and stable component operating point or engine match point, before the definitive measurements are recorded.

The term *transient conditions* are those in which a relatively slow variation of machine operation is deliberately induced (e.g. engine acceleration), and for which a single spatially averaged value is an adequate description of the flow at the time of measurement. Although the discussion in the following sections is not aimed at providing instrumentation capable of accurately quantifying the performance characteristics under transient conditions, the instrumentation system must be capable of detecting the boundaries of instability (e.g. surge, rotating stall etc.) and changes in performance due to transient operation. In many instances it will be necessary to provide rapid response instrumentation if a more detailed and accurate measurement is required but the definition of such instrumentation is beyond the scope of this document.

*Dynamic measurements* are those in which the conditions are varying at a high frequency and for which an instantaneous point measurement or spectral behaviour characteristics are required to adequately define the flow. Special instrumentation is required for this purpose. The specific problems associated with the measurement under dynamic conditions will not be considered in this document.

As well as designing an instrumentation system capable of providing measurements of adequate standard and with minimum influence on the flow itself, it is essential that the probe does not unduly hazard the machine. It is therefore necessary to assess all probes to ensure that they are of adequate strength to withstand all aerodynamic loads, including the extreme values which may occur during unsteady (e.g. surge) or high temperature conditions. It is also necessary to examine the vibration characteristics of all probes and in some cases it may be advisable to attach a strain gauge to the probe body so that its mechanical behaviour can be monitored during the test programme.

It should also be recognised that the insertion of a probe will create a disturbance in the flow which could result in a structural vibration of the main rig component. Although these aspects are not specifically discussed in this document it is essential that a thorough mechanical assessment of the total system be made so that engine and component tests can be carried out at a known minimum risk.

In the following subsections, the essential aspects of pressure and temperature measurement and the preliminary analysis requirement for each component are discussed and a minimum standard of instrumentation is recommended below which the acquired results could be of dubious value and in extreme cases could lead to erroneous conclusions. In addition to quoting the unit's performance, it is essential that a description of the instrumentation (and calibration data) used be quoted together with the record of the test environment and unit's mechanical standard and a description of the data reduction methods given.

## 2.2 General Considerations for Pressure and Temperature Measurement

In this document, the state of the art for steady state gas temperature and pressure measurement as applied to gas turbine component development will be described. These measurements have a wide variety of applications including such things as:

1. Assessment of component performance especially

efficiency, mass flow, and surge margin.

2. Study of blockage and aerodynamic losses.
3. Determination of nozzle coefficients.
4. Determination of gas velocity and Mach number.
5. Measurement of the spatial distribution of flow, boundary layer thicknesses, and flow separation.

In general, pressure and temperature measurements are the most fundamental aerodynamic measurements required in gas turbine component development. The number of measurements in any given test varies widely from just a few in simple tests to well over a thousand in complex tests of major components.

The types of pressure measurements required are: the total pressure at various stations in flow passages, static pressures both in passages and on surfaces, and differential pressures for determination of such things as air angle and dynamic head. The gas temperature measurement normally used is the total or stagnation temperature. Measurement of static temperature, while it might be desirable in some cases, is not feasible with fixed intrusive probes which are the current state of the art for both pressure and temperature measurement. Optical techniques such as CARS (Coherent Anti-Stokes Raman Scattering) can measure static temperature (as well as density and composition) directly but are applicable only in special cases and will not be covered in this document. In gas turbine work, the pressure and temperature measurements needed extend over approximately the following ranges:

Pressure	10 to 4000kPa
Temperature	200 to 2200K
Ma	0.05 to 1.2*

In general, this document covers recommended practices which are appropriate for most of the above ranges. It does not cover the temperature range above the limits of readily available sensors (1700K for noble metal thermocouples) nor does it cover any of the unique problems of designing probes for transonic and supersonic flow regimes.

The successful application of pressure and temperature measurements to gas turbine development requires that a very clear definition of the measurement process and its objectives be established and used as a basis for the instrumentation system design. Some of the critical considerations are:

1. The characteristics of the facility in which the test vehicle will be run including its aerodynamic characteristics, data acquisition system, and vehicle control system.
2. The specific objectives for which the data will be used. Is only overall efficiency required or is additional information needed such as stage-by-stage losses, spatial distribution of losses, flow coefficient determination, etc?
3. Are absolute results required or is the principal objective the assessment of the effect of changes such as the comparison of a baseline compressor and the same compressor with modified blade designs?
4. The accuracy required should be given careful consideration. The higher the accuracy specified, the more costly a test will be. On the other hand, a test in

\*Much higher Mach numbers might be encountered in inlets and nozzles.

which the uncertainty is so large that the results cannot be unambiguously interpreted is of little value and can sometimes be dangerously misleading.

5. The location of measuring stations must be selected and an adequate array of sampling points defined at each station. This very difficult issue is always a compromise between selecting a large enough array of data points to satisfy the test objectives but not so large an array that probe blockage effects significantly affect the vehicle performance.
6. The requirements for pretest checkout and on-line data reduction and display must be defined. For each test, provide the operators with predictions of the results to be expected and establish a data validation plan which is designed to warn of faults in the measurement systems or in the facility.

An extensive background of work exists covering the theory and application of aerodynamic probes and the relevant literature is cited in the sections of this document on pressure and temperature measurements (Sections 5 and 6). These sections provide guidance and recommendations for applying the state of the art in aerodynamic probe design to the unique problems encountered in gas turbine development.

A variety of new methods for measuring gas dynamic quantities have evolved in recent years, nevertheless, pressure and temperature probes are still by far the most useful measurement devices for component development. Although the technology on which these probes are based originated many years ago, recent trends in gas turbine design have placed increasingly stringent demands on the instrumentation design theory and practice.

Higher pressures and temperatures, more highly loaded and closely spaced stages coupled with the need to validate three-dimensional design systems have put a premium on the design of small, less intrusive probes and rakes and on the integration of these sensors into airfoils and other flowpath structures. Design of probes with high tolerance and unambiguous response to unsteadiness and other time varying flows is also an increasing requirement.

In general, it is found that pressure and temperature probe designs must be carefully tailored to the test vehicle and test objectives. This document cannot give specific directions on probe designs and measurement system designs which cover any and all situations. It does, however, describe the most important considerations and makes recommendations which, if followed, will allow the reader to get high-quality experimental data from component test programs.

### 2.3 Measurement Identification Codes

The codes described in this section relate specifically to identification tags and have been abbreviated to keep the number of characters to a minimum. These codes apply to components in rigs as well as in engines. Rig installations are addressed as though the component were installed in an engine.

It must be noted that the measurement identification codes are used in conjunction with installation drawings and that they are configured to permit the rapid location of the referenced points. It is recognized that there may be configurations or requirements that are not covered by these recommended practices, ARP246B or ARP755A.

The engine or component manufacturer's drawings and publications must clearly define the notations and practices applied in those cases.

For written documents, the nomenclature defined in Section 2.3.1 is to be applied. The nomenclature recommended for probes and sensors are based upon the principles defined in SAE ARP 755A "Gas Turbine Engine Performance Station Identification and Nomenclature" and SAE ARP246B "Orientation of Engine Axis, Coordinate and Numbering Systems for Aircraft Gas Turbine Engines".

#### 2.3.1 Measurement Identification

For aerodynamic gas path temperature and pressure measurements the recommended Measurement Identifications on cable and tubing are as follows:

Measured Parameter.....	P,S,X,T
Engine Station.....	1,2,3.....9
Component Station.....	1,2,3.....999
Angular Position.....	A,B,C,D.....Y
Sensor Number.....	01,02,03.....99
Directional Probe.....	L,R,C,U,D.

An example of the code is 

S	2	112	C	03
---	---	-----	---	----

 which would normally be written or stamped on labels as S2112C03 where,

- S Static pressure
- 2 Compressor
- 112 Position along the gas path within the compressor
- C Angular position of probe  $30^\circ \leq C < 45^\circ$  relative to top dead centre, clockwise looking upstream from a downstream location.
- 03 Location of sensing head on the probe.

The code applies to primary air flow through the core and bypass. Secondary internal air flow and parameters related to auxiliary functions may be identified by adding suitable codes before or after the recommended code to clearly segregate those functions. When applied, the modifiers must be clearly identified on the drawings and in the text of documents.

#### 2.3.1.1 Measured Parameters

- P Total Pressure
- S Static Pressure
- X Delta Pressure
- T Temperature

#### 2.3.1.2 Engine Stations

The station identifications increment in ascending order along the mean path of aerodynamic gas flow from intake to exhaust.

- 0 Free stream air condition
- 1 Inlet/Engine interface
- 2 First compressor front face
- 3 Last compressor discharge
- 4 Burner discharge
- 5 Last turbine discharge
- 6 Available for mixer, afterburner, etc.
- 7 Engine/Exhaust nozzle interface
- 8 Exhaust nozzle throat
- 9 Exhaust nozzle discharge.

For conventional straight through flows the stations are readily seen to move from left to right. In the case of engines with reversing flows e.g. reverse flow combustors, the

sequence should remain in order as compared to the straight through engine.

In addition to the primary air flow, multiple streams such as the bypass flow in a turbo fan engine are identified using the digit 1 for the station number for the innermost bypass duct and the equivalent primary airflow as the second digit.

- e.g. 12 First compressor front face tip section  
 13 End of compressor bypass flow  
 17 Bypass duct/exhaust nozzle interface  
 18 Bypass exhaust nozzle throat.

The digit 9 will be used to identify ejector nozzle flow or for a second bypass duct.

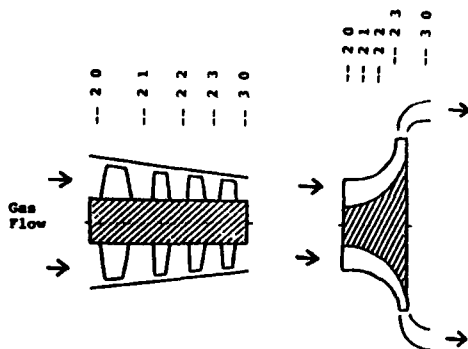
- e.g. 98 Ejector exhaust nozzle throat.

When a component is to be tested separately or in conjunction with other components, the codes must be consistent with the engine station number i.e. Compressors, Station 2; Turbines, Station 4; etc.

The recommended station identifications for various sample configurations are illustrated in Figures 2.3-1 to -11.

### 2.3.1.3 Component Stations

Each component can be subdivided into a number of discrete locations.



For the example given, a compressor station 2 has been split into 3 locations. Each of these three locations can be further divided into 99 subdivisions. Therefore the codes run from 2001... 2101... 2299... 2399. It is recommended that the component stations be numbered in ascending order in the direction of the gas flow. If, subsequently additional sensor locations are added that break the sequence of the numbers, then out of sequence numbering is acceptable as long as it is clearly specified in the text. It is good practice to "design in" as many probable locations as possible at the start of the program and hence keep additions to a minimum.

The position code can be applied in various combinations to suit the application. Depending on the number of stages in the station under consideration, the code may be used as illustrated in the following:

- (a) First digit identifies the component. The second digit identifies a major subdivision and the third and fourth digits give further subdivisions. The major subdivision may, for example, represent individual stages in a compressor. This is limited to nine major subdivisions

(1 to 9). An example is shown in the figure above, 20; 21; 22; 23; represent the major divisions of the compressor. The third and fourth digits represent subdivision 63 between major stations 22 and 23 (a total of 99 subdivisions are possible between stations 22 and 23).

Example 

S	2	2	63	A	01
---	---	---	----	---	----

- (b) For bypass flows the second digit identifies the equivalent of the primary flow station being used in conjunction with 1 or 9 as the stream identifier (first digit) as described in Section 2.3.1.2. The last two digits permit position codes from one to ninety-nine (1 to 99).

Example 

T	12	56	A	01
---	----	----	---	----

- (c) For subsystem airflows, e.g. to and from bleed cavities, seals, etc., the third location in the station code identifies the intended destination or source of the flow. Examples of the use of identifiers are:-

B for Bleed  
 C for cavity  
 S for seal.

Example 

S	2	B	5	6	A	01
---	---	---	---	---	---	----

This represents a bleed flow from the compressor at compressor position 5 (station 25). 6A01 gives the specific location of the measurement in the bleed orifice or cavity through which the bleed flows.

NOTE: It is important that the coding method and identifiers be clearly defined in the reference documents.

### 2.3.1.4 Angular Positions.

The engine cross sections, as viewed in the upstream direction from a gas path down stream location, are divided into segments of 15° increments starting at top dead centre (TDC) and moving in a clockwise direction. The segments are identified with alpha characters.

0° < A < 15°	180° < M < 195°
15° < B < 30°	195° < N < 210°
30° < C < 45°	210° < P < 225°
45° < D < 60°	225° < Q < 240°
60° < E < 75°	240° < R < 255°
75° < F < 90°	255° < S < 270°
90° < G < 105°	270° < T < 285°
105° < H < 120°	285° < U < 300°
120° < I < 135°	300° < V < 315°
135° < J < 150°	315° < W < 330°
150° < K < 165°	330° < X < 345°
165° < L < 180°	345° < Y < 360°

Z = Sensor points mounted OFF-engine/intake

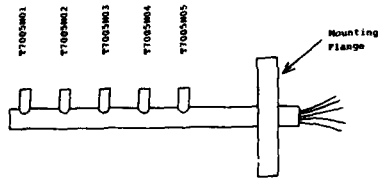
### 2.3.1.5 Sensor Number

The reference point for all free mounted rakes is the mounting flange.

- (a) Radial Rakes

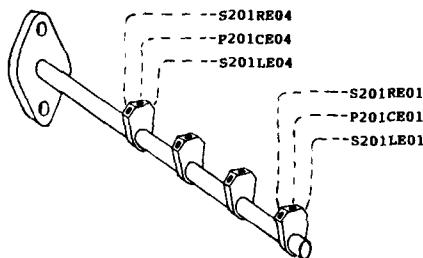
The outermost sensing point on the rake from the mounting flange is identified as 01. The points on the

rake are sequentially numbered in ascending order towards the mounting flange.



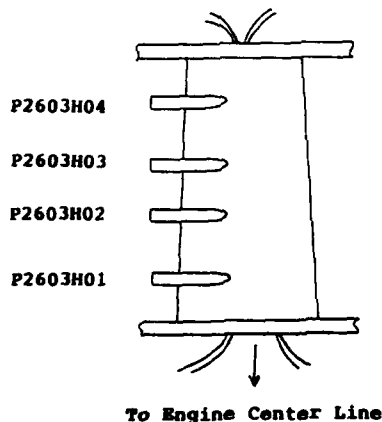
This sequence has the advantage of consistency during the construction of probes in that the numbering is always in the same direction and also that the installed direction of the probe does not have to be considered. In some cases the probe may be horizontal relative to the engine/component centreline.

In the case where the heads have multiple sensing points at the same location, e.g. cobra probes, the sense point numbers are incremented as illustrated. (L = left, C = centre, R = right, U = up, D = down). The position on the sensing head (L, C, R, U or D) is inserted at the location of the fourth digit in the position identifier.



The numbering sequence is left to right, clockwise looking from the flange towards the tip of the probe at each sensor location. (or for vanes, looking towards the engine/component centreline).

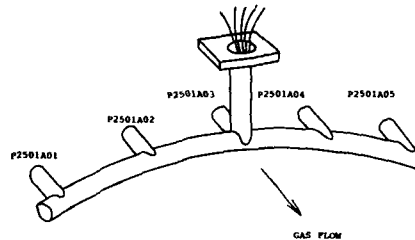
#### (b) Blade/Vane Mounted Sensors



The number starts with 01 closest to the engine centreline regardless of the direction in which the instrument lines exit the blade/vanes.

#### (c) Wake Rakes (or Circumferential Rakes)

Where viewed from a downstream location in the upstream direction, the probe at the furthest counter clockwise position is 01. The sensor points are identified sequentially in ascending order in a clockwise direction.



In the case where multiple sensing points are at the same location, follow the example as given under Radial Rakes (2.3.1.5 (a)).

#### (d) Longitudinal Rakes

The probe heads are numbered with 01 being the point furthest upstream with the identifications numbered in ascending order in the downstream direction.

Multiple head sensors are to be identified as given under Radial Rakes (2.3.1.5 (a)).

#### 2.3.2 Identification Tags on Instrument Lines

The method of identifying the instrumentation lines on a test section must take into consideration the environment, location and handling required to route the lines in the test facility.

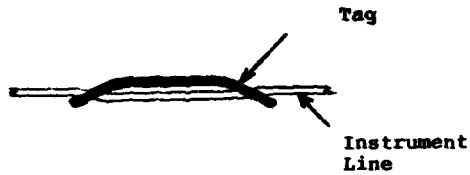
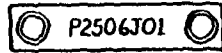
Each installation must be considered on its own merits. The following is a check list of considerations that should be taken into account when selecting a particular method or material for attachment to the lines.

1. Will the identification be subjected to a hostile environmental e.g.  
High/low temperatures.  
Chafing due to vibration  
Corrosive gases/fluids?

Remember that plastic can equally well be destroyed by brittleness when cold as by melting when hot and that high temperature plastics, when embossed with identifications, can lose that embossing when hot. Also, vibration does not just refer to the natural vibration due to air flow such as propeller blade wakes, bleed flows, bypass flows, etc.

2. Will the lines have to pass through small orifices or as bundles through the test facility wall etc? In this case the physical profile of the tag on the lines is important.
3. For "normal" extension cable and metal tubing, metal tags are recommended. In this case, normal refers to lines that are robust and will tolerate both the handling by the test facility crew and the attachment of the tag while satisfying the requirements in 1 above.

Aluminium or stainless steel are preferred. Two hole attachment is recommended as illustrated.



Note: Remove all sharp corners and edges, in particular around the holes through which the line passes.

4. If the environment that the identification tags will normally reside in is considered to be within that which plastic heatshrink, wrap around or numbered rings will survive without being cut, pulled-off or otherwise disfigured then they may be considered for use. This is where it is important that eight digit codes are used because it can easily be checked that the code on the line is complete.

Note: Avoid colour coding as there are individuals who are colour blind.

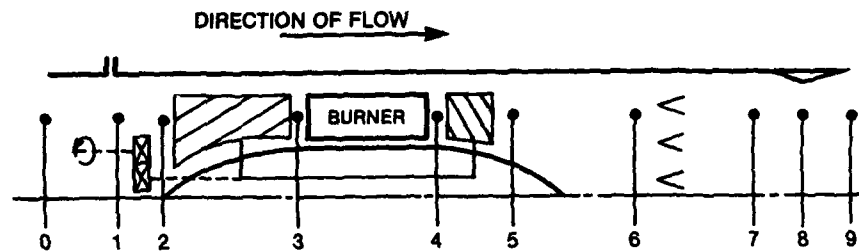


Fig.2.3-1

### SINGLE SPOOL TURBOJET/TURBO SHAFT

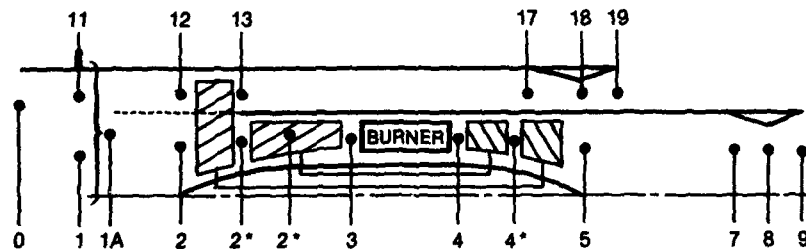


Fig.2.3-2

### TWIN SPOOL TURBOFAN

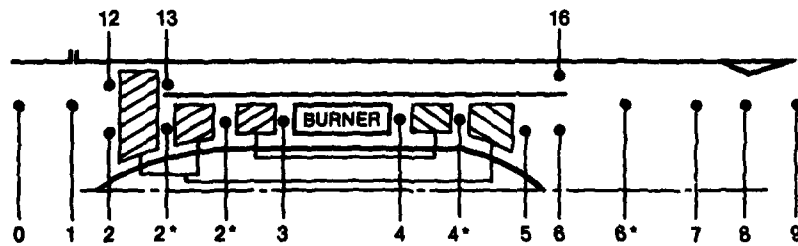


Fig.2.3-3

### MIXED TWIN SPOOL TURBOFAN

\* See Section 2.3.1.3.

Figs 2.3-1 to 11 Recommended engine station identification for various configurations\*

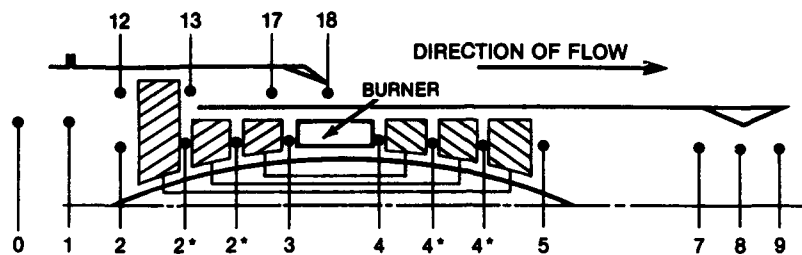


Fig.2.3-4

## TRIPLE SPOOL TURBOFAN

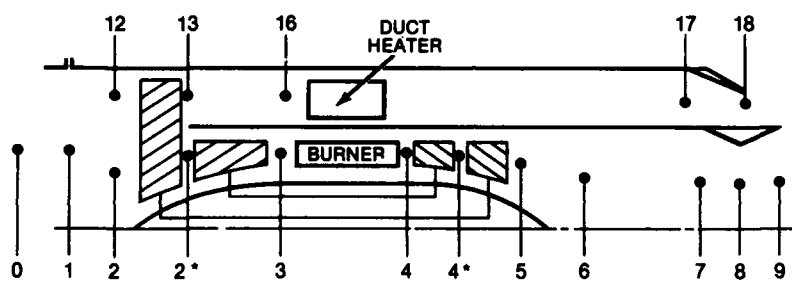


Fig.2.3-5

## TWIN SPOOL DUCT HEATER

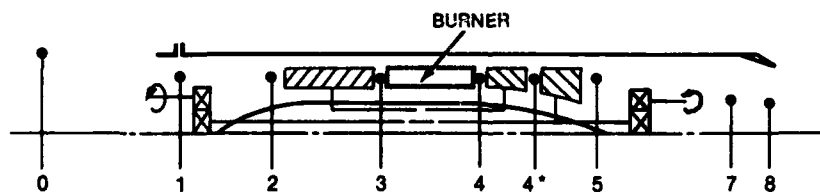


Fig.2.3-6

## FREE TURBINE TURBO PROP/TURBO SHAFT

\* See Section 2.3.1.3.

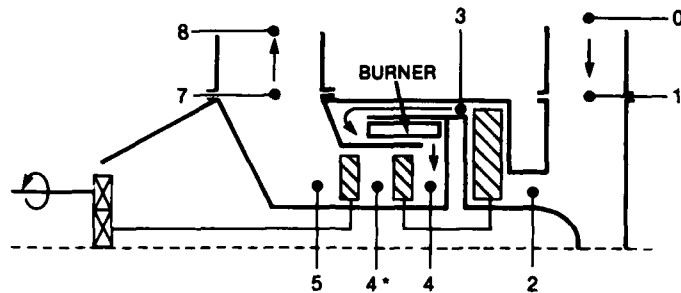


Fig.2.3-7

## FREE TURBINE TURBOPROP/TURBOSHAFT

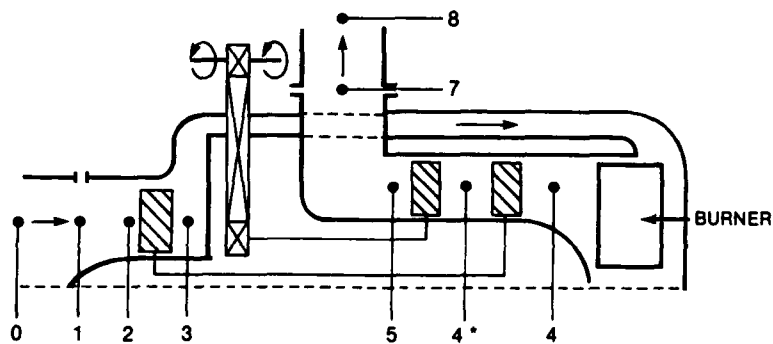


Fig.2.3-8

## FREE TURBINE TURBOPROP/TURBOSHAFT

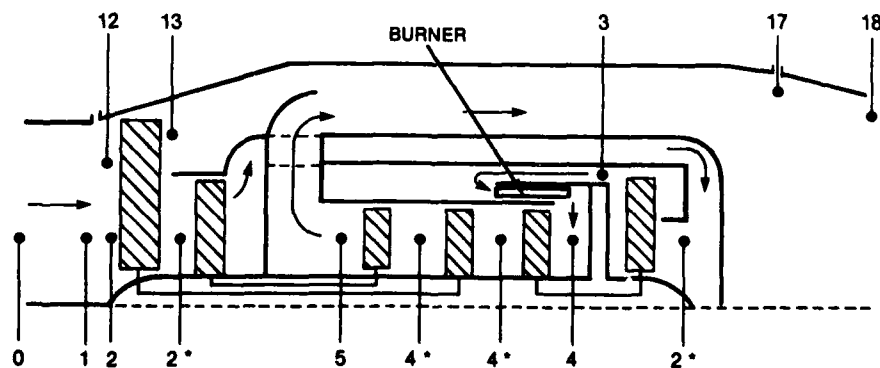
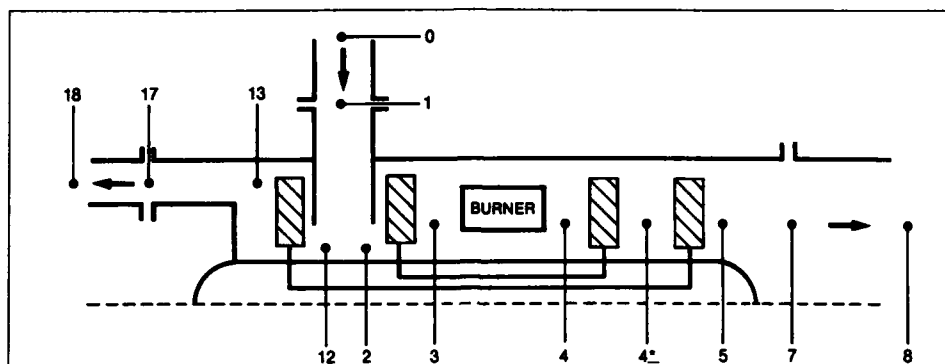


Fig.2.3-9

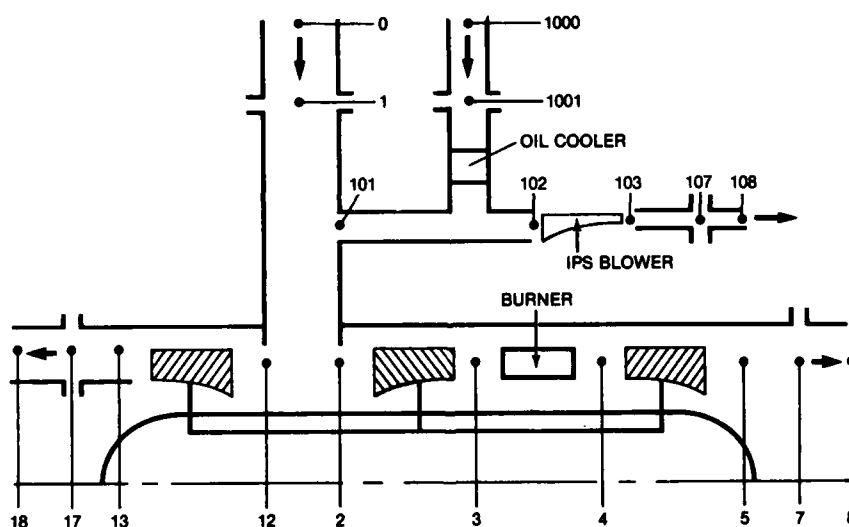
\* See Section 2.3.1.3.

## THREE SPOOL TURBOFAN



**AUXILIARY POWER UNIT**  
(Independent secondary compressor drive)

Fig.2.3-10



**AUXILIARY POWER UNIT**  
**WITH 2 STREAM INLET PARTICLE SEPARATOR**

Fig.2.3-11

\* See Section 2.3.1.3.

## 2.4 Test Cell Environment

### 2.4.1 Introduction

Aircraft Turbine engines under development test in a test cell are often supplied with air by ducting at the front and exhaust into a diffuser at the rear, particularly when simulated altitude performance is being investigated. In these circumstances it is important to measure the total pressure and temperature at engine entry and also to measure the environmental pressure surrounding the engine and into which the nozzle exhausts. Figures 2.4-1 and 2.4-2 show typical installations of engines in altitude test cells in which the engine is in a "connected" test mode. This type of

installation enables the air entering the engine to be conditioned to the correct simulated forward speed, whilst the air exhausted from the pressure chamber surrounding the engine is kept at the correct simulated altitude pressure. In sea level engine tests there is no need for complicated inlet ducting. The engine is often connected to a simple bellmouth entry at the front and exhausts into a simple diffuser at the rear.

Where test rigs for component testing are concerned, the measurement of inlet and exhaust pressures and temperatures in the inlet and exhaust ducting should be given similar considerations to those for full engine testing.

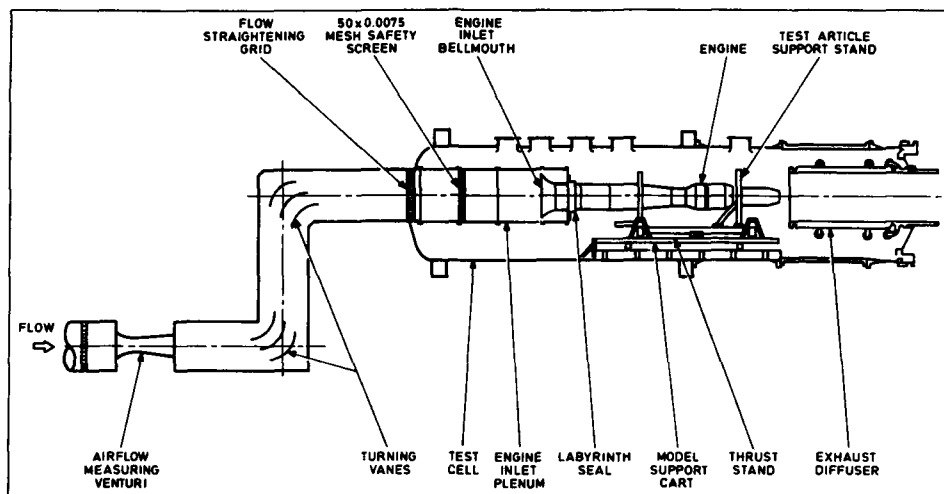


Fig. 2.4-1 Typical engine installation in an altitude test cell

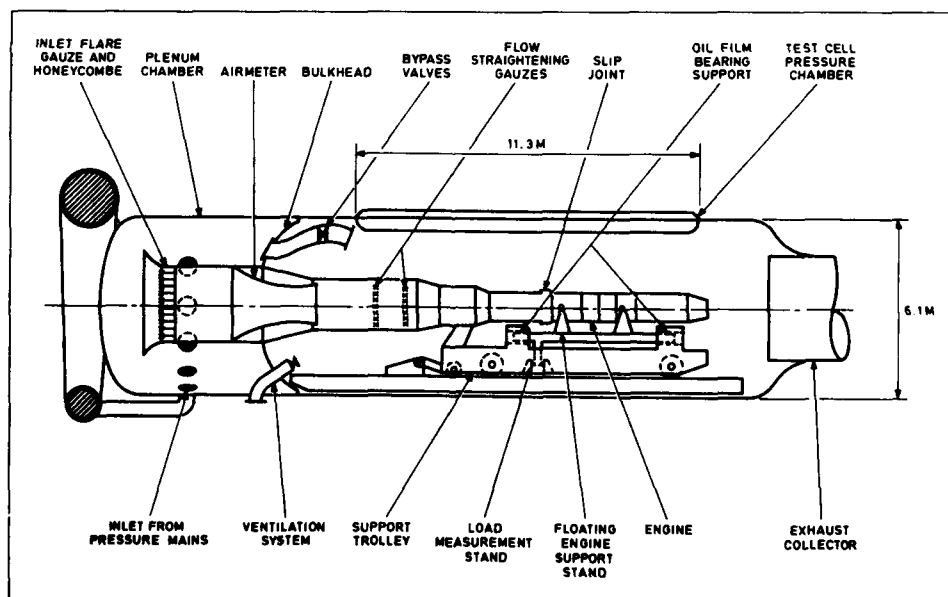


Fig. 2.4-2 Typical engine installation in an altitude test cell

Special requirements for pressure and temperature measurements in component testing are highlighted in the respective sections devoted to each component which may be found in later sub-sections.

The quantity of measurements needed to define the total pressure and temperature in the inlet ducting approaching the engine in the test cell or component in a test rig is dependent on the quality of the flow field. The quality of the flow field, in turn, may be dependent on the test objective or the design of the inlet ducting. The test may be deliberately simulating a distorted flow field by the insertion of distortion plates or gauzes (also called screens), and in this case, the quantity of measurements to define the flow field may well be extensive. On the other hand, a simple bellmouth intake suitably designed to minimise boundary layer growth may provide a uniform flow field that requires minimal instrumentation probes to define total pressure and temperature.

These examples of extremes of inlet flow fields illustrate the problem of defining a unique standard to be applied uniformly to the measurement of total inlet pressure and temperature.

The normal history of events in steady state engine performance tests for a given inlet duct geometry is initially to use extensive pressure and temperature probes to investigate the quality of the flow field, and then later, to gradually reduce the number of probes, having established the requirements. Ideally the probes should eventually all be removed so that the very disturbance to the flows by the probes and supports themselves is removed. Future measurement systems, i.e. laser anemometers, etc., should enable this ideal to be accomplished.

#### 2.4.2 Engine Performance Definitions

Measured engine performance in a test cell requires the inlet pressure and temperature measurements as well as the cell pressure to determine major parameters such as thrust, airflow and specific fuel consumption. For example:

Engine Gross thrust in an altitude test facility may be a function of:-

- (a) Load cell force
- (b) Inlet duct total and static pressure and temperature
- (c) Cell pressure
- (d) Inlet duct area
- (e) Inlet airflow

Inlet airflow may itself be a function of a total pressure and temperature measurement.

Unique relationships cannot be identified for these parameters since their derivations are dependent on test cell configuration and geometry and calculation method. However, the importance of the total pressure and temperature measurements can be gauged by the size of the influence coefficients which can have a magnitude as high as 3 for a high by-pass ratio engine, for example, an uncertainty of 1% in inlet total pressure can lead to an uncertainty of 3% in net thrust. This indicates that, to achieve an uncertainty within  $\pm 1$  percent in the major parameters, pressures and temperatures must be known to uncertainties within  $\pm 1/3$  percent. This example only allows for errors in pressure and temperature and does not account for errors in other parameters which would be additive, giving even larger uncertainties.

In addition to the considerations of direct measured values above, measured engine performance often requires applied corrections using the inlet total pressure and temperature and exhaust pressure to determine the performance at specified altitude or sea level conditions. The necessity for corrections is usually due to the inability to set or reach the exact pressure and temperature required. These specific requirements are often needed for the demonstration of particular guarantee values for the engine around the flight envelope. These corrections normally make use of engine performance parameters called 'referred' quantities based on dimensional analysis.

Classical referred quantities are defined as:-

$$\delta = \frac{P_{T \text{ actual}}}{P_{\text{reference}}}$$

$$\theta = \frac{T_{\text{actual}}}{T_{\text{reference}}}$$

$$\text{Referred Pressure} = \frac{P}{\delta}$$

$$\text{Referred Temperature} = \frac{T}{\theta}$$

These classical referred quantities may be modified in some cases where empirical data indicate that a small variation in the classical exponent applied to  $\theta$  and  $\delta$  is warranted for a particular engine. Additional corrections are also required to correct separately for the variation in flight speed. These corrections are required for gross thrust for all flight conditions. For other parameters, this correction is needed only if the final nozzle or nozzles are unchoked. Corrections for this effect may be determined from empirical data, from analysis, or use of an engine performance computer simulation.

It is not only necessary to make accurate pressure and temperature measurements for the above correction considerations using the best measurement technology, but it is also necessary to know the shape of pressure and temperature profiles and gradients. In some test cases, corrections may need to be made to account for abnormal profiles or gradients which are not representative of in-flight conditions. This is an important factor when performance guarantees have to be demonstrated at a specified flight condition in a test facility. Correction factors can be derived from tests where the profiles for pressure and temperature can be controlled and the effects quantified.

#### 2.4.3 Engine Altitude Testing

##### 2.4.3.1 Inlet total pressure measurement

In simulated altitude testing, the upstream ducting usually contains some means of airflow measurement, for example a venturi or choked nozzle, which itself requires instrumentation probes and perhaps diffuser ducts which may cause unstable pressure distributions. Of course, these disturbance factors are minimised where possible and gauzes inserted to improve the pressure profiles at the engine entry plane if necessary.

Engine inlet total pressure is usually measured with the use of a multi-arm total pressure probe rake. The number of arms depends on physical size and each arm can contain a number of probes. The probes are normally positioned radially on each arm (spoke) so that they sample the

pressure in the centre of equal annulus (circumferential) areas.

In addition to the main pressure probe rake described above, sometimes boundary layer comb rakes, spaced circumferentially, but not necessarily at the same position as the main rake spokes, are installed in the inlet ducting. The spacing of the individual probes on a single comb usually sample equal annulus areas and if possible the innermost probes can be positioned to encompass the radial position of the outermost probe on the main rake. It may be found that these boundary layer comb pressure readings are unnecessary in the determination of mean duct total pressures if the main rake is already sampling the boundary layer pressure profile. However, it is better to install comb rakes as an insurance against the case where the boundary layer is not sampled by the main rake; the main rake will, in these circumstances, over-estimate the true mean total pressure. Figure 2.4-3 shows a typical array of engine inlet pressure probes in the inlet ducting for an altitude test cell.

#### 2.4.3.2 Inlet total temperature measurement

The gradients in total temperature in the inlet ducting for altitude engine testing are usually small, of the order of 2 to 3°C. Nevertheless, like inlet pressure, defined engine performance is sensitive to the accuracy of inlet temperature measurement. However, it is unnecessary to sample the duct area as comprehensively as in the case of total pressure. It is normal to install a small number of probes at varying depths of immersion from the duct wall and spaced circumferentially in such a position as to avoid interference with the pressure sampling system. Two different types of probe can be employed giving independent checks on the temperature reading (i.e. thermocouples and resistance bulbs). Figure 2.4-3 shows a typical array of total temperature measurement probes integrated with the pressure measurement array for an altitude test cell.

#### 2.4.4 Sea Level Engine Testing

A great majority of sea level engine testing facilities are built such that the engine is mounted on a stand in a building. The air to the inlet of the engine is fed through an opening in one side of the building and the engine exhaust is extracted via a diffuser through the opposite side of the building, see Figure 2.4-4. This type of installation leads to some air passing around the engine and therefore requires corrections to be applied to the measured frame thrust to obtain the true gross thrust. These corrections are:—

- (a) A ram drag correction
- (b) A pressure drag correction
- (c) An entrainment drag correction.

The ram drag is a momentum term caused by the engine itself acting as an ejector and inducing air into the building past the engine itself. The engine itself is therefore not in a true static condition.

The pressure drag is likewise caused by the same effect. All surfaces including the inlet flare, engine mounting, etc., are subjected to a pressure difference which must be accounted for in the thrust derivation.

The entrainment drag is again a momentum correction caused by the artificial increase in velocity due to the presence of the exhaust diffuser.

These cell corrections are sometimes determined empirically by a series of tests involving the same engine tested in the indoor facility being tested on an outdoor test

stand where the engine is subjected to a true static condition.

Alternatively, to evaluate these corrections by determining the various cell forces, several areas must be determined and pressure and velocity surveys must be carried out radially and longitudinally in the space surrounding the engine. It is also worthwhile testing the engine with varying distances between engine exhaust nozzle and the exhaust diffuser in order to evaluate the entrainment drag term.

#### 2.4.4.1 Inlet ducting

The inlet ducting for sea level static engine testing is usually short and profiled to minimise boundary layer growth. This characteristic gives a very flat pressure profile with negligible temperature gradient. The consequences of such characteristics is that pressure and temperature sampling in the inlet duct can be kept to a minimum. Obviously if deliberate distortions are being introduced to examine engine behaviour under these conditions then instrumentation standards outlined for the altitude testing should be adopted. Extensive instrumentation would also be installed if recirculation within the test cell chamber created temperature and pressure gradients in the inlet ducting.

In some sea level test facilities, particularly small engine facilities, it may be desirable to duct the engine inlet air direct to the engine inlet face from outside the building (see Figures 2.4-5 and 2.4-6). In this case the inlet ducting would incorporate an air mass flow measuring section which may require both total and static pressure measurements. In addition, the engine inlet total pressure and temperature should be measured at the engine inlet plane with suitably positioned instrumentation as described in the altitude engine testing section. It may even be desirable to instrument and calibrate the inlet ducting in a separate facility before installation on the engine test stand. In the case of other small engines, APUs or small project engines where the inlet ducting is necessarily of non-uniform shape, special rakes will need to be positioned such that mean total pressures can be determined. These types of installation are often accompanied by non-axial flows and the probes chosen for total pressure measurement will need to be less directionally sensitive.

#### 2.4.5 The design considerations for the total pressure and temperature sampling probes

The testing that involves either a complete powerplant or an individual component involves, not only expensive test plant, but also expensive test articles. The following factors need to be taken into account when probe design is considered:—

- (a) damage likely as a result of mechanical failure of a probe
- (b) blockage and flow disturbance
- (c) accuracy and reliability in the measurement environment
- (d) cost and ease of manufacture
- (e) ease of installation.

These factors will have to be given various degrees of priority depending on each individual application. The size of the probe may well be more important in the turbomachinery application than in the complete powerplant test. On the other hand, the mechanical strength will be more important in the engine case where the test article has a higher capital cost. Since the total pressure and temperature are commonly measured by pitot and

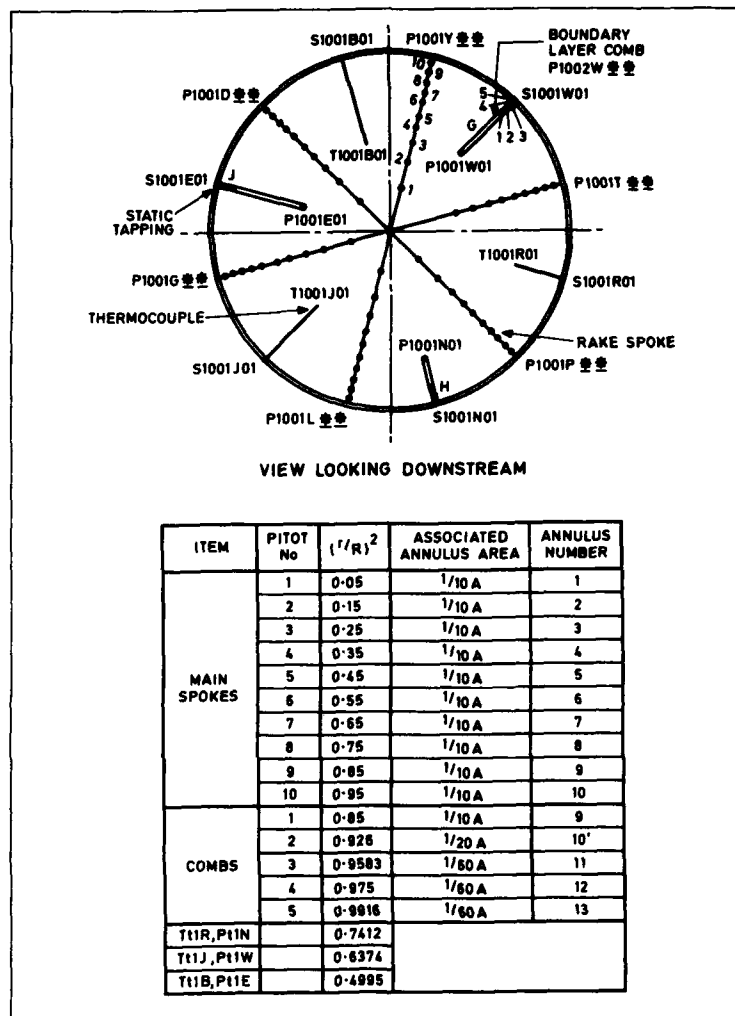


Fig. 2.4-3 Inlet duct instrumentation at engine inlet plane

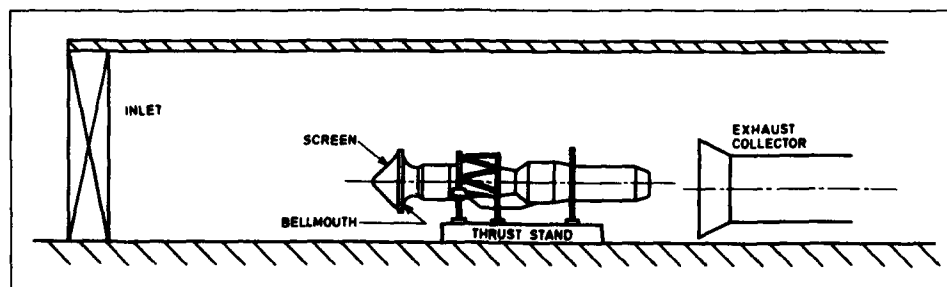


Fig. 2.4-4 Typical engine installation in a sea level test stand

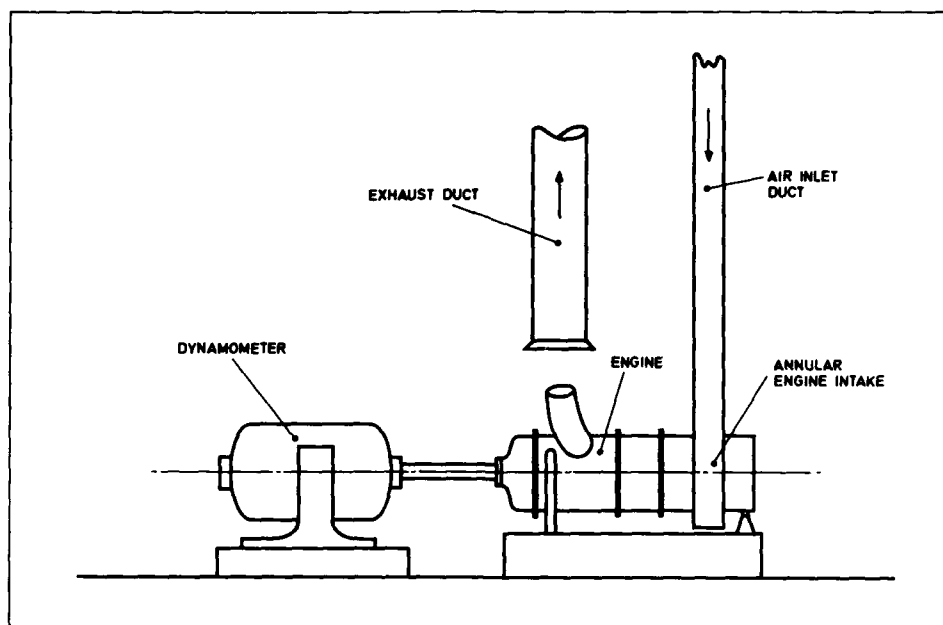


Fig. 2.4-5 Small turboshaft engine sea level test cell

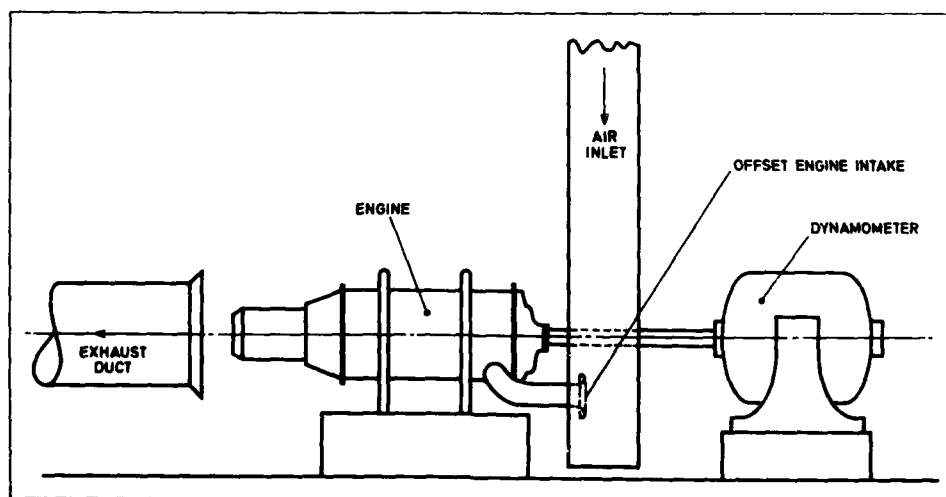


Fig. 2.4-6 Small turboshaft engine test cell

thermocouple rakes these design considerations apply not only to the probe, but also to the probe support. In some installations the probe support may well influence the design because of its need to carry multi-pressure or temperature paths which lead to a relatively large cross-sectional area.

#### 2.4.6 Inlet Static Pressure Measurement

In some applications, in particular mass flow measurement it is often required to measure the static pressure in the inlet ducting at some particular measurement plane. Static pressure measurement is in many ways more difficult than total pressure measurement. The main reasons for this difficulty arise from the effects of hole size, compressibility, hole edge form, upstream surface irregularities, flow incidence relative to the surface and hole inclination. The majority of these effects can be minimised by attention to detail in the manufacture of the static pressure hole and the surrounding surface area. The remaining effects must be avoided by careful positioning of the static pressure measurement so that flow irregularities are avoided and compressibility minimised. There are methods of correcting pressure for static hole size and these can be found in Reference 2.4-1 and 2.4-2. Having highlighted the care needed in each static pressure measurement the static pressure at a measurement plane should be sampled in several circumferential locations so that any variations can be accounted for in deriving the average.

#### 2.4.7 Exhaust Duct Pressure Measurement

The majority of simulated engine altitude testing and some sea level engine testing necessitate the engine to exhaust into some type of diffuser within an enclosed pressure chamber or building. Frequently the diffuser design is a compromise solution for the total possible engine airflow range. It is therefore possible for secondary flows (recirculation) to be generated within the pressure chamber or building. The derivation of the engine thrust requires the static pressure to which the engine is exhausting to be known accurately. If this pressure is influenced by the secondary flows then careful surveys of the engine exhaust pressure need to be made.

In addition, secondary flows can cause static pressure gradients to occur along the length of the engine and inlet ducting. In this case it is necessary to determine the external forces applied to the engine etc., in order to establish the true engine thrust. Static pressure measurements need to be taken adjacent to all surfaces which may contribute a pressure force to the engine thrust balance. The positioning of these probes can only be made after a careful audit of the particular installation being tested.

### 2.5 Intake

#### 2.5.1 Introduction

The purpose of an engine intake is to condition the freestream airflow so that it is acceptable to the inlet of the engine and to achieve this match with the overall minimum energy loss. The intake as an engine related component is only considered in this document in terms of testing in ground level facilities attached to the engine and not in a flight vehicle for flight testing purposes.

There is a wide variety of intake types and geometries, depending on the aircraft function. Military aircraft which generally have a supersonic speed requirement use a complex intake that might incorporate external and internal compression via mild shock waves to slow down and

compress the air efficiently. Subsonic civil transport aircraft are not subjected to such arduous flight conditions and can therefore use a simple pitot design.

Engine intake performance is usually explored in wind tunnels using extensively instrumented models and incorporating flow visualisation techniques. These tests will enable the performance to be defined over a range of incidence, forward speed and mass flow. It is not the intention of this document to identify the details of this type of test. However, engine development testing does sometimes include the total engine/intake combination and it is this type of test which is given consideration in the following sections.

#### 2.5.2 Intake performance definition

The intake performance related to a gas turbine engine is normally judged on the ram pressure recovery, for which the classical performance definition is:—

$$\eta_R = \frac{P_{T1}}{P_{AMB} \left( 1 + \frac{\gamma - 1}{2} M_i^2 \right)^{\gamma/(\gamma - 1)}}$$

The important pressure measurement in these equations is  $P_{T1}$  the engine face total pressure. Therefore in any test which includes the engine and intake, i.e. free jet testing of an engine/intake combination or a sea level test of an intake/engine behind a propeller, the engine face total pressure needs to be measured.

#### 2.5.3 Intake Pressure and Swirl Measurements

The design of the intake is often a compromise between ultimate performance and mechanical simplicity. In these circumstances the intake may well produce non-ideal pressure profiles at the engine face, particularly at off-design conditions. In order to obtain the true mean total pressure for the engine face throughout the flight envelope a comprehensive total pressure measurement survey is needed. The procedure is much the same as that described for the total pressure measurement in the test cell environment, see Section 2.4. However, the directional tolerance of the measurement probes should be considered in the case of intake testing. Alternatively, probes which determine flow angles may well be incorporated so that a mean total pressure can be derived from the measurements.

#### 2.5.4 Intake flow distortion

One of the most important departures of the intake flow from the ideal of uniform axial flow is the variation of total pressure across the engine face. The term applied to this variation is 'distortion'. Wherever the turbulence levels are low the total pressure distortion may be regarded as steady. Time variant (dynamic) distortion is not considered in this document since unsteady pressure measurements are not addressed here.

The steady state distortion of total pressure is characterised by measurements of the spatial non-uniformity of time averaged total pressure. Some degree of radial non-uniformity will always exist due to the presence of the boundary layer at the duct wall, but this can be neglected in most cases with respect to the effect on the engine rotating components. However, circumferential variations in total pressure can have a significant effect on compressor surge margins and therefore it is important to establish both the quality of the intake flow and the tolerance of the engine to

such flow non-uniformity. There is no universally adopted definition of a flow quality descriptor; some agencies use a definition based on intake sectors:—

$$\text{Distortion Coefficient} = \frac{P_{T1} - P_{Tn}}{q}$$

where  $P_{T1}$  = mean total pressure at engine face  
 $P_{Tn}$  = mean total pressure in the lowest pressure sector of the engine face, of angle  $\theta$   
 $q$  = mean dynamic head

The sector  $\theta$  must be of a significant size and  $60^\circ$  is a value often chosen. Other agencies use more complex descriptors which combine the circumferential and radial distortion factors. One such descriptor is:—

$$\text{Distortion Coefficient} = K\theta + b.KRAD$$

where  $b$  is a factor dependent on engine type and  $K\theta$ ,  $KRAD$  are respectively circumferential and radial factors based on total pressure measurements around  $n$  concentric rings with  $m$  equispaced points on each ring. The factors are defined as:—

$$K\theta = \frac{2}{mq \sum \left( \frac{1}{D_i} \right)} \cdot \sum \left[ \frac{1}{D_i} \left( \left( \sum P_r \cos \theta \right)^2 + \left( \sum P_r \sin \theta \right)^2 \right)^{1/2} \right]$$

$$KRAD = \frac{1}{q \sum \left( \frac{1}{D_i^2} \right)} \cdot \sum \frac{|P_r - (\bar{P}_r)_n|}{D_i^2}$$

$\theta$  is the circumferential location  
 $D$  is the ring diameter

References 2.5-1, -2, -3, -4 and -5 describe the various choices and implications of distortion parameters and should be consulted for further information. No further comment is offered here, but all distortion descriptors for intake flow quality are very dependent on the total pressure measurements at or near the engine intake face. Once again some degree of compromise in the number of probes may be necessary, dependent on scale and the particular distortion definition chosen. However, within these constraints the pressure instrumentation array should be selected to capture the extent of any low pressure region at the engine intake face and often the probes in the array are located at the centroids of equal area. It may also be possible to use engine inlet guide vanes, if these exist, as carriers for the total pressure probes necessary in a flow distortion investigation.

### 2.5.5 Special problems

If a particular engine installation has to be positioned in the wake of a propeller or propfan, then the intake itself may well be immersed in an airflow containing total pressure distortion and swirl. In these circumstances it may be necessary to survey the total pressure and temperature profiles of the air entering the intake as well as taking measurements at the engine intake face. In this way the actual intake performance can be measured. However, if the engine performance accounting includes the propeller/intake as one unit this degree of complexity will not be necessary. Small engines, APUs and small prop jet engines bring their own special problems in total pressure measurements. Their intakes are often non-uniform in shape, contain inertial separators for debris rejection, or are

ultra short with strange shapes. In these cases it is difficult to make specific recommendations, but special rakes may well have to be incorporated which need careful positioning and a large tolerance to directional flow. In these cases it is important to maintain the position, number and geometry of the probes throughout all phases of the intake tests, model, engine/intake and flight tests and to maintain the same accounting system.

### 2.5.6 Boundary layer measurements

The boundary layer may be quite large, particularly at subsonic flight speeds at high altitude, and may have a significant influence on engine performance. It is also important to identify areas of flow separation that might have been created by the upstream ductwork or for example by the intake at incidence etc.

In the above instances it is prudent to install total pressure sampling rakes for boundary layer measurements, incorporating the rakes with the engine face total pressure sampling system. Several circumferential positions should be allocated so that any non-uniformity is detected.

### 2.5.7 Static pressure measurement

It is often desirable in intake/engine testing to determine the mass flow rate at the engine face or at the total pressure measurement plane and a measurement of static pressure is required to fulfil this need. All the difficulties highlighted in static pressure measurement for engine inlet ducting in the section on Test Cell Environment apply equally well here and will not be repeated. However, the need to sample the static pressure at several radial and circumferential locations in the same plane as the total pressure measurement to obtain a good average value must be emphasised.

In addition it may also be desirable to measure static pressure profiles longitudinally along parts of the ductwork in order to help in the understanding of its performance or flow behaviour. The choice of position and the number of sampling holes is very geometry dependent and must be left to professional judgement.

## 2.6 Compressors, Fans and Associated Ducts

### 2.6.1 Introduction

This section is limited to a discussion of the measurement requirements for the determination of steady state overall (not interstage) aerodynamic performance of a compressor, with its associated ducting, for a high speed machine using air as a working fluid. Low tip speed machines and testing of specialist components (e.g. cascades) will not be considered. As well as recommending typical locations for instrumentation (Sections 4, 5 and 6 provide instrumentation details) special emphasis is given to those aspects of test procedures which lead to uncertainty in the levels of derived performance (see Section 3 for uncertainty analysis).

### 2.6.2 Engine vs Component Testing and Instrumentation Required

The decision as to whether or not the performance measurements should be made on an engine or a rig component will be dependent upon the objectives of the programme and the associated cost-effectiveness. The objectives will also define the type of test which could range from basic research, through a component development programme (in support of an engine project) to an engine

development exercise. These considerations will also establish the array of instrumentation required. A research test, for example, will probably require a comprehensive array of instruments to determine an absolute performance level, whereas an engine development programme could in many cases be carried out with much reduced levels of instrumentation. This is because in an engine development programme it is often sufficient merely to detect changes in performance resulting from small changes in unit configuration. Also because access for engine instrumentation is often limited and operational hazards usually impose further restrictions, rig testing usually forms a major item in support of an engine programme. However in this case a "rig to engine" performance correlation is sometimes required to provide adequate "read across" as it is seldom possible to completely establish the real engine environment. Thus with this type of testing it is highly desirable that, in addition to a comprehensive array of instrumentation, the engine instrumentation be also used on the rig. These latter aspects of Engine to Rig correlation are discussed in more detail in Section 2.1.1.

A typical arrangement for the location of instrumentation for the determination of overall performance of a split flow fan is shown in Figure 2.6-1. The wall static pressure tappings and the total pressure and temperature rakes at interconnecting and bypass duct exits will be required if the performance of those items is to be investigated and debited to the fan. A similar instrumentation of a core compressor is required and once again instrumentation of the upstream inter-connecting duct, bleed flow representation and combustion chamber entry diffuser may need careful consideration if those items are to be regarded as part of the core compressor. Thus the upstream and downstream limits of a component must be clearly defined and the instrumentation chosen so that a realistic measure of the component's performance between the two interfaces can be determined. For example, a total pressure rake placed downstream of a vane but outside its wake will not detect the real influence of the vane. In such cases rakes must be verniered through the wake, a "wake rake" or traversing must be considered. The types of instrumentation and the

density of sampling points are further discussed later in this document.

### 2.6.3 Factors Affecting the Uncertainty of Test Results

Considering the case of component testing it is essential that the rig geometry and environment simulate as near as possible engine conditions; otherwise, correction factors may be required to relate rig results to the engine. For research programmes similar problems arise when relating one compressor to another — often tested on different facilities.

Some of the aspects which should be considered are:—

- (i) Intake geometry effects on inlet and exit flow profiles (e.g.) flow distortions and boundary layer blockage produced by aircraft intake, propeller swirl, inter-connecting ducts, splitters, vanes, combustion chamber, etc.
- (ii) Compressor mechanical configuration (e.g.) blade geometrical tolerances, blade row stagger setting, tip clearances, surface finish, deterioration and erosion, rotor blade centrifugal untwist, etc.
- (iii) Parasitic losses, (i.e.) losses which are not recorded in flow path measurements (e.g.) disc windage.
- (iv) Secondary flow differences between rig and engine (e.g.) flows induced on centrifugal compressor back face, root well flow in axial compressors, cooling flows and leakages.
- (v) Heat transfer differences between rig and engine (e.g.) temperature gradient and soaking time effects on clearances, instrumentation system calibrations, etc.
- (vi) Spool interaction effects — compressors in series.
- (vii) Test Procedures (e.g.) Rig scale, pressure and temperature levels (i.e. Reynolds No. and specific heat effects), imposed by-pass ratio, bleed flows, humidity, etc.
- (viii) Rig-to-Engine differences in exhaust volume and its influence on flow stability and surge line.

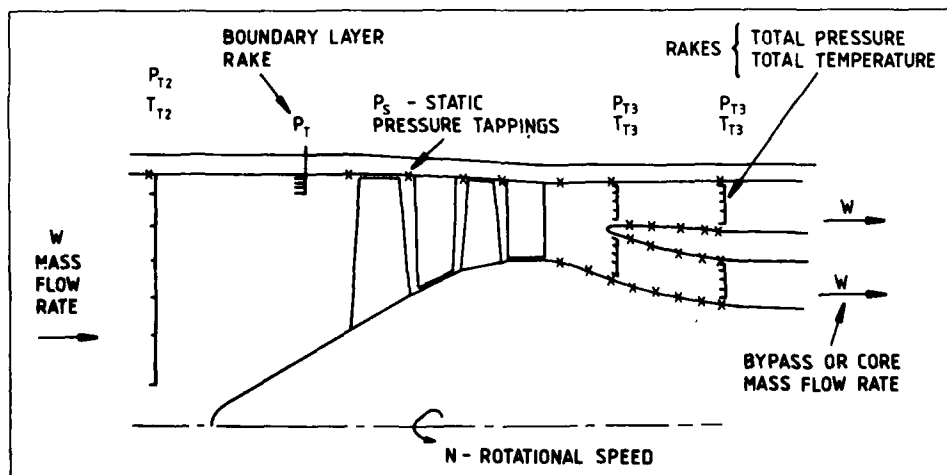


Fig. 2.6-1 Example showing typical locations of instrumentation for overall calibration

Many of these influences can only be minimised by ensuring that the rig configuration, environment and mechanical standard are an adequate representation of the engine. It is, however, an accepted procedure that all overall performance characteristics should be corrected for Reynolds number effects by one of the established methods (e.g. References 2.6-1 and 2.6-2). The method used and the base Reynolds number to which the results have been reduced must be quoted.

Although the above items can have very significant effects on the performance of a compressor, correction methods will not be discussed. It is, however, a requirement to select an instrumentation system and test procedure which is capable of determining regions and boundaries of unsteady flow (hysteresis, rotating stall, surge, etc.) and to quote all relevant mechanical features (e.g. instrumentation configuration, tip clearances, etc.).

#### 2.6.4 Definition of Performance Parameters

The parameters normally used to describe the overall performance of a compressor are:—

- (i) Pressure Ratio  $\frac{P_{13}}{P_{12}}$
- (ii) Mass Flow Function  $\frac{W_2/\sqrt{T_{12}}}{P_{12} A_2}$   
or  $\frac{W_2/\sqrt{T_{12}}}{P_{12}}$   
or  
Referred Mass Flow  $W_R = \frac{W_2 \sqrt{T_{12}/T_R}}{P_{12}/P_R}$
- (iii) Non dimensional speed  $\frac{N}{\sqrt{T_{12}}}$   
or  
Referred speed  $N_R = \frac{N/\sqrt{T_R}}{\sqrt{T_{12}}}$
- (iv) Efficiency-isentropic —  $\eta_{isen}$   
or  
Efficiency-polytropic —  $\eta_{poly}$
- (v) Bypass ratio —  $W_{bypass}/W_{core}$   
or  
Bleed ratio —  $W_{bleed}/W_2$
- (vi) Reynolds Number  $\frac{VL\rho}{\mu}$ , for axial flow compressors  
usually based on first rotor mid radius relative condition and characteristic length (L) (eg. blade chord)

The instrumentation arrays, averaging techniques, etc., for determining meaningful values of pressure and temperature to derive the above parameters are discussed in other sections of this document.

Compressors which have been designed for a uniform or a simple radially varying flow profile are normally required to be tested with imposed inflow distortions representing the environment which may occur at certain aircraft operating conditions. The representation of these flow distortions is usually achieved by placing a gauze (also called a screen) upstream of the compressor. A detailed measurement of the flow profiles throughout the unit can most readily be achieved by rotating the gauze in a series of steps which are related to the pressure and temperature rake configurations.

The parameters normally used to quantify the effects of inflow distortion and the methods used in analysis and presentation of results are not discussed here but are given in References 2.5-1 through 2.5-5.

The definition of the essential accuracy of the overall (final) parameters is not necessarily straightforward. The essential absolute accuracy (and related absolute uncertainty) for use in a performance specification or research test may need to be substantially higher than in development testing which could be carried out on a comparative (build-to-build) basis.

The derivation of efficiencies (isentropic and polytropic), from the pressure and temperature measurements requires careful consideration as various definitions have been proposed (and used). The three most commonly used definitions are based on (a) enthalpy of dry air, (b) constant specific heats at mean of inlet and outlet temperatures, (c) fixed specific heat ratio (e.g. 1.4); this latter method being regarded as normally inadequate.

The definitions of overall compressor efficiency (isentropic and polytropic) are given below.

#### Isentropic Efficiency

$$\eta_{isen} = \frac{\text{Isentropic enthalpy rise for measured pressure ratio}}{\text{Actual enthalpy rise for measured temperature rise}} \\ = \frac{H'_1 - H_2}{H_1 - H_2}$$

For constant specific heat ratio ( $\gamma$ ) this reduces to,

$$\eta_{isen} = \frac{T'_{13} - T_{12}}{T_{13} - T_{12}} \\ = \frac{T_{12}}{T_{13} - T_{12}} \left[ \left( \frac{P_{13}}{P_{12}} \right)^{\frac{1}{\gamma(\gamma-1)}} - 1 \right]$$

#### Polytropic Efficiency

$$\eta_{poly} = \frac{\text{Isentropic enthalpy gradient}}{\text{Actual enthalpy gradient}} \\ = \frac{dH'}{dH} = \text{constant throughout the compression} \\ = \frac{\ln(\text{actual pressure ratio})}{\ln(\text{isentropic pressure ratio})}$$

For constant specific heat ratio ( $\gamma$ ) this reduces to

$$\eta_{poly} = \frac{\ln \left( \frac{P_{13}}{P_{12}} \right)}{\ln \left( \frac{T_{13}}{T_{12}} \right)^{\gamma(\gamma-1)}}$$

The relationship between  $\eta_{isen}$  and  $\eta_{poly}$  for constant  $\gamma$

$$\eta_{isen} = \frac{(T'_{13}/T_{12}) - 1}{(T_{13}/T_{12}) - 1} = \frac{\left( \frac{P_{13}}{P_{12}} \right)^{\frac{1}{\gamma(\gamma-1)}} - 1}{\left( \frac{P_{13}}{P_{12}} \right)^{\frac{1}{\gamma(\gamma-1)/\eta_{poly}}} - 1}$$

The values of enthalpy and specific heat ratio can be obtained from standard data. It is recommended that efficiencies based on enthalpy be used as the alternative definitions can lead to erroneous results. Table 2.6-1 shows some typical values based on the three different definitions.

**TABLE 2.6-1**  
**Typical Examples Showing Effect of Alternative Definitions**  
**of Compressor Efficiency**

Efficiency Definitions	R	20	20	3	3
$T_{T2}$		288	488	288	388
$\Delta T_{21}$		441.3	682.8	120.0	158.6
Enthalpy	$\eta_{poly}$	90	90	90	90
	$\eta_{isen}$	85.4	85.7	87.5	88.4
Specific Heat Ratio at Mean Temp	$\eta_{poly}$	89.8	88.9	90.4	89.9
	$\eta_{isen}$	85.1	84.2	88.9	88.3
Fixed Specific Heats e.g. $\gamma = 1.4$	$\eta_{poly}$	92.1	97.8	90.1	91.6
	$\eta_{isen}$	88.3	96.7	88.5	90.2

### 2.6.5 Corrections to Flow Path Performance Parameters

In Section 2.6.3 a range of factors which can affect the perceived performance of a compressor were listed. Many of these can only be minimised by careful simulation of the test configuration and environment. However, there are some aspects for which established correction procedures should be applied or configuration measurements quoted. Typical examples of the magnitudes of the effects of these "corrections" are discussed below; a thorough "uncertainty analysis" should also help to quantify these effects.

Discrepancies in derived efficiency can be produced as a result of errors in the measured value (or derived average over a surveyed area) of pressure ratio or temperature rise. These errors are most pronounced in low pressure ratio units where a slight error in pressure ratio is reflected in a substantial error in derived efficiency (Figure 2.6-2). Similarly an error in measured mean temperature rise will also appear as an error in efficiency and will once again be greatest on low pressure ratio units (Figure 2.6-3). For rig testing, particularly of low pressure ratio fans, a torque meter could be considered as an alternative to the direct measurement of temperature rise. However, with torque meters several allowances (torque meter heating, bearing loss, disc windage, etc.) must be taken into account during data reduction and quantified through an uncertainty analysis. A torque meter is, however, often installed in addition to thermocouple rakes to provide an alternative source of temperature rise data. *Note:* When using a torque meter with split flow fans, or core compressors with bleed, it is necessary to provide a proper measurement of bypass or bleed mass flow and their temperatures so that an "accurate" value of the work done on each flow path can be derived from the reading of the single torque meter.

Another factor which can have a significant effect on compressor performance is Reynolds number because of its influence on the boundary layer (laminar, turbulent, transition and separation). The boundary layer will also be influenced by surface roughness. It is, therefore, important for those cases where tests are carried out at Reynolds numbers unrepresentative of the engine environment or where results are to be published at a reference Reynolds number that a correction procedure such as those of Reference 2.6-1 or 2.6-2 should be applied. It is important that the basis of the correction method be quoted with the published test results. An example of the magnitude of a typical Reynolds number correction is given in Figure 2.6-4.

Tip clearance, as indicated in Section 2.6.3, can also have a major influence on the performance of a compressor in terms of both efficiency and surge margin. A typical variation in efficiency with respect to clearance (as a percentage of blade span) is shown in Figure 2.6-5 (Reference 2.6-3). The clearances shown in Figure 2.6-5 are measured when the unit is "cold" and stationary. In many cases, clearance probes are installed to directly measure the running clearances as they will be different from the static values.

Tests with deliberately imposed inflow total pressure distortions are often a major aspect of a compressor test programme, but this type of testing requires special techniques and is beyond the scope of this document. This form of compressor testing has already been mentioned in Section 2.6.4 and further information is available in References 2.5-4 and 2.5-5. However, in testing with nominally uniform inflow an intake wall boundary layer will be present and the resulting profile should be measured (with a fixed rake covering this region) and its influence accounted for when presenting results.

### 2.6.6 Presentation of Results – Summary

The overall aerodynamic performance of a compressor should be presented using the parameters defined in Section 2.6.4 including a correction to a specified Reynolds number level. All instability boundaries (e.g.) surge and rotating stall should be defined.

In the case of split flow fans it is essential that tests be carried out at an appropriate level of bypass ratio and that these levels be quoted. The overall characteristics of both bypass and core performance should be presented separately and each based on the inlet condition of the appropriate stream tube. These pressure ratios and efficiencies may be plotted against the unit's total mass flow. An overall characteristic based on an average of both bypass and core section performance may be presented but this is somewhat limited in meaning.

In the case of core compressors all bleed flows must be properly accounted for and performance changes resulting from variable geometry (IGV and stator restagers) must be clearly identified.

Included in the presentation of results it is essential that an instrumentation layout, relevant test facility environment and test procedure be given. Other important mechanical aspects of the compressor itself, such as tip clearances and rotor blade untwists (while running) should also be provided.

## 2.7 Combustion Chamber

### 2.7.1 Introduction

Instrumentation requirements for combustion chambers are set to satisfy objectives to measure:

- combustor pressure drop
- combustor efficiency
- combustor pattern factor and radial profile shape.

The measurement problem is particularly difficult because of the exothermic chemical reaction and hostile temperature environment. Large gradients of temperature at the combustor discharge require that hundreds of measurements be taken. As a result, meaningful thermodynamic performance measurements are assigned to combustor rig tests rather than the engine.

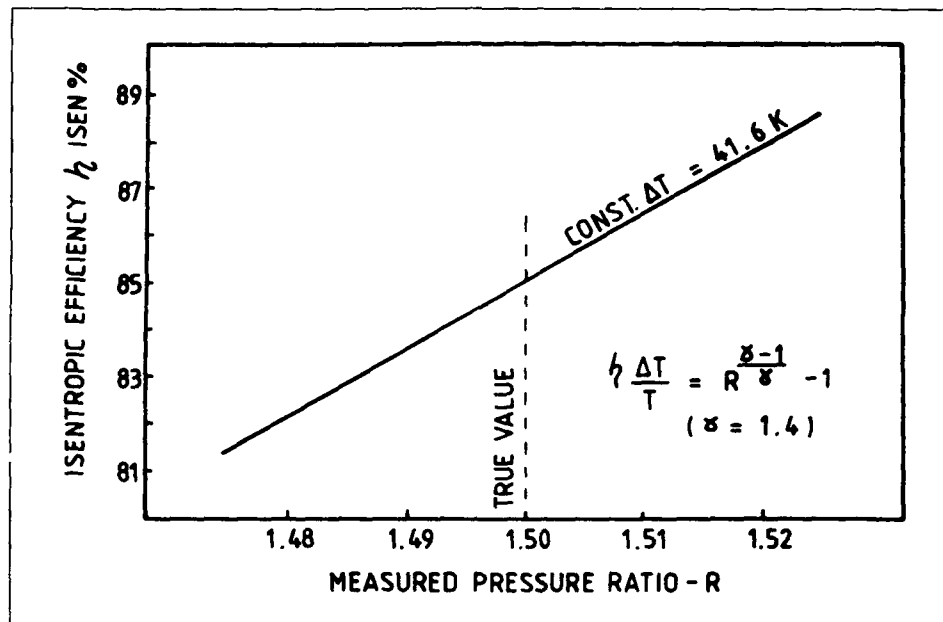
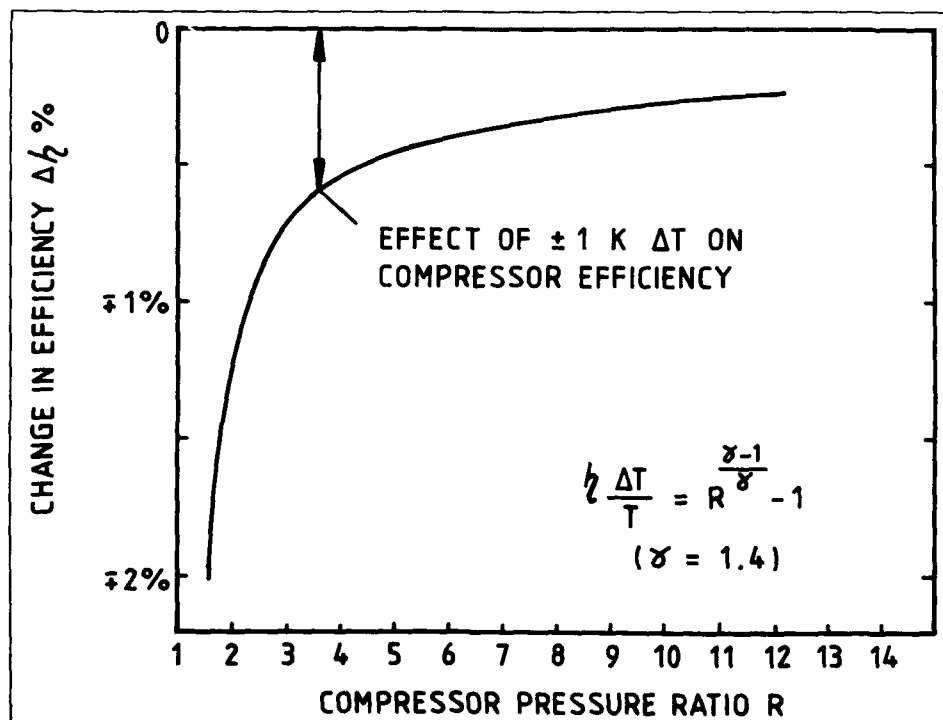


Fig. 2.6-2 Effect on derived efficiency of error in measured pressure ratio for fan

Fig. 2.6-3 Effect on derived efficiency of  $\pm 1 \text{ K}$  error in measured temperature rise

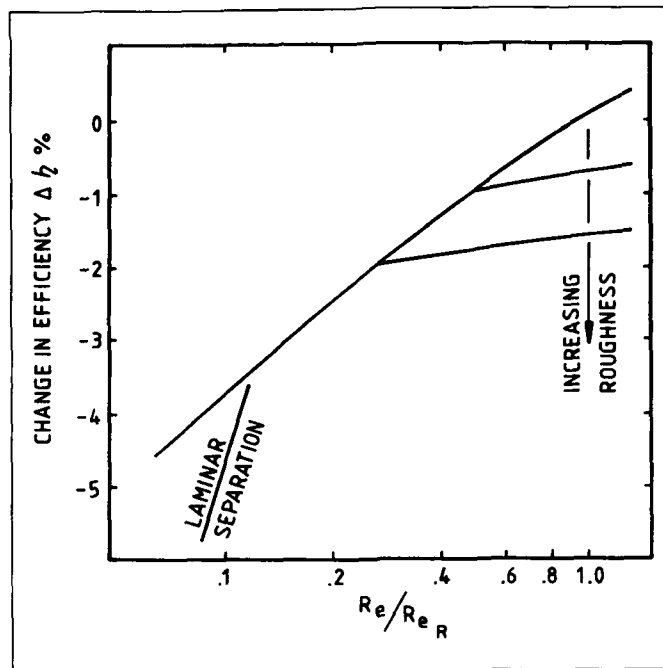


Fig. 2.6-4 Typical influence of Reynolds number and roughness on compressor efficiency

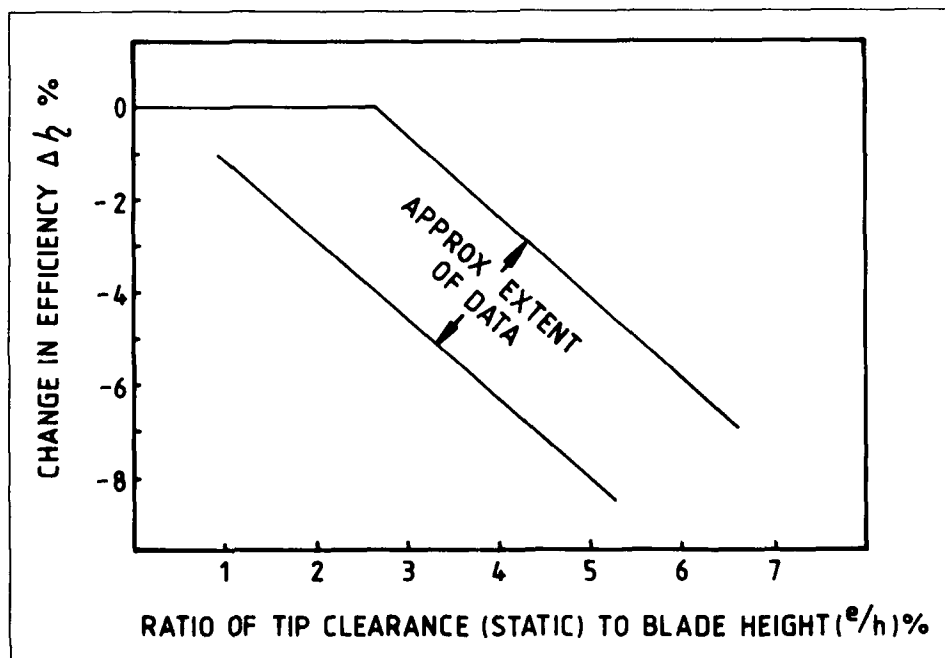


Fig. 2.6-5 Typical influence of tip clearance on compressor efficiency

### 2.7.2 Definition of Performance Parameters

- (i) Dimensionless Pressure Drop =  $(P_{T3} - P_{T4})/P_{T3}$
- (ii) Efficiency =  $\frac{\text{Actual Heat Release}}{\text{Theoretical Heat Release}}$
- (iii) Outlet Pattern Factor =  $\left[ \frac{T_{T4 \text{ Max}} - T_{T3 \text{ Av}}}{T_{T4 \text{ Av}} - T_{T3 \text{ Av}}} \right] - 1.0$

where  $T_{T4 \text{ Max}}$  is the maximum temperature measured by any probe

### 2.7.3 Combustor Inlet

Combustor inlet pressure and temperature measurement requirements are similar to those at compressor discharge. Probes should be aligned in the flow direction with negligible error up to  $\pm 10^\circ$  probe angle of attack. Rakes should be calibrated for recovery. Thermocouple wire with high sensitivity and good stability characteristics is recommended and the wire calibration should be obtained and checked. (See Section 6.3).

Several radial rakes, each having sufficient probe immersions to survey radial gradients are acceptable. Care should be taken to select the quantity and size of rakes so as not to create unacceptable blockage. Since the combustor inlet usually contains a diffuser and struts or simulated compressor outlet vanes, proper accounting for these parasitic losses (plus rake losses) must be made to book-keep combustor inlet pressure. Wake rakes may be required to ascertain strut or vane discharge pressures. If inlet screens are placed in the flowpath to produce particular compressor discharge pressure and velocity profiles, they should be at least ten annulus heights forward of the rakes so that the profile is stabilized at the measurement plane. Combustor inlet rakes are illustrated in Figure 2.7-1.

Inner and outer wall static pressure taps should be placed on the walls at the plane of rake measurement. These taps allow the calculation of velocity and mass flow at the rake probe measurement locations. Static pressures along the diffuser walls should also be used to measure diffuser performance (static pressure recovery).

### 2.7.4 Combustor Discharge

At the combustor discharge, pressure and temperature measurement rakes are usually placed at the plane of the turbine nozzle vane inlet.

Combustor discharge pressure is usually fairly uniform in the circumferential direction since velocities are low and there are no large wake sources. As a result, a quantity of radial rakes that do not cause unacceptable blockage are normally sufficient to adequately survey combustor discharge pressure. The number of immersions on each rake must be chosen dependent upon the radial profile. Again, probes should be insensitive to angle-of-attack.

However, numerous temperature samples are needed in the circumferential and radial directions due to the large gradients created by discrete zones of burning. A circumferentially traversible rake system is desirable to survey the 100 to 200 circumferential and radial locations deemed adequate to define the average temperature and pattern factor.

Obviously, the thermocouples must be capable of surviving in the high temperature environment. Platinum-rhodium thermocouples are often used. The probes should be designed to minimize recovery, radiation, conduction, and convection errors. Calibrations and corrections should be made for these effects. To avoid catalytic reaction on the thermocouple at low temperatures, a coating (such as aluminium oxide) should be applied.

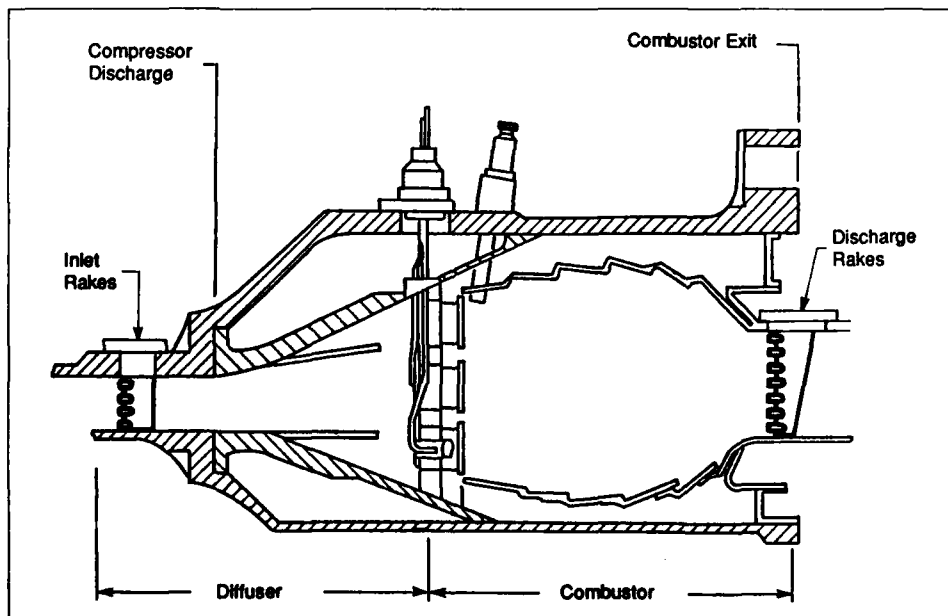


Fig. 2.7-1 Combustor performance instrumentation

Thermocouples can be designed for relatively slow response since readings are steady state. However, if traversing is employed, a fairly quick (3 second or less) time constant should be a goal to minimize stabilization time between the many readings required to survey the combustor discharge.

Inner and outer wall static pressure measurements are also required on several locations around the circumference to allow velocity and mass flow calculations to be made at the rake locations. See Figure 2.7-1 for instrumentation locations.

Combustor airflow and fuel flow must be accurately measured. Gas sampling is often made as a check on combustion efficiency. Special probes are designed for this, but their requirements are beyond the scope of this document.

## 2.8 Turbines and Associated Ducting

### 2.8.1 Introduction

This section is limited to a discussion of the measurement requirements for the determination of the aerodynamic steady state performance of a turbine. Blade cooling will not be considered except insofar as the cooling flows affect the main gas path performance measurements.

The problems associated with turbine testing, instrumentation and data reduction are in many ways very similar to those of the compressor and therefore the reader is referred to Section 2.6 of this document.

### 2.8.2 Engine vs Component Testing and Rig Configuration

Ideally it would be preferable to carry out all turbine performance measurements on an engine as the real

working environment would exist. However, there are serious difficulties in making detailed measurements in an engine and relating these measurements to results from other experiments. Some of these difficulties are:—

- (i) Inability to operate the turbine over a wide range of conditions
- (ii) Provision of low blockage, robust probes capable of withstanding the harsh engine environment and capable of providing high accuracy measurements
- (iii) Limited access and the difficulty of determining and defining mean stable conditions at the interface planes
- (iv) Inability to accurately measure and make proper allowances for cooling and leakage flows or to determine other parasitic losses which do not show up in the main flow path measurements
- (v) Problems in the direct measurement of mass flow rate and shaft power
- (vi) Cost and limited availability of development engines.

As with compressors the extent of the instrumentation and choice of test vehicle (engine or component test) will be dependent upon the objective of the investigation. An engine test may be required for development purposes or to demonstrate the potentially attainable performance levels, whereas component testing could be carried out on a turbine module extracted from an engine programme ("engine parts rig") and adapted with minimum modification for testing on a cold flow test facility. A typical layout of an engine parts rig is shown in Figure 2.8-1. A major requirement in an "engine parts rig" test is that the engine geometry and environment is simulated as nearly as possible.

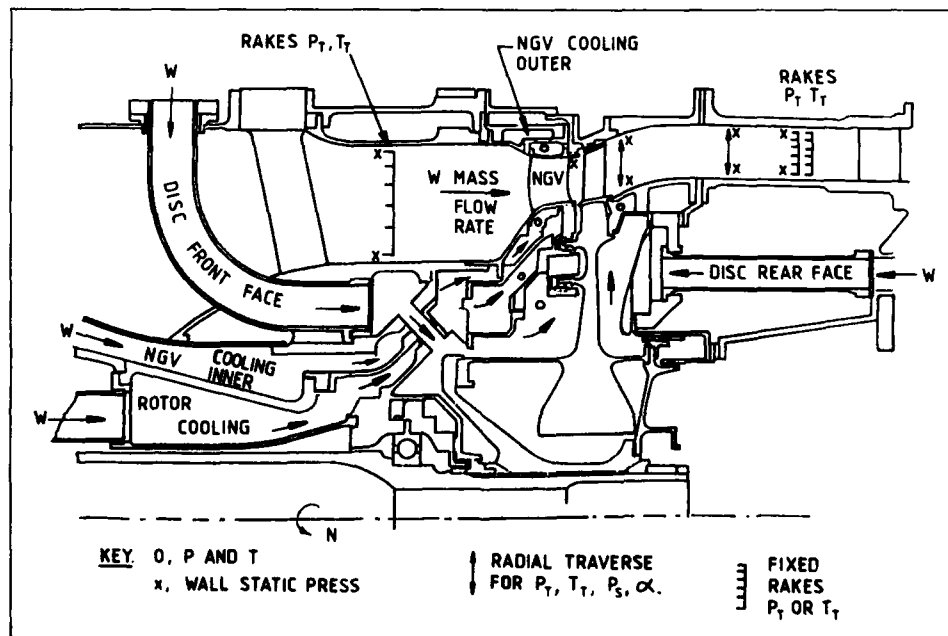


Fig. 2.8-1 Engine parts turbine — typical location of instrumentation for overall calibration

One of the purposes of such tests could be the determination of the influence of cooling flows on overall turbine performance or the development of a "rig to engine correlation".

Alternatively, component testing (to establish fundamental technology) could be carried out on an idealised cold flow turbine model in which the representation of cooling flows, for example, is not attempted. A typical cold flow model turbine is shown in Figure 2.8-2 and a typical arrangement of a single shaft test bed is shown in Figure 2.8-3.

The performance measurements made on a so-called ideal turbine rig, an engine parts rig and on an actual engine test can be significantly different. It is not unusual, for example, to see differences of the order of 1 to 2 percent in efficiency between ideal and engine part rigs or between engine part rigs and actual engine tests. In spite of these problems of relating model turbine test results directly to an engine, considerable resource is devoted to model turbine tests due to the large cost advantages resulting from testing at lower temperatures, pressures and rotational speeds which permits the use of simplified constructional methods.

### 2.8.3 Definition of Performance Parameters

The aerodynamic performance of a turbine is usually presented in terms of:—

- (i) Pressure ratio —  $P_{14}/P_{15}$
- (ii) Mass flow function —  $W_4\sqrt{T_{14}}/P_{14}$
- (iii) Non dimensional speed —  $N/\sqrt{T_{14}}$
- (iv) Specific work function —  $\frac{H_4 - H_5}{T_{14}}$
- (v) Isentropic efficiency  $\eta_{\text{isen}} = \frac{H_4 - H_5}{H_4 - H_5'}$

Efficiency is also sometimes defined as:

Isentropic efficiency  $\eta_{\text{isen}}$

$$\eta_{\text{isen}} = \frac{T_{14} - T_{15}}{T_{14}} \times \frac{1}{1 - \left(\frac{P_{15}}{P_{14}}\right)^{1/\gamma-1, \gamma}}$$

Where  $\gamma$  is taken at the mean of the inlet and outlet temperatures and for the appropriate gas composition.

The total pressures and temperatures, required above, can be derived in several different ways and as a result uncertainty can be introduced into the derived performance parameters. The main methods in use are as follows:—

- (i) *Inlet*  
Total temperature, measured directly,  
Total pressure, measured directly  
OR derived using wall static pressure, mass flow, temperature, area (etc.,) (i.e.) continuity.
- (ii) *Exit*  
Total temperature, measured directly,  
OR derived from torque meter/dynamometer and measured mass flow.  
Total pressure, measured directly by fixed instrumentation or by traverse,  
OR derived from wall static pressure and measurements of mass flow (including allowance for bleed flows),

derived or measured temperatures, flow angle and area with allowances for blockage of instrumentation, etc., (i.e.) continuity).

Note: If a torque meter or dynamometer is used either allowances must be made for disc windage, bearing or other similar losses or, that these losses are representative of engine conditions and are thus debited to the turbines aerodynamic performance.

Clearly a wide variation in apparent overall performance can result through the use of the alternative methods of deriving the basic performance data. Currently there seems to be no consensus of opinion as to which of the methods is the most meaningful; the accuracy will depend upon the relative standards of instrumentation, the correction factors used and the type of turbine being investigated. The factors to be considered when selecting the instrumentation details and configuration are discussed in the following sections of this document (Sections 3, 4, 5 and 6).

Hence as it is not possible to recommend a preferred practice it is therefore very important with any turbine test to fully describe the instrumentation, correction factors and the methods used for determining the performance characteristics.

### 2.8.4 Corrections to Flow Path Performance Parameters

In addition to the problems mentioned in the previous section related to obtaining the basic pressure and temperature data there are other aspects of turbine performance assessment which need to be considered when attempting to simulate a realistic test environment. These additional problems arise because of:—

- (i) Close coupling of combustion chamber and nozzle guide vane assembly and the associated pressure and temperature profiles
- (ii) Difficulties simulating the engine entry and exhaust duct geometry and other environmental and geometric aspects in a rig turbine
- (iii) Allowance for radial variation of swirl and pressure and temperature profiles at entry to an LP turbine rig
- (iv) Differences in heat transfer effects between the rig and engine components
- (v) Difficulties in representing, measuring and accounting for cooling flows including the effects of unrepresentative temperature differences between cooling flow and main stream
- (vi) The effects of variation in specific heat between a hot engine and cold flow rig tests resulting from differences in gas composition, dissociation, temperature level, condensation Reynolds No etc.
- (vii) Other parasitic losses and leakage flows which do not show up in flow path measurements
- (viii) Difficulties of obtaining measurements and quantifying the effects of the mechanical standard of the unit, e.g. surface finish, running tip clearance, etc.

Perhaps one of the most difficult items to represent are the cooling flows which can be ejected either from the blade tip, blade surface or trailing edge. The effects can be considered from two points of view. The first involves the effect of the assumption regarding how much of the potential work in the cooling flow is recovered and thus its contribution in the determination of efficiency. The second involves the

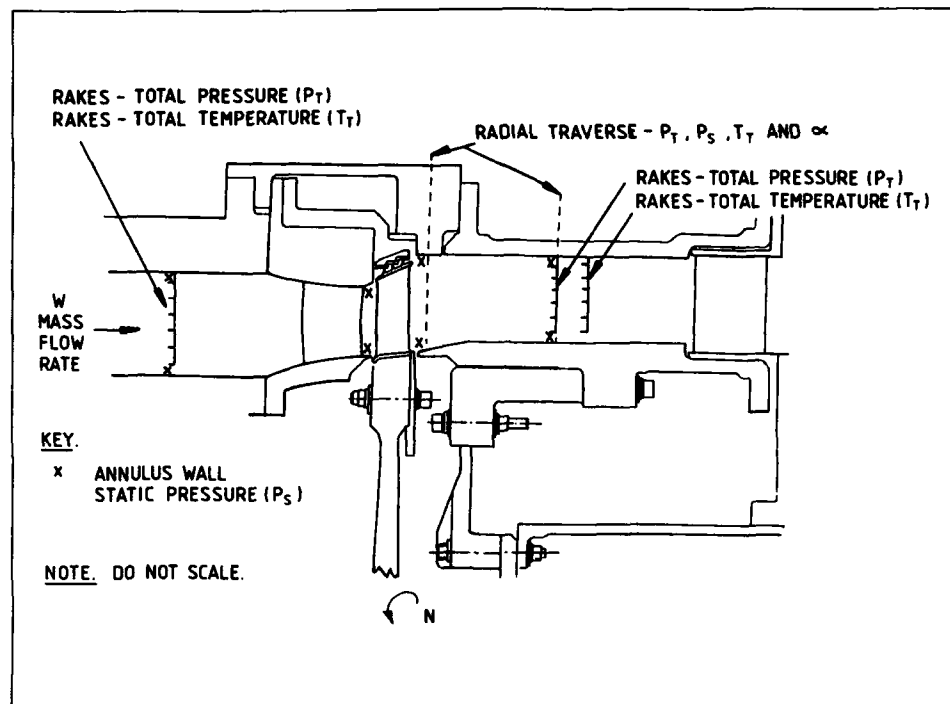


Fig. 2.8-2 Model turbine — typical locations of instrumentation for overall calibration

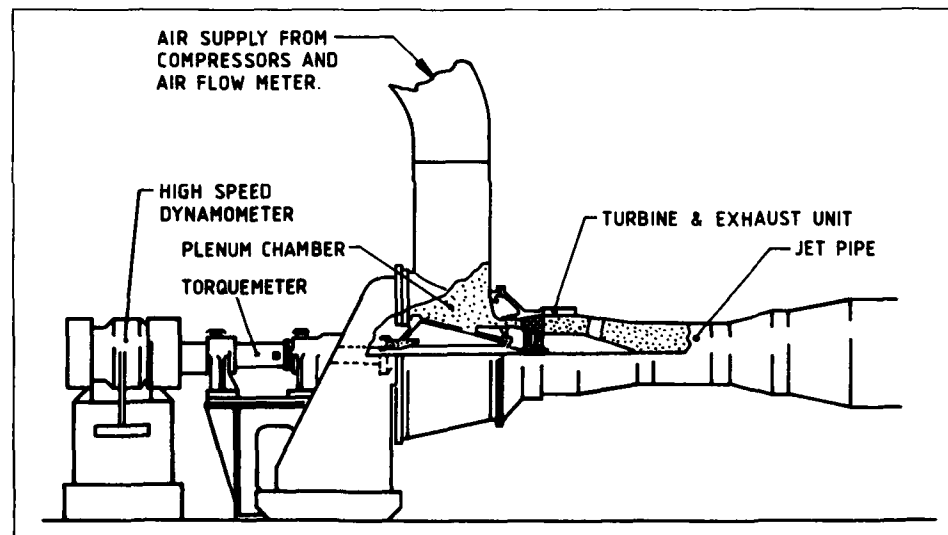


Fig. 2.8-3 Typical arrangement of single shaft test bed

influence of cooling flows on the behaviour of the boundary layer of the blade. Also in component testing consider the case of endeavouring to represent a cooled engine turbine, in which up to 15% of the flow leaving entered as cooling air. Hence if an engine condition was to be investigated on an idealised model turbine (without cooling flows) then certain allowances may need to be made, for example, to the blade profile, throat area, trailing edge thickness, etc., to simulate the cooling flows and establish realistic blade row matching.

In the case of LP turbine component testing a set of variable inlet guide vanes may need to be incorporated to simulate the flow conditions at entry which would be generated by an upstream HP turbine.

At turbine exit a representative exhaust system, in place of a parallel exit measuring section, may be used if the performance of the exhaust duct and its effect on the turbine is to be investigated. The performance of the exhaust system is normally defined using a pressure loss function:

$$\frac{P_{T5} - P_{T6}}{P_{T5} - P_{S5}} \quad \text{OR} \quad \frac{P_{T5} - P_{T6}}{P_{T5}}$$

with the appropriate allowance for swirl.

Testing of a combined HP and LP turbine system on a two shaft test facility requires a matrix of test conditions and these need careful considerations if a representative range of operating points is to be selected. This type of rig may also be required with an LP turbine which has no inlet stator.

As with compressors the influence of Reynolds number is important particularly in terms of efficiency and for this reason all turbine test data should be measured and quoted at Reynolds numbers as close as possible to those of the engine operating point. If, however, testing has been carried out at an unrepresentative Reynolds number any correction method used should be clearly described. Note: the Reynolds number in turbines must be related to some reference condition and a characteristic dimension such as, for example, last blade row relative conditions and axial chord at mid radius.

### 2.8.5 Presentation of Results — Summary

The overall aerodynamic performance of a turbine should be presented using the parameters defined in Section 2.8.3. The objectives of the programme will establish the type of unit, (engine, engine parts rig or idealised model turbine) on which the measurements are to be made and also the possible form and layout of the instrumentation and methods of deriving basic pressure and temperature information. For example, temperature drops through the turbine can be measured directly or derived from torque meter or dynamometer and, as a consequence, a relatively large degree of uncertainty in the recorded value could be introduced. Many other aspects such as the difficulty of representing and accounting for cooling flows can also add to the uncertainty in the perceived aerodynamic performance of the turbine.

It may be possible to minimise some of these uncertainties in development testing by carrying out back to back testing in which only differences in performance are required following small changes in turbine geometry or cooling flows, etc.

Because there are several methods in use for deriving pressures and temperatures within a turbine, and it is not possible to determine which procedure gives the most

meaningful result, a preferred practice cannot be recommended. It is, therefore, essential that, when presenting results, the rig environment, instrumentation system, data reduction and analysis methods are fully described. Also, as with compressors a description of the mechanical standard of the unit must be provided.

Details of possible configurations for pressure and temperature instrumentation are discussed in later sections of this document.

## 2.9 Afterburner

### 2.9.1 Introduction

Pressure and temperature instrumentation requirements for afterburners are set to satisfy performance objectives to measure:

- Dry operation pressure drop
- Reheat operation pressure drop
- Efficiency

Development of afterburners also involves stability, emissions, lightoff, and blowout characteristics, but these are beyond the scope of this document. The measurements of thrust, airflow and fuel flow, while critically important to the measurement of afterburner performance, also are not addressed within the scope of this document.

Afterburner development is primarily accomplished on engine tests since performance and operability characteristics are so dependent upon the flow conditions from the turbine, ducting, and/or mixer upstream of the afterburner. Rig testing is usually accomplished in a new engine program prior to engine availability so as to properly size the afterburner, properly position its flame holders, and allow confirmation of the basic design. Fine-tuning of performance should be accomplished on engine tests.

### 2.9.2 Definition of Performance Parameters

Dimensionless Pressure Drop =  $(P_{T5} - P_{T7})/P_{T5}$

$$\text{Efficiency} = \frac{\text{Actual Heat Release}}{\text{Theoretical Heat Release}}$$

Where the actual heat release is derived from:

Thrust  
Mass Flow Continuity  
or a detailed exhaust gas profile integration.

### 2.9.3 Afterburner Inlet

At the afterburner inlet plane, total pressures and temperatures are usually measured with radial rakes as illustrated in Figure 2.9-1. The probes should have good recovery over a wide angle of attack. The quantity of rakes may depend upon the engine configuration. For a simple turbojet engine where only exhaust gas from the turbine enters the afterburner, profiles are usually consistent around the circumference, such that fewer rakes are needed. In the turbofan, where a mixer is employed to mix the turbine and bypass duct gases, more rakes may be required to assess the less uniform environment. Total pressure and temperature sensors are sometimes attached to the spraybars to better sample the circumferential variations. Sometimes spraybars are removed to allow rakes to be installed to better define the circumferential flow field. Wall static pressure measurements are also required to properly calculate the average momentum weighted flow conditions, and to provide a check that the diffuser is flowing full.

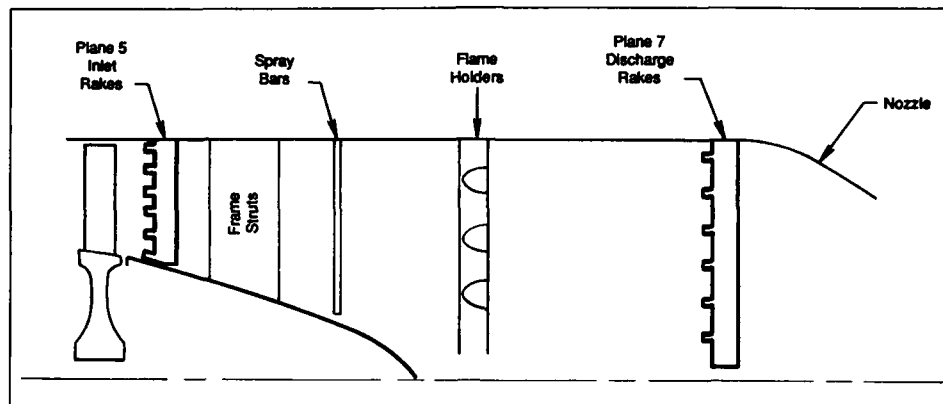


Fig. 2.9-1 Afterburner performance instrumentation

#### 2.9.4 Afterburner Discharge

At the afterburner discharge, measurements should ideally be taken at the nozzle throat. Since this disrupts the nozzle performance, instrumentation may be installed in an adapter ring which is inserted between the afterburner and the nozzle, moving the nozzle aft. It is important to maintain the effective volume of the afterburner up to the rake plane because this volume defines the residence time for the combustion process.

Since the temperature level is so high at the plane of measurement (upwards of 1700°C or greater), total pressure should be measured with water cooled, copper-tipped rakes. However, it is most difficult to measure temperature in this environment. For this reason, gas sampling is recommended to deduce the temperatures at the various probe locations within the stream. By analysing the chemistry of the gas sample, the temperature, enthalpy, and velocity can be calculated at the probe locations. The average heat release can then be calculated by integration of the local gas properties measured within the annulus. Alternatives are to deduce average stream properties and heat release from a continuity solution or a thrust solution, eliminating the need for gas sampling measurements.

Radial rakes are recommended for the total pressure and gas sampling measurements. Each rake should contain several measurement immersions. Rakes should be spaced so as to sample behind and at equal increments between the flameholder spokes. Wall static pressures are required to provide (along with total pressure and temperature) enough information to calculate mass flow and velocity at each probe location.

### 2.10 Propelling Nozzle

#### 2.10.1 Introduction

The primary functions of an exhaust nozzle are to provide a desired match of the engine components and to convert the engine exhaust energy into thrust in an efficient manner.

There is a wide variety of nozzle types in use, depending on the requirements of a particular engine type and application. When the engine has more than one flow stream such as in a turbofan, a nozzle is required to properly match each stream. Commonly used types of exhaust systems include

coannular, compound, and compound-mixer nozzles as illustrated in Figure 2.10-1. These nozzles can have fixed or variable convergent or convergent-divergent geometry.

The purpose of this section is to address recommended pressure and temperature instrumentation practices relative to determination of nozzle performance as an engine component. The scope of this section covers nozzle component performance measurement in both rig and engine testing.

#### 2.10.2 Nozzle Parameter Definition

Nozzle performance is typically presented in terms of maps or coefficients, depending on the type of nozzle involved. With either method, pressure and temperature measurements, along with flow, thrust, and geometric area measurements, are required to define a nozzle's performance. Figures 2.10-2 through 2.10-6 illustrate typical exhaust nozzle performance correlations.

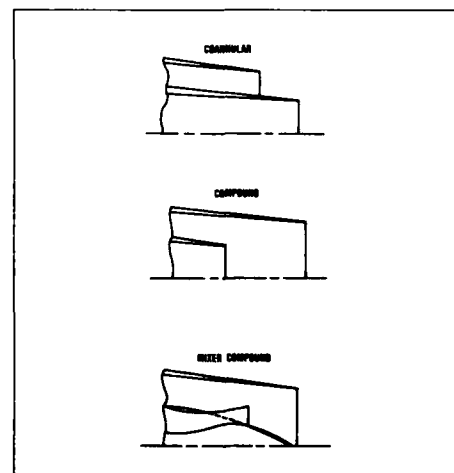


Fig. 2.10-1 Examples of exhaust systems for turbofan engines

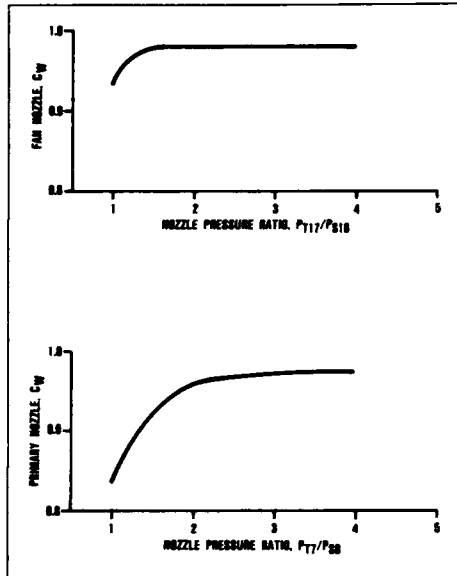


Fig. 2.10-2 Examples of coannular nozzle flow coefficient correlations

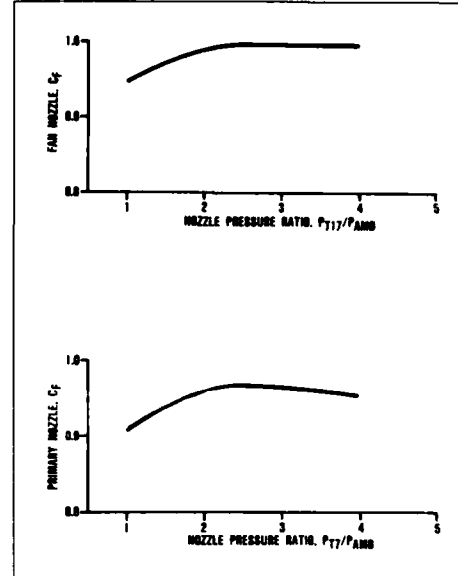


Fig. 2.10-3 Examples of coannular nozzle thrust coefficient correlations

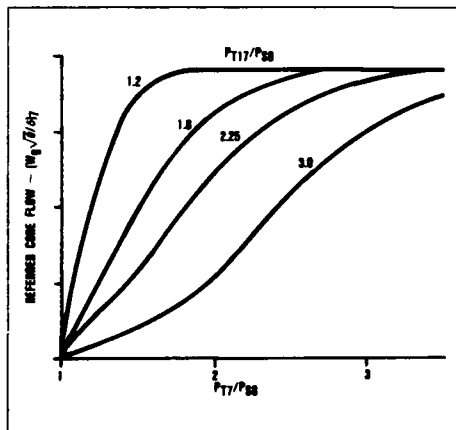


Fig. 2.10-4 Example of core gasflow correlation for compound and mixer-compound nozzles

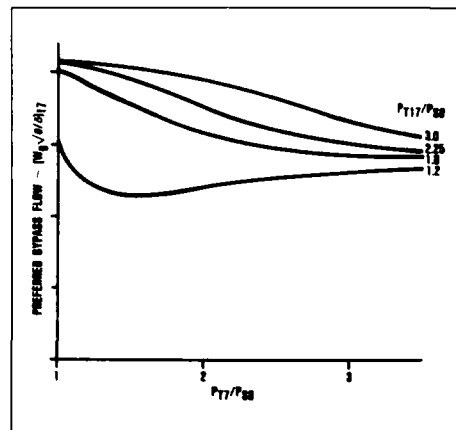


Fig. 2.10-5 Example of bypass airflow correlation for compound and mixer-compound nozzles

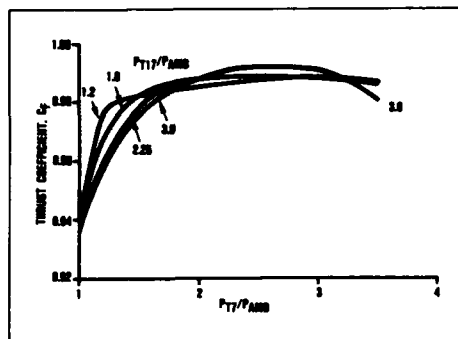


Fig. 2.10-6 Example of compound and mixer-compound nozzle thrust coefficient correlation

Nozzle coefficients typically consist of the following:

The thrust coefficient is defined as:

$$C_F = \frac{F_G}{F_{GI}} = \frac{\text{Actual Gross Thrust}}{\text{Ideal Gross Thrust}}$$

The discharge flow coefficient is defined as:

$$C_w = \frac{W_A}{W_{AI}} = \frac{\text{Actual Mass Flow}}{\text{Ideal Mass Flow}}$$

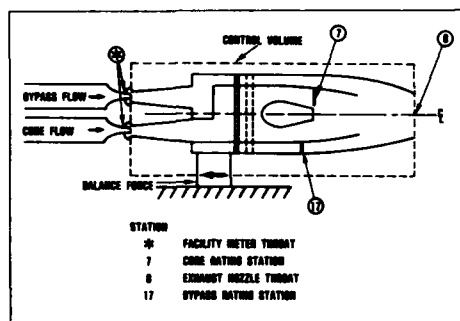


Fig. 2.10-7 Station notation for rig

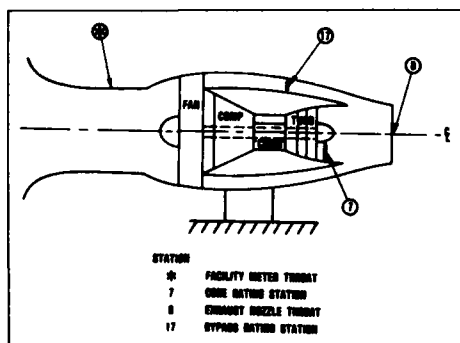


Fig. 2.10-8 Station notation for engine

The nozzle thrust and discharge coefficients are calculated with use of inlet total pressures and temperatures measured at the nozzle rating station. This is usually upstream of the nozzle exit for each flow stream (see Figures 2.10-7 and 2.10-8).

There is a variety of nozzle equations used to define the ideal nozzle flow and thrust. These equations basically differ in the amount of the deviation from ideal nozzle performance that is to be reflected in the basic equations and the amount that is to be reflected in the tested coefficients. This section presents examples of these equations to illustrate the need for pressure and temperature measurements to determine a nozzle's performance. However, this section is not intended to represent an in-depth treatment of the subject of nozzles.

The ideal thrust for each stream can be defined as:

$$F_{GI} = W_A \sqrt{\frac{2\gamma RT_T}{(\gamma - 1)g_c}} \left[ 1 - \left( \frac{P_T}{P_{AMB}} \right)^{(1-\gamma)/\gamma} \right] \quad (2.10-1)$$

This equation provides the ideal thrust, assuming isentropic expansion to atmospheric pressure. While this would require an ideal, infinitely variable exit area convergent-divergent exhaust nozzle to accomplish, this same equation is often used to calculate the ideal thrust for any type of nozzle, including plain convergent types.

The ideal mass flow for each stream can be defined by one of the following equations:

For unchoked flow for either convergent or convergent-divergent exhaust nozzles:

$$W_{AI} = \frac{P_T A_{throat}}{(P_T/P_{S,amb})^{1/\gamma}} \sqrt{\frac{2\gamma g_c}{RT_T(\gamma - 1)}} \left[ 1 - \left( \frac{P_T}{P_{S,amb}} \right)^{(1-\gamma)/\gamma} \right] \quad (2.10-2)$$

or

$$W_{AI} = \frac{P_T A_{exit}}{(P_T/P_{S,amb})^{1/\gamma}} \sqrt{\frac{2\gamma g_c}{RT_T(\gamma - 1)}} \left[ 1 - \left( \frac{P_T}{P_{S,amb}} \right)^{(1-\gamma)/\gamma} \right] \quad (2.10-3)$$

For choked flow for either convergent or convergent-divergent exhaust nozzles:

$$W_{AI} = P_T A_{throat} \sqrt{\frac{\gamma g_c}{RT_T} \left( \frac{2}{\gamma + 1} \right)^{(\gamma + 1)/(\gamma - 1)}} \quad (2.10-4)$$

where the flow is choked when the nozzle pressure ratio is greater than or equal to the critical (choking) nozzle pressure ratio (CNPR).

The ideal critical nozzle pressure ratio is defined for  $P_T/P_{S(throat)}$  as

$$CNPR = \left( \frac{\gamma + 1}{2} \right)^{\gamma/(\gamma - 1)} \quad (2.10-5)$$

For most practical exhaust nozzles for aircraft turbine engines, the actual critical nozzle pressure ratio deviates significantly from this ideal. For example, the actual critical pressure ratio for convergent nozzles is a strong function of nozzle geometry and often exceeds 3.

This definition holds for either convergent or convergent-divergent nozzles, since the pressure ratio is defined for conditions at the nozzle throat. For a convergent nozzle,  $A_{throat}$  and  $A_{exit}$  are the same and so  $P_{s_{throat}}$  and  $P_{s_{exit}}$  are also the same. For a convergent-divergent nozzle, the  $P_{s_{throat}}$  is usually calculated as a function of nozzle geometry and measured nozzle inlet total and exit static pressures.

It is sometimes useful to use the same definition of ideal nozzle performance for either convergent or convergent-divergent nozzles in terms of overall nozzle pressure ratio so that the differences in nozzle performance can be directly compared in terms of nozzle coefficients.

Please note that, in consistent SI units,  $g_c$  in the above equations is equal to 1.0.

To evaluate the nozzle thrust and flow coefficients, the measurements needed are  $P_T$ ,  $P_S$ ,  $T_T$ ,  $P_{s_{exit}}$ ,  $P_{AMB}$ ,  $A_{throat}$ ,  $A_{exit}$ , and  $W_A$ . The parameters  $P_T$ ,  $P_S$ , and  $T_T$  are measured at the nozzle rating station for each flow stream entering the nozzle.  $P_{s_{exit}}$  is measured at the nozzle exit. The actual mass flow ( $W_A$ ) is usually measured external to the nozzle through facility meter throats (see Figures 2.10-7 and 2.10-8).

### 2.10.3 Pressure and Temperature Measurement

Pressures and temperatures, for a given nozzle operating condition, are measured at the nozzle rating station by immersing total pressure and total temperature probes into the flow stream. If the pressure, temperature, and velocity profiles at the nozzle rating station are fairly uniform, then relatively few rakes and probes are required. However, since the stream conditions (total pressure and total temperature) for most engines are not uniform across the flow stream at the nozzle rating station, several instrument rakes with multiple area-weighted-probes are typically inserted into the flow stream to survey the flow conditions.

To determine the type of instrumentation needed, there must be some knowledge of the flow stream total pressure and total temperature profiles, and a knowledge of how the data is to be reduced. If there is a large variation in flow properties in the radial or circumferential directions, then the number of measurements and manner in which the data is to be reduced will have a pronounced effect on the errors associated with the calculated nozzle thrust and flow coefficients.

To calculate the nozzle coefficients, an average total pressure and total temperature for the flow stream must be calculated. This can be done by one of several averaging or weighting methods, including area, mass flow, and mass-momentum weighting. For uniform profiles, any one of the several averaging methods will give similar results. However, for non-uniform profiles, the method chosen could have a large impact on the value of the nozzle flow and thrust coefficients. A detailed analysis of several averaging techniques is presented in Reference 2.10-1.

If the prime objective of testing is to obtain component performance maps with which to calculate actual engine performance, then as stated in Reference 2.10-1 on page 153, "Thermodynamic cycle calculations by any of these pressure averaging methods will give correct final results (engine performance), provided the same method is used throughout the engine. However, the various component efficiencies will not be the same."

If the prime objective is to determine true component performance for comparison between rig and engine test data and to estimate engine thrust from rig derived coefficients, and the nozzle pressure, temperature, and velocity profiles at the nozzle rating stations are not uniform, then the averaging technique chosen is very important. Of the several different methods presented in Reference 2.10-1, mass-momentum averaging of pressures (Dzung's method) and mass-flow averaging of temperatures are recommended for non-uniform profiles.

Since the flow ( $W_A$ ) related with the flow stream property ( $P_T$ ,  $P_S$ , or  $T_T$ ) at the point of interest must be known to calculate the weighted properties, the parameters  $P_T$ ,  $P_S$ , and  $T_T$  must be measured at the same location. As a result, it is recommended that dual element probes ( $P_T$  and  $T_T$ ) be used to measure the flow properties. Instrumentation rakes should be placed in locations where there is minimal duct curvature and the static pressure is essentially constant across the flow stream. In this case only the hub and shroud need to be instrumented to measure the static pressure. If the instrumentation must be located where there is significant curvature, then tri-element probes ( $P_T$ ,  $P_S$ , and  $T_T$ ) should be used to obtain an accurate flow profile definition.

The engine test will present the worst case for both radial and circumferential variations in the flow properties; therefore, test instrumentation needs to be defined relative to actual engine flow conditions.

The number of rakes and probes per rake needed to define the flow stream is dependent on the flow stream distortion. Flow stream distortion will vary for each type of engine and will depend on strut locations, oil cooler location, burner configuration, etc. To determine the required number of rakes and probes per rake, a survey of the flow stream profiles should be conducted. A study can then be made to determine the required number of probes and rakes which will provide uncertainty levels that are acceptable. The procedure to determine sampling error is clearly outlined on page 12 of Reference 2.10-1 under "Sampling Error". To determine the allowable uncertainty for each parameter ( $P_T$ ,  $P_S$ , and  $T_T$ ), the individual contributions of each parameter to the uncertainty of the nozzle coefficients must be determined. The method for determining this uncertainty contribution is outlined in detail in Reference 2.10-1 on page 10 under "Error Evaluation". The uncertainty method is essentially based on Reference 2.10-2.

It is difficult to specify an acceptable level of uncertainty because the instrument rakes disturb the flow by creating blockage and a total pressure loss. There is a trade-off in terms of measurement accuracy and flow disturbance. There is also an increase in testing complexity and cost with an increase in the number of measurement probes and rakes.

Instrumentation for small engines requires special consideration since space becomes a problem and the desired number of area weighted dual element probes cannot always fit on a single instrument rake. In such a case, single element probes may be used or the number of probes per rake may be decreased. This results in an unavoidable decrease in measurement accuracy.

### 2.10.4 Sample Case

A sample case to illustrate the requirements influencing instrumentation selection and the uncertainty analysis of

tested flow and thrust coefficients for a particular nozzle system and instrumentation definition is presented in Section 8. This example shows the effect of the uncertainty of each measured parameter on thrust and flow coefficients.

#### 2.10.5 Engine vs. Isolated Nozzle Testing

Engine testing is required to confirm full scale nozzle performance, and engine cycle match. In order to properly compare data from engine testing with the result of isolated nozzle testing, the nozzle rating station should be at the same location relative to the nozzle exit for both cases. The instrumentation used to measure the nozzle performance in both the rig and engine should also, if possible, be the same. This eliminates the need for a correction for instrumentation differences. In addition, differences in the aerodynamic and thermodynamic properties of the nozzle working fluids are usually present between engine testing and isolated nozzle testing. Accounting of differences in properties such as gas swirl, wakes from rakes and struts, gas composition, nozzle Reynolds number, nozzle leakage, and non-one-dimensional pressure and temperature profiles should be included in the comparison. The schematic of Figure 2.10-8 illustrates typical rating station locations for an engine test.

To arrive at the ideal nozzle performance for a turbofan engine, the core and bypass flow split must be determined (individual gas flows through the core and bypass). The total airflow into the engine inlet is usually measured with use of a calibrated bellmouth inlet or venturi section. The flow split is sometimes determined by use of a flow calibrated instrumented measurement station in each flow stream, but it is also commonly determined by semi-empirical means. Two common empirical methods for calculating the flow split are: (1) Use of an energy balance of the complete engine system to determine the ratio of bypass-to-core flow, or (2) use of a calibrated HP turbine flow function to determine the core flow and subtraction of this flow from the total flow rate to determine the bypass flow.

#### 2.10.6 Thrust Reverser and Afterburning Nozzles

##### 2.10.6.1 Thrust Reverser

The nozzle coefficients for a thrust reversing nozzle in its stowed configuration are defined in the same manner as for a conventional nozzle. Therefore, the instrumentation for a thrust reverser nozzle in its stowed configuration should be defined in the same manner as for a conventional nozzle. Instrumentation recommendations for a thrust reverser nozzle in its deployed configuration are beyond the scope of this document.

##### 2.10.6.2 Afterburner

The instrumentation for an afterburner nozzle can be defined in the same manner as for a conventional nozzle. Measurements are taken at the individual flow stream rating stations upon which the nozzle coefficients are based. For the dry mode, the individual flow streams are typically considered to be mixed at the throat and a pressure loss from the nozzle rating stations to the nozzle throat is applied to the mixed flow stream. The nozzle coefficients are then rated on the basis of the mixed properties at the nozzle throat. For the afterburner on, or 'wet' mode, the rating station measurements, in conjunction with the friction, mass, and heat addition effects, are used to calculate the mixed properties at the nozzle throat. The nozzle coefficients can then be expressed in terms of the mixed flow stream properties at the nozzle throat.

Therefore, for both the dry and wet modes, the overall nozzle performance is typically defined by use of both a pressure loss from the nozzle rating station to the nozzle throat and the nozzle coefficient obtained from full scale or model tests.

In some applications, the nozzle rating station is downstream of the afterburner. In this case, the nozzle is treated as a simple, single-stream convergent or convergent-divergent nozzle. In some cases, a specially designed rake has been used to directly measure pressures at the nozzle throat.

#### 2.10.7 Summary of Recommendations

- The instrumentation for the nozzle rig and engine should be common and the nozzle rating station for each test should be at the same location.
- The instrumentation should be defined for the conditions of the engine since this will constitute the worst case flow profile.
- For the typically non-uniform pressure, temperature, and velocity profiles found in most engines at the nozzle rating stations:
  - Each flow stream should be instrumented with rakes that have dual element probes, if space permits.
  - Instrumentation rakes should be placed in locations where there is minimum duct curvature and the static pressure is essentially constant across the flow path.
  - The data should be reduced using mass-flow weighting to determine the average stagnation temperature and mass-momentum weighting to determine the average total pressure.
- For a non-typical case of very uniform pressure, temperature, and velocity profiles at the nozzle rating stations, the use of single-element probes and area weighting to determine the average total pressures and temperatures may provide satisfactory results.

#### 2.11 Component Testing in Engines

##### 2.11.1 Purpose

One of the advantages of the gas turbine engine is that the engine may be subdivided into a system of individual components. Thus, individual components may be developed on rigs and once they have demonstrated their individual design performances on their rigs, they should, theoretically, be expected to meet this same performance in the engine.

Quite often in practice, however, the component performance demonstrated on rigs is not achieved in the engine. This can be due to a variety of reasons which are discussed in Sections 2.6 and 2.8. Common reasons for this anomaly are that the engine component geometry or engine operating environment may not have been completely simulated on the rig, or an unknown problem needing identification and correction may exist in either the rig or engine hardware. Since it is the component performance produced in the engine that is paramount, it is necessary to obtain flow path pressure and temperature measurements in the engine in order to establish the performance of the components when operating in the engine environment. During a typical engine development program, there is usually concurrent testing of the same component configurations on rigs and in engines for purposes of cross-

checking both absolute levels and trends of component performance.

### 2.11.2 *Rig Versus Engine Instrumentation*

It is desirable that the rig instrumentation include, in addition to the normal rig instrumentation, a full complement of the instrumentation to be used in engines identified as "performance development" engines. Some performance development engines may have extensive flow path instrumentation, while others may include simpler and less intrusive instrumentation. However, the instrumentation should be sufficient to enable the identification of profile differences between the rig and engine. A common problem is that the large pressure, temperature, and flow angle variations associated with some components often require more flow path instrumentation for an adequate survey than is considered acceptable for most engine tests due to accessibility and flow path blockage considerations. In general, accurate pressure and temperature measurements are more easily obtained on component test rigs than in the full scale engine, since the rig is designed with instrumentation considerations in mind. More available space and better access to measurement planes are the primary benefits of the rig. Another advantage for the rig is that, in cases where aerodynamic similarity is used to simulate an operating condition and the aerodynamic forces are reduced, for example on a cold air turbine test rig, less sturdy instrumentation can be employed on the rig, resulting in less flowpath blockage.

### 2.11.3 *Rig-to-Engine Correlation*

Adjustments for measured component performance differences due to instrumentation differences between engine and rig may be developed from measurements conducted on the rig. In this process, the rig must include a set of "engine" instrumentation along with its more extensive rig instrumentation. The rig test data is reduced with use of both the engine instrumentation measurements and the more extensive rig instrumentation measurements. Correction factors are then developed from this information to apply to component performance measured during engine testing. This particular correction is only for the difference between rig and engine instrumentation, and in many instances, may not represent the most significant difference between rig and engine component performance.

The overall engine performance achieved represents the matched output of the system of individual components as they perform in the engine environment. Therefore, it is important that the rig simulate, as closely as is practical, the geometry and operating environment of the component as it operates in the engine. In the ideal case, this should include the simulation of component inlet profiles, secondary flows, running clearance, and geometry. The alternative to a complete simulation of engine environment on the rig is the development of a rig-to-engine correlation which reflects the differences in geometry and environment between the rig and the engine. As indicated previously in Section 2.8, it is not unusual for the component operating in the engine to demonstrate a different efficiency, typically lower than that demonstrated on the rig.

### 3. UNCERTAINTY ANALYSIS

#### 3.1 Introduction

The estimation of uncertainty is an essential requirement for all measurements. Without such an estimate, interpretation of the measurement may be difficult or impossible. In the measurement of turbine blade temperature, for example, an error of  $\pm 25$  K, may mean the difference between an adequate life prediction on the low end and early failure on the high end. Uncertainty of this magnitude is intolerably large to the blade designer and might reveal an urgent requirement for the development of improved measurement methods. This is also true for gas pressure and temperature measurements. Estimates of uncertainty can strongly influence the methods used to test engines and components and the interpretation of results. The evaluation of a design improvement can at times be totally

confounded by experimental error and lead to costly and time-consuming repetition of experiments which may be intrinsically incapable of resolving the effects sought.

During the last decade, a great deal of effort has gone into defining a methodology for the evaluation of measurement uncertainty by organizations such as the ASME, SAE, AIAA, ISO, the history of which is described in Reference 3-1 (See Figure 3-1 for the relationships between the principal documents covering this subject). In addition, AGARD Working Group 15 has applied uncertainty analysis in their evaluation of the Uniform Engine Test Program, UETP, which had as its objective the intercomparison of engine test facilities, Reference 1.2-1. In this report, a guide to the existing literature on the subject is given and the application of the methodology to the measurement of gas pressure and temperature will be

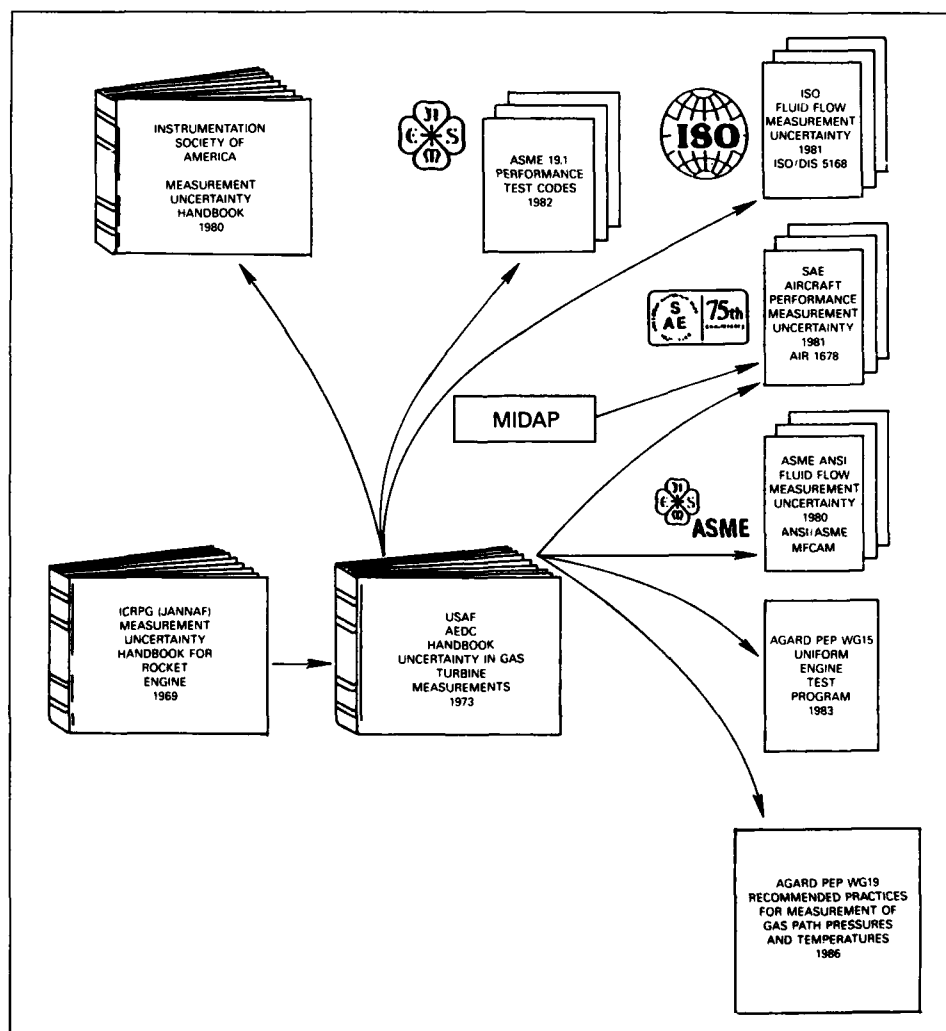


Fig. 3-1 Measurement uncertainty documents

described. Examples for specific measuring systems are described which include all sources of error and the method by which these individual errors are combined into an overall system uncertainty. The magnitude of the estimated uncertainty which is given in the sample cases (Section 8) is also intended to indicate the results that are achievable through the use of the measurement practices described.

### 3.2 Overview of Concepts and Definitions

The "Uncertainty of Measurement" is defined by the ISO as "an estimate characterizing the range of values within which the true value of a measurand lies" (Reference 3-2). An alternative definition is, "The maximum error reasonably expected for the defined measurement process."

The first step in the estimation of uncertainty is to prepare a carefully and completely defined description of the measurement process. This description must account for all of the basic measurement systems which will be used in the process, the test facilities, the test objectives, the sequence of tests to be performed, and the analysis or math models which will be used to combine and interpret the basic measurements.

In this document, two examples of uncertainty analysis are given in which the basic measurements are primarily gas pressure and temperature. One example involves the measurement of nozzle coefficients (Section 8.1). The second involves the measurement of compressor efficiency (Section 8.2). The latter case is covered briefly in ANSI/ASME PTC 19.1-1983 Part I, "Measurement Uncertainty," (Reference 3-3) and is also treated in detail for a particular compressor test in Reference 3-4.

More complex testing, such as determination of in-flight thrust (References 3-5, 3-6, 3-7, 3-8) or the comparison of engine test facilities (AGARD Uniform Engine Test Program, Reference 1.2-1), would require a more elaborate measurement process definition than is necessary for a single compressor test.

The simpler cases used in this document are intended to illustrate in more detail than has been done previously the uncertainty evaluation for tests in which the basic measurements are temperature and pressure only.

After defining the measurement process, the procedure for carrying out the uncertainty analysis is as follows (based on Reference 3-1):

- Analyse the formulas and data reduction by which the final answer will be obtained to determine what measurements must be investigated in the uncertainty analysis.
- Study the measurement systems and make an exhaustive list of all possible elemental errors, including calibration errors, data acquisition errors, data reduction errors, and any other errors which might affect each measurement.
- Obtain estimates of each elemental error and classify them into two categories depending on whether the error would be expected to vary at random or to remain fixed during the defined measurement process (see Section 5 of Reference 3-2 for more discussion on the categorizing of error sources). The magnitudes of the estimated errors should, insofar as possible, be based on actual data such as statistical analysis of calibration records, known least count of an A/D convertor, etc. Less desirable is the use of instrument

manufacturers' specifications since they cannot be expected to reflect the performance of the instrument in the environment of the defined measurement process. Least desirable, although sometimes necessary, is the use of estimates based on "engineering judgment."

The theoretical basis of the measurement which we have taken as an example is the comparison of the actual compression of the component with the ideal isentropic compression using as the definition of efficiency:

$$\eta = \frac{\Delta H'}{\Delta H} \approx \frac{(\bar{P}_{13}/\bar{P}_{12})^{\gamma-1/\gamma} - 1}{(\bar{T}_{13}/\bar{T}_{12}) - 1} \quad (3-1)$$

where  $\Delta H'$  = ideal enthalpy rise  
 $\Delta H$  = actual enthalpy rise

It is not sufficient to merely state these equations in defining the math model since they do not unambiguously define the experiment. For a more complete definition refer to Figure 3-2 which shows typical axial compressor characteristics.

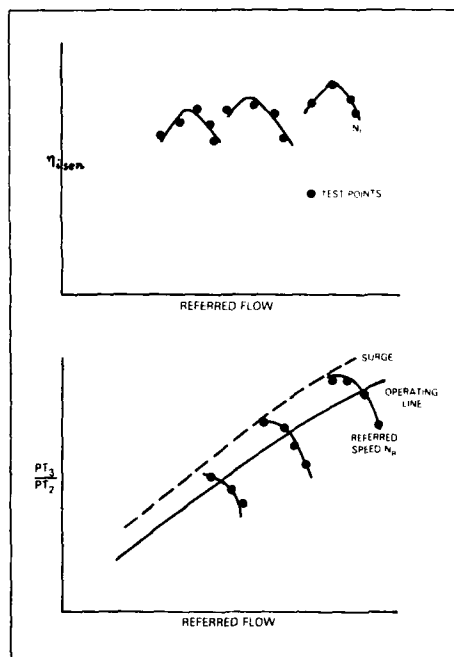


Fig. 3-2 Compressor characteristics

The definition of the experiment might then be as follows:

- Set an operating point (i.e. a referred rotor speed and a referred mass flow). Where:

$$NR = \text{referred rotor speed} = N/\sqrt{\Theta}$$

$$WR = \text{referred mass flow} = W/\sqrt{\Theta/\delta}$$

and  $N$  = measured rotor speed

$W$  = measured mass flow

$$\Theta = T_{12}/T_o^*$$

$$\delta = P_{T2}/P_o^*$$

To = ISO Standard Reference Temperature

Po = ISO Standard Reference Pressure

Note that the setting of the operating point involves a number of measured quantities, N, W, T, P, and defining mathematical expressions. All these quantities also have an uncertainty associated with them which must be included in the uncertainty model for the efficiency measurement.

- At each steady state operating condition (1), established by setting WR and NR, "record" the values of the  $(P_{T2i}, T_{T2i})$ ,  $(P_{T3i}, T_{T3i})$  required to calculate the station average total pressure and temperature upstream and downstream of the stage. The process by which this recording is made, i.e. the data acquisition process, must also be carefully defined since the test vehicle and its controls will have a tendency to drift slowly with time within limits determined by the control system design (or within the acuity limits of the particular operator if under manual control) and in addition the whole system will respond to changes in ambient conditions (temperature of duct walls, ambient wind velocity at the inlet, etc.). Ideally one might suppose that if all measurements were made at the same instant in time, small drift effects would not be an issue. This would be the case if there were no short time fluctuations due to steady state turbulence, blade passing and other non-steady effects, but these fluctuations are always present to some degree. Whether or not the elemental measurement systems respond to them depends on how these systems are designed. The usual strategy for steady state instrumentation is to design the system such that the elemental measurement systems have low-pass filtering properties that cause their outputs to be a time average over a short period in time. The filter characteristics are chosen such that the effect of turbulent fluctuations are eliminated but fast enough so that the system settles rapidly to a new value after a change in operating point. The filters are also intended to reject electrical noise above a frequency which also depends on the desired time response of the system. Note that the time average value so obtained may have to be further corrected in turbulent or unsteady flow (Reference 3-10) because of effects such as the term  $(\frac{1}{2}\rho v^2)$  in the formula:

$$\bar{P}_T = \bar{P}_s + \frac{1}{2}\rho \bar{v}^2 + \frac{1}{2}\rho \overline{v'(t)^2} \quad (3-2)$$

where the instantaneous velocity  $v(t) = \bar{v} + v'(t)$  and  $v'(t)$  is the time dependent velocity fluctuation.

Additional corrections may be necessary for momentum or airflow angle weighting effects associated for example with large fluctuations present in passing blade wakes. These corrections become another element of the math model for the test.

Most data acquisition systems do not read all of the parameters simultaneously but rather sequentially and in some cases are organized to read the same parameter more than one time in a single data scan. Obviously, then the data

\*If  $\gamma$  varies between station 2 and 3, these definitions may have to be expanded (see below).

acquisition extends over a finite period in time and can include redundancy, so another mathematical model which needs to be included in the overall uncertainty model is the scheme for converting the array of measured values in one data acquisition scan sequence into equivalent values at a selected instant in time. A wide variety of practices are used here ranging from the assumption that all values recorded during the scan sequence are effectively instantaneous through the use of selective scan sequences which tend to minimize errors due to drift. The most sophisticated schemes use redundant data acquisition in which the data analysis math model is designed to detect short-term and long-term drift and excessive scatter and also to eliminate outliers through either automatic or manual editing.

Equation 3-1 above is the principal equation which defines the math model portion of the defined measurement process. For this case it is, as the above discussion shows, not the only equation. The quantities  $P_T$  and  $T_T$  in this equation are not directly measured but are calculated from measurements since they are weighted, station averaged quantities. Consequently, the second portion of the math model for this case is the equation which relates the individual measured quantities to the spatial and time average at the station.

$$\bar{P}_T(i) = F[P_{Ti}(x_1, t_1), \dots, P_{Ti}(x_j, t_j)] \quad (3-3)$$

$$\bar{T}_T(i) = G[T_{Ti}(x_1, t_1), \dots, T_{Ti}(x_j, t_j)] \quad (3-4)$$

where  $\bar{P}_T(i)$  and  $\bar{T}_T(i)$  are space and time averages defined by the functions F and G of the measured quantities.

Each  $P_{Ti}(x_j, t_j)$  or  $T_{Ti}(x_j, t_j)$  is a single elemental measurement as obtained by a given probe located at  $x_j$  and recorded at time  $t_j$  by its associated measuring system while the system is at the  $i$ th operating point. The "reading" obtained is a function of operating point (NR(i) and WR(i)). It may also be a function of time as explained above and perhaps other interfering or modifying parameters as well (Reference 3-11). The test environment program and data analysis should be designed to detect and either eliminate or correct for dependencies of the elemental measured quantities on all parameters other than those which are under the experimenter's control. Such a test is said to be under well-defined statistical control. The post-test analysis of data then permits the overall uncertainty to be estimated as described later in this section.

A further element of the math model is the relationships by which  $\gamma$  is calculated in Equation 3-1.  $\gamma$  varies significantly with temperature and air composition, especially for combustion products, and the relationship used to compute the mean value for use in Equation 3-1 must be specified. Any uncertainties in this computation become bias errors in the final test results. This topic is discussed further in Section 2 of this report. The effects of the variation of  $\gamma$ , and also of the gas constant R, must sometimes be included in the definitions of referred rotor speed and mass flow. This is especially important in comparing turbine rig tests with the same turbine running in an engine.

The test specification includes a definition of the calibration procedures to be used. It should also describe the test itself. For our example, this would consist of a plan for the measurement of pressure and temperature at well-defined locations upstream and downstream of the fan at a series of fixed flow conditions and pressure ratios or rotor speeds. This series should include appropriate repetitive points designed to allow the disclosure of effects related to time or

changes in ambient conditions. The post-test analysis of the results can be carried out by the methods of regression and analysis of variance (Reference 3-12) applied to the experimental data as plotted in Figure 3-2.

Finally the defined measurement process must include a detailed definition of the elemental measurement systems [i.e. the systems which measure the  $P_{Ti}(x_j, t_j)$  or  $T_{Ti}(x_j, t_j)$ ], with a measurement uncertainty model for each. This topic is covered in some detail in Sections 5, 6 and 8 of this document. The methodology currently in use starts with three categories of measurement error as follows:

#### Calibration Error

Errors which arise at each step of the calibration hierarchy which establishes the traceability of the working sensor and the data acquisition equipment through working standards and laboratory standards to the national standards institution. The thermocouples (or RTDs) and pressure transducers in aerodynamic probes are traceable in this way.

#### Data Acquisition Error

Errors which arise from the data acquisition system, that is from voltmeter, signal conditioners, A/D converters, recording devices, etc.

#### Data Reduction Error

Errors arising from sources such as calibration curve fits, computer resolution, approximations in math models, computational models for obtaining of station average values from samples in space and time, etc.

In this report, we will treat each of these sources of error for pressure and temperature measurement systems plus, for purposes of clarity, we will add a fourth which we will call "errors of method\*," covering error sources which do not fit obviously into the above three categories. The important thing will be to identify all significant sources of error and then to describe how estimates can be made of the magnitude of this error.

#### Errors of Method

Errors arising from the use of particular probe and rake designs or from the test vehicle, test facility, or their environment. Examples are:

Probe Errors — uncertainty in radiation and conduction corrections, static pressure correction, blockage, stream line distortion, response to unsteadiness, etc.

Test Vehicle Errors — uncertainty in the operating condition, speed control, blade tip clearance, vane angle settings, etc.

Test Facility Errors — uncertainty in inlet flow profiles, duct area, leakage, bleed flow, etc.

For each error source, a "bias" and "precision" must be assigned which are measures of the uncertainty arising from that source.

The general definitions used in this error analysis are based on the material in The Measurement Uncertainty

Handbook (Reference 3-13). The basis of these definitions is the idea that the total uncertainty of any given measurement consists of a bias and a precision as shown in Figure 3-3. The precision is an estimate of the standard deviation which would be achieved in repetitive tests under the same conditions. The bias is an estimate of the difference between the mean of these repetitive measurements and the "true" value of the quantity being measured.

Each  $i_{th}$  error source in an elemental measurement has a bias ( $b_i$ ) and a precision ( $s_i$ ) associated with it. The magnitude of the individual errors must be estimated and then combined to form an overall uncertainty estimate. The two recommended methods for combining the individual errors are:

$$U_{ADB} = \pm (B + t_{95}S/\sqrt{N}) \approx \pm \sqrt{\sum_{i=1}^M b_i^2} + t_{95} \sqrt{\sum_{i=1}^M \frac{s_i^2}{N}} \quad (3-5)$$

or

$$U_{RSS} = \pm \sqrt{B^2 + \left(\frac{t_{95}S}{\sqrt{N}}\right)^2} = \pm \sqrt{\sum_{i=1}^M b_i^2 + \left(\frac{t_{95} \sqrt{\sum_{i=1}^M s_i^2}}{\sqrt{N}}\right)^2} \quad (3-6)$$

where  $b_i$  = bias, the fixed or systematic error associated with the  $i_{th}$  error source.

$s_i$  = standard deviation of the random error associated with the  $i_{th}$  error source also called the precision index).

$N$  = number of repetitions of the defined measurement process. (Note: this is not the number of measurements used to determine  $S$ , see  $t_{95}$  below and glossary.)

$M$  = number of error sources in the elemental measurement system model.

$t_{95}$  = parameter defining the 95th percentile point of the Student's "t" distribution. It depends on the sample sizes used to estimate the  $s_i$ . If all were 30 or more,  $t_{95} = 2.0$ . If various smaller sample sizes were used to estimate the  $s_i$ , then the Welch-Satterthwaite method (Reference 3-13) must be used to determine  $t_{95}$ .

The interpretation of the quantities  $U_{ADB}$  and  $U_{RSS}$  has been studied by Abernethy (Reference 3-1) using Monte Carlo methods (Reference 3-20) and is as follows:

$U_{ADB}$  = 99 percent of the time the true value is expected to lie within  $\pm U_{ADB}$  of the measured value.

$U_{RSS}$  = 95 percent of the time the true value is expected to lie within  $\pm U_{RSS}$  of the measured value.

The ranges  $\pm U_{ADB}$  or  $\pm U_{RSS}$  are frequently referred to as confidence intervals at the 99 percent or 95 percent level. They are also said to provide 99 percent or 95 percent "coverage" of the true value.

Where a final result is a function of two or more elemental measurements, the uncertainty of the elemental measurements can be combined into an overall uncertainty by the methods of error propagation (Reference 3-13). The method is based on use of the first derivative terms in a Taylor's series expansion of the derived quantity and the

\* Both RAE and AEDC use a fourth error category (References 3-14, 3-15) which they call respectively; "real effects" and "environmental/installation." The ISO Flow Standard, ISO/DIS 5168 Section 5.7 uses the term "errors of method" and this is the term we will use. AIR 1678 (Sect. 2.1.2) uses the term "Model Errors."

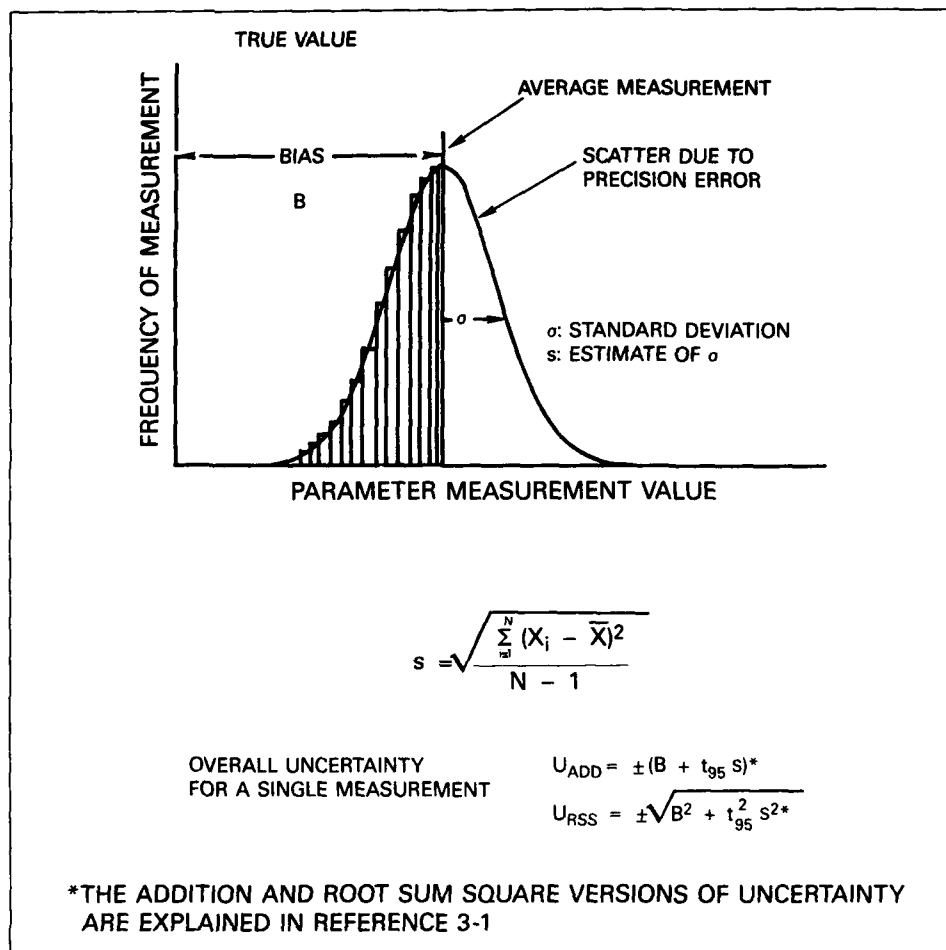


Fig. 3-3 Precision and bias

assumption that the uncertainty of the elemental measurements are mutually independent.

For example, given that compressor efficiency is defined from pressure and temperature measurements as in Equation 3-1 above, the result is as follows:

$$s_n^2 = \left(\frac{\partial \eta}{\partial P_{11}} SP_{11}\right)^2 + \left(\frac{\partial \eta}{\partial P_{12}} SP_{12}\right)^2 + \left(\frac{\partial \eta}{\partial T_{11}} ST_{11}\right)^2 + \left(\frac{\partial \eta}{\partial T_{12}} ST_{12}\right)^2 \quad (3-7)$$

$$B_n^2 = \left(\frac{\partial \eta}{\partial P_{11}} BP_{11}\right)^2 + \left(\frac{\partial \eta}{\partial P_{12}} BP_{12}\right)^2 + \left(\frac{\partial \eta}{\partial T_{11}} BT_{11}\right)^2 + \left(\frac{\partial \eta}{\partial T_{12}} BT_{12}\right)^2$$

The partial derivatives are frequently termed "influence coefficients" because they determine the relative importance of the elemental measurement uncertainty terms on the final result.

The dilemma in applying this methodology is in achieving a means for evaluating the ability of the elemental measurement system to measure the "true" value of the quantity since the true value is never known. The problem is

eased somewhat if an international standard exists for the measured quantity as is the case for length, mass and many other quantities. However, there are no standards for the fluid dynamic quantities  $P_T$ ,  $P_S$ , or  $T_T$  which are the subjects of this document. The elemental measurement system uncertainty model must include, based on the actual system hardware design, a measurement uncertainty hierarchy. This hierarchy has at its base the primary standard for the measurement and maps the sequence of calibrations or other evaluations which contribute to the overall uncertainty in the measurement of the physically, or aerodynamically, defined quantity which is the objective of the measurement.

To make this point clearer, consider the measurement of total temperature in a flowing gas which is not isothermal with its surroundings. This is the typical condition for the measurement in a gas turbine engine. Assuming the transducer is a thermocouple, a well-defined calibration hierarchy traceable to national standards organizations can be constructed for the thermocouple wire. The

thermocouple wire junction, however, cannot be expected to run at the gas stream total temperature and additional error sources must be physical effects that need to be made negligible or corrected for and the uncertainty in these corrections produces error sources. This is one of the sources of error which we refer to as errors of method. These error sources are described more fully in the section of this report covering temperature measurement and are extensively discussed in Reference 3-10. They include:

- Recovery — A measure of a probe's ability to adiabatically stagnate the flow. This is a function of Mach No. and Reynolds No.
- Conduction Corrections
- Radiation Corrections
- Yaw and Pitch Corrections
- Corrections for response to unsteady flow
- Corrections for catalytic effects (downstream of combustor)
- Probe blockage and streamline distortion corrections

A similar argument applies to the measurement of pressure. Available pressure standards apply to *stationary* gases. The extension of the pressure measurement to moving fluids is also described, for example, in Reference 3-10. A total pressure probe must recover essentially all the dynamic head whereas a static pressure probe must be completely insensitive to dynamic head. The probe and intervening tubing is essentially a fluid transmission line which transmits the fluid dynamic quantities  $P_T$  or  $P_s$  into a stationary gas pressure at the pressure transducer. The calibration of the pressure transducer is then traceable to international standards. Again, the sources of error are fully described under the pressure measurements section of this report but include such things as:

- Pressure recovery as a function of yaw and pitch
- Reynolds Number effects
- Mach No. effects
- Corrections for response to unsteady flow
- Probe blockage and streamline distortion corrections
- Static pressure tap geometry effects

The overall uncertainty analysis then consists of the following steps:

1. Estimating uncertainty prior to testing.
2. Post-test evaluation of uncertainty.

### 3.3 Estimating Uncertainty Prior to Testing

As described in the overview above, the "Defined Measurement Process" is the basis for all subsequent facets of the estimation of uncertainty. The generation of a defined measurement process is treated generally in References 3-1, 3-5, 3-7, 3-15. Taking a compressor test as an example, which is one of the two specimen cases presented in Section 8, we start with a Definition of Test Objectives as follows:

Determine the efficiency of a compressor at a fixed referred rotor speed at various pressure ratios. Vary the pressure ratios by throttling the flow downstream. The total uncertainty objective for the efficiency measurement is  $\pm 1.0$  percent at the 95 percent confidence level\*. Other elements in defining the measurement process are:

\*The trade-offs on uncertainty, credibility and cost are discussed in Reference 3-15.

1. Establishing a sequence of points and repeat points to be measured. Define all elemental measurements needed, including not only pressures and temperatures but rotor tip clearance, axial position, ambient humidity, rotor speed, pressures and temperatures related to mass flow, etc.
2. Identifying the criterion for setting the point, (i.e. limits and stability of rotor speed and mass flow, math model for correcting to reference ambient conditions).
3. Selecting the stations at which measurements will be made and the number of points to be sampled. A corollary to this is the documentation of assumptions or calculations of flow profiles and their uncertainty as well as assumptions about the treatment of the boundary layer. In addition, the math model by which station averages are to be calculated from point measurements must be defined.
4. Define the data acquisition strategy, (i.e. filtering and time averaging properties, scan sequence, use of in-scan calibration and confidence checks).
5. Select and document probe and rake designs considering especially response to fluctuations, blockage and flow distortion, conduction/radiation, recovery errors, and yaw and pitch response. In all cases this documentation will require information acquired by calibration of probes in a free jet or similar facility and calculations to predict effects not obtainable by measurement.
6. Define the calibration hierarchy for all elemental measurements and collect calibration history data necessary to define bias and precision errors for each step.
7. Combine with the calibration hierarchy, data acquisition, data reduction, and errors of method components to form the overall uncertainty model for each measured parameter. Note that errors of method include effects related to probe design as well as error sources due to the facility.

A fundamental requirement for the defined measurement process is the specification of bias and precision in the definition of this uncertainty model.

In deciding which error terms will be categorized as precision error and which as bias error, use the following criterion:

Any error sources which remain fixed throughout the duration of the test are counted as bias errors. This duration can be as short as a few minutes and can be as long as several months. The duration is an implicit part of the defined measurement process and is established by intervals defined for the key processes such as recalibration, reconfiguration, and reinstallation. Error sources which are expected to vary at random during the test are included as precision errors. Thus precision errors of transfer standards for example can be "fossilized" (Reference 3-2), as bias errors in the test if the standard is used to calibrate a working standard before the test and not again.

8. Specify the relevant math models which will be used to compute the end result, in this case the referred rotor speed, the airflow and station average pressures and temperatures, and finally the stage efficiency.

9. Propagate the elemental error, to determine the overall uncertainty of the measurement. The procedures for combining error including the effects of degrees of freedom, (i.e. number of independent measurements used to estimate each error source) and correlation coefficients are included in Reference 3-13. The result of this is the *pretest prediction of uncertainty* and can be compared with the test objectives. If the uncertainty is too great, several strategies exist for correction ranging from basic improvement in the measuring systems to increased use of repetitive measurements. The latter strategy reduces only the short-term precision error portion of the uncertainty by the factor  $1/\sqrt{N}$  where  $N$  is the number of test repetitions. Efforts to improve the basic measurement systems may be feasible; however, increased accuracy can be costly (Reference 3-11) and in some cases, may not be possible without major advances in measurement technology.

### 3.4 Post-Test Evaluation of Uncertainty

Once testing is in progress, the test data obtained should be subject to post-test uncertainty analysis. This is quite different from the pretest prediction in that it does not begin with the elemental measurement uncertainties but analyses the dispersion of the actual data obtained as a function of the controlled parameters. In the example of compressor efficiency measurement, the quantities  $P_{T3}/P_{T2}$ ,  $T_{T3}/T_{T2}$  and the overall efficiency would be calculated from the elemental measurements  $P_i$ ,  $T_i$ , etc., plotted against mass flow and speed and subjected to statistical regression analysis to determine the standard error of the estimate achieved. If the time interval over which the measurements are made is the same as the time interval implicit in the defined measurement process e.g., one test day, then the standard error or the estimate can be directly compared to the estimated precision. Obviously, if very little data is taken, valid statistical deductions cannot be made and the pretest uncertainty analysis is the best guide to actual uncertainty. In a well designed test this should not be the case. In our example, the data accumulated for each constant speed line would be subject to regression analysis. The dispersion around the mean line is then a measure of the precision achieved in the test and should be compared to the precision calculated in the pretest uncertainty analysis. It is very important to include statistical tests for normalcy (Reference 3-11) of the data since non-normal (that is, non-Gaussian) behaviour is a strong indication that some parameters of the test are out of control and shifting in a non-random fashion. If the data is normally distributed, wild points can be discarded by various outlier rejection criteria. If the post-test precision is larger than the pretest estimate, the dispersion of the data around the mean line can be subjected to analysis of variance in order to detect dependency on parameters that might be out of control. To do this, it is necessary to record at each data point as much potentially relevant information as possible such as date, time, facility configuration, ambient conditions and anything else which may interfere with or modify the parameters being measured.

A methodology for validation of data while the test is in progress is described in Reference 3-16, and a method for rapid computation of results is presented in Reference 3-17.

### 3.5 Combining Pretest and Post-Test Results

Ideally when the measured post-test precision and the pretest predictions of precision agree, one can conclude that the results being obtained in the test program are as good as one could expect to achieve with that particular set of instrumentation systems. When a significant difference exists between predicted and actual precision, it is indicative of a problem either with the measurement systems or the test vehicle and facility. The measurement systems can be either more or less variable than was estimated in the pretest prediction. The test vehicle and facility on the other hand can introduce unexplained variability if some parameters are out of control. These effects are frequently referred to as "Environmental Factors" and, if their magnitude can be estimated, they should be included with errors of method in the uncertainty analysis.

Notice, however, that the pretest bias prediction has not been eliminated and so the total uncertainty still includes the precision plus the bias. Although the bias with respect to the "true" value can never be known, it is possible, once agreement has been obtained between pre-and post-test precision in a given facility, to test bias differences between different facilities (Reference 1.2-1), between altitude and sea level tests (Reference 3-18), and between results obtained in individual component test versus results obtained with the same component in a full engine. Each of these tests for bias would require an uncertainty analysis based on a carefully defined measurement process and math model as outlined above.

In general, although the bias or systematic error with respect to the "true value" cannot be known, systematic error information can sometimes be obtained in practice via the following approaches (References 3-2 and 3-19).

- (a) Interlaboratory or interfacility tests make it possible to obtain the distribution of systematic errors between facilities.
- (b) Comparisons of standards with instruments in the actual test environment may be used. (Note again that, while this can be applied to measuring systems using stationary gases as a standard, there are no standards in flowing gases).
- (c) Comparison of independent measurements that depend on different principles can provide systematic error information. For example, in a gas turbine test, airflow can be measured with (1) an orifice, (2) a bellmouth nozzle, (3) compressor speed-flow rig data, (4) turbine flow parameters, and (5) jet nozzle calibrations. As another example, the efficiency of a turbine component can be measured by determining the real vs. ideal thermodynamics as in Equation 3-1 or by measuring shaft work (torque and speed) and the enthalpy change per unit time of the gas (i.e. mass flow and temperature change).
- (d) When it is known that a systematic error results from a particular cause, calibrations may be performed allowing the cause to vary through its complete range to determine the range of systematic error.
- (e) When none of the above are available, bias must be estimated by experienced experimenters.

#### 4. SPATIAL SAMPLING, PROBE ARRAYS AND DATA EDITING

##### 4.1 Introduction

The spatial distribution of probes within a flow measurement plane is of prime importance to the assessment of accurate component performance. This section presents guidelines which should be considered when designing probe arrays for performance measurement of components tested in rigs or in engines. Design objectives of probe arrays should include:

- How performance is to be calculated, averaged, and weighted.
- Consistency with performance calculations in the engine cycle model.
- Consistency between rig and engine tests.
- Complexity of the profiles to be measured.
- Engine instrumentation capabilities.
- and most importantly, capability to measure as close to the real component performance as possible.

Guidelines are also presented for procedures to edit defective probe data within the array. How the probes are edited can sometimes significantly impact the planar average, and thus, performance assessment.

##### 4.2 Averaging Considerations

When the spatial variations of pressure, temperature, and velocity are fairly small, average levels will be little affected by the averaging technique, be it the area-weighted, mass-weighted, or momentum-weighted technique. In such a case, fewer rakes and probes are required, and static pressure measurements needed for the definition of mass flow and velocity distributions may be deleted.

However, uniform flow is seldom found at the inlet and exit planes of components within gas turbine engines. As a result, a simple area-weighting of pressure and temperature will calculate a significantly different result relative to the recommended average techniques of reference 4-1. For most planes of measurement, these recommendations are:

1. The mass-weighting of stagnation enthalpy.
2. The momentum-weighting of stagnation pressure (Dzung method), or the Pianko method of averaging stagnation pressure.

For any averaging method, a sufficient quantity of probes must be placed in the annulus to measure the radial and circumferential gradients of total pressure and temperature. When either the mass-weighting or momentum-weighting techniques is chosen, additional instrumentation must be employed to allow the static pressure and swirl to be measured or estimated at the total pressure and temperature probe locations. Static pressure and swirl are needed to allow calculation of velocity and mass flow at the probe locations.

- Static pressure instrumentation is usually applied at the outer and inner walls. Where static pressure gradients are not constant or linear across the flowpath, stream tube curvature calculations can be made to estimate the gradient. Radial traverses of static pressure can also be made to more accurately define the gradient.

- If circumferential and radial swirl gradients are not constant or uniform, traverses of swirl are suggested. Alternatively, design gradients can be used to estimate swirl at the probe locations.

At the outset of an engine program, a decision must be made as to how the various component performance levels are to be measured and averaged. Engine cycle book-keeping of the components should be consistent with this decision. While probe arrays within the flowpath will not be much affected by the averaging technique, the decision will significantly impact the need for static pressure and swirl measurement instrumentation.

##### 4.3 Profile Considerations

The radial and circumferential gradients of pressure and temperature strongly influence the quantity of probes necessary to obtain an accurate average of the annulus. Factors which should be considered are:

- Design or previously measured radial or circumferential gradients.
- Boundary layers or areas of potential separation.
- Strut or vane wakes.
- Inlet distortion.
- Discrete zones of energy addition, such as that created by the combustion process.
- Pylons or other obstructions forward or aft of a component which can significantly affect the radial or circumferential energy input distributions.

Considering the above factors, it is difficult to generalize the number of probes or types of rakes needed to adequately sample a measurement plane. Guidelines are listed below to aid in the design of the probe array.

- In an inlet flow field where no strong wakes from upstream blade rows or struts are present, radial rakes are adequate.
- Where vane or strut wakes are present, arc or wake rakes are preferred (Figure 4-1). If radial rakes must be used, they should be circumferentially incremented relative to the upstream cascade so as to sample the wake flow as well as the clean flow between vanes (Figure 4-2).
- In a plane where velocity is fairly uniform around the circumference, fewer rakes are needed.
- In a plane where the energy and velocity fields are circumferentially distorted due to the presence of large struts, pylons, flow dividers, or other obstructions, more rakes are needed, spaced so as to define the gradients and allow circulation of flow continuity. Radial or circumferential traversing is an option to minimize the number of rakes. (Figures 4-3 and 4-4).
- There are cases when it may be necessary to combine readings from multiple rake array tests to obtain average performance. This could occur when enough rakes cannot be inserted at one time to sample all of the radial and circumferential positions needed. As an alternate approach, it may be advantageous to design rakes which traverse radially or circumferentially.
- During circumferential inlet distortion testing of compression systems, it is sometimes convenient to rotate the distortion screen, taking readings at several screen positions. By combining the readings, a more complete description of the performance can be

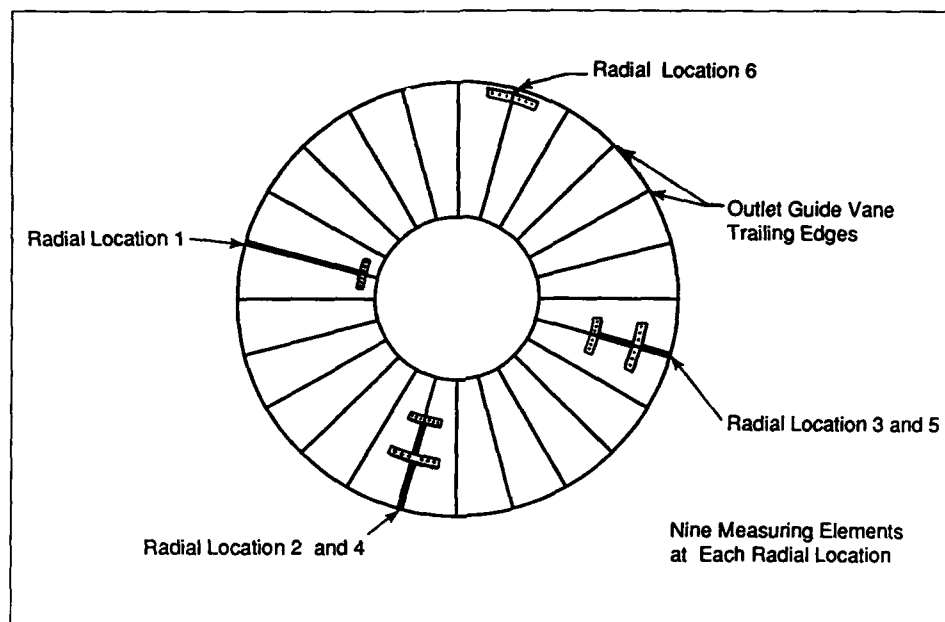


Fig. 4-1 Wake rake installation

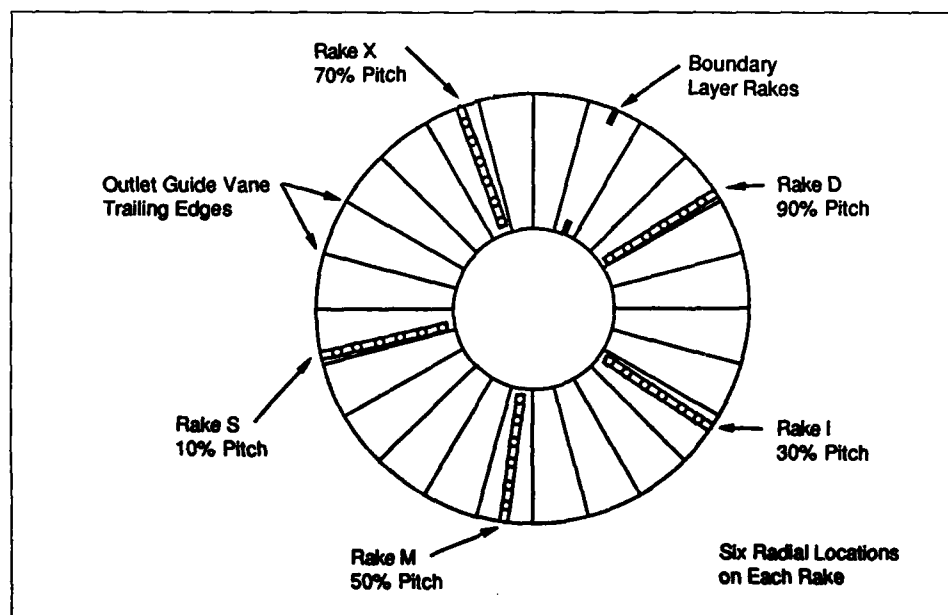


Fig. 4-2 Radial rake installation

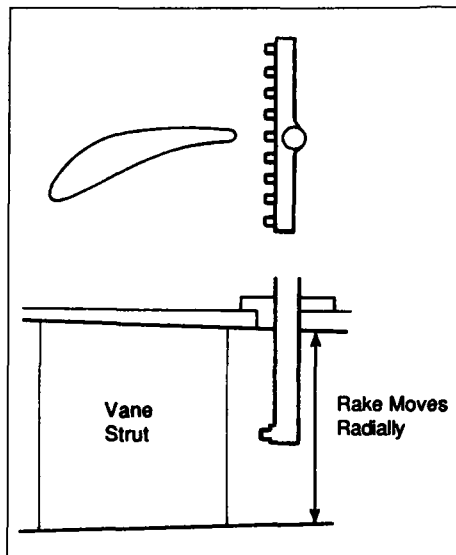


Fig. 4-3 Radially traversing wake rake

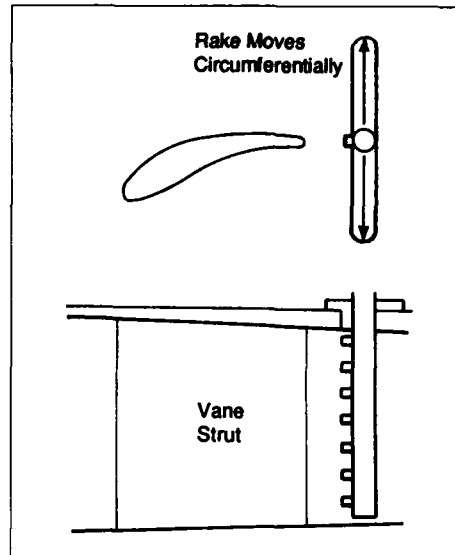


Fig. 4-4 Circumferentially traversing radial rake

measured using a limited number of rakes in the measurement planes.

- Wall static pressures (both inner and outer walls) should be located at the rake probe head measurement plane to allow the calculation of local velocities and the closure of mass flow continuity. Static taps should be placed as close as possible to the rakes, but to the side to assure that the static pressure measurement is not influenced by the flow field around the rakes (Figure 4-5). Depending on the location of the static pressure taps, probe blockage may have to be accounted for in the analysis.

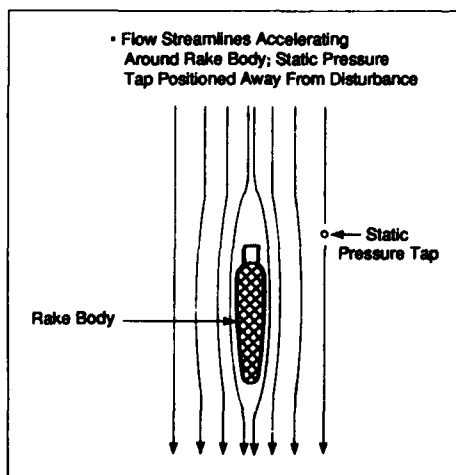


Fig. 4-5 Static pressure tap positioning

- Wherever possible, it is preferable to use combined pressure and temperature elements within the probe stagnation shield. This eliminates the need to translate measurements to calculate velocity. In a plane where the velocity and energy fields are fairly uniform, this recommendation is of less importance.
- The radial distribution of probes is also influenced by the velocity and energy gradients. Generally, where flowpath annulus heights are large and where hub-to-tip radius ratios are low (such as at a fan discharge plane) a larger number of radial probe locations are preferred. Where annulus heights are small and radius ratios are high, fewer immersions are needed. On machines where probe size relative to annulus height makes it impractical to sample many immersions, less may be accepted. Most importantly, radial gradients should dictate the number of immersions.
- Where areas of flow separation are suspected, boundary layer rakes should be installed to aid in the calculation of average performance parameters. (Figure 4-2).
- It is recommended that probes be placed radially at centres of equal areas when the flow field is relatively uniform.
- Combustor components may have to be surveyed at many circumferential locations (150 to 200) at their discharge planes due to the large gradients of temperature generated by discrete zones of combustion. Rakes which traverse in the circumferential direction are often employed.

#### 4.4 Component Versus Engine Test Considerations

Component test vehicles or flow models can usually be instrumented thoroughly enough to satisfy performance averaging goals. However, engine system test

instrumentation capabilities are often compromised, resulting in more doubt or error being introduced as to the true levels of component performance. This being the case, best efforts should be made to establish performance with limited instrumentation using the suggestions listed below:

- Component rig instrumentation quantities and locations must be chosen to very accurately measure the component performance. If possible, this instrumentation should be duplicated on the engine. Since the amount of instrumentation is usually limited in the engine test, at least some rakes should be placed in the same positions as on the rig to allow correlation and comparison of performance and profiles between engine and rig. If engine instrumentation cannot be positioned at the ideal rig locations, then instrumentation should be added to the rig to conform to the engine capabilities.
- Correlations derived from component tests can often be used to "fill out" the more limited measurement arrays available on engines. Care must be exercised, though, to be sure that influences from other upstream or downstream components are measured which may not be present during component tests.
- It is sometimes convenient, or even necessary, to select measurement planes or probe arrays within a gas turbine engine which will not measure losses from such items as upstream structural members or diffusers. As a result, the downstream component measured performance book-keeping includes these losses. These external factors should be identified and considered when comparing performance levels between similar type components measured in different engine (or even test rig) environments. Sometimes the losses can be directly measured on component tests, with the results used as correlation factors on engine tests.

#### 4.5 Instrumentation Editing

When measuring performance on component or engine tests, it is a rarity when at least a few probe readings are not defective. Obviously, every effort should be made to correct the defective ones. However, many problems cannot be corrected, and the test must be resumed, calculating performance in such a way as to best account for the probes missing from the array.

It is a general rule that a value should be substituted for the

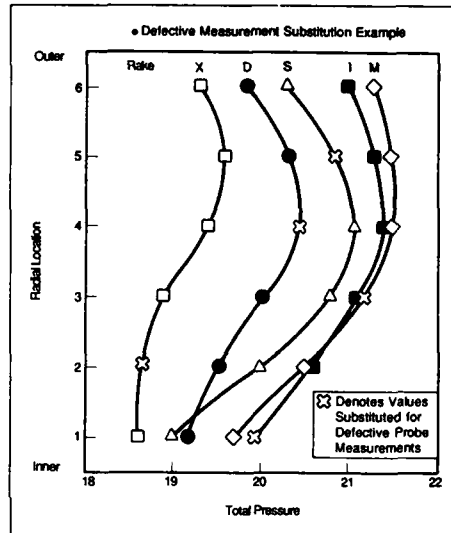


Fig. 4-6 Radial profiles

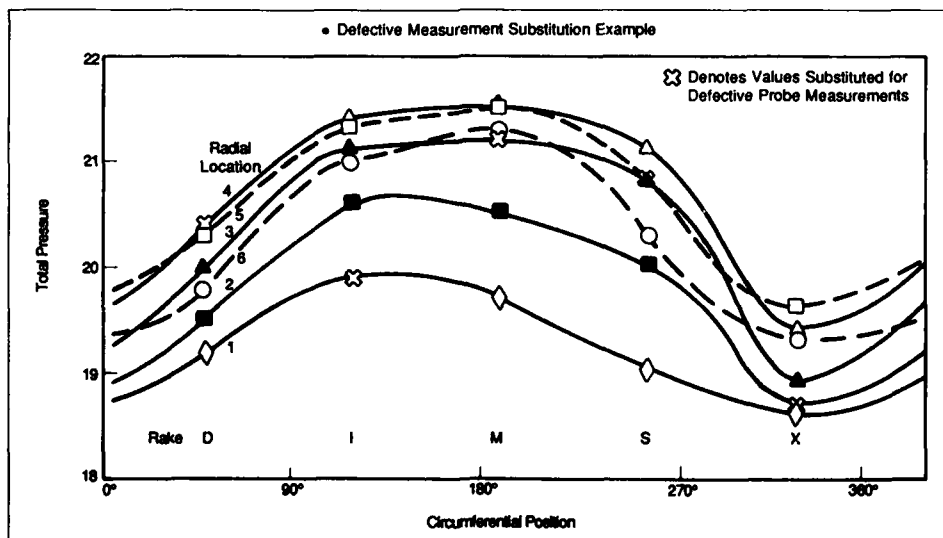


Fig. 4-7 Circumferential profiles

missing probe. The question is, what is the best method for making the substitution?

- The answer is easiest (and obvious) when all "good" probes within the array have little variation. A simple substitution of the average of the good values is sufficient.
- When all "good" probe values at the same radial immersion have little variation, then it may be best to substitute the immersion average value for the missing or defective probe. However, an inspection of the other immersions is necessary to make sure that the circumferential position of the probe does not show an abnormality. If it does, then the substituted value should take this trend into account.
- Likewise, when all good probes at a given circumferential position read similarly, the average of those probes may be best substituted. Again, the above warning applies. The other circumferential positions

should be inspected to make sure that the radial position of the missing or defective probe does not show an abnormality that may need accounting for.

- When the measurement plane exhibits large radial or circumferential gradients, the substitution problem becomes more complex. In this case, the circumferential and radial gradients should be plotted, and a value substituted which best fits the interpolated value of these gradients. Figures 4-6 and 4-7 illustrate substitution examples for pressures measured by the radial rakes in Figure 4-2. In this example, substitutions are made which fit both the radial and circumferential trends established by the good measurements. If a substituted value is not consistent with the measured gradients, it should be justified by a physical explanation. Sometimes data from past tests or rig tests can serve as a reference for substantiating the substituted value. It is often the case that a probe will become defective during a test, and a substituted value can be correlated from earlier data.

## 5. PRESSURE MEASUREMENT

### 5.1 Definition of the System

#### 5.1.1 Pressure Measurement Systems

The definition of the pressure measuring system includes all components from the sensor, sensor support and connecting tubing through the transducer, data acquisition, and processing system to the medium by which the measurement result is delivered to the user. The complete system includes calibration, data validation, and uncertainty estimation as well. A diagram of the components of one example, a complete measuring system, is shown in Figure 5.1-1.

#### 5.1.2 The Sensor and Sensor Support

The sensor for pressure measurements consists of an open-ended tube facing into the gas stream for total pressure measurement or flush with a wall for static pressure measurement. For high response measurements, a transducer can be mounted near or at the entrance to the tube to yield high frequency response; but, for most steady state and transient measurements, the transducer is located some distance from the sensing end of the tube. This document will concentrate on steady state measurements.

The configuration of probes and rakes varies widely depending on their use. Sometimes individual sensors are

used; but, frequently, arrays oriented radially across a passage, radially near a wall (boundary layer rakes), or circumferentially behind a stator (wake rakes) are used. Sensors can be attached to the leading edges or other surfaces of airfoils. In order to achieve higher density spatial sampling, probes and rakes can be traversed in one, two, or three dimensions or rotated about their axis. Examples of these are given in the section on pressure probe design.

The distortion produced by intrusive probes of all types must be controlled; and consequently, the designs used will depend on the size of the passage in which the measurement is being made and the steepness of the local pressure gradient as well as on the expected variations with time.

The transducer can be any of a number of types of devices which convert pressure to a readable signal. Manometers used commonly in the past have now given way to transducers generating electric signals, and these will be the principal type considered in this document. Typical electric pressure transducers sense the deflection of a mechanical member such as a diaphragm or Bourdon tube and convert this deflection into an electric signal using various devices such as a linear differential voltage transformer or a strain gage bridge. The principles of the pressure transducer are described in References 5.1-1 and 5.1-2 and descriptions of many commercially available models are in Reference 5.1-3.

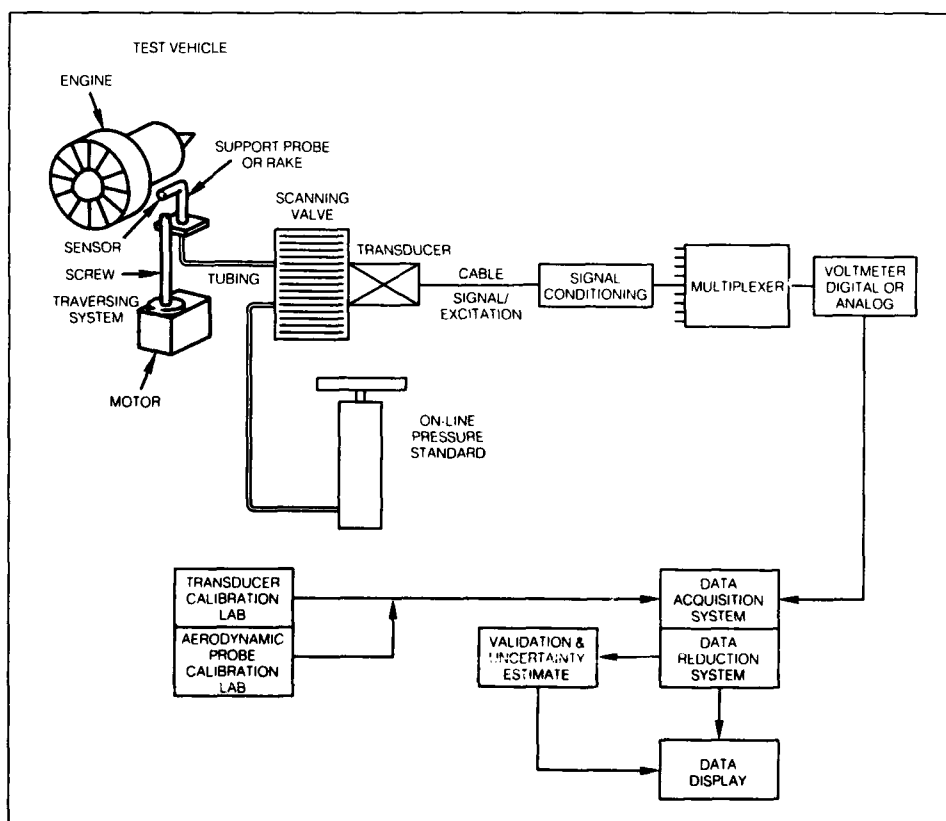


Fig. 5.1-1 A pressure measuring system

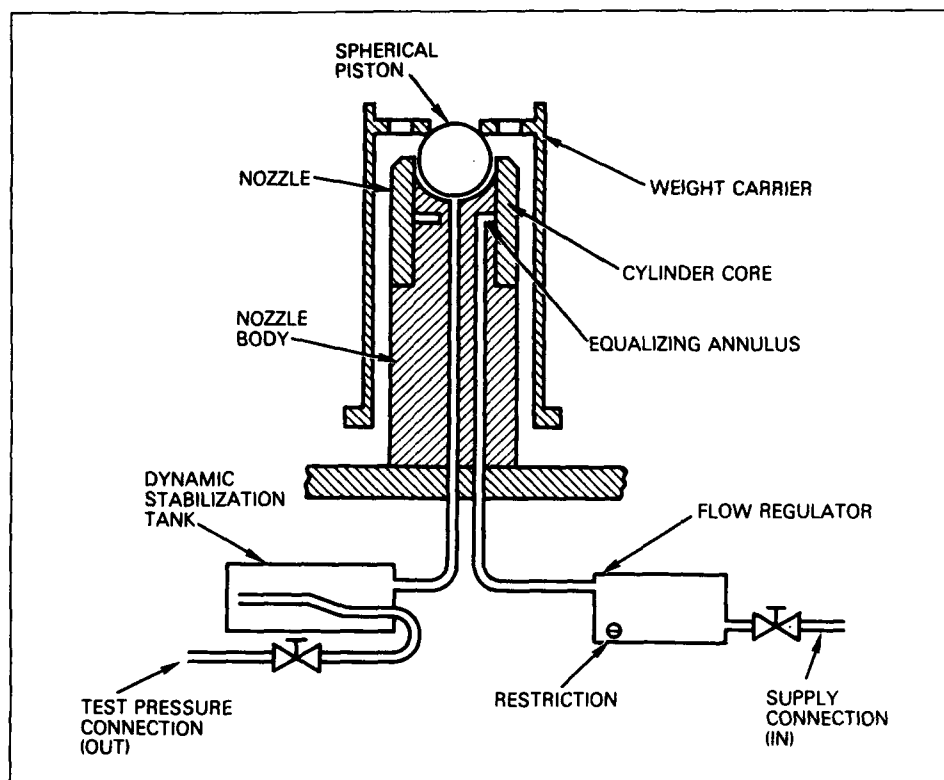


Fig. 5.1-2 Deadweight piston gauge

TABLE 5.1-1

Comparison of British, French, German, and American Terminology for Pressures

	<u>British Units</u>	<u>French Units</u>	<u>German Units</u>	<u>American Units</u>
$P_T$	Total or Stag-nation Pressure	Pression Totale	Gesamtdruck	Total or Stag-nation Pressure
$P_s$	Static Pressure	Pression Statique	Statische Druck	Static Pressure
$P_T - P_s$	Dynamic Pressure	Pression Dynamique	Dynamischer Druck	Dynamic or Vel-ocity Pressure
$1/2 \rho v^2$	Dynamic Head	Pression Kinetique	Kinetischer Druck Geschwindig-keits Druck	Dynamic or Vel-ocity Pressure

For compressible subsonic gas flows the dynamic pressure is given by

$$(P_T - P_s)_{comp} = q = \frac{\rho v^2}{2} \left( 1 + \frac{M^2}{4} + (2 - \gamma) \frac{M^2}{24} + \dots \right) \quad 5.1-2$$

Evaluations of electronically scanned multiple transducer arrays are given in References 5.1-4 and 5.1-5.

A wide range of signal conditioning and data acquisition systems are used for pressure measurement ranging from all analog systems employing oscillograph read out and using either direct or FM tape recorders for data storage to multiplexed high speed systems. Generally, the current state of the art is for multichannel high speed systems to be analog, and for lower speed and steady state systems to be digital. Practices are, however, changing rapidly paced by the advancing microelectronic, optic, and fibre optic technology which is producing multi-array transducers, and the capability to do very high speed digitization, transmission, and storage of wide band signals.

A very important practical requirement in pressure measurement is the use of appropriate functional checks on the system before or during the system's use to ensure that the intended performance is actually being achieved. Suggestions on functional checks involving leakage, time response, etc., are given in the text of this document. An additional important requirement is the post-test validation of the measured data and the generation of a measurement uncertainty estimate.

The measurement philosophy considered to be fundamental in this document is: "No measurement is

complete without an estimate of its uncertainty". The means for generating such an estimate have been extensively debated by national and international committees, and there is the beginning of a consensus on the subject which is summarized in Section 3 of this document.

### 5.1.3 Pressure Definitions Standards and Units Used in NATO Countries

#### *Pressure Standards, The Calibration Hierarchy*

Pressure is not a fundamental quantity but is derived from the standards for force and area. For gas pressure in the range of interest in gas turbine testing the fundamental standard used for calibration of transducers is the deadweight piston gage calibration Figure 5.1-2. Primary calibration services are available from standards organizations in the various NATO countries (see for example NBS Special Publication 250, "NBS Calibration Services Users Guide 1986-88"). Pressure measurement uncertainty at the primary level given by NBS for the range 1.4 kPa to 17 Mpa is  $\pm 57$  ppm. This is the first step in the pressure transducer calibration hierarchy shown in Figure 5.1-3. Ordinarily, the uncertainty at the primary level does not contribute significantly to the overall uncertainty since many other sources of uncertainty are present in most tests.

The quantities normally of interest in gas turbine measurements are static pressure, total pressure, and

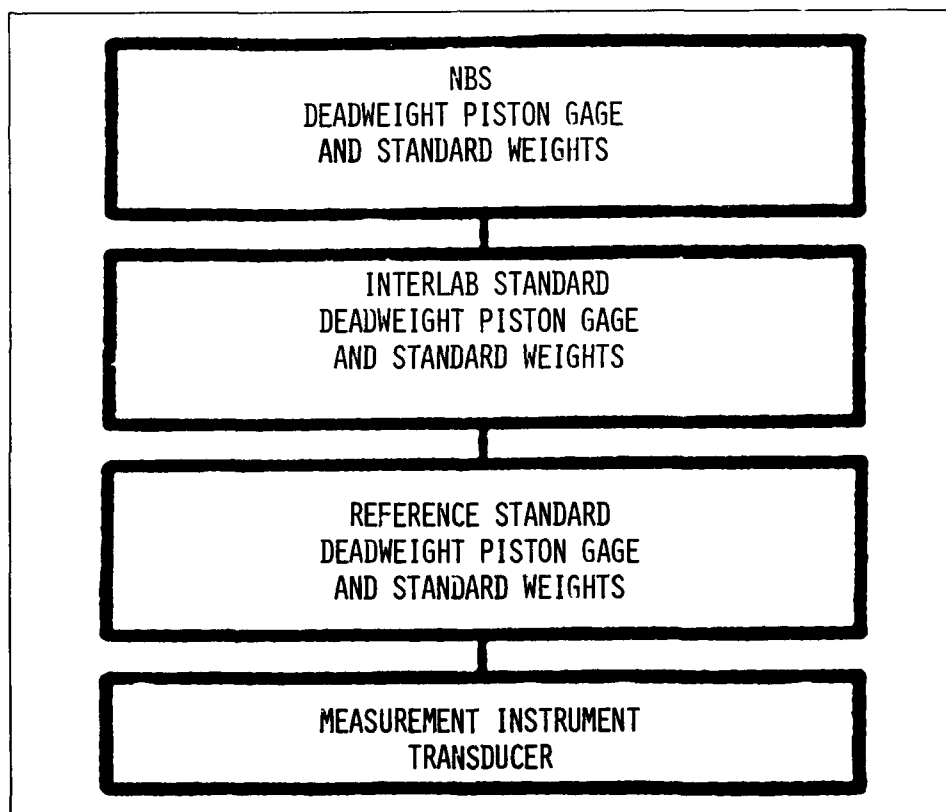


Fig. 5.1-3 Pressure transducer calibration hierarchy

dynamic pressure. The terminology used in NATO nations is described in Reference 5.1.6 (see Table 5.1-1) and can be summarized as follows:

The static pressure is conceptually defined as the pressure measured by an instrument at rest relative to the fluid. As this cannot be obtained directly in a flowing gas, the static pressure is taken from a hole in a wall (wall tap) or from a probe shaped so that, at the position of the pressure hole which we will call the "sensor", the true static pressure can be obtained with acceptable uncertainty. This requires that the hole be small, flush with the surface, that the local streamlines be parallel to the plane of the hole, and that the

sensor support does not significantly alter the local static pressure. If the fluid is brought to rest by an isentropic process, the pressure increases to a maximum value called the total (stagnation or pitot) pressure. The dynamic (or velocity) pressure is the pressure equivalent of the directed kinetic energy of the fluid. For an incompressible fluid this is equal to one-half the product of the density and the square of the velocity (i.e. the kinetic energy per unit volume of the fluid). The relationships are illustrated by the manometer measurements shown in Figure 5.1-4. For incompressible flow, the dynamic pressure is:

$$(P_T - P_S)_{inc.} = q = \frac{\rho v^2}{2} \quad 5.1-1$$

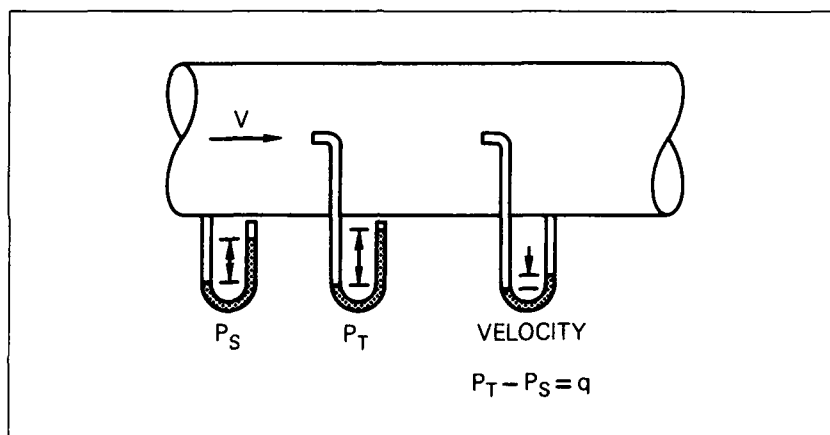


Fig. 5.1-4 Types of pressure measurement

TABLE 5.1-2 Pressure conversions

To Obtain	Multiply No. of	Atmosphere	mm Hg	mm H <sub>2</sub> O	Torr	Bar	mm Hg	mm H <sub>2</sub> O	mm Hg	mm H <sub>2</sub> O	mm Hg	mm H <sub>2</sub> O
Atmosphere	1	760.0	1013.25	1013.25	760.0	1.01325	760.0	1013.25	760.0	1013.25	760.0	1013.25
mm Hg (atm)	14.696	1	1.36	1.36	14.696	0.133322	1	1.36	1.36	1.36	1.36	1.36
mm H <sub>2</sub> O	2116	144	1	1	2116	0.0001433	1	1	1	1	1	1
Torr	760	51.71	0.3601	1	760	0.0001333	1	0.76	0.76	0.76	0.76	0.76
Bar	1.013	0.0001	0.0001	133.3	1	10 <sup>5</sup>	10 <sup>5</sup>	1.333	1.333	1.333	1.333	1.333
Bore	1.013	0.0001	0.0001	133.3	10 <sup>5</sup>	1	10 <sup>5</sup>	1.333	1.333	1.333	1.333	1.333
mm Hg	1013	0.0001	0.0001	133.3	10 <sup>5</sup>	1000	1	13.33	13.33	13.33	13.33	13.33
mm of Hg (°C)	76	5.171	0.3601	10 <sup>-1</sup>	76.01	7.601	1	2.54	0.1008	10 <sup>-1</sup>	10 <sup>-1</sup>	10 <sup>-1</sup>
mm of Hg	760	51.71	0.3601	1	760	0.76	10	25.399	1.008	1	10 <sup>-1</sup>	10 <sup>-1</sup>
in of Hg (°C)	29.92	2.033	1.414	3.007	29.92	2.033	0.3607	1	7.366	2.937	2.937	2.937
in of H <sub>2</sub> O (°C)	408.8	27.59	0.1908	0.0001	408.8	4.088	0.0001	6.304	12.00	1	0.0001	0.0001

\* Exponent Convention: In the above table E + 04 = 10<sup>4</sup>

where the Mach No. =  $M = \frac{V}{(\gamma RT)^{1/2}}$

It is important to realize that the pressure standards referred to by the national standards organizations as embodied in the hierarchy of Figure 5.1-3 are for stationary fluids. They apply to the transducer calibration only and correspond to the aerodynamic quantity  $P_s$  when the velocity at the sensor is zero. Consequently the calibration hierarchy must be extended to cover the quantities of interest in flowing gases. The extension covers the system components from the transducer to the sensor in the flow (i.e. the pitot probe, wall tap, etc.). This portion of the system, unlike the transducer calibration, is not traceable to national standards institutions since no artifacts or procedures have been developed for flowing gases that constitute a universally accepted standard.

SI units are the preferred units; in general, however, since various other units such as psi, atmospheres, and mm of Hg are in common use, it is good practice to always state explicitly the units being used. A table of conversion factors for the most common units is given in Table 5.1-2.

## 5.2 Pressure Probe Design

Gas turbine engines offer a variety of physical and aerodynamic conditions under which total and static pressure and flow direction have to be measured. Such conditions are operating pressure and temperature ranges, pressure gradients and fluctuations, space limitations and the expected static and dynamic stress requirements for measuring probes. The designer will soon become aware that in most cases turbines are not built to carry the optimum instrumentation from the aerodynamic point of view. The probe design will always represent a compromise between the limits of probe dimensions due to space available, strength criteria and the best possible aerodynamic probe characteristics to meet the required measurement accuracy.

After discussing commonly used techniques to design

pressure sensors, some practical probe design examples will illustrate the limits of good aerodynamic probe design from the aerodynamic point of view.

### 5.2.1 Commonly Used Techniques for Pressure Probe Design

The main factors which determine the probe design are:

- direction of mean flow and its variation in direction over operating conditions
- pressure gradients
- interaction between sensor, sensor support, adjacent sensor, duct wall and upstream/downstream blade rows.
- probe installation effect on the flow field.

#### 5.2.1.1 Direction of Mean Flow and its Variations Over Operating Conditions

Generally, total pressure measurement is obtained by placing the open end of a tube into the flow field facing the oncoming flow. However, depending on the operating range of an engine and by the passing wakes, the direction of flow can vary widely, determining the design requirements of the sensor.

Whenever possible a simple square-ended tube should be used to measure total pressure. The effect of inside to outside diameter ratio for circular entrance tubes on flow direction insensitivity is shown in Figure 5.2-1 (Reference 5.2-1). From this, it is evident that thin walled tubes are to be preferred. An increase in insensitivity can also be achieved by bevelling the inlet of the tube as shown in Figure 5.2-2 (Reference 5.2-1).

When the direction of flow varies widely, Pitot tubes enclosed in a cylindrical shield are preferable. Depending on the design, an insensitivity of up to  $\pm 45^\circ$  can be achieved (Figure 5.2-3). Extensive test results on this subject are summarized in References 5.2-1 through 4).

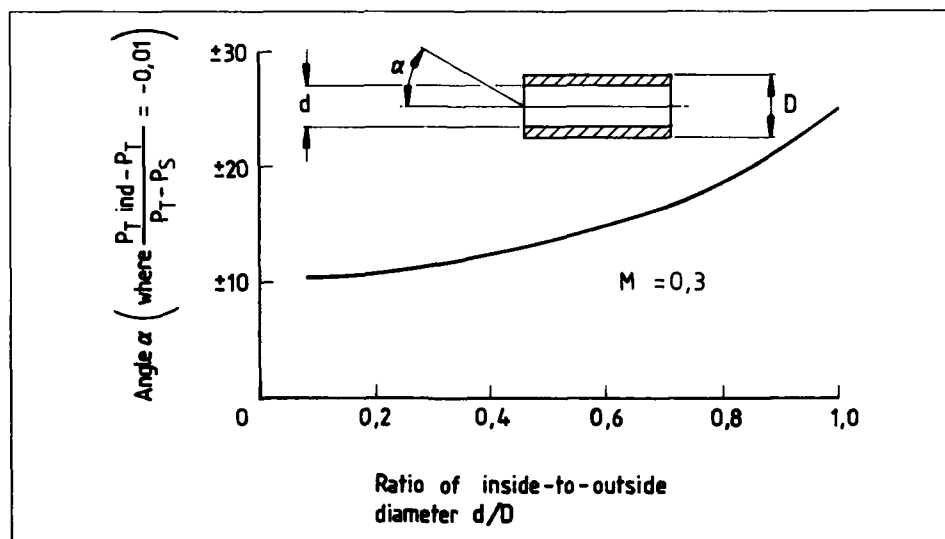


Fig. 5.2-1 Variation of angle  $\alpha$  with ratio of inside to outside diameter

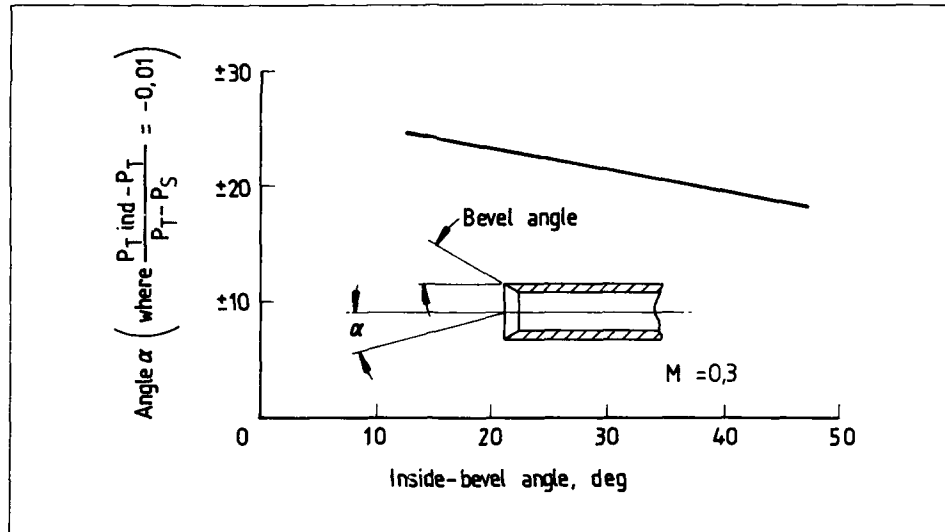
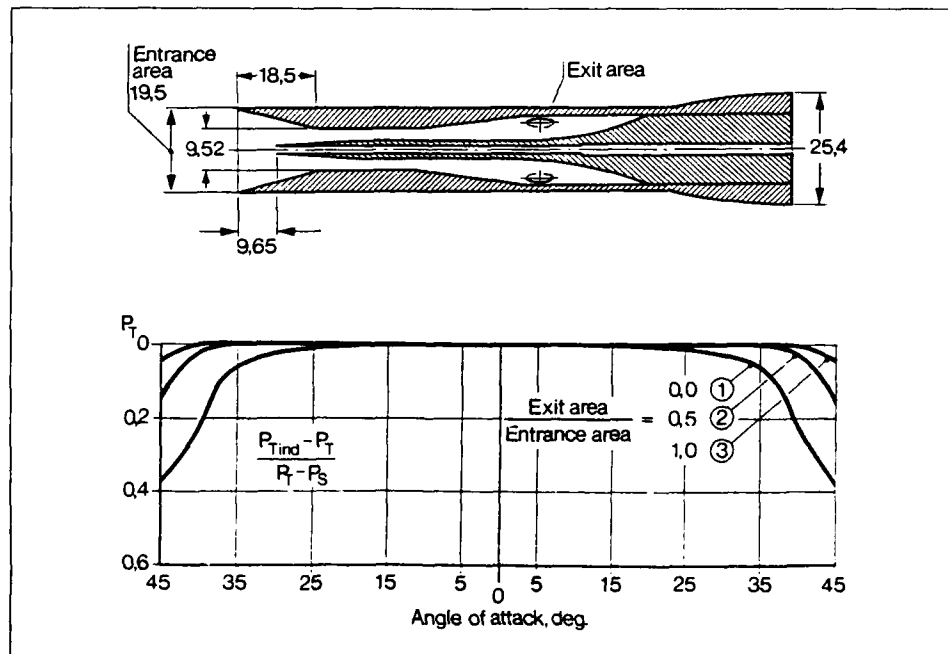
Fig. 5.2-2 Variation of angle  $\alpha$  with inside bevel angle

Fig. 5.2-3 Variation of total pressure error with angle of attack

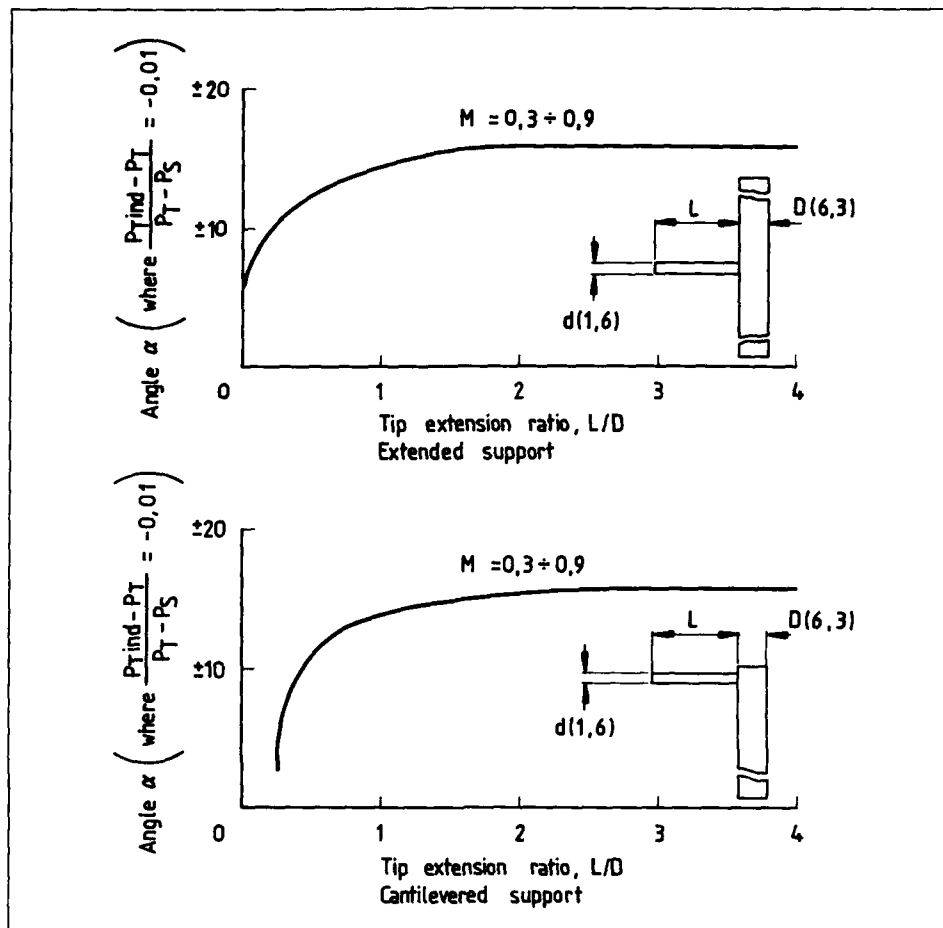


Fig. 5.2-4 Variation of angle with tip extension ratio  $L/D$

The preceding information is based on the assumption that the sensor support would not affect the measurement. However, Figure 5.2-4 (Reference 5.2-1) illustrates that for ratios  $L/D < 3$  this effect can not be neglected, as stem interference will change the flow direction sensitivity of the probe.

#### 5.2.1.2 Pressure Gradients

Total pressure gradients in a cross section of compressors and turbines can be very severe, especially in boundary layers and wakes behind vanes. A pressure probe, consisting of a sensing element mounted on a support, will deflect the flow so that the indicated pressure is not representative of the actual pressure at the centre line of the tube. The stream lines of the flow field become displaced by the presence of the probe. This displacement is a function of the ratio of the length of the sensing element to the diameter of the support. A ratio  $d/D > 3$  is reported (Reference 5.2-5) to minimize this displacement by up to 10% of the support diameter (Figure 5.2-5). This is very important to consider when

measurements have to be performed behind struts or within boundary layers.

#### 5.2.1.3 Interactions Between Pressure Sensing Elements, Sensing Element Support and Adjacent Sensing Elements

The effect of interaction between sensors and supports of total pressure probes within pressure gradients is already covered in the preceding section. This states that the measured total pressure is somewhat higher than the true pressure at the centre line of the measuring sensor.

As presented in Reference 5.2.6 this correction is valid for distances of centre line of the tube to the wall of the duct up to  $y > 2D$  ( $D$  = tube diameter). For distances  $y < 2D$  the measured pressure is lower than the pressure which exists at the centre line of the sensor (as presented in Figure 5.2.6).

The interaction effects become more important for probes, such as Prandtl probes, which allow for the measurement of total and static pressure simultaneously. Figure 5.2-7

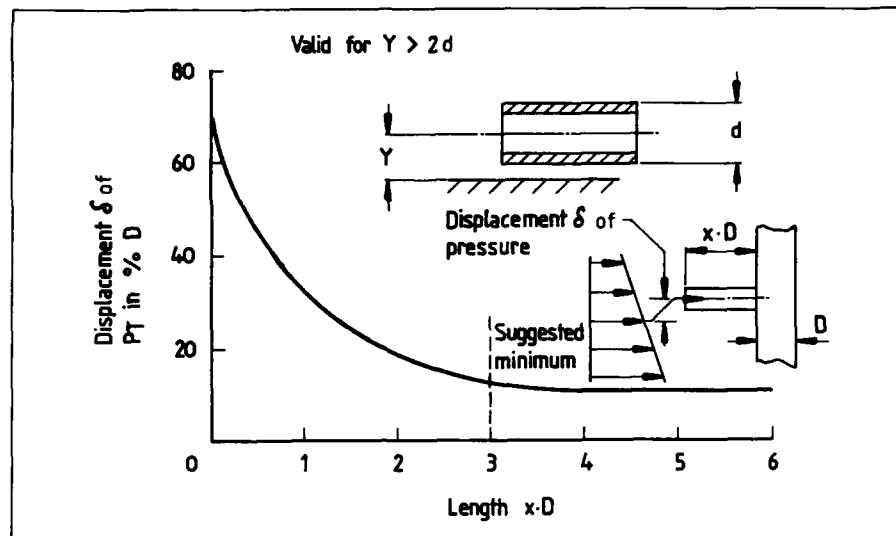


Fig. 5.2-5 Effect of probe length in a pressure gradient field

illustrates the effect of support location on static pressure error for a Prandtl tube (Reference 5.2-7). The effect of adjacent sensing elements on static pressure measurement (Figure 5.2-8) is also reported in Reference 5.2-7.

#### 5.2.1.4 Probe Installation Effects on the Flow Field

The designer has to be aware that the probe is an alien element within the flow field. A probe inserted in a gas stream changes the velocity in the near vicinity of the probe, hence the mass flow rate, the static pressure and the Mach No. in the measuring section. Figure 5.2-9 (Reference 5.2-7) demonstrates the change in flow conditions in a circular duct due to insertion of the probe support. Drag coefficient (support frontal area) and fractional blockage (duct area) have to be overcome by designing a aerodynamically shaped probe support.

#### 5.2.2 Probe Calibration

Each probe can only be manufactured within certain

tolerances. The effects of the tolerances on measuring pressure increase with the miniaturization of the probes. In order to achieve precise results in pressure measurement, it is necessary to calibrate each individual sensor.

Many engine development programs are collaborations of several partners. To make tests results comparable, it is recommended to do some probe cross-calibration tests. This recommendation is supported by discrepancies in cross calibration test results performed with a wedge type probe in 11 difference calibration nozzles throughout Europe (Reference 5.2-8).

#### 5.2.3 Pressure Probe Design Examples

The preceding considerations pointed out the main factors determining the probe design. The basis for designing a probe should be to find the smallest and least expensive probe for a given application with the smallest acceptable error margin consistent with the total uncertainty requirements.

According to their application probes can be classified as follows:

- Total pressure probes  
For measuring total pressure in a stream where direction of flow may vary with operating conditions and time if behind a rotating component.
- Static pressure probes  
For measuring total and static pressure at the same point when direction of flow is known.
- Directional probes (2-dimensional)  
For measuring total and static pressure and yaw angle (pitch angle known).
- Directional probes (3-dimensional)  
For measuring total and static pressure, yaw and pitch angles.

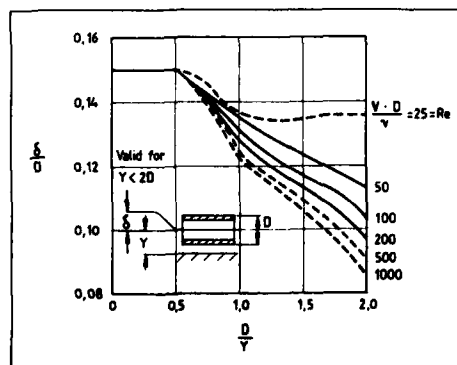


Fig. 5.2-6 Effect of shear flow and wall in boundary layer

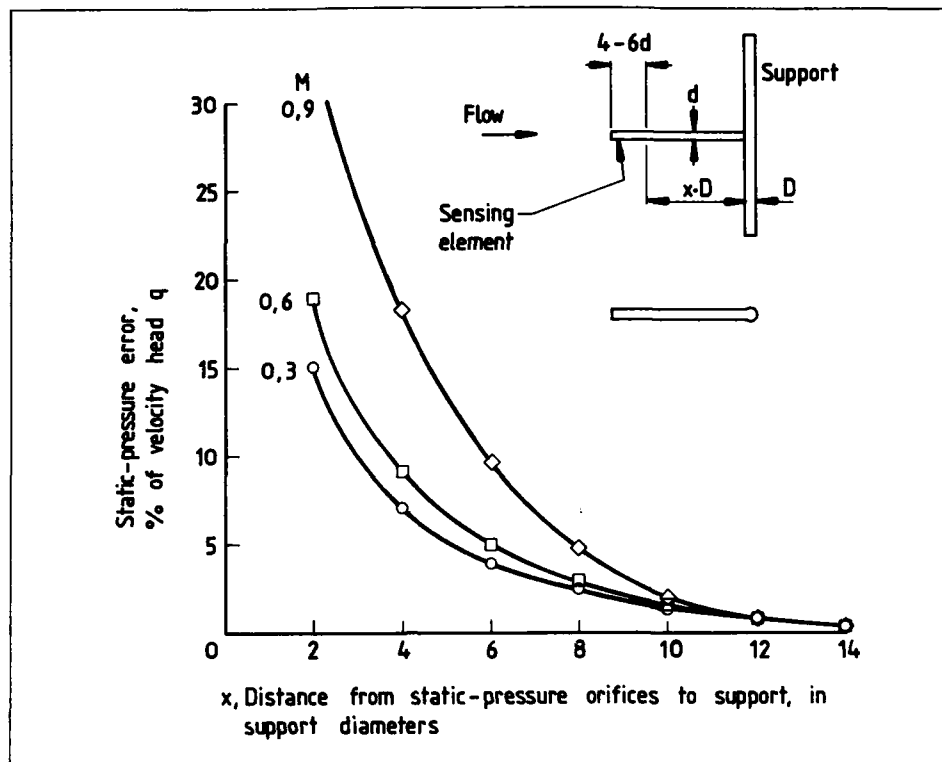


Fig. 5.2-7 Effect of support location on static pressure error

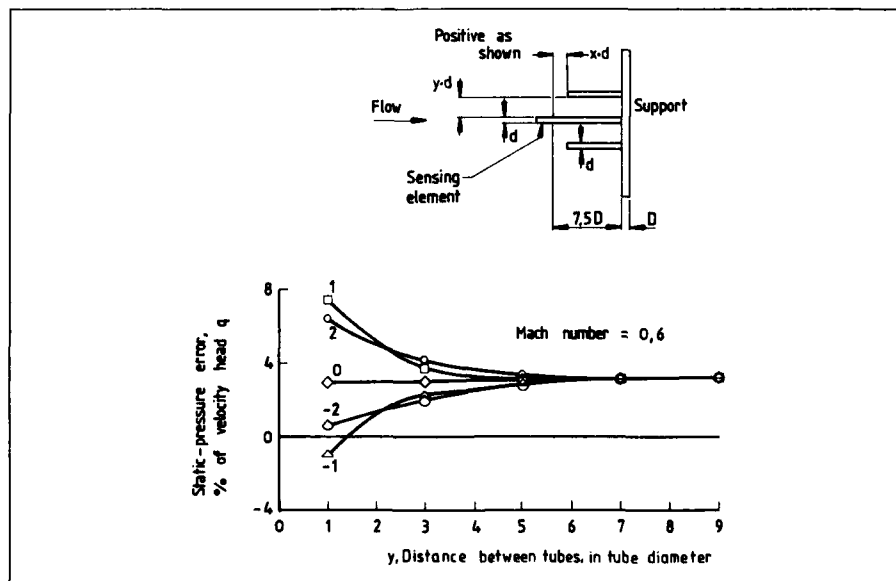


Fig. 5.2-8 Effect of tube proximity on static pressure error

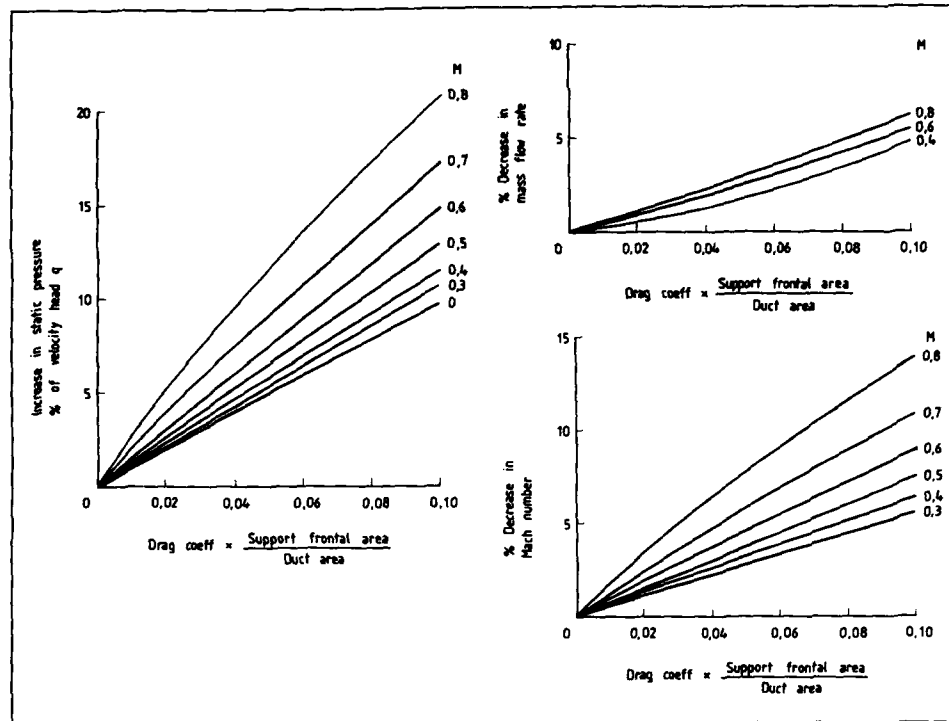


Fig 5.2-9 Change in flow conditions in a circular duct due to insertion of a probe support

### 5.2.3.1 Total Pressure Probes

When the direction of flow is known or within total pressure gradients, simple chamfered impact tubes mounted on a support should be used as discussed in 5.2-1. But in most cases direction of flow is unknown or varies with operating condition and time, so a Kiel type sensor is recommended if space is available.

- Rake "A" is designed to measure the total pressure at six radial positions (Figure 5.2-10). The sensors are insensitive to yaw angle variations of up to  $\beta \pm 20^\circ$  as shown by the calibration curve. A directional head is mounted at one radial position to control changes in flow direction (yaw angle), assuming that there is no change in pitch angle over  $\pm 5^\circ$ . True total pressure is indicated up to a Mach Number of 0.8. Reynolds number and turbulence errors are negligible.
- The wake rake "B" shown in Figure 5.2-11 is a very useful device for measuring pressure profiles behind struts. In combination with a radial traverse unit, a complete pressure profile between two struts can be measured in one hook up. However, because of the large size of the rake, attention has to be given to the strength of the shaft, the sensor carrier and to blockage effects.
- Space limitation between compressor or turbine stages often requires the use of vanes as pressure sensor

supports. This technique has some attractive advantages, e.g.

- instrumentation is relatively inexpensive, due to no provision for installation in the casings
- blockage is almost negligible
- multistage turbines can be analysed in detail on a stage to stage basis.

The pressure tubes should be routed within the surface of the pressure side if the strength of the vanes allows one to do so, (Figure 5.2-12). The remaining slots can then be filled by cement, epoxy or solder in order to smooth the surface. When the pressure tubes have to be guided along the surface on the pressure side of the vane, they can be fixed by metal sheets spot welded on to the vane (Figure 5.2-13).

The "Kiel type" sensor can be bonded, torch brazed or brazed by inductive heating on to the leading edge of the vane. The latter brazing procedure is very controlled and therefore in most cases rework of the vane surface is not necessary.

### 5.2.3.2 Static Pressure Probes

Static pressure is by far the most difficult pressure measurement to make. The types of static pressure measurement include wall taps, which are small holes drilled in the flow boundary wall or on airfoil surfaces, and stream statics using Prandtl probes, cylinder, cobra or wedge probes.

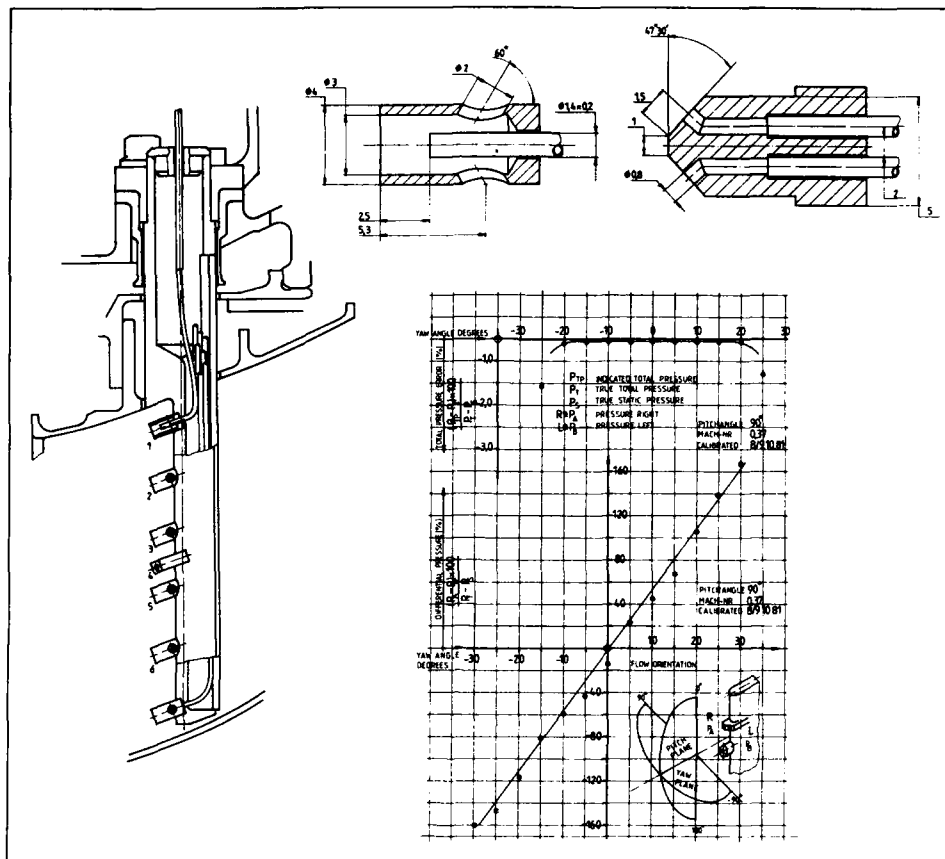


Fig. 5.2-10 Rake "A"

Wall taps provide static pressure measurement without greatly disturbing the flow streamlines. Rayle (Reference 5.2-9) investigated the influence of orifice geometry on static pressure measurements. Some additional test results are presented in Reference 5.2-10 and 11. It was found that a radius supplied to the edge of the orifice produces a positive change in the pressure reading, while a countersink produces a negative change (Figure 5.2-14).

The size of the static tap hole also affects the accuracy of the static pressure reading. Theoretically, a zero diameter static tap will yield an errorless reading. But small holes are difficult to machine burr-free, they have a long response time and they easily become plugged by solid or liquid particles in the gas. In practice, hole diameters of 1.0 – 1.2 mm have proved adequate. Figure 5.2-15 illustrates possible designs of static pressure taps.

The method "A" (Figure 5.2-15) guarantees the best possible machining accuracy and should be preferred if the wall thickness allows one to do so. Method "B" (Figure 5.2-15) is the most common configuration, because typically the engine casings are very thin. But care has to be taken to smooth the tube end to the inner contour of the wall.

- Pitot-static probes are suitable for flow velocity or mass flow measurements in straight ducts or where the air stream direction is fairly well known.

Pitot static probes are defined as a coaxial combination of a pitot and a static tube. Basically, they are L-shaped tubes with an impact hole in the tip and several static holes in the head. The shape of the tip determines the sensitivity of the probe to flow direction changes. The length of the head determines the sensitivity to Mach number errors.

In practice, a compromise length has to be chosen for ease of installation.

Figure 5.2-16 shows the measuring head of a pitot static probe, which can be installed within an air-meter in front of an engine. The pressure curve along a tube with a hemispherical head is shown in Figure 5.2-17 (Reference 5.2-12). The influence of beam and orientation of static pressure holes is illustrated in Figure 5.2-18 (Reference 5.2-13). The diameter of static pressure tapings should be within  $d = 0.2 - 0.74 D$  to avoid significant errors (Reference 5.2-14). For detailed information regarding pitot tubes and their use refer to Reference 5.2-19 with 129 references.

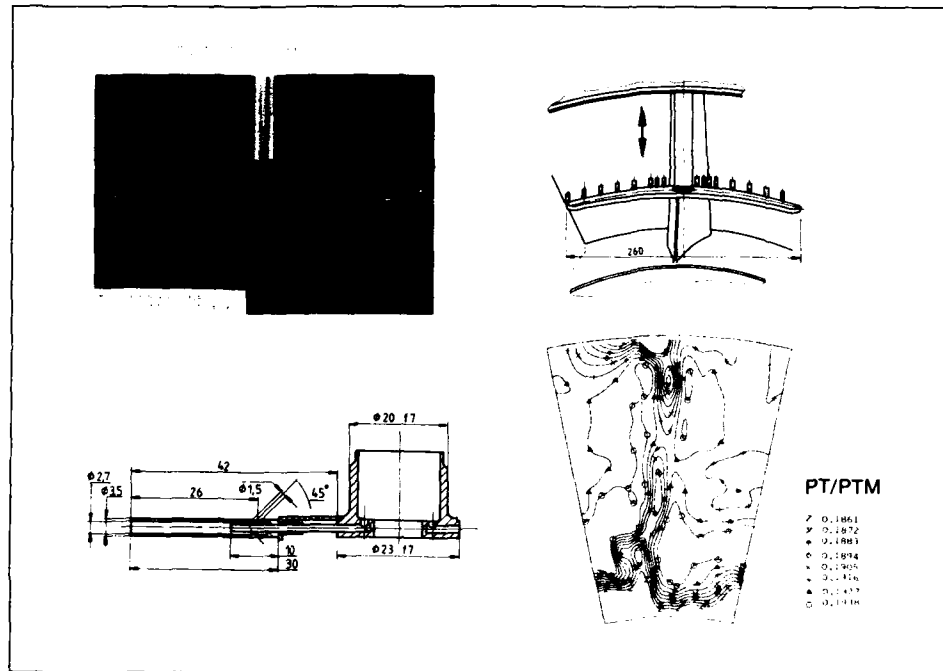


Fig. 5.2-11 Wake rake "B"

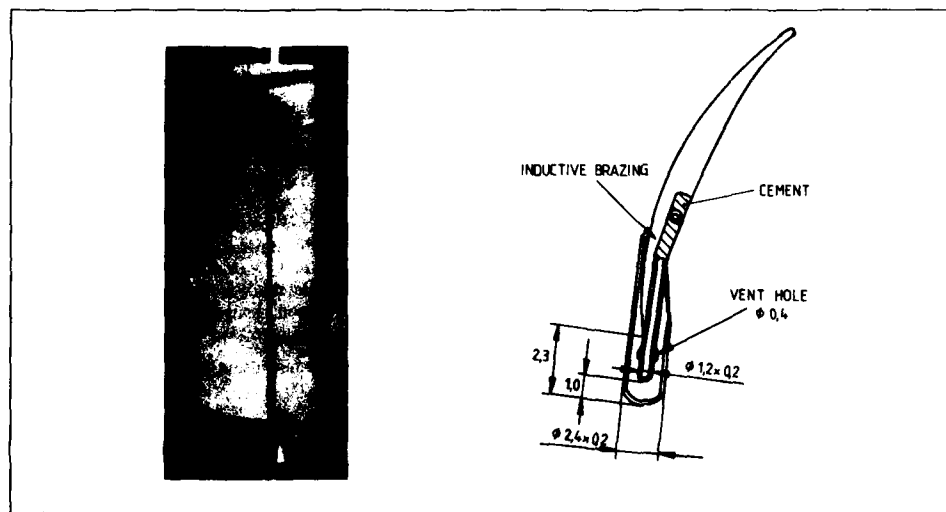


Fig. 5.2-12 Instrumented vane "C"

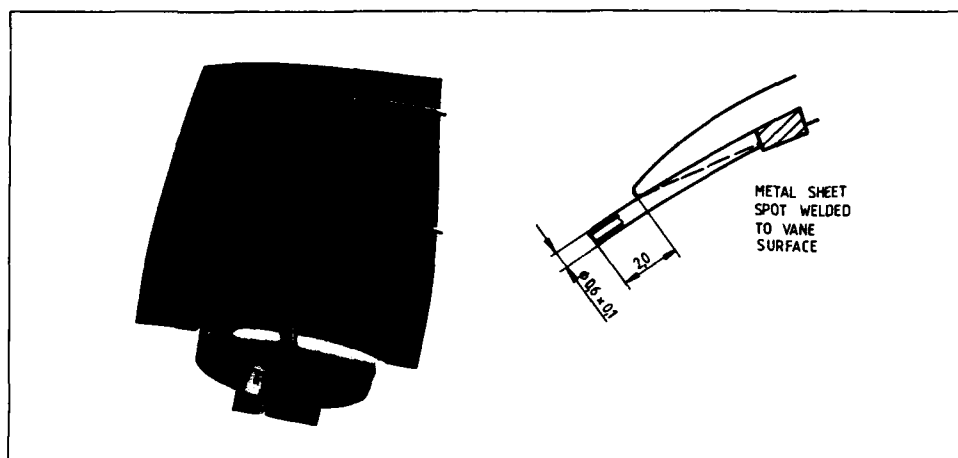


Fig. 5.2-13 Instrumented vane "D"

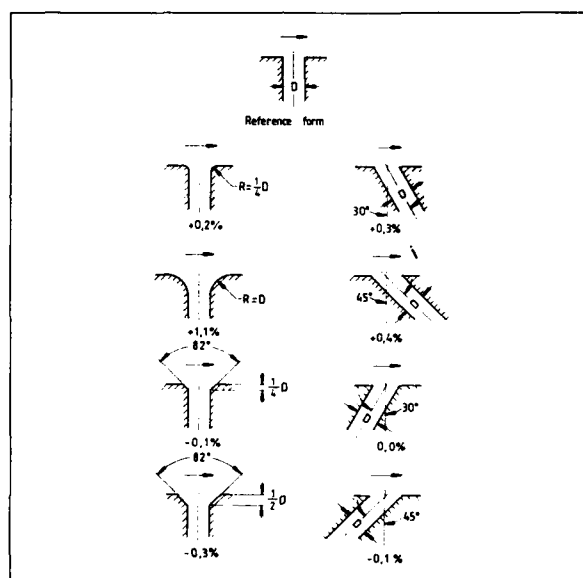


Fig. 5.2-14 Effect of orifice edge form on static pressure measurement

### 5.2.3.3 Directional Probes, 2-dimensional

Directional probes (2-dimensional) are used to measure total and static pressure and yaw angle. In most cases the probe is rotated about its axis so that the sensor is aligned with the flow direction in the yaw plane.

In this chapter, it is not possible to give a broad survey of all available probe designs. Figure 5.2-19 presents the three most commonly used probe types with special features, i.e. a cylindrical probe, a wedge probe and a cobra probe.

The calibration curves (Figure 5.2-20) for these probes

allow the calculation of total and static pressure and yaw angle, assuming that the probe is held facing into the flow in the yaw plane with a self-balancing actuator.

- The cylindrical probe "E" is designed with the directional holes normal to the stream surface. This probe is for use in flow fields with moderate pressure gradients. To increase the sensitivity to yaw angle changes and to decrease the sensitivity to pitch angles up to  $\pm 20^\circ$  the probe has a prism shaped measuring section. An additional tapping is located near the tip of the probe to measure total pressure. The calibration

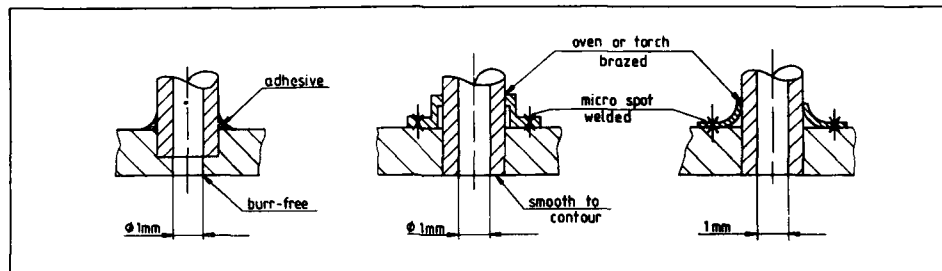


Fig. 5.2-15 Design of pressure taps

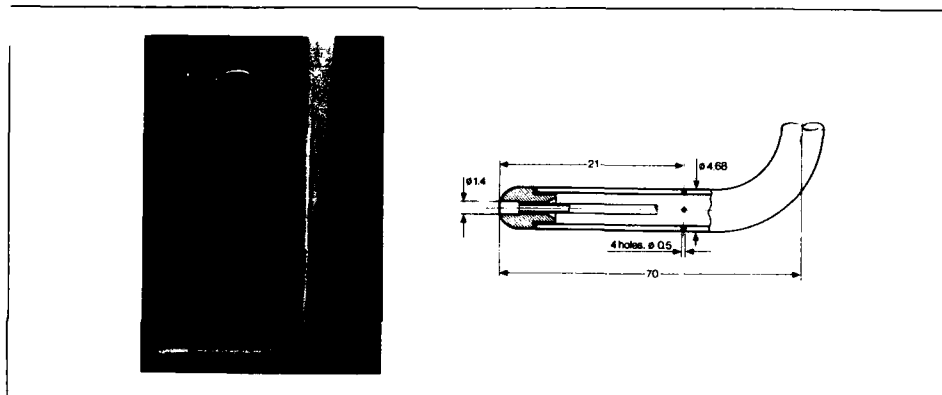


Fig. 5.2-16 Typical design of a pitot static probe

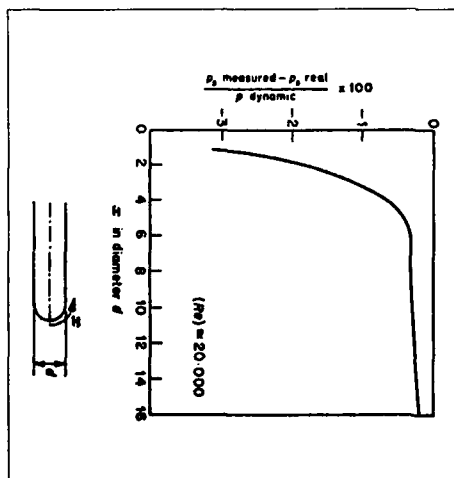


Fig. 5.2-17 Pressure curve along a tube

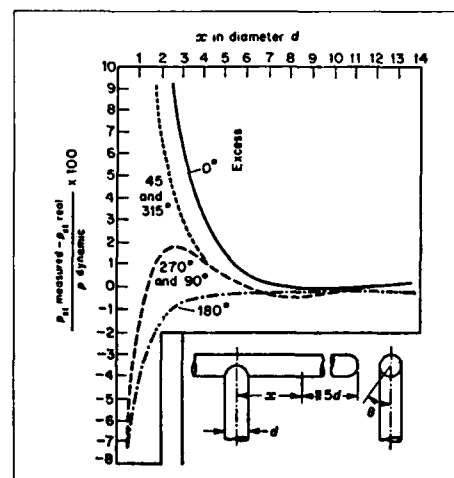


Fig. 5.2-18 Influence of beam and orientation of a hole

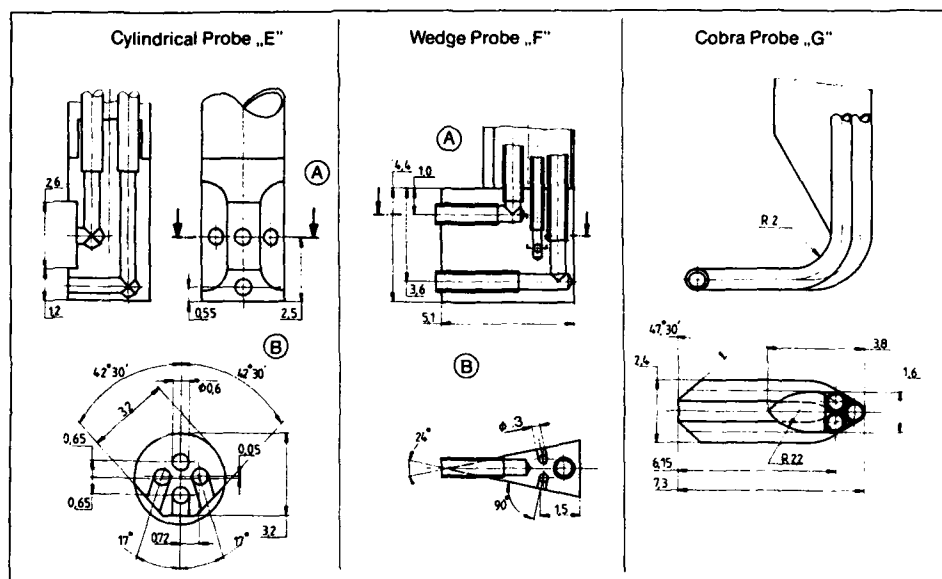


Fig. 5.2-19 Measuring head of a cylindrical probe, a wedge probe and a cobra probe

results, however, indicate a significant difference between indicated and actual total pressure for this tapping due to the influence of the probe tip on flow direction.

- The wedge probe "F" measures total and static pressure and yaw angle. The advantage of this probe is its low blockage. The probe has two total pressure sensors, which reduce the measuring time. As indicated by the calibration curves, there is no significant difference between indicated and measured total pressure for both sensors. The probe is insensitive to pitch angles up to  $\pm 15^\circ$  within 1% of the dynamic pressure for total pressure measurement.
- The cobra probe "G" is comprised of three tubes normal to the stream surface and allows the measurement of total and static pressure and yaw angle. The probe can traverse within the boundary layer, but is not suitable for pitch angles over  $\pm 5^\circ$ .
- Small engines do not always allow enough room for the installation of traverse probes in combination with a traverse unit. Therefore, the test engineer is sometimes forced to measure total and static pressure with fixed rakes. Rake "H" (Figure 5.2-21), a cobra type probe enables measurements to be taken at three different radial positions, but is not suitable for pitch angles over  $\pm 5^\circ$ . To calculate the total and static pressure and yaw angle each sensor is individually calibrated (Figure 5.2-22).

#### 5.2.3.4 Directional probe (3-dimensional)

Three dimensional probes are used to measure total and static pressure, and yaw and pitch angle. Fig. 5.2-22 shows a typical five hole probe with a hemispherical head designed to measure the flow field characteristics behind a turbine stator. The very small sensing head is aligned to the mean

flow direction and allows measurement close to the wall. A typical calibration field is also shown in Fig. 5.2-22. Detailed information about calibration procedure is presented in Ref. 5.2-15. Fig. 5.2-22 illustrates the velocity and total pressure distribution over a vane space measured by means of the five hole probe.

#### 5.2.3.5 Probes for Special Applications

It is obvious that the development of the gas turbine and its components often require special probes, such as miniature traverse probes or combination sensing probes for measurement of temperature, pressure and flow direction. For information about special probes please refer to Ref. 5.2-16 through 21.

#### 5.2.4 Mechanical Integrity of Probe Design

The strength requirements for probe design are determined by the aerodynamical and mechanical operating conditions (Ref. 5.2-21), such as

- total temperature
- total pressure
- Mach-number
- angle of attack
- engine rotational speed
- blade passing frequencies

In general, probe design should take care of:

- optimal aerodynamic shaping to reduce drag
- avoidance of stress raisers
- reduction of mass concentrations at the end of the probe

Whenever a probe design is critical with respect to the strength requirements, the static and dynamic stress should be controlled by an attached strain gauge.

Probe material should be the same as that of the casing where it is installed. Fig. 5.2-23 shows a choice of material to

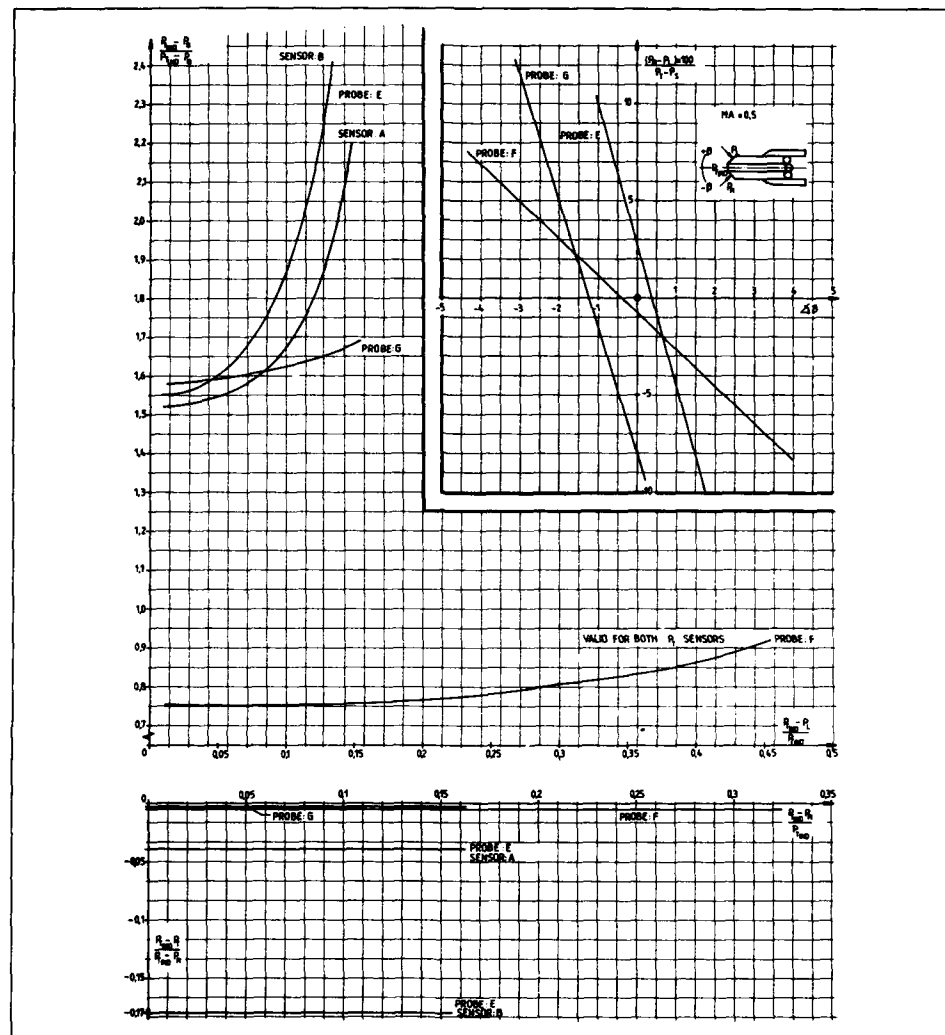


Fig. 5.2-20 Calibration curves for probe "E", "F", "G"

be used in the different engine modules.

### 5.3 Recommended Practices

#### 5.3.1 Pressure Sensors and Sensor Supports

##### General Description

Pressures in gas turbines are measured with a wide variety of probes, rakes, wall and airfoil surface taps, leading edge sensors, cobra and wedge probes, etc. The definitions used in this document refer to the "sensor" as the open tube and its support located at the position in the flow where the measurement is required. Ideally the measurement made corresponds to the true value at the centre of the opening. The tubing from this location to the transducer is essentially a pneumatic transmission line which conveys the pressure information from the sensor to the transducer. The

transducer in turn converts the pressure signal to a discernible output, electrical or otherwise, used for observation or recording.

##### Probe and Rake Design

The recommended practices for probe and rake design are embodied in Section 5.2 of this document. They are summarized as follows:

#### 1. Aerodynamic Design

Use probe designs whose performance has been documented such as those in Section 5.2 or in the reference literature. Alternatively, develop the equivalent body of information for required probe designs. In any case, the performance of individual probe designs must be checked in a suitable calibration facility to assure that design objectives are being met.

The critical factors in the design are:

- Tolerance to variation in flow direction
- Size of expected pressure gradients
- Interaction between sensor, sensor support, and walls
- Probe installation effects on the flowfield including both streamline distortion and effects on the performance of the component under test
- Probe response to non-steady flow.

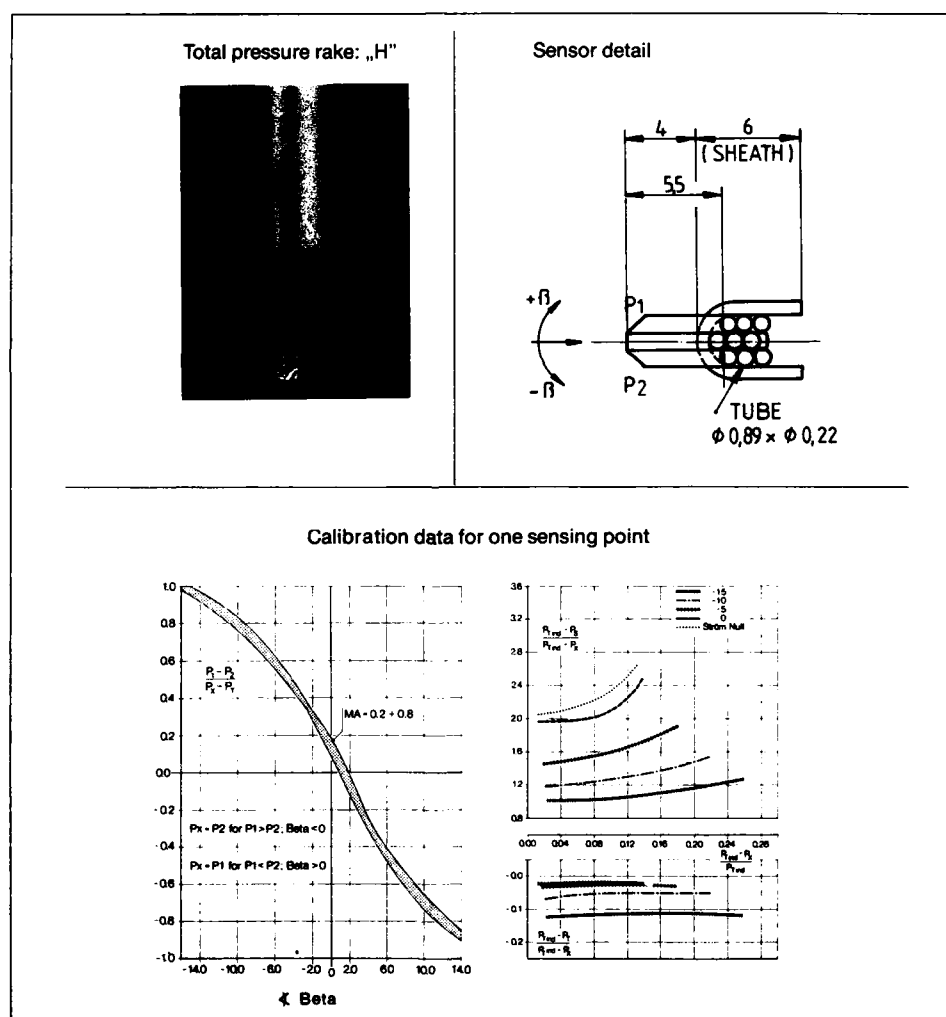
## 2. Mechanical Design

The probe structural material and mechanical design must take into account both steady state air loads, anticipated vibratory loads, and, for probes in high temperature regions, thermal stress loads. The detailed criteria is a matter of individual practice; however, probes located upstream of rotating components

should be designed with a very generous safety factor because of the potential damage consequent on probe failure. Any probe failures which do occur should be carefully analysed and the lessons learned used to improve the design and/or fabrication technology for that type of probe. For new probe designs, it is common practice to apply strain gauges on the first installation of the probe to assure that the results of the structural design are valid.

## 5.3.2 Traversing Systems

When the number of points to be sampled is large, fixed rakes with multiple sensors produce excessive blockage, and it then becomes necessary to use a single probe or small rake and traverse it through the flow to achieve the necessary density of measured points. A wide variety of 1, 2,



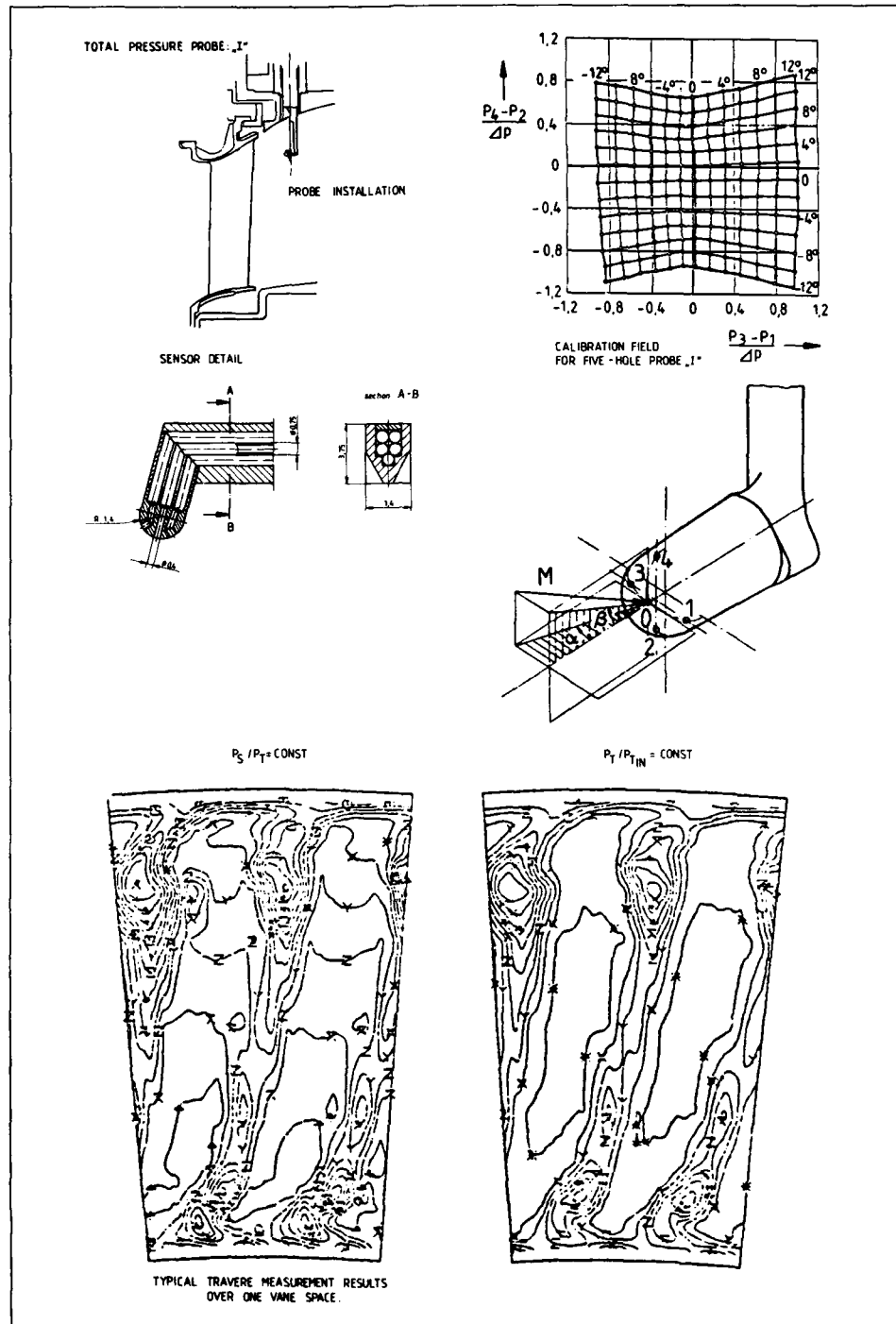


Fig. 5.2-22 Five hole probe

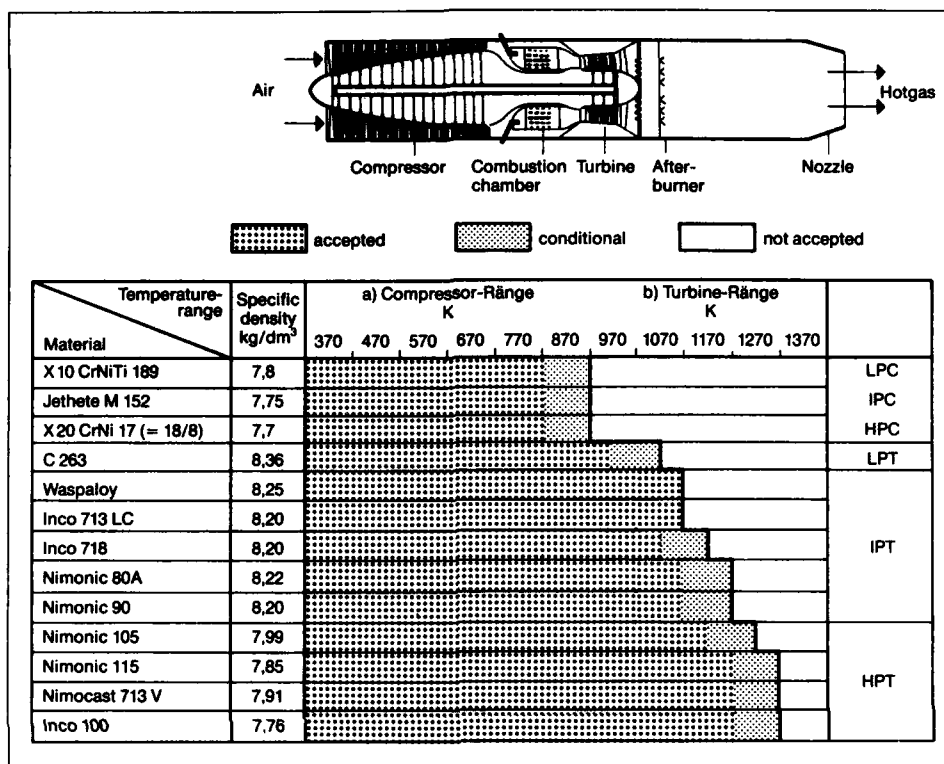


Fig. 5.2-23 Selection of probe material

and 3 axis traversing systems have been used such as the 2 axis system shown in Figure 5.3-1. Considerations when using traversing are as follows:

#### 1. Speed vs. Settling Time

Since it takes time to move a probe from point to point and running time can be expensive, one normally wants to move the traversing system as rapidly as possible. This is also desirable from the point of view of maintaining fixed operating condition in the test vehicle since stability is easier to maintain over shorter periods of time. However the speed of traverse is limited by the settling time of the system, and the dwell time at any specific location should never be so brief that the pressure readings do not have time to settle to their final values to within the accuracy required. When an overall uncertainty of 1 percent is required, a good rule of thumb is to allow time to settle to 0.1 percent final value (i.e., 1/10 of the desired uncertainty). With close-coupled transducers, the response time may be so fast that continuous traversing is possible. With long lines to remote transducers, however, the rate of traversing will be limited by the line response time.

#### 2. Positioning Accuracy

The positioning uncertainty of a traversing system should, in general, be small compared to pressure gradients in the flow. Again as a rule of thumb, if 1

percent uncertainty in pressure measurement is desired, the position accuracy requirement can be obtained by estimating the maximum gradient in the measurement region and determining what displacement corresponds to 1 percent change in pressure and then requiring that the position accuracy produce no more than 0.1 percent error in pressure. Typical requirements for position uncertainty are  $\pm 0.1$  mm.

For angular alignment of total pressure probes since with kielhead and similar designs the acceptance angle is typically  $\pm 30^\circ$  (the exact amount depends on the particular probe and the accuracy needed) and although alignment is necessary it does not need to be very precise. For pressure measurements used in determining air angle, however, the angular uncertainty required must be within  $0.1$ – $0.3^\circ$ .

Frequently, differential thermal expansion of test vehicle hardware as well as distortion under operating loads can have a significant effect on the position of a traversed probe, and these displacements must be taken into account. Useful additions to traversing probes designed to move radially across an angular flowpath are the use of a proximity probe to detect the position of the inner wall and the utilisation of mechanical and electrical limit stops to prevent rig or probe damage.

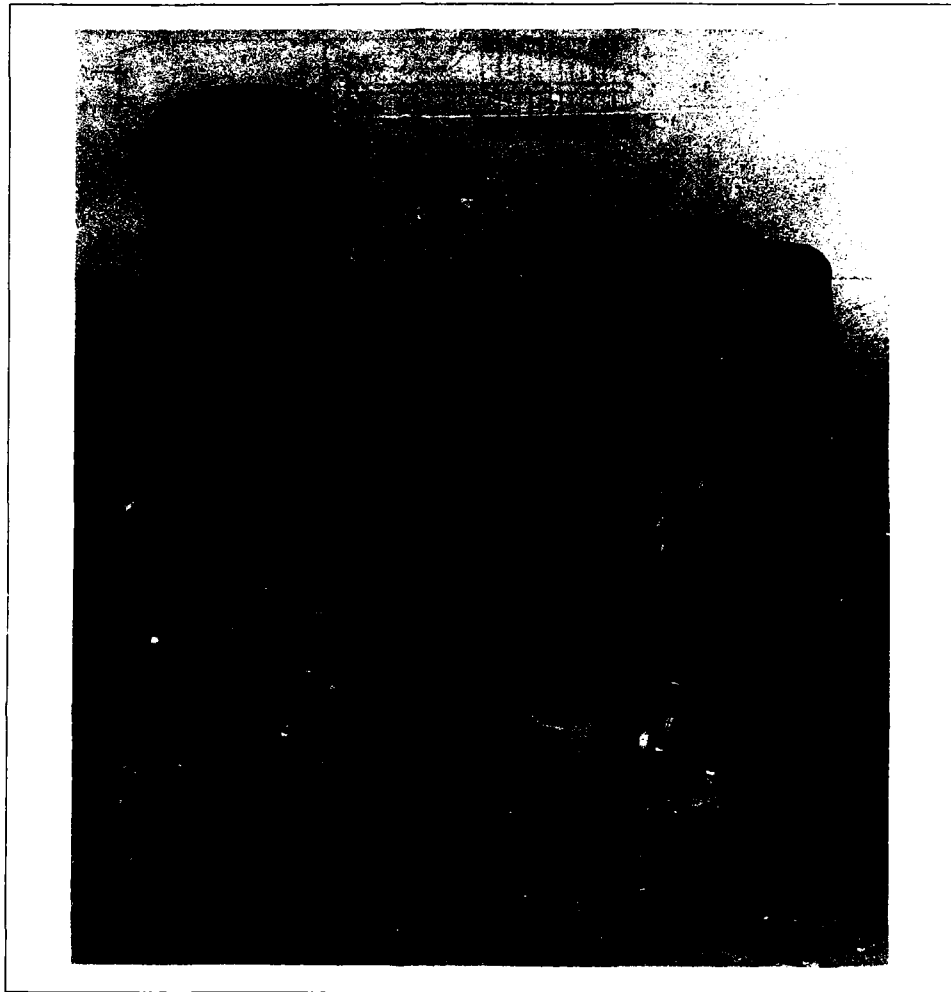


Fig. 5.3-1 Traverse system

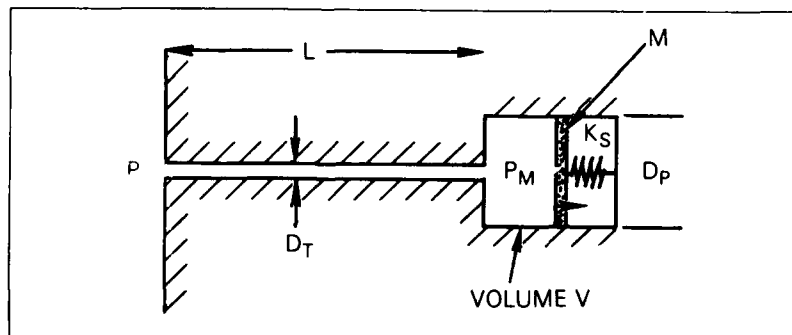


Fig. 5.3-2 Transducer/tubing model

### 3. Variable Blockage

As the probe is traversed to greater insertions in the flowpath the amount of flow blockage changes. The effect is especially pronounced when traversing between airfoils and, in general, in small passages with complex flow. No general prescription for overcoming this problem is known. Assurance that results achieved are valid requires integration of all data from fixed and moveable probes, from static taps on walls and airfoils, and finally with alternative methods of measurement such as laser velocimetry.

#### 5.3.3 Pneumatic Signal Transmission

The dynamic effects of volumes and connecting tubing used in pressure systems are discussed in References 5.1-1 and 5.1-2. The simplest model used in assessing the system is shown in Figure 5.3-2. Additional references are 5.3-1 and 5.3-2.

The analysis given by Doebelin, Reference 5.1-2, applies to small disturbances and yields the following relationship between the measured pressure  $P_m$  and the actual pressure  $P$ :

$$\frac{1}{w^2} \ddot{P}_m + \frac{2\xi}{w} \dot{P}_m + P_m = P$$

The pressure transducer and tubing behave like a damped second order system with undamped natural frequency  $= w$  and damping constant  $= \xi$ . For gas systems with tubing volume,  $V_t$ , comparable to chamber volume,  $V$ , the magnitude of  $w$  and  $\xi$  are as follows:

$$w = \sqrt{\frac{\gamma \bar{P}}{\rho}} \left/ \left( L \sqrt{\frac{1}{2} + \frac{V}{V_t}} \right) \right.$$

$$\xi = \frac{16\mu L}{Dt^2 \sqrt{\gamma \bar{P} \rho}} \sqrt{\frac{1}{2} + \frac{V}{V_t}}$$

where  $L$  = tubing length  
 $V$  = transducer volume  
 $V_t$  = tubing volume  
 $\gamma$  = ratio of specific heats  
 $\rho$  = mass density  
 $\bar{P}$  = average pressure  
 $Dt$  = tubing diameter  
 $\mu$  = fluid viscosity

Note that  $\sqrt{\frac{\gamma \bar{P}}{\rho}}$  is the velocity of sound in the tubing (a).

The response of this second order system to a step change depends on the magnitude of the damping constant. If the damping is negligible, oscillations at the undamped natural frequency will persist for several cycles and a settling time is difficult to define. If  $\xi$  is near optimum (i.e.  $\xi \approx 0.6$ ), the settling time  $\tau$  to reach within 10 percent of the final value is (see Chapter 3 of Reference 5.1-2);

$$\tau \approx \frac{2.4}{w} = 2.4 \frac{L \sqrt{1/2 + V/V_t}}{a}$$

This is essentially the effective acoustic propagation time in the tubing.

If the damping is large, the response is dominated by viscous fluid transport in the tubing. In this case, the second order term is negligible and the system responds as a first order system with response time,

$$\tau = 2\xi/w$$

For large changes in pressure the simple model above becomes nonlinear because  $\rho$  and  $P$  are not constant. Solutions for the nonlinear case (i.e., large pressure changes) and for the simple model shown in Figure 5.3-2 are given in Reference 5.1-1. In addition, many systems are physically more complex than the model because of bends, tees, diameter changes, etc. For this reason, it is important to experimentally check the dynamic response of complex pressure systems to assure that data acquisition after a change in operating condition does not begin until the pressure readings have settled to their final values to within the limits required by the uncertainty model.

An example of a set up for testing the dynamic response of a pressure system designed to measure steady state or transient pressure is shown in Figure 5.3-3. In this system, a pressure source is attached to the sensor end of the system through a quick-acting diaphragm valve. The system is pressurized, held at steady state and then the diaphragm is rapidly released. Recording of the transducer output in response to this step change then yields the system time response. It is essential to demonstrate that the response behaves as expected for the range of pressure changes expected. Typically, a damped second order response should be found and that the system is approximately linear. This latter is checked by varying the amplitude of the input pressure signal and determining whether the characteristics of the response remain constant. The speed of the valve opening must be rapid compared to the designed time response of the system. For engine operability-type pressure measurements, which is the fastest response time needed for most performance measurements (i.e. determination of operating point at stall), the highest frequencies present in the time varying pressure signal that it is necessary to resolve are about 100 Hz. For this case, a quick acting valve as described above with millisecond response is adequate. For calibration of systems designed to measure acoustic signals, rotor blade wakes, etc. much faster steps are required such as obtainable in a shock tube (Reference 5.1-2).

#### Unbiased Time Averages in Pressure Probes

The work of Grant, Reference 5.3-3, and Weyer and Schodl, Reference 5.3-4, have demonstrated that if fluctuations in pressure are occurring on time scales short compared to the system response time and, as shown in the last section, whenever fluctuations are large, the average pressure read at the transducer may differ from the average pressure at the sensor even under steady state conditions. An example of the magnitude of this bias error is shown in Figure 5.3-4. The bias depends on both the magnitude and the shape of the fluctuating wave form. The magnitude of the bias can be estimated (assuming the wave form shape is known approximately) using the methods described by Grant in Reference 5.3-3. In addition, Grant's method allows criteria to be applied to the pressure sensor design which minimize bias error due to pulsatile fluctuations. These criteria are intended to minimize errors due to non-linear averaging processes within the probe and include criteria for controlling the errors due to:

- Local losses at bends
- Transition to turbulent flow in the tubing
- Compressibility
- Tube resonances

When fluctuations are large or when the Grant criteria cannot be satisfied in the probe design, it is necessary to use

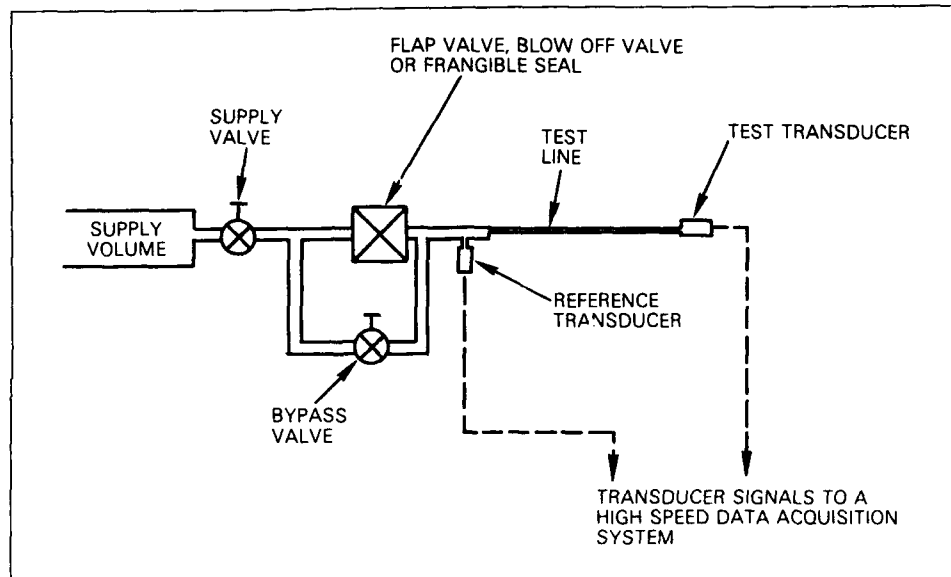


Fig. 5.3-3 Measurement of dynamic response of a pressure system

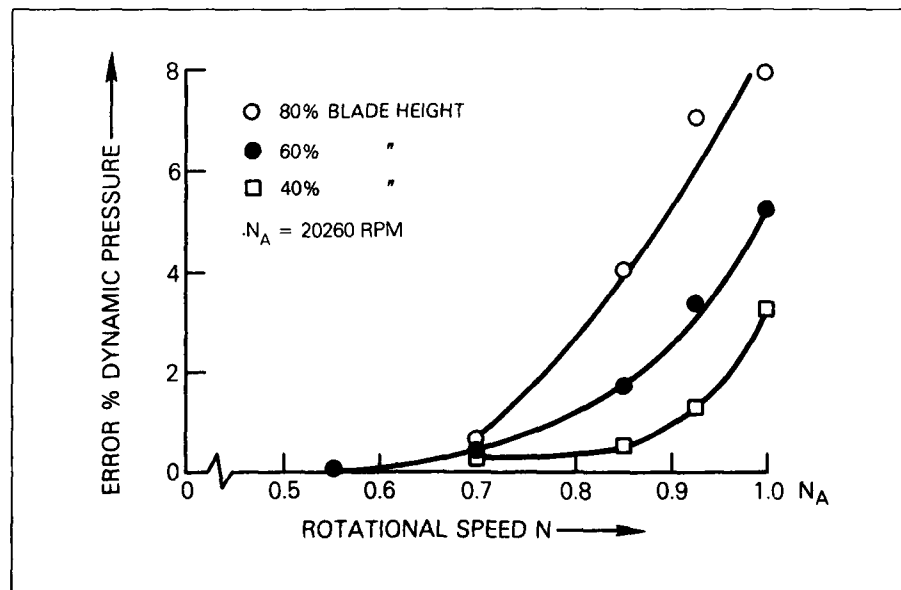


Fig. 5.3-4 Error of total pressure measurement behind a transonic compressor rotor

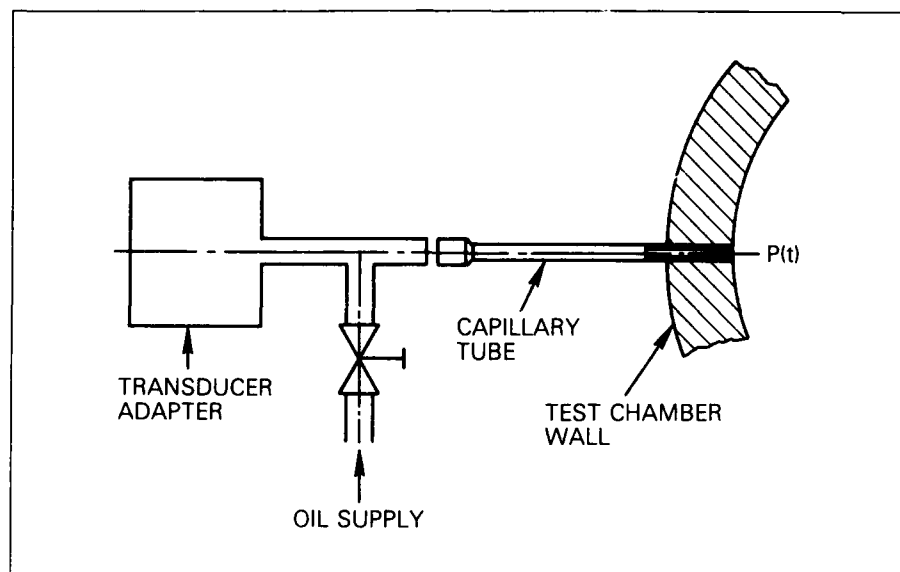


Fig. 5.3-5 Fluid-filled probe

fluid-filled probes as described in Reference 5.3-4 and shown in Figure 5.3-5.

#### Manifolded Pressure Probes

Connecting an array of sensors to a plenum and measuring the plenum pressure is a common practice in pressure measurement. The plenum pressure is equal, under certain restrictive assumptions, to the average pressure at the individual sensors. The restriction is basically that the pressure differentials across each sensor tube (impact tube or static tap) are small such that flow through each port is proportional to  $(P_i - P_p)$  and also that the geometry and, therefore, the flow coefficient of each port is the same. In this case using the fact that at equilibrium the total flow entering and leaving the plenum is zero, the plenum pressure is the average of the individual pressures.

$$\sum_{i=1}^n (P_i - P_p) = 0$$

$$\text{and } P_p = \frac{1}{n} \sum P_i$$

where  $P_i$  = pressure at the  $i$ th port  
 $P_p$  = plenum pressure

If  $P_i - P_p$  is large for any  $i$ 's, the flow in that port becomes proportional to  $\sqrt{(P_i - P_p)}$  and the plenum pressure is no longer a simple average of the individual pressures. This is a function of the tube Reynolds number. If large variations occur in the pressure at the individual sensors, then internal flows may occur in the manifold which may affect the manifold pressure measurement and also lead to biased results.

#### Pressure Scanning Valves (Reference 5.3-5)

##### 1. Principle of Operation

A pressure scanning valve is a pneumatic switch,

capable of multiplexing a number of pressures, sequentially, to a single pressure transducer. Such valves have been made in a variety of ways, but the most widely used types are valves such as those made by the Scanivalve Corporation. These valves employ a matched pair of lapped surfaces, one of which rotates with respect to the other. The valve most commonly used in turbomachinery test facilities is capable of switching 48 ports to a single transducer. A cross-section of the switching module is shown in Figure 5.3-6. Note that the transducer is typically flush mounted in very close proximity to the valve in order to minimize the volume of gas subject to changes in pressure. The rotor of the valve is driven by a stepper motor, and the position of the valve is given by a digital encoder.

##### 2. Scanning Speed

The maximum rate at which pressure ports can be scanned is related to the accuracy desired for the measurement. The response time depends on the time for pressure equilibrium to be achieved in the travelling volume between the scanner and the gauge diaphragm. The time required to achieve equilibrium is a function of the size of the travelling volume and the magnitude of the pressure change. Using a flush-mounted transducer as pictured in Figure 5.3-6 scan rates up to 20-25 ports/sec. can be considered practical from an aerodynamic standpoint. However, actual rates used are usually somewhat slower. To achieve still higher scanning rates while maintaining adequate residence time on each port to achieve equilibrium, individually controlled units can be stepped in sequence such that, for 12 units, the overall rate is 12 times that for a single unit.

Through this scheme, the transducers of an arbitrary number of valves are read in sequence. When data from the

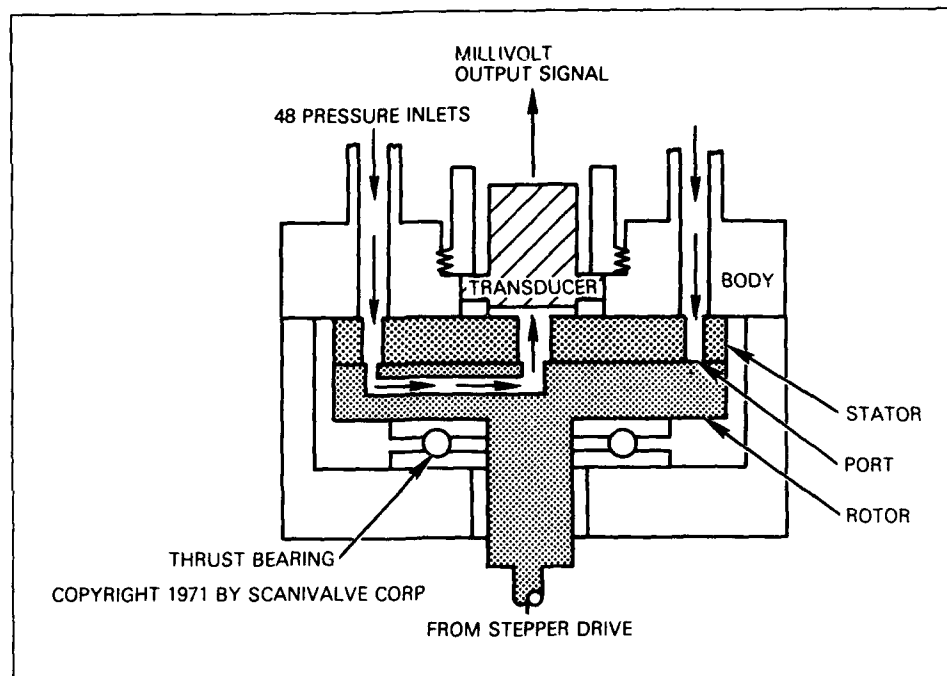


Fig. 5.3-6 Pressure scanner module

first valve has been recorded, that valve immediately indexes to its next port and waits while all other valves are read in sequence. This control scheme is applied to all other valves in the group. Thus the settling time available for any one valve is the time required for all valves to be read in sequence.

#### 5.3.4 Pressure Transducers

##### Specification and Calibration

Pressure transducers are defined here as the devices which convert the pneumatic signal into an electrical signal. A wide variety of such devices are available with strain-gauged diaphragm, vibrating cylinder, capacitive and Bourdon tube types being the most commonly used in the turbine engine industry. Most commonly used transducers such as the strain-gauged diaphragm type are analog, open loop transducers in which the pressure sensitive member deflects proportionally to the applied pressure, and the electrical output is continuous. A cut-away of a typical strain-gauge diaphragm transducer is shown in Figure 5.3-7. Also, in common use are certain intrinsically digital transducers such as the vibrating cylinder and beam types in which the number of vibration cycles in a fixed time are counted. Finally, certain very precise pressure transducers and pressure generators are closed loop or null balance types in which the pressure sensitive element is restored to zero deflection before a reading is taken. For details on specific types, the reader is referred to the references and to manufacturers' literature. A comprehensive review and summary of characteristics of pressure transducers including a listing of suppliers is given in References 5.1-3

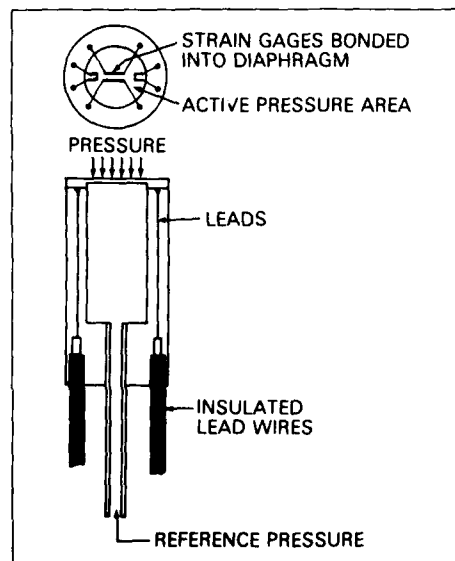


Fig. 5.3-7 Cut-away view of strain-gauged diaphragm transducer

and 5.1-6. In specifying a transducer for application in turbine component testing, the following are the important considerations:

**Range:** Most manufacturers recommend a maximum pressure based on a specified departure from linear response. Ordinarily, a transducer should be selected which will operate for the given test at 50 to 90 percent of its full scale range.

**Overrange:** This is usually the maximum pressure the transducer can sustain without damage. Overrange operation can result in calibration shifts in some transducers. Where overrange operation is necessary, some transducers provide positive stops to avoid distressing the diaphragm, or other mechanical member.

**Reference Pressure:** Arrangements available include: gauge — referenced to ambient through an open tube, absolute — referenced to zero in a sealed internal cavity, differential — referenced to a second pressure source. Some transducers are provided with sealed internal gauge references.

**Sensitivity:** Electric output per unit pressure input such as millivolts per psig. Usually refers to the average value over the operating range.

**Resonance Frequency:** In a diaphragm transducer, the resonant frequency of the diaphragm. For non-steady measurements, the resonant frequency should be typically five times the maximum frequency to be measured. In steady state measurements, it is only necessary to ensure that excitation of the transducer resonant frequency is avoided.

**Output Impedance:** Important for the design of the data acquisition system. Affects input filter characteristics.

**Non-linearity:** A variety of specific definitions are used but typically refers to the maximum deviation of any calibration points from a best straight line fit. Where detailed calibration curves are used linearity may not be as important as stability of the calibration.

**Hysteresis:** This is the tendency of the transducer to produce a different output when a given pressure is approached from a higher value or a lower value. It can have a number of specific definitions but is typically quoted as the maximum difference to be expected in percent of full scale.

**Temperature Range:** This can mean either the temperature range over which the stated transducer specifications are valid or alternatively the range over which the transducer can operate without damage. In transducers having built-in temperature compensation, the former is frequently called the compensated temperature range and the latter the operating temperature range. The upper and lower temperature limits are used to specify the range; and, where the exact meaning is not clear, one should check with the manufacturer.

**Thermal Sensitivity Shift:** All pressure transducers exhibit more or less temperature dependence and most include some built in means of compensation. The remaining effects are specified as percent change in sensitivity over the given temperature range.

**Thermal Zero Shift:** In addition to the sensitivity shift, most transducers exhibit a temperature dependent zero shift which requires internal compensation. The residual effect is again typically specified as max. zero shift over the operating temperature range.

**Acceleration Sensitivity:** Most transducers are more or less sensitive to shock and mechanical strains. One of several indicators of such sensitivity is this specification given as percent full scale per acceleration.

**Media Compatibility:** Since some portion of the sensitive part of the transducer must come in contact with the medium in which the pressure is to be measured, restrictions are frequently placed on the nature of this medium. In gas turbine applications, the transducer must be tolerant of water and combustion gases. Transducers designed for use with liquid water, fuel, or oil are sometimes referred to as "wet" transducers.

**Accuracy:** The meaning of the term "accuracy" sometimes specified by the transducer supplier should be obtained from that supplier. It frequently is defined as the root sum square of linearity, hysteresis, and repeatability as obtained under some prescribed conditions in the supplier laboratory tests. The user should consider it as a guide only and in any given measurement system, the "uncertainty" attributable to the transducer should be obtained via the defined measurement process and calibration hierarchy as described elsewhere in this document.

**Precision/Repeatability:** Again, the transducer supplier should be queried for the specific definition when these terms are included in the transducer specification. Within the measurement uncertainty protocol used in this document, this normally should be the "precision error" obtained by the supplier in his own evaluations and should be used as a guide only.

The above transducer specifications are important considerations in the selection of a transducer but are not sufficient in themselves to allow the accuracy of a transducer to be deduced. The sensitivity and transducer zero drift with time, temperature, vibration and strain environment such that the accuracy must ordinarily be determined in the environment of actual use by statistical analysis of actual in-place calibration records.

#### Calibration

Calibration of the transducer can be accomplished off-line or on-line. In an off-line calibration, the transducer is typically calibrated before and after the test measurements are taken and the time span between the calibration and the tests can be from several hours to several days. This has several disadvantages. Unless the transducer is located in a temperature-controlled environment, its calibration will generally change with ambient temperature changes. Also, its output will vary with changes in its power supply voltage. In addition, the performance of any amplifier interposed between the transducer and the analog/digital converter will affect the final output. All of these devices must be calibrated, and the calibrations must be maintained.

In systems which use scanning valves, the best solution to these problems is the use of on-line calibration. With a pressure scanning valve, the use of on-line calibration results in the entire pressure measurement system including amplifiers, power supplies, and voltmeters being calibrated every time a scan is accomplished. This is done by including several pressures of accurately known magnitude among those scanned by each valve. Then a new calibration is performed for each valve during each scan by the data reduction software, prior to converting all remaining test pressures to engineering units. In this manner, all errors due to temperature drift, power supply drift, and scale factor errors are substantially eliminated. The overall error is then reduced to the nonlinearity of the transducer between calibration pressures, the accuracy of the calibration pressures themselves, and the accuracy of the analog/digital converter. The precision of the on-line calibration process is

determined by statistical analysis of successive calibrations by recording the "as is" differences between the transducer being calibrated and the standard pressure ("as is" = before adjustment). The uncertainty of the standards used in this on-line calibration are counted as "bias" in the total uncertainty model.

When using transducers in which hysteresis is a significant error source, it is possible to set up a scanning valve with a vacuum applied to every other port and in this way assure that the transducer always approaches the measured pressure from one direction. This, of course, cuts the number of measurement channels in half; and, therefore, it should only be used when sufficient channel capacity is available and when there is clear evidence that it is necessary to achieve the required accuracy goals. Some pressure measurement system designers argue that, in turbomachinery testing, the fluctuations inherent in controlling the operating point and the normal unsteadiness of the flow cause the transducer to experience small upward and downward excursions which make hysteresis correction unnecessary and indistinguishable in practice from repeatability. Given an on-line calibration capability, an analysis of the system calibration history will disclose whether or not hysteresis is significant.

#### *Transducer Arrays — Electronic Pressure Sensors*

##### *1. Principle of Operation*

The advent of miniature semiconductor strain gauge

transducers and solid state electronics have made electronic multiplexing relatively competitive with pneumatic multiplexing in cost. This offers the additional advantages of much higher scanning rates and greater flexibility in designing an installation because of the small size of the units. Units are now available with up to 48 input channels. A 48-channel module is pictured in Figure 5.3-8. It contains 48 silicon integrated circuit pressure transducers, a low-level multiplexer and instrumentation amplifier, and a pneumatically operated valve which allows each sensor to be automatically switched from its input pressure to a calibration manifold at any time during a test. By re-calibrating frequently although not necessarily for every data point, zero, span, non-linearity, and thermal errors can be nearly eliminated so that the overall accuracy approaches that of the calibration pressures just as with a pressure scanning valve.

##### *2. Scanning Speed and Flexibility*

Electronic pressure scanners may be operated at data rates of 10,000—20,000 samples per second — about 1,000 times faster than a pressure scanning valve. This speed advantage can be used in a variety of ways including the capturing of transients as well as the averaging of many scans per data point in order to reduce electronic and pneumatic noise. These systems are typically controlled by a programmable

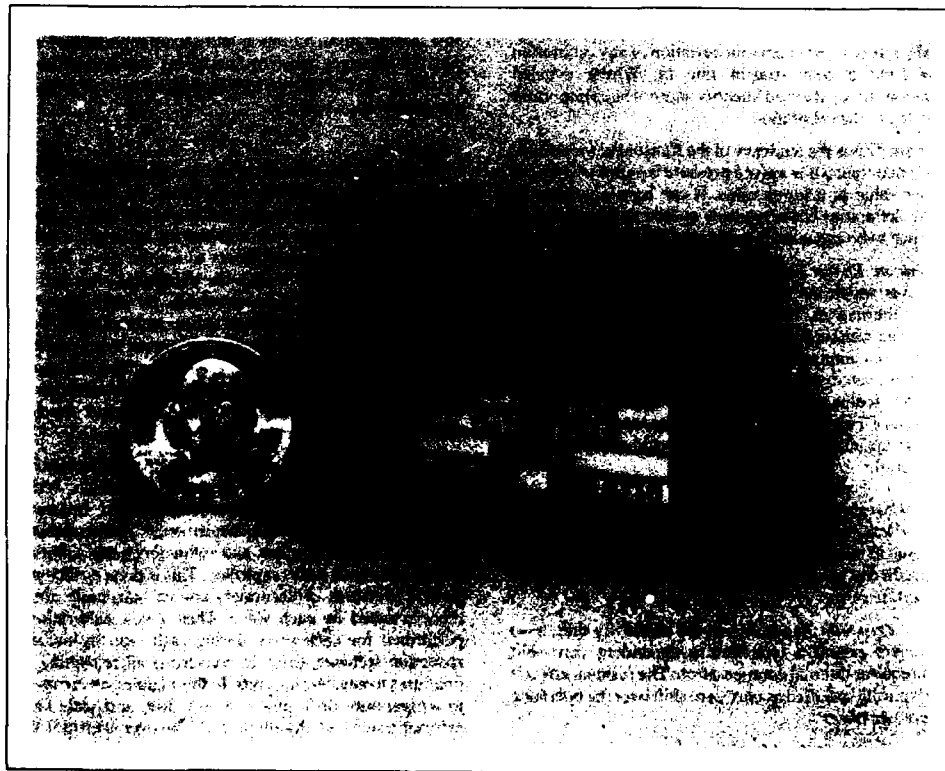


Fig. 5.3-8 Electronic pressure scanning module

microprocessor allowing great flexibility in both the configuration and operation of a complete pressure measurement system.

#### *Transducer Calibration Reference Pressures*

##### **1. Primary Standard**

The accuracy of a precision pressure measuring system can be no greater than the accuracy of the sources of pressure used for its calibration. Hence, the accuracy and long-term reliability of these sources is basic to achieving good and consistent performance from any pressure measuring system. The least controversial and most reliable standard is a so-called "primary" standard. A pressure regulator employing dead-weights is a device of this type. An accurate calibration pressure is produced by bringing into equilibrium the pneumatic pressure on one side of a piston of known area by weights of known mass on the other side. A device of this type is illustrated in Figure 5.1-2. This example uses a spherical piston (a hardened ceramic ball) of a controlled diameter in a tapered controlled clearance nozzle as the piston-cylinder combination.

In operation, a constant supply pressure is introduced through a flow regulator, building pressure under the ball, lifting it toward the top edge of the nozzle. As the equator of the ball is positioned at the top of the nozzle, the ball uncovers more of the nozzle until escaping air is equal to that supplied by the regulator. At this position, equilibrium is reached, and the ball is supported by the air pressure under it. This pressure, which is also the output pressure, is proportional to the weight load. During operation, the ball is centred by a dynamic film of air, eliminating physical contact between the ball and nozzle.

When weights are added or removed from the weight carrier, the ball rises or lowers affecting the airflow. The regulator senses the change in flow and adjusts the pressure under the ball to bring the system into equilibrium, changing the output pressure accordingly. Thus, regulation of output pressure is automatic with changes in weight mass on the spherical piston.

Since the force is applied by a weight in these gages, the two most important corrections which must be made in order to achieve high accuracy are for local gravity and for buoyancy of the weights (References 5.1.1 and 5.1.2).

The calibration uncertainty of such a device is typically 0.025 percent of output pressure. Repeatability of production units is 0.005 percent of output reading. Devices of this type, when used as working standards, must be functionally checked periodically against laboratory standards since accumulation of dirt on the piston and cylinder surfaces can affect their accuracy. Under ideal environmental conditions, they are extremely stable.

##### **2. Secondary Pressure Standards**

An alternative to a primary pressure standard is a secondary standard which is periodically recalibrated against a primary standard. The best of these employ a quartz crystal element caused to vibrate at its resonant frequency or a quartz Bourdon tube. These units have the disadvantages of requiring periodic recalibration and of being electronic devices subject to occasional failure and repair. However, they have the advantage

of being inherently digital devices which are directly compatible with computer-controlled instrumentation and calibration systems. As employed in a pressure calibration system, the calibration pressures are produced by conventional pressure regulators having no inherent measuring capacity of their own. The calibration pressures are then measured during a calibration with one or more of these secondary standards.

#### **5.3.5 System Functional Checks**

##### *Error Detection*

##### **1. Leaks**

Given an accurate pressure scanning system with frequent calibration, the principal sources of error are leaks and hook-up errors. There are many techniques for leak testing pressure lines one at a time including leak-down rate tests, smoke tests, bubble tests, and helium leak checks. One technique that is fast and simple for many turbomachine component tests is to pressurize the entire test vehicle and take a data scan. Only a small overpressure is required, and it is not important if the test vehicle itself has numerous minor leaks to its surroundings. What is important is that the air in the test vehicle is basically stagnant. Since the vast majority of pressures measured are from either probes or static taps located within the vehicle, they should all read the same if they are leak free. Any leaking pressure lines will be immediately apparent from a data scan.

When pressurization of the entire test vehicle is not possible, leak checking must be carried out on individual probes and rakes. Records of leak check results should be kept.

##### **2. Hook-Up Errors**

Hook-up errors are among the hardest of all to find because they frequently have little impact on the averaged test results. The best way to avoid them is by very thorough labelling of pressure lines as they are installed in a test vehicle and great care in making the connections. However they will still sometimes occur. Whenever the measurements are distributed in such a manner that they can be mapped onto a line or a surface, a great aid to finding hook-up errors is displaying radial or circumferential profiles or contour plots of the data. Hook-up errors can then show up as outliers in otherwise smooth plots. This "profiling" of the data should be standard practice for functional checking of the system.

#### **5.4 Pressure Measurement Uncertainty Analysis**

As described elsewhere in Section 3 of this document, systematic methods are evolving and being accepted by the international technical community for estimating the uncertainty of measurements (Reference 5.3-7). The initial step required in making such an estimate is to create a model of the measurement process which permits the sources of all error to be identified as well as provides a framework to account for the presence of interfering and modifying inputs to the measurement system which affect the output. Referring to Figure 5.1-1 which represents a measurement system configuration, one can trace a path from the physical quantity being measured, in this case say total pressure, to the output presentation to the observer as follows:

#### 5.4.1 Measurement System Model

Measurand, Total Pressure  $P_T$  at a specific required location in a flowing gas:

- **Pressure Recovery** — Pressure probes should be designed for negligible recovery error over the full range of expected flow angles. Where this cannot be

Components of the Model	Sources of Error
A. Pressure Probe Components	
1. Sensor & Sensor Support including traversing system probe calibration lab.	<ul style="list-style-type: none"> <li>• Blockage, Hole Size vs. Gradient</li> <li>• Streamline Displacement</li> <li>• Pressure recovery Calibration vs Mn</li> <li>• X, Y, Z positioning error</li> </ul>
2. Connecting tubing including scanning valve, tees, etc.	<ul style="list-style-type: none"> <li>• Time response</li> <li>• Averaging Properties — Bias</li> </ul>
B. Transducer with excitation and signal conditioning	<ul style="list-style-type: none"> <li>• Primary Calibration Hierarchy</li> <li>• Excitation Voltage Error</li> <li>• Temp. &amp; Common Mode Pressure Corrections</li> </ul>
C. Data Acquisition System (Output = Volts)	
<ul style="list-style-type: none"> <li>• On-Line Pressure Standards</li> <li>• Filtering</li> <li>• Multiplexing, Voltage Measurement</li> <li>• Digital Resolution (Least Count)</li> </ul>	<ul style="list-style-type: none"> <li>• Voltage Measurement Error</li> <li>• Secondary Calibration</li> </ul>
D. Data Reduction Recording & Display (Output = Pressure)	
<ul style="list-style-type: none"> <li>• Conversion voltage to pressure</li> <li>• Data reduction software</li> <li>• Weighting &amp; average, space &amp; time</li> <li>• Dynamic compensation</li> </ul>	<ul style="list-style-type: none"> <li>• Calibration curve or table</li> <li>• Weighting &amp; averaging errors</li> <li>• Computational Resolution</li> <li>• Corrections for time delay effects</li> </ul>

The following discussion will elaborate on the error sources listed above and describe means for estimating magnitudes.

achieved, an uncertainty estimate should be made from the probe calibration data.

The system in Figure 5.1-1 provides on-line pressure standards for secondary calibration of the scanivalve transducer during each data scan as described in Section 5.3-4. A more detailed description of this approach is given in Reference 5.3-8.

All of the above sensor and sensor support errors are *errors of method*. Since they are not expected to vary at random in a given test, they are *bias* errors.

#### 5.4.2 Pressure Probe Error Sources

- **Blockage** — Good design practice attempts to make uncertainty in the pressure measurement due to blockage negligibly small, but it is very difficult to achieve this. Effects should be determined by systematic removal of probes, by traversing, by arrays of wall statics and by analysis. The magnitude varies greatly depending on the particular circumstances.
- **Hole Size vs. Gradient** — Estimate from information given in Section 5.2. Calculated gradient permits the application of a known position bias usually with negligible uncertainty.
- **Streamline Displacement** — This effect is due to the sensor support, and it can be large. Again, it must be estimated from information given in Section 5.2 or other references or from calculation. It is usually applied as a known position bias with negligible uncertainty.

#### 5.4.3 Calibration, Data Acquisition, and Data Reduction Error Sources

A variety of pressure measurement system designs are possible each of which will differ in detail and, therefore, require a different elemental measurement system uncertainty model. Specific systems are described in the specimen cases (Section 8.1 and 8.2). The two primary techniques used in pressure transducer calibration, as discussed previously, are:

1. Pre-and Post-test Calibration
2. On-line Calibration

The first technique can be further broken down into methods in which the transducer is calibrated in a standards lab and those in which it is calibrated in the installed location. On-line calibration is done, by definition, with the transducer installed. Since the mechanical forces applied in transducer installation as well as the local environment can affect the transducer calibration, in-place calibration is recommended. In addition, all transducers tend to drift somewhat with time and use; and therefore, the on-line calibration approach is recommended. For purposes of illustration in this section, a system like that shown in Figure 5.1-1 will be assumed. This system uses scanning valves and

employs primary standards at the test site to do both primary and on-line secondary calibration of the pressure transducers. Calibration of a system of this type is described in Reference 5.3-8. The system has the following features:

1. Deadweight piston gauges are available in an environmentally controlled room at the test site in sufficient number to allow primary on-site calibration of all transducers at 6 points over their range. This calibration is done with the transducer mounted in the scanning valve in the same environment as when in use.
2. In addition, deadweight piston regulators are plumbed into each scanning valve to allow in-scan, on-line, secondary calibration of each transducer at 60 percent and 80 percent of its range.
3. Each scanning valve has one port devoted to a "zero" source also, either a vacuum for absolute pressure measurements or ambient for gauge pressure measurements.
4. The on-site, working standard, deadweight piston gauges are periodically checked against deadweight piston gauges traceable to a national standards laboratory via quartz Bourdon tube transfer standards in a standards laboratory. Since each deadweight gauge is a primary calibration source, this is a functional check only. These gauges, for example, require periodic cleaning, or they will not perform to their design limits. The uncertainty of this functional intercomparison with the primary gauges then sets a limit on the uncertainty of the working standard. No calibration adjustments are made to the working standard.

5. The transducers in each scanning valve are subjected periodically to an in situ 6-point calibration using the on-site working standard deadweight gauges. This calibration establishes the calibration curve shape. As described in Reference 5.3-8, the curve shape is more stable than the zero intercept and average slope of the transducer.
6. The secondary calibration of the transducer is carried out by connecting the zero pressure source and the 80 percent of span working standard pressure source to two ports of the scanning valve. On each data scan, the zero and the mean slope of the 6-point calibration curve is adjusted to agree with the applied standards. A record of the zero and 80 percent span adjustments is kept.
7. A third port of the scanning valve is supplied with pressure from a working standard source at 60 percent of full scale called the "confidence pressure". This pressure is recorded *after* adjustment of the calibration curve and a record of this data is kept.

Since the secondary calibration is carried out in situ through the same system used for the test, error sources due to electrical excitation, signal conditioning, and the recording device are included in the record of the 60 percent confidence channel check.

As an example of the results achievable, the uncertainty in pressure measurement for this system due to calibration data acquisition and data reduction error sources is as follows:

	Bias (B)	% of Reading Precision (S)
1. <i>Curve Shape Error</i> Obtained from the records of 6-point calibration data for each transducer. A second order curve fit to the 6 points is used as the calibration curve, and the Standard Error of Estimate (SEE) is determined from regression analysis. The accumulated record of SEEs is pooled to estimate this error magnitude. Since the calibration curve is fixed in any given test, it is treated as <i>bias</i> . (*Note that although the number of degrees of freedom is small in any one calibration, the pooling of SEEs from many calibrations yields over 30 degrees of freedom; and, therefore, Student's $t_{0.95} \approx 2.0$ .)	$\pm 0.03$	
2. <i>Working Transducer Error</i> Obtained from the record of confidence checks at 60 percent FS against a working standard deadweight gauge. Differences are recorded on each data scan and are accumulated data used to calculate a bias and a precision error.	$\pm 0.01$	$\pm 0.03$

	Bias (B)	% of Reading Precision (S)
3. <i>Working Standard Deadweight Gauge (DWG)</i> Records are kept of the comparison ( $Y_i$ ) of the Working Standards against a lab transfer standard quartz Bourdon tube gauge. The variability in successive comparisons is calculated as follows: $S = \sqrt{\frac{\sum (Y_i - \bar{Y})^2}{N - 1}}$ <p>This is assumed to be a measure of the random variability of the DWG during a test and treated as precision error. In addition, it is used as a function check. When the difference in any comparison exceeds a selected value, the DWG is cleaned and overhauled.</p>	$\pm 0.012$	
4. <i>Lab Transfer Standard Quartz Bourdon Tube</i> Calibration against lab primary dead-weight gauges which are traceable to NBS. The records of this "as-is" calibration of these gauges yield bias and precision. The total error is fossilized as bias since it is fixed throughout test.	$\pm 0.015$	
5. <i>Primary Laboratory Deadweight Gauges</i> Return periodically to NBS who quote $B = 0.01$ percent of reading and $2S = 0.015$ percent of reading fixed (fossilized) in any test.	$\pm 0.025$	
6. <i>Port-to-Port Precision</i> Obtained by applying a standard pressure to all ports through the test stand installed tubing and connectors.		$\pm 0.010$
7. <i>Reference Pressure</i> From records of calibration of the system ambient pressure transducer.	$\pm 0.030$	$\pm 0.030$
	$\sqrt{\sum B^2} = 0.052$	$\sqrt{\sum S^2} = 0.046$

#### Total Uncertainty

The total uncertainty due to transducer calibration, data acquisition, and data reduction error sources is:

$$U_{ADD} = \pm (\sqrt{\sum B^2} + 2\sqrt{\sum S^2})$$

(99 percent confidence)

$$= \pm (0.052 + 0.091) = \pm 0.143\%$$

$$U_{RSS} = \pm \sqrt{\sum B^2 + \sum (2S)^2}$$

(95 percent confidence)

$$= \pm \sqrt{0.00270 + .00828} = \pm 0.105\%$$

## 6. TEMPERATURE MEASUREMENT

### 6.1 Definition of System

#### 6.1.1 Introduction

Just like the measurement of pressures, temperature measurements are among the essential parameters which will be used to optimise a turbine engine (checks, performance, engine control, safety).

For development tests, the range to be covered extends from  $-60^{\circ}\text{C}$  to about  $2000^{\circ}\text{C}$  and the number of parameters to be acquired may, in some cases, comprise between 500 and 1000.

In this section, we will not cover metal temperature but only gas temperature, the measurement accuracy of which must be very carefully controlled to meet the requirements of engine development.

The section will mainly cover the use of the thermocouple as this type of sensor is widely used by engine manufacturers. Resistance temperature detectors (RTDs) are also mentioned.

As stated later in this section, sensing elements (thermocouples and resistance temperature detectors, to quote the most widely used sensors), have their own limitations which must be known to guarantee the measurement accuracy. This accuracy will depend not only on the sensing element itself, but also on the design of probe into which the element will be inserted, and to the measurement systems which will acquire the parameters.

Before going any further, the "total temperature" and "static temperature" concepts should be defined:

- The total temperature  $T_t$  of a fluid flow at a velocity  $V$  is equal to the thermodynamic temperature of the fluid, when this fluid is stopped in an adiabatic manner (in general, by a fixed sensor immersed in the flow). This temperature is a "generating parameter" of the flow, i.e. a characteristic of its energetic condition.
- The static temperature  $T_s$  of a fluid flow is the temperature which would be measured by a sensor moving along at the velocity  $V$  of the flow. This temperature is typical of the fluid thermodynamic condition, and the thermodynamic relationship between the total temperature and the static temperature is written as follows:

$$T_t = T_s + \frac{V^2}{2C_p}$$

or

$$T_t = T_s \left( 1 + \frac{\gamma - 1}{2} M^2 \right)$$

where  $C_p$  = Specific heat at constant pressure  
 $\gamma$  = Specific heat ratio.

#### 6.1.2 Temperature Measuring Systems

##### 6.1.2.1 General

For a test bench, when a temperature measurement system is considered, it is essential that all the components of the system, from the sensing element up to the signal processing unit, should be considered (calibrations, data validation, uncertainty assessment).

The next figures describe typical temperature measurement systems used during engine tests:

Figure 6.1-1: System with thermocouple and  $0^{\circ}\text{C}$  reference.

Figure 6.1-2: System with thermocouple and UTR reference (UTR = Uniform Temperature Reference).

Figure 6.1-3: System with resistance probes (the principle of 2-, 3-, or 4-wire wirings will be detailed in paragraph 6.3.2.2).

Thermocouples are generally used as sensing elements of temperature probes (one measuring point) or rakes (several measuring points).

Sometimes, miniaturized resistors are used to make the sensing elements of probes or rakes installed in inlet ducts. The probe or rake manufacturing must be based on the following main criteria:

#### *The intended application*

Measurement of steady state or high rate transient temperature.

#### *The operating conditions*

- Temperature, gas velocity and pressure levels.
- Temperature of adjacent walls (protection against the effect of heat conduction and/or radiation).
- Required level of sensing element output signal.

#### *The dimensions, determined by:*

- The number of sensors in one rake.
- The mounting boss diameter.
- The space available in the flowpath.
- The requirement for minimized flow disturbance.

#### *The mechanical integrity dependent on:*

- operating conditions.
- vibration environment.
- life.
- size.

#### *The accuracy*

Closely dependent on operating conditions, the accuracy is also determined by the quality of wire calibration and free jet calibration and by the measuring instrument used during the tests.

After the probes and rakes, the thermocouple lines will be routed up to the reference junction. Lines made with the same quality wire as thermocouples are recommended and connections should preferably be made in low temperature zones.

In general, as far as the thermocouple reference junctions are concerned, two systems are used in test benches:

- either an ice point reference box (Peltier effect box),
- or UTR, uniform temperature reference box (close to the ambient temperature, with measurement of this temperature).

In both cases, the reference junctions and the acquisition systems are connected to each other by pure copper lines in order to avoid generating parasitic electromotive forces.

The signal will normally be acquired by means of analog or digital recorder system.

When evaluating the measurement uncertainty, in particular when the temperature is measured with an automatic data recording system, the various elements of the measuring channel must be considered:

- thermocouple wire calibration.
- reference junction calibration.
- analog to digital (A-D) converter/MUX calibration.

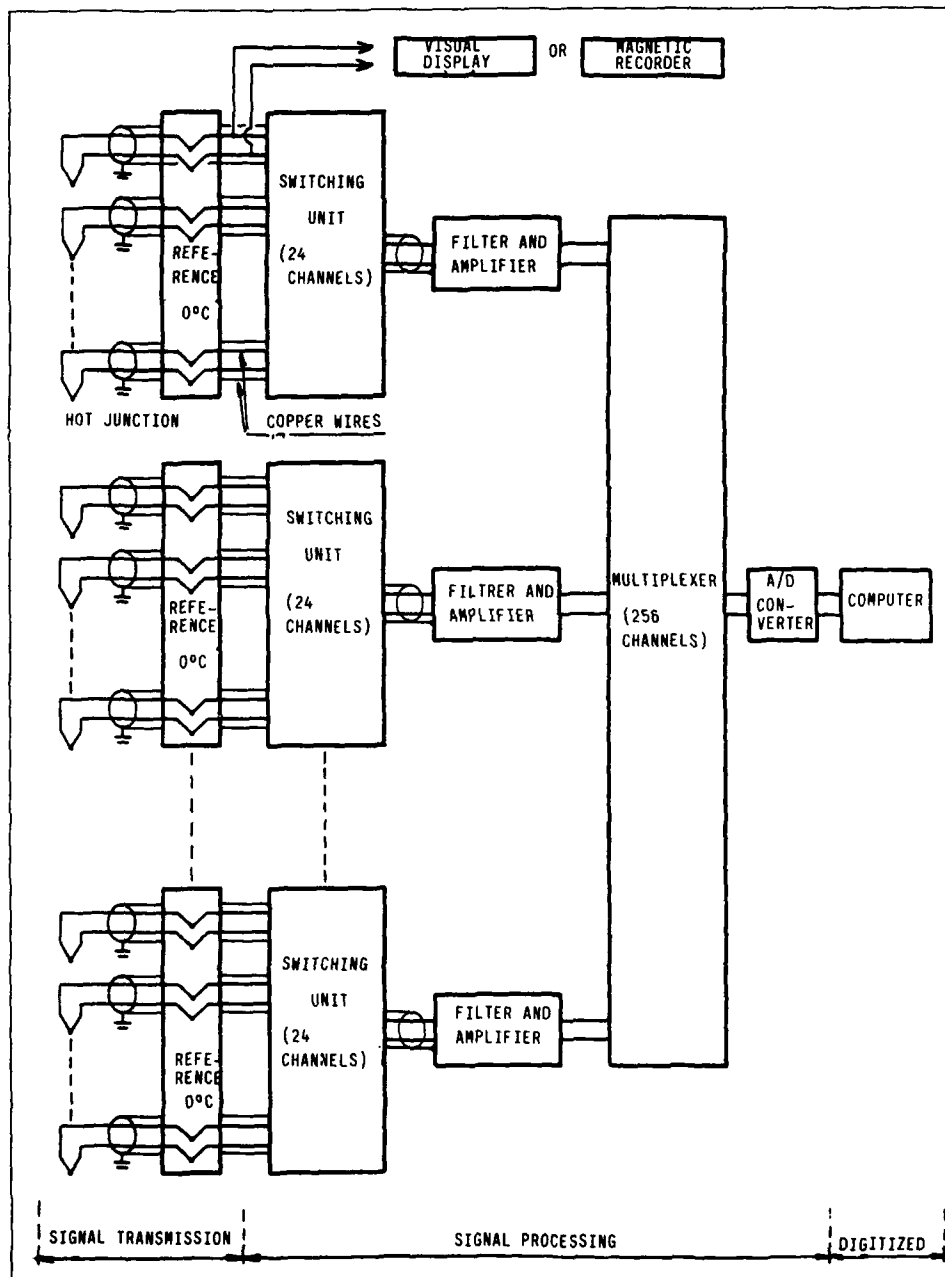


Fig. 6.1-1 Thermocouple temperature measurement system (0°C reference)

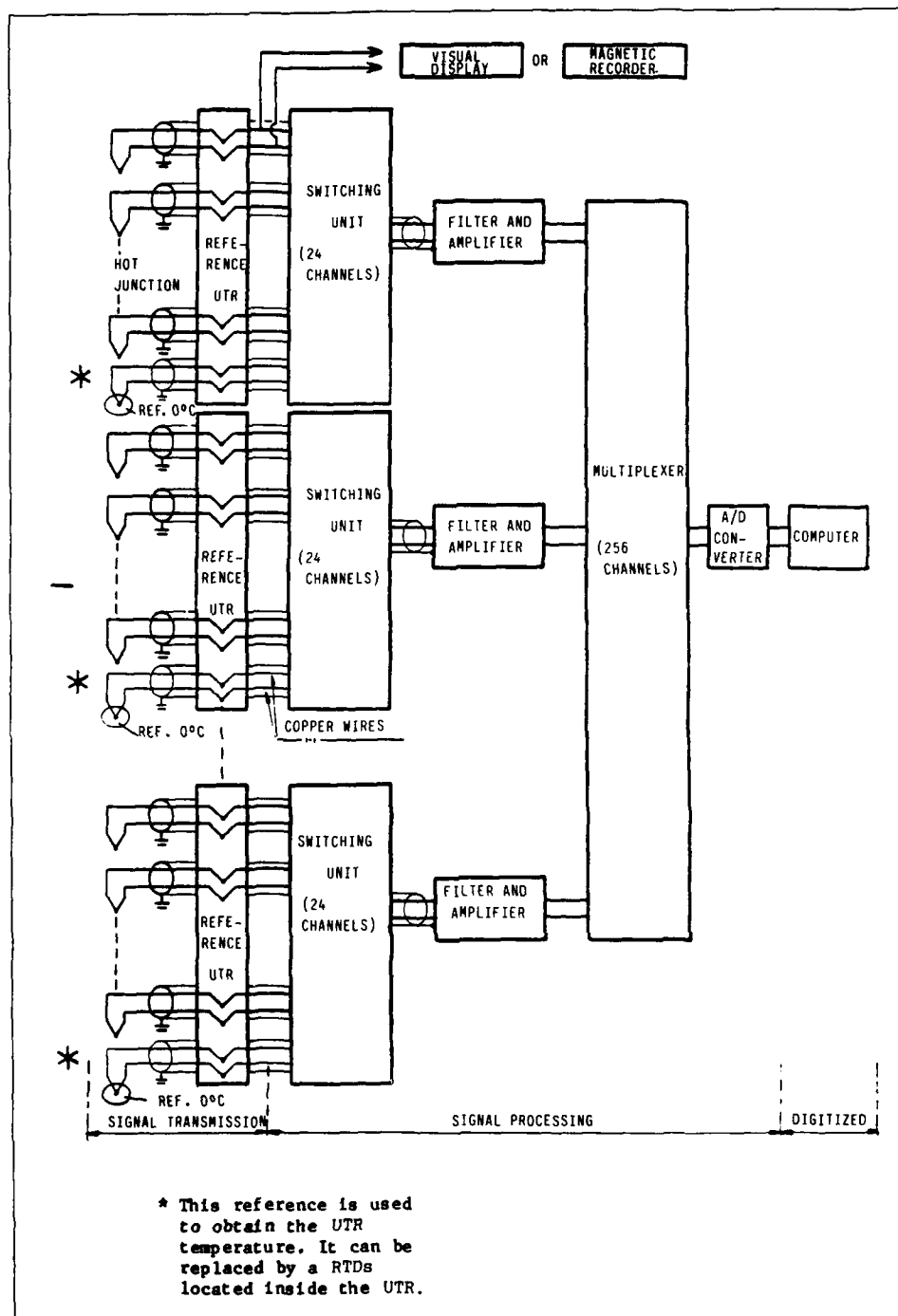


Fig. 6.1-2 Thermocouple temperature measurement system (UTR)

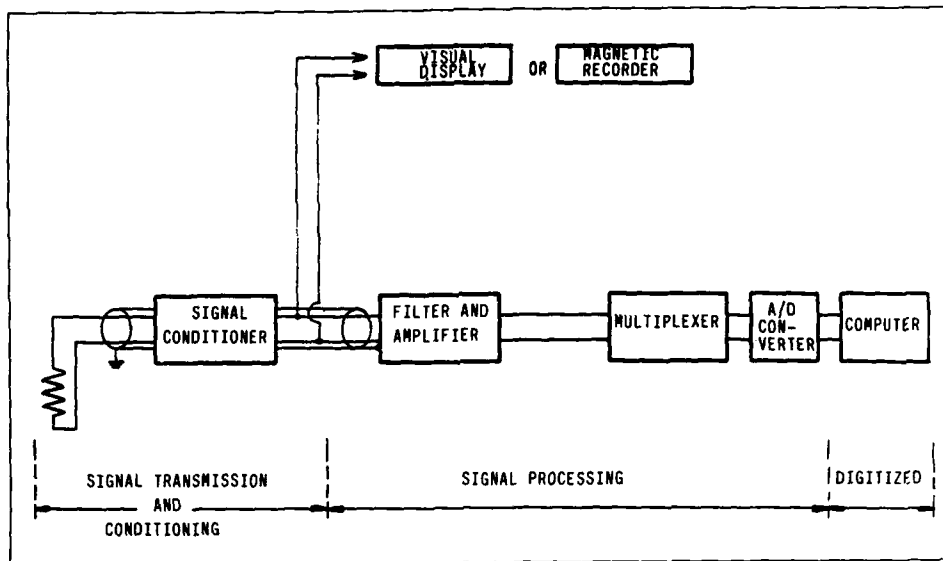


Fig. 6.1-3 Resistance temperature measurement system (single channel)

- probe recovery calibration.
- extension wire calibration.
- reference junction uniformity
- voltage to temperature conversion and truncation interpolation rounding-off

Various checks before, during and after the tests shall be carried out to support the quality of data, as described in section 6.3.5 below.

To be comprehensive, the measured data shall be issued with an uncertainty assessment.

In addition, the representativity of data relative to temperature profiles observed in flowpaths shall be assessed.

#### 6.1.2.2 Temperature Units and References Units (ref. 6.1-1 and 6.1-2)

The international scale currently applicable to temperature measurements is the International Practical Temperature Scale of 1968 (I.P.T.S-68).

The unit of the basic physical value called thermodynamic temperature, symbol  $T$ , is the Kelvin, symbol  $K$ . This value represents the  $1/273,16$  fraction of the thermodynamic temperature of the triple point of water. Thus, the temperature of the triple point of water is  $273,16 K$ .

Practically, as the degree Celsius is still in use, the Celsius temperature (symbol  $t$ ) can be expressed from the freezing point of water which is  $0,01 K$  below the temperature of the triple point of water i.e.  $273,15 K$ . In this case:

$$t^{\circ}C = T - 273,15$$

Simultaneously with the international scale, the use of other scales should be noted:

In some countries, the Fahrenheit scale ( $^{\circ}F$ ) which assigns "32" to freezing water and "212" to boiling water. Conversions to/from the Celsius scale use the following formulae:

$$t^{\circ}C = 5/9 (t^{\circ}F - 32)$$

$$t^{\circ}F = 9/5 (t^{\circ}C) + 32$$

*Note:* These conversions are for absolute values of temperature. Remember that for differential temperature e.g.  $1500^{\circ}C - 1400^{\circ}C = 100^{\circ}C$ , the conversion factor is  $9/5$  and the  $100^{\circ}C$  differential =  $180^{\circ}F$  differential.

#### References of I.P.T.S-68

The I.P.T.S-68 is based on temperature values assigned to a number of reproducible equilibrium states and on specified measuring instruments calibrated at these temperatures. Interpolation between fixed point temperatures is achieved by means of formulae used to establish the relationship between the readings of these instruments and the International Practical Temperature values.

Between  $-259,34^{\circ}C$  and  $630,74^{\circ}C$  (Antimony point), the platinum resistance thermometer is used as interpolation standard. The sensing wire must be pure annealed platinum free from strains (see paragraph 6.3.1.5).

Between  $630,74^{\circ}C$  and  $1064,43^{\circ}C$  (Gold point), the interpolation standard is the thermocouple type S:

10% Rhodium Platinum/Platinum

Above  $1064,43^{\circ}C$  the International Practical temperature of 1968 is defined using the laws governing the black body heat radiation as a function of temperature (use of an optical pyrometer).

*Note* (ref. 6.1-3 and 6.1-4)

It should be noted that I.P.T.S-68 should be revised in the

near future (I.P.T.S-90?). The changes would affect:

- the references at low temperatures.
- the extension of the use of resistance thermometers as a standard, which may replace the thermocouple type S.

## 6.2 Temperature Probe Design

Gas turbine engines offer a variety of physical and aerodynamic conditions under which temperatures have to be measured. Such conditions are operating pressure and temperature ranges, gradients and fluctuations, gas composition as well as space limitations and expected static and dynamic stress requirements for measuring probes. Therefore, the probe design will always represent a compromise between the limits of probe dimensions due to space available, strength criteria and the best possible aerodynamic probe characteristics to meet the required measurement accuracy.

The most common gas temperature sensors used in turbomachinery development are thermocouples. Compared with other sensors, such as resistance thermometers and thermistors, their advantages are:

- small size.
- adaptability to high temperature application.
- ease of manufacture.
- less expensive than all other comparable sensors.

The subject of this section is to point out essential theoretical and practical aspects of thermocouple probe design.

The object of the thermocouple probe design is to produce an environment which will allow a thermocouple to measure gas temperature with the required accuracy. The probe design depends on the severity of the surrounding conditions, the space available, the required life time, the maintenance and the static calibration of the thermocouples.

The most important aerodynamic and thermodynamic

factors affecting thermocouple probe design are:

- velocity error  $Y_v$
- conduction error  $Y_k$
- radiation error  $Y_R$
- catalytic error  $Y_C$

Possibilities to minimize these errors are covered in the following discussion.

### 6.2.1 Velocity Error $Y_v$

In a probe, the gas is not brought to rest isobarically. The indicated temperature  $T_i$ , therefore, is below the total temperature  $T_T$  of the gas. A typical total temperature sensor is shown in Fig. 6.2-1 defining the geometrical and aerodynamic parameters at the thermocouple junction.

The velocity error  $Y_v$  of a thermocouple junction can be expressed in terms of the velocity of the gas flow at the junction and the recovery factor  $r$ .

$$Y_v = T_T - T_i = (1 - r) \frac{\frac{\gamma - 1}{2} M_j^2}{1 + \frac{\gamma - 1}{2} M_j^2} \cdot T_T \quad (6.2-1)$$

where the thermocouple recovery factor  $r$  is defined as

$$r = \frac{T_i - T_s}{T_T - T_s} \quad (6.2-2)$$

Equation (6.2-2) represents the ratio of the actual to the total thermal energy that will be available from the adiabatic deceleration of the gas stream at the junction. The recovery factor  $r$  of a bare wire thermocouple is a function of the thermocouple geometry and can be varied only between narrow limits. For bare thermocouple wires recommended values of  $r$  for probe designs are:

$$\begin{aligned} \text{wires normal to flow} & \quad r = 0.68 \pm 0.07 \\ \text{wires parallel to flow} & \quad r = 0.86 \pm 0.09 \end{aligned}$$

These values are valid for  $M = 0-1.0$  and given by Moffat

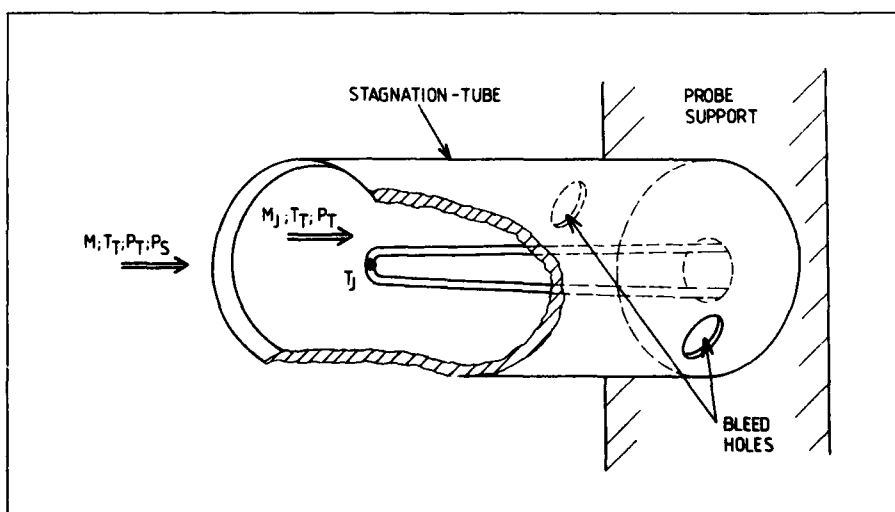


Fig. 6.2-1 Generalized total temperature sensor

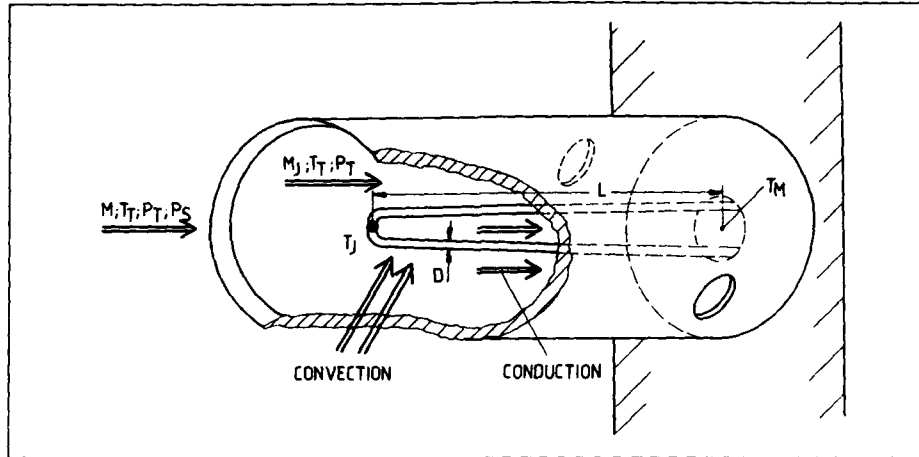


Fig. 6.2-2 Generalized total temperature sensor

(Ref. 6.2-1), who summarized various test results presented in the literature.

Thus the velocity error  $Y_v$  can be minimized by decreasing the Mach number  $M_j$  at the thermocouple junction by means of a stagnation tube. The Mach number  $M_j$  is a function of the free stream Mach number  $M_f$ , the inlet to exit (bleed hole) area ratio of the stagnation tube and the density of the gas.

Assuming free stream static conditions at the bleed holes and stagnation stream conditions within the stagnation tube,  $M_j$  can be calculated from:

$$M_j = \frac{M_f}{(A_E/A_B)} \left[ 1 + \frac{\gamma - 1}{2} \cdot M_f^2 \right]^{-(\gamma - 1)/2} \quad (6.2-3)$$

Referring to equation (6.2-3)  $M_j$  can be influenced by the area ratio ( $A_E/A_B$ )

#### 6.2.2 Conduction Error $Y_K$

It is assumed that the thermal energy transferred from the fluid to the junction wires by means of forced convection is equal to the thermal energy transfer by means of conduction along the thermocouple wires.

The thermocouple junction is generally treated as a one dimensional fin (Fig. 6.2-2), in order to obtain an expression for the conduction error  $Y_K$

$$Y_K = T_j - T_m = \frac{T_j - T_m}{\cosh L \left[ \frac{4h_c}{D \cdot k_s} \right]^{1/2}} \quad (6.2-4)$$

Referring to equation (6.2-4) conduction error  $Y_K$  can be reduced by

- decreasing  $(T_j - T_m)$ .
- increasing  $L/D$ .
- increasing the coefficient of convection heat transfer  $h_c$ .
- decreasing the coefficient of thermal conductivity  $K_s$  of the thermocouple wire.

#### 6.2.2.1 Decreasing $(T_j - T_m)$

The mount temperature  $T_m$  is the temperature at the base of

the thermocouple and is determined by the action of the external environment on the support and stagnation tube structure. The designer can control the effects of the duct wall temperature by insulation between probe and duct wall and also between thermocouple wires and probe stem, but the temperature depression affected by the shield assembly caused by radiation and velocity effects is harder to control.

#### 6.2.2.2 Increasing the Ratio $L/D$ (wire length/wire diameter)

The most effective method of reducing conduction error is to increase the ratio  $L/D$  up to the limit given by the mechanical stability and the space available. Fig. 6.2-3 is presented in Ref. 6.2-1 and illustrates the effect that the ratio  $L/D$  can have on conduction error for a thermocouple wire normal to flow.

In practical probe design,  $L/D = 10-15$  seems to be achievable and sufficient with respect to the mechanical stability of the junction for wires parallel to flow.

#### 6.2.2.3 Increasing the Coefficient of Convective Heat Transfer $h_c$

The convective heat transfer can be influenced by the probe geometry, the stagnation tube gas Reynolds number and the free stream turbulence. The Nusselt number is used to correlate data for different thermocouple junction wire diameters and to account for the changes in the thermal conductivity of the gas stream  $K_f$

$$h_c = \frac{Nu \cdot K_f}{D} \quad (6.2-5)$$

Moffat (Ref. 6.2-1) summarized various data presented in the literature and recommends the following equations for the relationship between  $Nu$  and  $Re$  (Fig. 6.2-4);

$$\text{wires parallel to flow: } Nu = (0.085 \pm 0.009) Re^{0.674} \quad (6.2-6)$$

$$\text{wires normal to flow: } Nu = (0.44 \pm 0.06) Re^{0.5} \quad (6.2-7)$$

$$Re = \frac{\rho \cdot V \cdot D}{\mu} \quad (6.2-8)$$

Referring to equation (6.2-5) convective heat transfer can be influenced by changing the wire size and the flow within the stagnation tube. Smaller wire diameter will give higher

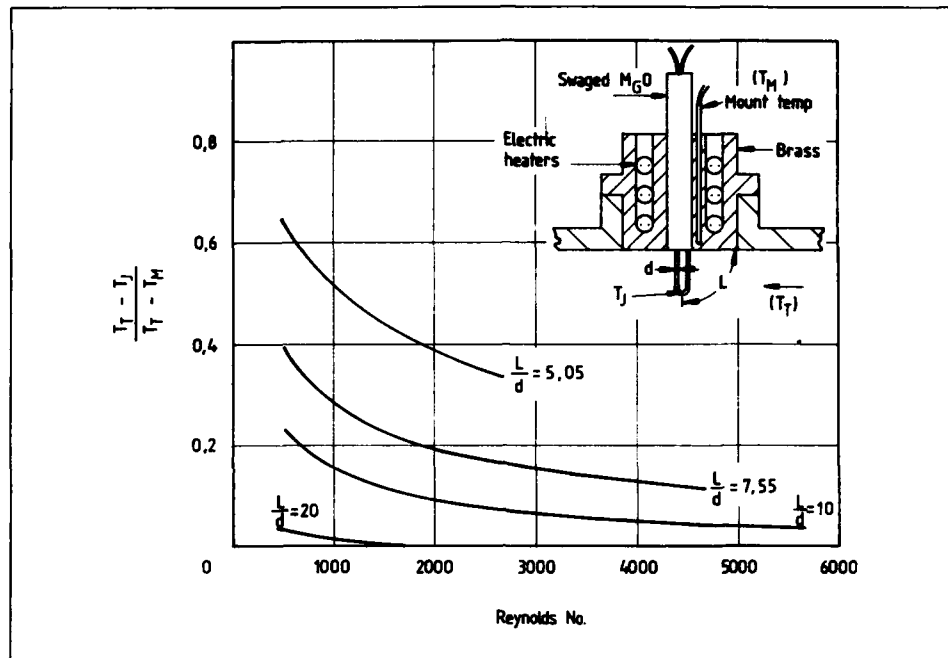


Fig. 6.2-3 Effect of the ratio of wire length to wire diameter on conduction error

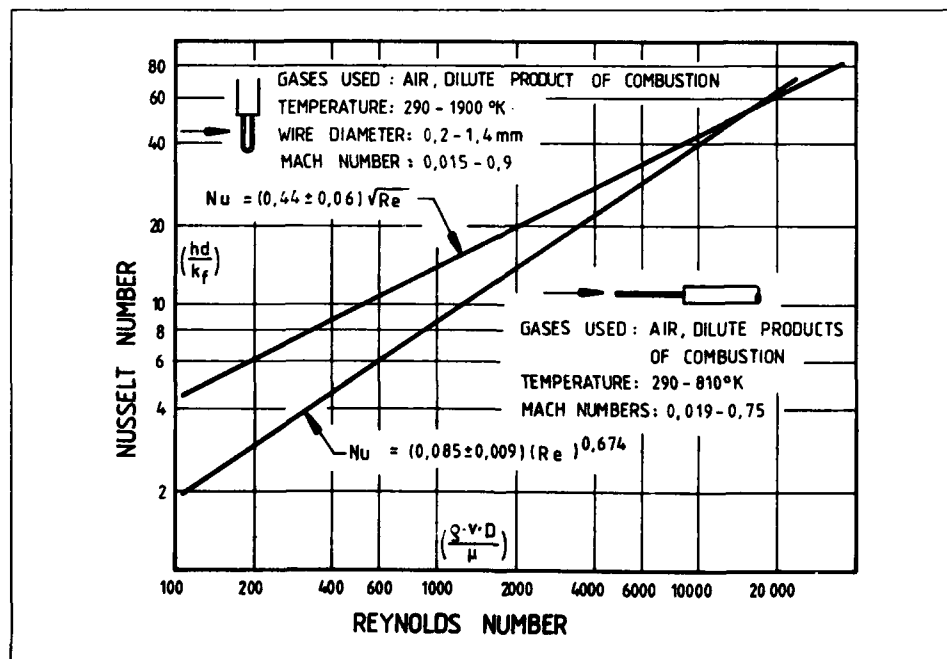


Fig. 6.2-4 Nusselt number versus Reynolds number for thermocouple junctions of round wires

values of  $h_c$ . The internal velocity can be increased up to a level of the maximum allowable velocity error.

#### 6.2.2.4 Decreasing the Coefficient of Thermal Conductivity $K_s$ of the Thermocouple Wire

The choice of thermocouple materials is generally determined by the temperature level to be measured.

Table 6.2-1 compares the coefficient of thermal conductivity  $K_s$  of various thermocouple materials. When using Copper-Constantan thermocouple wires in probe design, care has to be taken because of the very high coefficient of thermal conductivity of copper.

TABLE 6.2-1

Material	Cu	Const.	Fe	CH	AL	Pt Rh	Pt
Thermal Conductivity	at 290 K		at 290 K	at 550 K	at 1000 K		
[w/mK]	390	40	75	15	60	30	70
	at 750 K		at 1000 K				
	360		35				

#### 6.2.3 Radiation Error $Y_R$

Radiation error has to be split into three components (Fig. 6.2-5); radiation of the thermocouple junction, gas radiation and flame radiation.

- Radiation error  $Y_R$  caused by radiation from the thermocouple junction to the enclosure.

Error  $Y_R$  of the thermocouple junction inside an enclosure is expressed by the equation

$$Y_R = T_T - T_J = \frac{\sigma \cdot \epsilon}{h_c} (T_T^4 - T_J^4) \quad (6.2-9)$$

(Equation (6.2-9) is valid for probe design, when the enclosure is large compared to the wire diameter)

The emissivity  $\epsilon$  is basically fixed by the thermocouple material, but will change during engine test in an

unpredictable way due to oxidation or deposition of solids in the gas. The convective heat transfer coefficient  $h_c$  is given by the maximum internal velocity. Only the wall temperature  $T_w$  is variable for the designer. The thermocouple has to be shielded by one or more shields arranged concentrically around the thermocouple to reduce the effect of radiation from the wall to the thermocouple. Fig. 6.2-6 shows a probe tested by King (Ref. 6.2-2) having five concentric shields around the sensor. King stated that the minimum effect of a shield will reduce the radiation error by approximately

$$Y_{R,S} = \frac{1}{n+1} Y_{R,B} \quad (6.2-10)$$

This statement was confirmed by test performed by Moffat (Ref. 6.2-3).

- Radiation error caused by gas radiation and flame radiation.

For this radiation error, no general expression can be developed. Radiation heat transfer from the gas to the thermocouple is generally considered to be small at atmospheric pressure and temperatures experienced in gas turbine combustors and is usually ignored. However it is appreciated that at high pressure radiation from water vapour, carbon dioxide and, in particular, carbon may be significant. In this case it is recommended to shield the junction from seeing the flame.

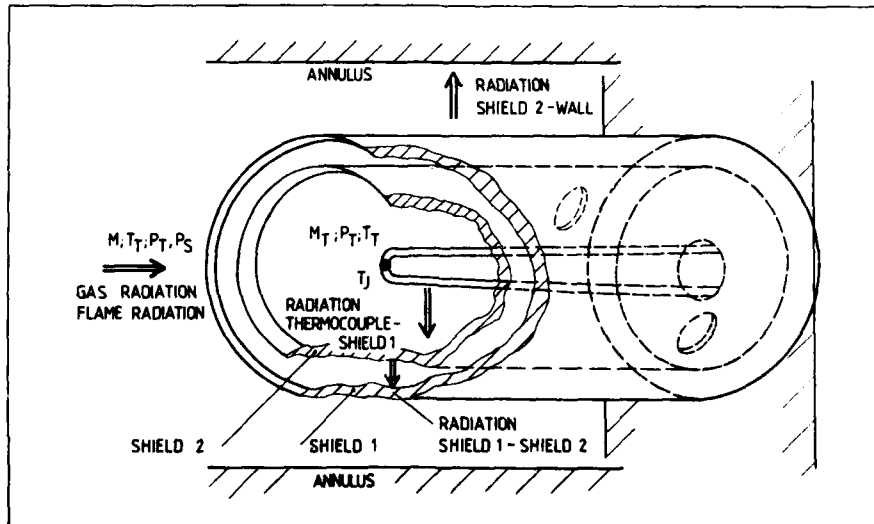


Fig. 6.2-5 Generalized total temperature sensor

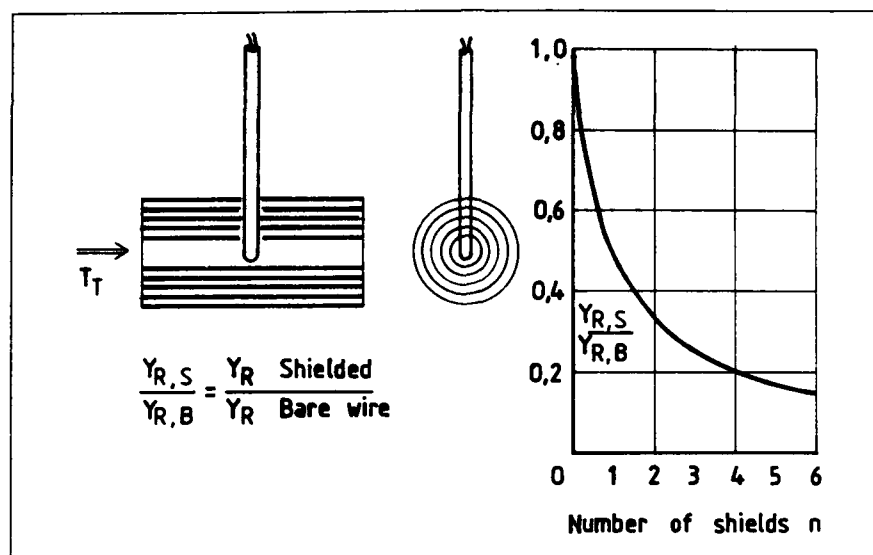


Fig. 6.2-6 Effect of radiation shields on radiation error

- Error due to catalytic effects  $Y_C$   
Surface reactions occur on platinum, rhodium and iridium in hot gases containing unburnt fuel and oxygen. This can lead to a temperature above the true temperature. Ceramic coating ( $Al_2O_3$ ) can prevent this effect.

#### 6.2.4 Static Calibration of the Temperature Probe

Static temperature calibration of the probe is desirable in order to minimize the measuring error. However, practice has shown that it is difficult to calibrate accurately an assembled probe, due to the fact that few calibration facilities have an area with constant temperature distribution in which a complex probe can be installed. Therefore the designer has to take care that it is possible to calibrate the thermocouple junction separately, and that during assembly of the probe no change in the static calibration data occurs by bending or brazing processes. In order to stabilize the thermocouple wire which is known to have drift characteristics it is recommended that heat treatment be considered. For example type K wire, when used above about 400°C should be heat treated at a temperature slightly in excess of the maximum operating temperature for at least 16 hours prior to static calibration.

#### 6.2.5 Temperature Probe Design Example

The preceding considerations pointed out possible errors in temperature measurements with thermocouple probes and how to minimize them. However, physical installation problems, vibration, dust, oil and fuel create measuring conditions which are often far from an ideal atmosphere. Finally, costs for probes and the time spent on measurements has to be considered. The designer has to take care of all these aspects to find the most reliable and accurate temperature probe design.

In the literature a number of design proposals for thermocouple probes with a single sensor can be found (Ref. 6.2-4 through 10). These probes are often designed to

measure the temperature profiles in a section by means of a traverse unit, which allows the probe to rotate around its axis as well as to move radially. It is obvious that this is a very expensive and time consuming method of measurement that is often impossible to carry out because of physical installation problems caused by the design of the engine.

Consequently, fixed rakes are more commonly used to measure the temperature profiles in a section of an engine. Rakes are probe assemblies containing two or more similar sensors or combinations of sensors at different radial positions.

A widely used technique to measure temperature profiles is to attach sensors to the leading edge of the vanes. This technique has some attractive advantages, e.g.

- instrumentation is relatively inexpensive, because no provision has to be made for installation in the casings.
- blockage is negligible.
- multistage turbomachinery can be analysed in detail on a stage by stage basis.

Fig 6.2-7 through 13 show some design examples for temperature rakes and instrumented vanes with their aerodynamic calibration data.

Rake "A" (Fig. 6.2-7) is a rake with three thermocouple sensors. The junction is arranged to be normal to the flow. The gas passes through the probe stem at the sensor position to minimize heat transfer from the junction to the stem. The side plates at the stem can be easily removed, allowing an individual static calibration of each thermocouple before and after a test. The operating limit is given by the type of wire insulation.

Rake "B" (Fig. 6.2-8) is a rake with six thermocouple sensors (Cr-Al) designed for high temperature and high pressure applications in areas with corrosive gases. Special precautions may be necessary to avoid ground loops. The thermocouples are bent less than twice the diameter of the

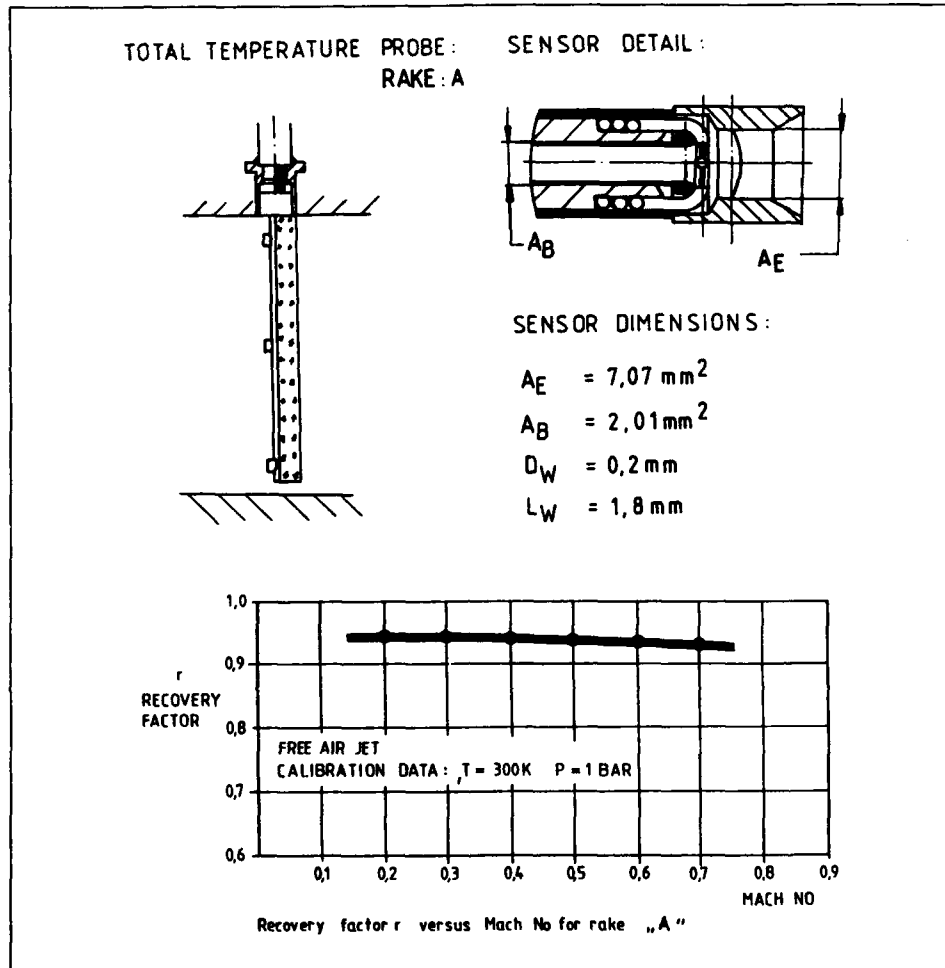


Fig. 6.2-7 Total temperature rake "A"

sheath, formed and heat treated for 16 hours at maximum operation temperature before static calibration. The rake assembly does not require any brazing so as to avoid static calibration changes during assembly. The thermocouples are held in position by specially formed metal supports within the stem.

Rake "C" (Fig. 6.2-9) is a rake with four thermocouple sensors designed for high temperature and high pressure application in small engines. Each thermocouple is placed normal to the flow in an individual chamber. The thermocouples are guided to the measuring positions from the head of the rake by individual tubes. These tubes allow installation of each thermocouple after assembly of the stem and also removal for repair.

Rake "D" (Fig. 6.2-10) is designed for a large cross section. To reduce the conduction error  $Y_K$  a ratio  $L/D = 18.5$  was achieved by forming a thermocouple loop. In addition the junction is insulated by a special part made of Polyimide with

a very low coefficient of thermal conductivity ( $k_i = 0,35 \text{ W/mK}$ ).

Rake "E" (Fig. 6.2-11) is also designed to minimize the conduction error by means of an insulation made of Polyimide.

Rake "F" (Fig. 6.2-12) is designed for small cross sections and for application in high temperature. The thermocouples are held in position by a special insert within the stem. The thermocouples are bent, formed and heat treated at the maximum operating temperature to stabilize the wire characteristics.

Rake "G" (Fig. 6.2-13) is designed to measure the temperature profile behind a combustion chamber (Ref. 6.2-11). The following criteria are the basis of the design:

- durability of the probe body and junction up to 2000 K and 20 bar. The probe body is watercooled. The

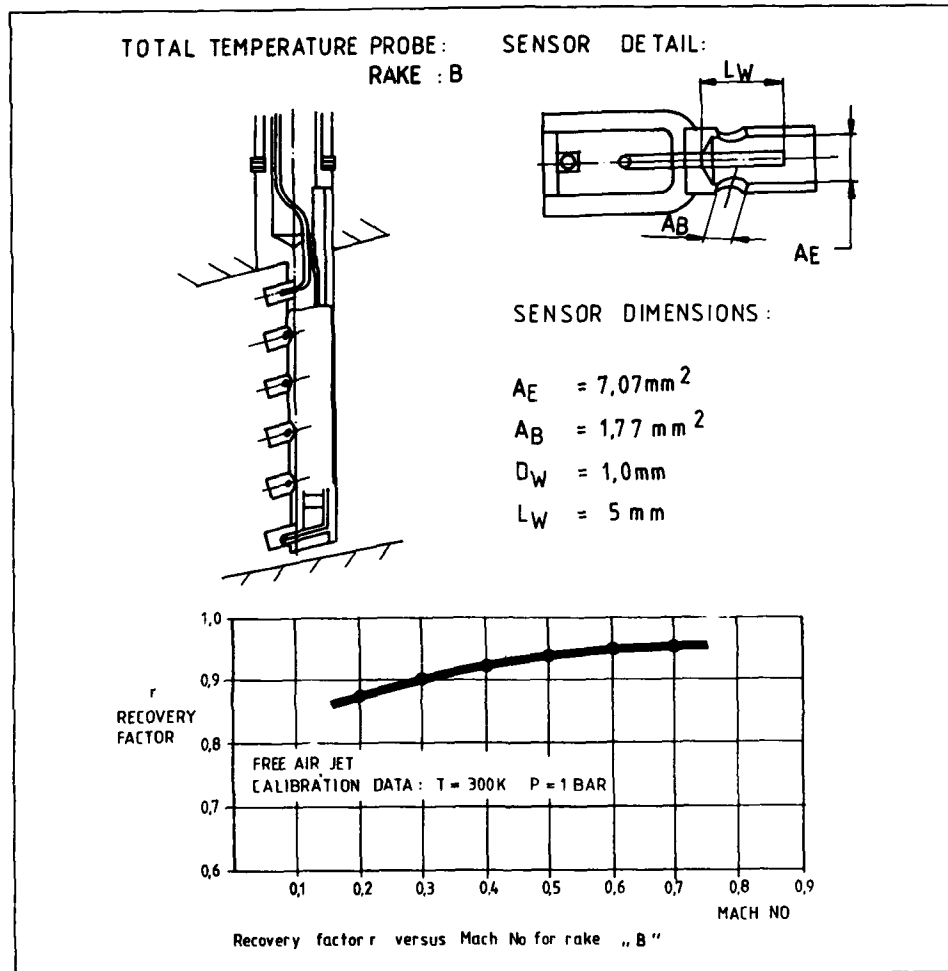


Fig. 6.2-8 Total temperature rake "B"

cooling water impinges on the hot leading surface of the probe and is drained along the inner structure. The thermocouple material is PTRh 10/PT;

- easy maintenance or replacement of the thermocouples. The teflon insulated 0,5 mm diameter thermocouple leads are separately guided within tubes in order to allow an easy replacement of each individual thermocouple;
- good reproducibility of geometrical junction configuration. The rake head is formed by ceramic tubes ( $\text{Al}_2\text{O}_3$ ) to hold the thermocouple junction. To increase the mechanical stability and to position the junction it consists of four wires (see Fig. 6.2-13);
- probe designed to measure gas temperature as near as possible to the wall;
- no catalytic effect on junction surface in the case of unburnt products in the gas.

The thermocouples are coated with a layer of  $\text{Al}_2\text{O}_3$  6–8  $\mu\text{m}$  thick. Disadvantages of the probe are high velocity, radiation and heat conduction errors. Hot gas calibration test had to be performed to create an analytical heat balance computer program. Fig. 6.2-14 demonstrates the thermocouple heat balance model and the temperature rake bead correction.

Instrumented vane "A" (Fig. 6.2-15) is a LP-Turbine vane tested in a cold flow rig. Polyimide insulated Cr-Al thermocouples are routed within the vane surface to the measuring position. An epoxy adhesive is used to fix the Kiel heads and thermocouple wires.

Instrumented vane "B" (Fig. 6.2-16) is a LP-Compressor vane with two thermocouple sensors at the leading edge. The Kiel heads are brazed by inductive heating on to the leading edge of the vane.

Instrumented vane "C" (Fig. 6.2-17) is a vane of a small

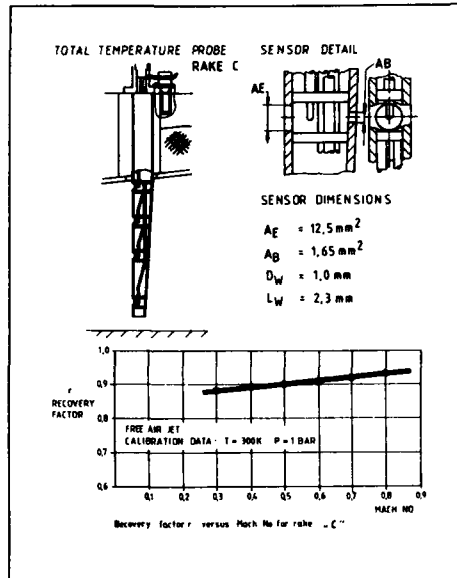


Fig. 6.2-9 Total temperature rake "C"

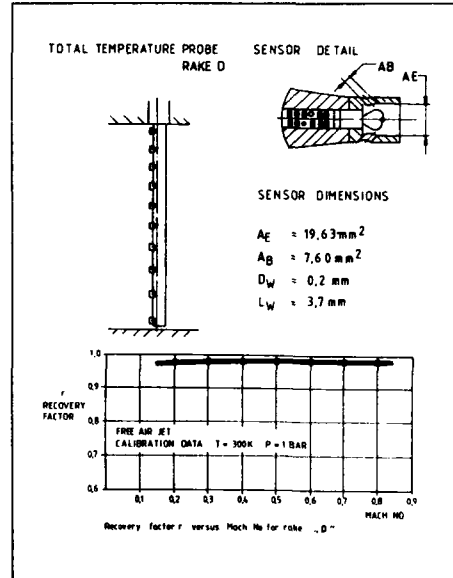


Fig. 6.2-10 Total temperature rake "D"

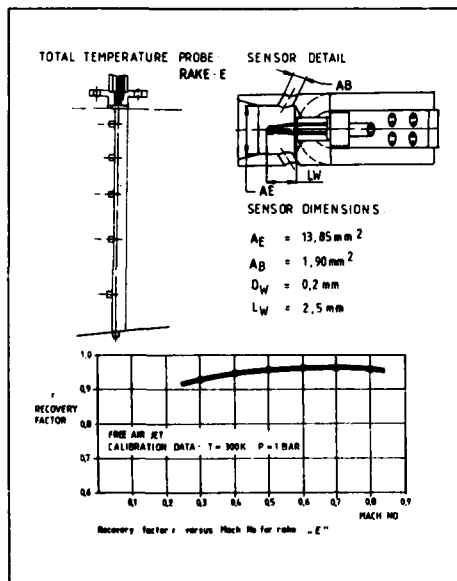


Fig. 6.2-11 Total temperature rake "E"

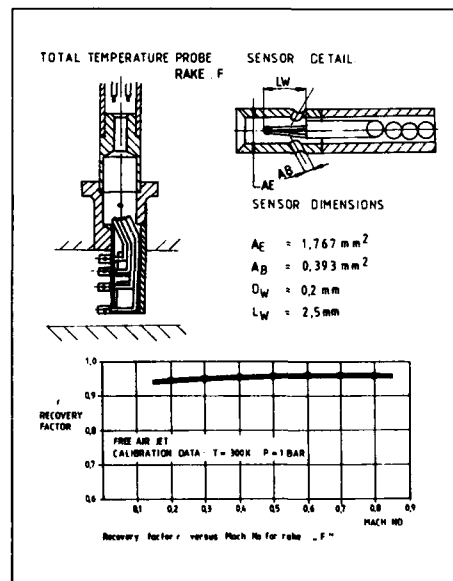


Fig. 6.2-12 Total temperature rake "F"

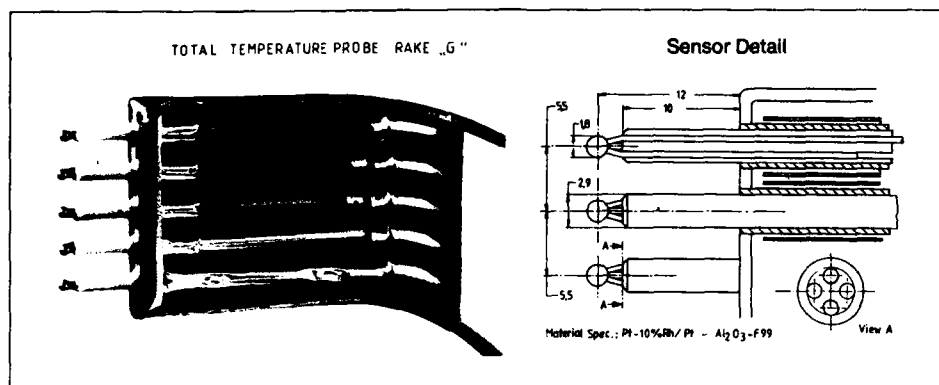


Fig. 6.2-13 Total temperature rake "G"

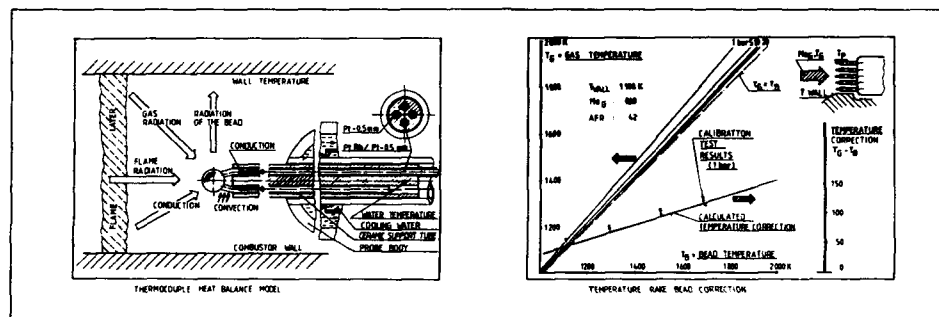


Fig. 6.2-14 Thermocouple heat balance model and temperature lead correction for rake "G"

compressor. The mechanical stability of the vane requires that the thermocouples are routed on the surface of the pressure side of the vane, fixed by micro spot welded metal sheets. A bare wire junction has to be used because the distance between rotor and stator does not permit the use of a Kiel head.

Instrumented vane "D" (Fig. 6.2-18) is a IP-Compressor vane manufactured in the same way as instrumented vane "B", but with different  $A_E/A_B$  ratio.

#### 6.2.6 Mechanical Integrity of Probe Design

The strength requirements for probe design are determined by the aerodynamic and mechanical operating conditions (Ref. 5.2-21) as:

- total temperature.
- total pressure.
- Mach number.
- angle of attack.
- engine rotational speed.
- blade passing frequencies.

In general, probe designs should take care of:

- optimal aerodynamic shaping to reduce drag.
- avoidance of stress raisers.
- reduction of mass concentrations at the end of the probe.

Whenever a probe design is critical with respect to the strength requirements the static and dynamic stresses should be determined with use of an attached strain gauge.

Probe material should be the same as that of the casings where they are installed. Fig. 5.2-23 shows a choice of material to be used in the different engine modules.

### 6.3 Recommended Practices

#### 6.3.1 Sensing Elements

##### 6.3.1.1 Sensing element calibration equipment used in test centres (Ref. 6.3-1 and 6.3-2)

To achieve the accuracy level required to meet the requirements of turbine engine development, calibration equipment must be available to test centres.

In general, in these calibration channels, the cold junction of thermocouples is immersed in an ice bath in a Dewar flask. Precautions are necessary to obtain satisfactory reference junctions (Ref. 6.3-2).

The 0°C and 100°C points are often used by engine manufacturers when calibrating the resistance and thermocouple probes. For temperatures below 0°C and up to 600°C approximately, the resistance and thermocouple probes are calibrated against a resistance thermometer (interpolation standard) which must be checked at periodic

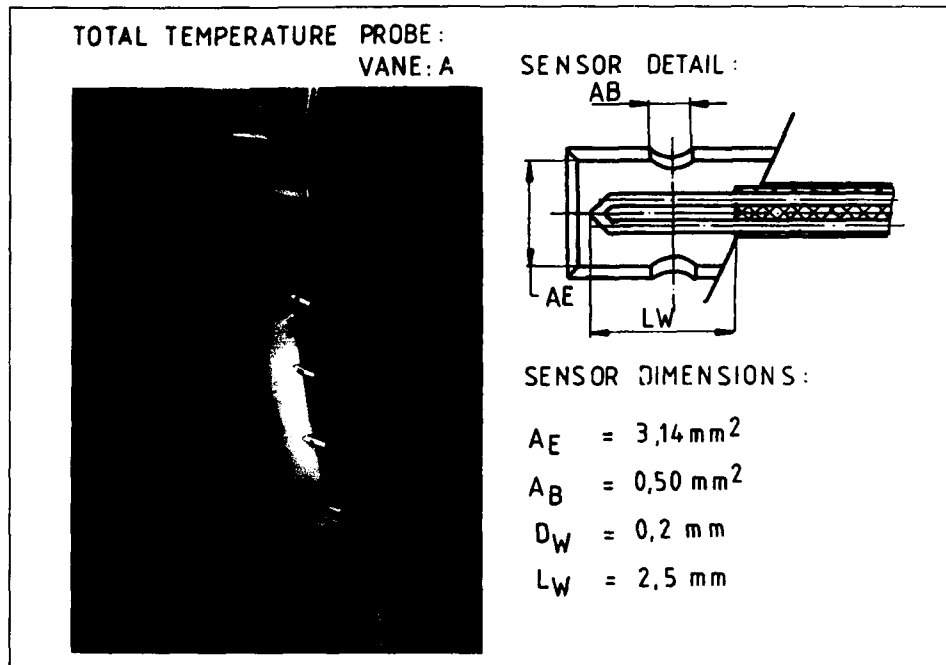


Fig. 6.2-15 Instrumented vane "A"

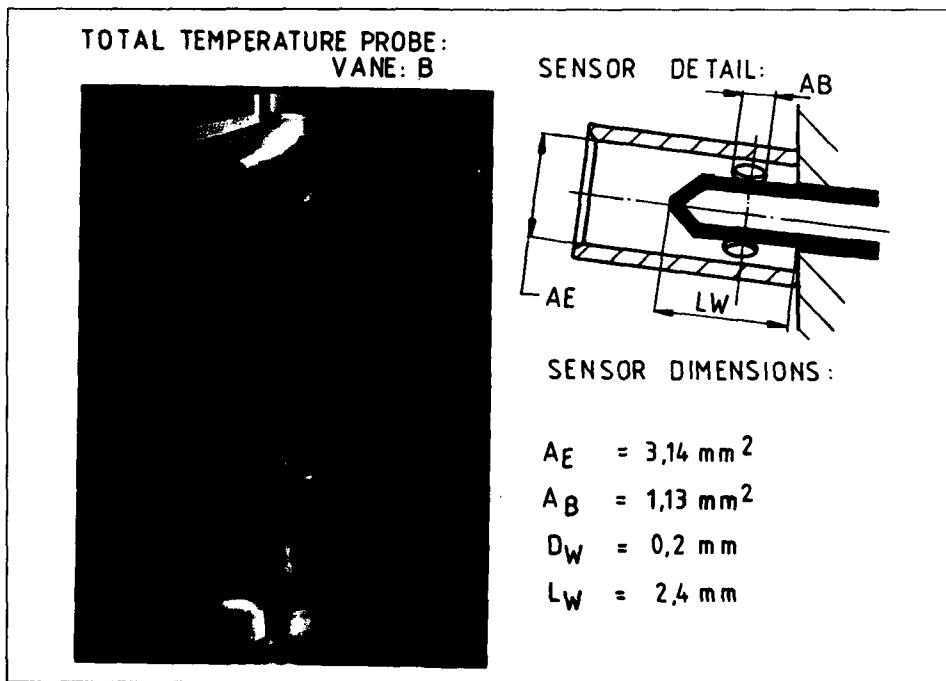


Fig. 6.2-16 Instrumented vane "B"

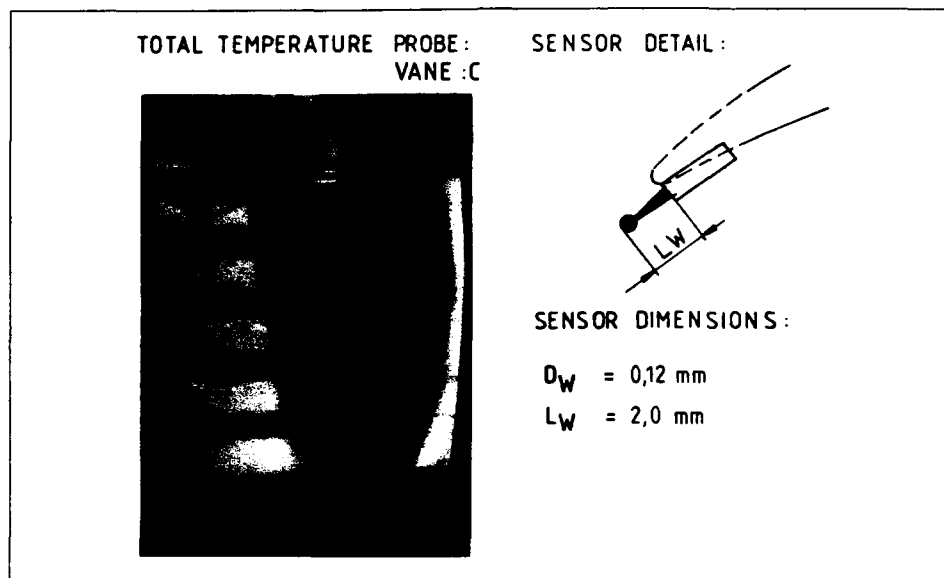


Fig. 6.2-17 Instrumented vane "C"

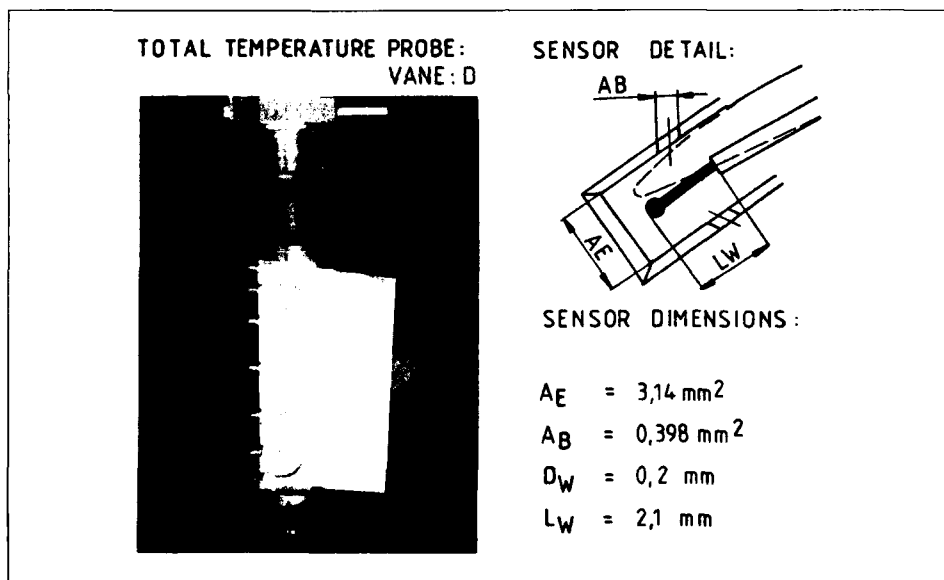


Fig. 6.2-18 Instrumented vane "D"

intervals (at least once a year) by an approved laboratory.

Depending on temperature ranges involved, the platinum thermometer and sensing elements to be calibrated are

heated in an oil bath (up to  $-200^\circ\text{C}$ ) or in a furnace at higher temperatures.

A precision heating chamber (with air stirring) may be a very convenient means of heating in the  $-70^\circ\text{C} \rightarrow +500^\circ\text{C}$

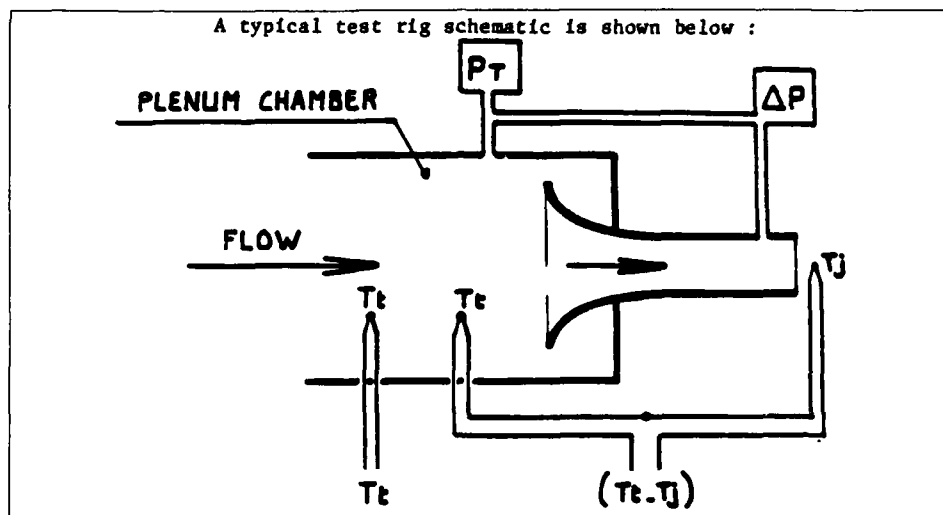


Fig. 6.3-1 Thermocouple recovery factor measurement wind-tunnel schematic

range. In the latter case, the sensor to be calibrated must be placed in high thermal inertia boxes in order to increase the temperature stability.

For temperatures above 600°C, sensing elements to be calibrated will be compared to an interpolation standard made of a 10% rhodium platinum-platinum thermocouple. In this case, an electric furnace should be used and the sensing elements to be calibrated should be placed very close to the reference thermocouple in the centre of the furnace, the assembly being protected against radiation effects by concentric cylindrical shields.

Simplified application "fixed reference points" (induction heating of small crucible containing pure metals such as those specified by I.P.T.S-68) constitute, subject to some precautions, an alternative calibration device.

Before performing such calibrations, validating the system by means of a reference thermocouple is recommended.

Whenever sensing elements are used (on engines or in laboratories) it should be highly desirable, considering the low level of signals involved, to use shielded lines to avoid induced electrical noise.

#### 6.3.1.2 Free jet aerodynamic calibration (See Ref. 6.3-3 and Section 6.2-1)

A thermocouple immersed in a flow recovers only a part of its kinetic energy. Ignoring losses by conduction or radiation, the capability of a thermocouple or sensor to recover the energy of flowing air is characterized by two factors:

— the aerodynamic recovery factor:  $r = \frac{T_t - T_s}{T_T - T_s}$

or

— the recovery ratio:  $R = \frac{T_t}{T_T}$

where  $T_j$  = temperature of the thermocouple junction (K)

$T_T$  = Total temperature of the flow (K)

$T_s$  = static temperature of the flow (K)

with  $\frac{T_T}{T_s} = 1 + \frac{\gamma - 1}{2} M_F^2$

where  $M_F$  = free stream Mach number

$\gamma$  = Air specific heat ratio.

The factors  $r$  and  $R$ , which provide similar indications, are related to each other by a relation depending on the Mach number only:

$$r = \frac{R \left( 1 + \frac{\gamma - 1}{2} M_F^2 \right) - 1}{\frac{\gamma - 1}{2} M_F^2}$$

Factors  $r$  or  $R$  close to unity may be obtained by reducing the flow velocity around the thermocouple. However, this velocity drop remains limited since a sufficient level of convection is required in order to offset conduction or radiation heat losses at the thermocouple.

Since some uncertainty is associated with the theoretical determination of  $r$  or  $R$ , these factors must be measured experimentally.

A typical test rig schematic is shown in Fig. 6.3-1.

The principle of calibration consists in comparing the signals delivered by the sensor or rake, the  $r$  and  $R$  factors of which must be determined, with those delivered by a reference thermocouple. This thermocouple is located in the plenum chamber of the test rig, and the tested sensor is located at the nozzle outlet where the Mach number is variable.

These tests should preferably be performed in ambient temperature flows. In these conditions, the radiation effects

are eliminated and the conduction effects are limited to those temperature deviations at the sensor or rake body (shapes with different recovery factors). In addition, by running the test at ambient temperature, temperature difference between the reference plane (plenum chamber) and the nozzle outlet where the sensor to be calibrated is installed are avoided.

If the facility is such that the flow temperature is above ambient, any temperature differences between the reference plane and the measurement plane will have to be characterized at the various operating conditions and introduced in the calibrations.

To minimize the uncertainty during calibrations, the temperatures should be measured preferably by connecting the reference thermocouple opposite to the tested thermocouple, rather than taking separate measurements.

For the same reason, the reference thermocouples and the those fitted in the sensors to be calibrated should be made from the same wire batch.

Factors  $r$  or  $R$  are deduced from the parameters shown on the schematic recorded at different steady Mach numbers.

The facility should preferably allow for sensor displacements (incidence and sideslip) in order to assess the effect of the flow incidence angle on these factors.

### 6.3.1.3 Selection of sensing elements

The most frequently used types of sensing element are thermocouples and resistance probes.

#### a) Thermocouples

The use of thermocouples is based on the thermoelectric effect. This effect — called the "Seebach effect" — is due to the association of two physical phenomena: the Peltier effect, or generation of an electromotive force due to contact between two dissimilar conductors, and the Thomson effect, or generation of an electromotive force in a metal bar submitted to a temperature gradient.

The basic circuit comprises two separate conductors, and includes a "hot" junction the temperature of which is unknown, and a "cold" junction, the temperature of which is constant and known (e.g.  $0^{\circ}\text{C}$ ). For a given couple of metals, the temperature of the hot junction is known by measuring the electromotive force produced in the circuit.

In general, the thermoelectric power of normal thermocouples is very low (few microvolts per degree).

The characteristics of main thermocouple types are summarized in Table 6.3-1.

TABLE 6.3-1

TYPE	THERMOELECTRIC POWER (REF 6.3-4)	RANGE	APPLICATION
Copper/Copper-Nickel (type T)	$51 \mu\text{V}/^{\circ}\text{C}$ from 0 to $350^{\circ}\text{C}$	$-50$ to $350^{\circ}\text{C}$	Engine Inlet LP compressor
Nickel-Chromium/ Nickel-Aluminium (type K)	$41 \mu\text{V}/^{\circ}\text{C}$ from 0 to $1000^{\circ}\text{C}$	$-50$ to $1000^{\circ}\text{C}$	Compressor Turbine outlet
Nickel-Chromium/ Copper-Nickel (type E)	$74 \mu\text{V}/^{\circ}\text{C}$ from 0 to $500^{\circ}\text{C}$ $80 \mu\text{V}/^{\circ}\text{C}$ from 500 to $900^{\circ}\text{C}$	$-50$ to $750^{\circ}\text{C}$	Engine Compressors
Platinel*	$40 \mu\text{V}/^{\circ}\text{C}$ approx	0 to $1200^{\circ}\text{C}$	Turbine
Nicrosil-Nisil* (type N)	$40 \mu\text{V}/^{\circ}\text{C}$ approx	0 to $1200^{\circ}\text{C}$	Turbine
30% Rhodium platinum/ 6% Rhodium platinum (type B)	$2.5 \mu\text{V}/^{\circ}\text{C}$ from 0 to $500^{\circ}\text{C}$ $7.2 \mu\text{V}/^{\circ}\text{C}$ from 500 to $1000^{\circ}\text{C}$	$1000^{\circ}\text{C}$ to $1700^{\circ}\text{C}$	Combustor outlet Turbine
Iridium/Iridium 40% Rhodium	$5 \mu\text{V}/^{\circ}\text{C}$ approx	$1000^{\circ}\text{C}$ to $1950^{\circ}\text{C}$	Combustor
10% Rhodium platinum (type S)	$11$ to $12 \mu\text{V}/^{\circ}\text{C}$	$500$ to $1600^{\circ}\text{C}$	Chiefly Calibrations
* Trade name	In general, these various thermocouples are identified by a colour code. The type of thermocouple is identified by the colour of the thermocouple cable sheath, while the polarity is identified by the colour of each wire. In some cases, the polarity may be identified by signs $+$ and $-$ , which avoids any confusion.		

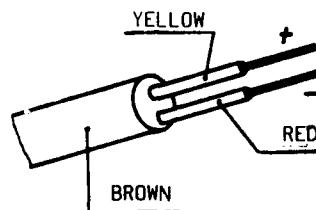


Fig. 6.3-2 Typical colour coding of type K thermocouples in the USA

It should be pointed out that all countries do not use the same colours, and that certain types of thermocouple are not even coded.

Therefore, users of thermocouple wire should be careful and make their own checks before using these wires.

Reference 6.3-5 and Table 6.3-2 provide an example of colour coding applicable to the major types of thermocouples.

b) *Resistance temperature detectors (RTDs)*

The use of RTDs is based on the following principle. The electrical resistance of a conducting wire varies with the temperature. Therefore, many metals or alloys can be used to make thermometric resistance probes. The most currently used metals are platinum and nickel. For high and medium accuracy measurements, platinum is generally used for the following reasons:

- It is the most stable, corrosion and chemical attack resistant of metals likely to be used; it has a very high chemical stability and melting point.
- It can be obtained to a very high degree of purity (better than 99.999%) and, therefore, the wire characteristics will be identical from one manufacturing batch to another.
- Its resistance vs temperature characteristic is free from hysteresis.
- Its resistivity is fairly high, producing a small size probe for precision measurements.
- The resistance variation vs temperature law can be represented by a simple mathematical function.

TABLE 6.3-2 National colour coding for insulation of thermocouples

TYPE	British to B.S 1843			American to ANSI/MC 96-1			German to DIN 43714			French to NFC 42-323 - 1965			Japanese to JISC 1610-1981		
	+ leg	- leg	overall sheath	+ leg	- leg	overall sheath	+ leg	- leg	overall sheath	+ leg	- leg	overall sheath	+ leg	- leg	overall sheath
T	WHITE	BLUE	BLUE	BLUE	RED	BROWN	RED	BROWN	BROWN	YELLOW	NO STANDARD	BLUE	RED	WHITE	BROWN
K	BROWN	BLUE	RED	YELLOW	RED	BROWN	RED	GREEN	GREEN	YELLOW	"	PURPLE	RED	WHITE	BLUE
E	BROWN	BLUE	BROWN	PURPLE	RED	BROWN	RED	BLACK	BLACK	YELLOW	"	ORANGE	RED	WHITE	PURPLE
PLATINEL	/	/	/	/	/	/	/	/	/	YELLOW	"	/	/	/	/
N	/	/	/	ORANGE	RED	BROWN	/	/	/	YELLOW	"	/	/	/	/
B	/	/	/	GREY*	RED*	GREY*	GREY*	RED*	GREY*	YELLOW	"	GREY	RED*	WHITE*	GREY*
Ir/Ir 40 % Rh	/	/	/	/	/	/	/	/	/	YELLOW	"	/	/	/	/
S	WHITE*	BLUE*	GREEN*	BLACK*	RED*	GREEN*	RED*	WHITE*	WHITE*	YELLOW	"	GREEN	RED*	WHITE*	BLACK*

\* : These color codes normally relate only to the extension grade  
/ : None established.

c) *Advantages and disadvantages of the two types*

TYPE	ADVANTAGES	DISADVANTAGES
THERMOCOUPLES	<ul style="list-style-type: none"> <li>- Small size</li> <li>- Point measurement</li> <li>- Short response time</li> <li>- Easily protected against thermal effects</li> <li>- Wide range of application</li> <li>- Diversity</li> <li>- Available as bare or sheathed wires</li> <li>- Low cost (except noble metals)</li> <li>- Self-generator</li> <li>- Easy to build into probes</li> </ul>	<ul style="list-style-type: none"> <li>- Measurement precision requiring a lot of care (calibrations)</li> <li>- Low output levels</li> <li>- Risk of ageing</li> <li>- Sensitivity to the environment</li> </ul>
RTDs PROBES	<ul style="list-style-type: none"> <li>- Accuracy</li> <li>- Fidelity</li> <li>- Selected as reference for calibration up to 600°C or fine measurements</li> <li>- Good interchangeability</li> <li>- Easy conditioning</li> </ul>	<ul style="list-style-type: none"> <li>- Size</li> <li>- Operating temperature limited to 600 - 650°C</li> <li>- Must be mounted in a strain-free environment</li> <li>- External power supply needed</li> <li>- Self-heating error and low recovery factor</li> </ul>

### 6.3.1.4 Specifications — Conformity Checks

#### a) Specifications

When purchasing sensing elements after a selection based on operating conditions, the tolerance classes must be clearly specified to achieve the accuracy level required for the tests.

For thermocouples, references 6.3-1 and 6.3-6 define tolerances relative to standard curves to which thermocouples can be ordered.

When purchasing resistance probes, the accuracy can be defined from reference 6.3-7, knowing that such accuracy can be improved (division by 2 or 3).

At acceptance testing, it shall be checked that sensing elements conform to the order.

#### b) Conformity checks

##### Thermocouples (Ref. 6.3-8)

The following checks shall be made on samples:

- tolerance conformity: calibration at three or four points within the thermocouple operating range;
- wire homogeneity: generation of high temperature gradients along the wire using a soldering iron or a flame. Typically, the error shall be less than 0.1°C.

After these checks, the wire batches shall be identified and stored until they are required for use.

For metal sheathed thermocouple wires insulated with magnesia, the wire ends shall be sealed to avoid internal humidity.

##### RTDs

In general, tight tolerances allow acceptance testing of the batches by sampling and interchangeability without any specific individual calibration.

### 6.3.1.5 Mechanical design of Thermocouples

Thermocouple manufacturing methods starting from bare wires or wires with a ceramic-insulated metal sheath are described in reference 6.3-1 and in paragraph 6.2

Thermocouples shall be selected on the basis of operating conditions and instructions shall be given to carry out checks and calibrations required to obtain the desired accuracy.

It should be noted that wire calibrations (as provided in paragraph 6.3.1.1) of sensing elements are difficult after such elements are installed in probes or rakes. Therefore, the following calibration procedures shall be applied:

- by sampling, for thermocouples made of bare wires or of wires sheathed with flexible insulating materials (Kapton, fibre glass, etc...) if the wire characteristics are sufficiently uniform to allow transposing the results from the sample to the complete batch. In this case, samples shall have undergone the same processes as thermocouples installed in probes or rakes.
- by individual calibration of each sensing element before its installation in probes and rakes. This method shall be applied systematically to thermocouples with metal sheaths insulated with magnesia. In actual fact, the manufacturing methods do not always provide assurance that wire characteristics will be sufficiently

uniform to achieve meaningful calibration by sampling.

Precautions should be taken if wires are spliced, in particular in a metal sheathed wire/flexible wire junction box. These precautions will chiefly cover the following aspects:

- quality of wires
- risks of polarity reversals
- tightness to humidity
- risk of short circuit (contact with the box or brazing alloy runout)
- location of splices in cool zones.

When thermocouples are connected to connectors, contact pins/sockets (from the same manufacturing batch if possible) shall be of the same types as the thermocouple leads, chiefly if temperature gradients may exist at this location. In all cases, these connections shall be located in low temperature zones. At this location, shielding continuity shall be verified.

Finally, as already stated about calibrations, the use of shielded cables will reduce the noise level during test data acquisition.

In all cases, on completion of manufacturing, it shall always be ensured that type and polarity of thermocouples are properly identified.

For unsteady temperature measurements with thermocouples (Ref. 6.3-9 and 6.3-10), the time constants will be reduced by reducing the lead diameters. However, this process has its own limitation in the minimum mechanical integrity required from leads in the adverse environment of a turbine engine. An associated processing system is the only means to provide improved performance.

##### RTDs (Ref. 6.1-3)

The manufacturing of very high precision platinum resistance probes requires considerable precautions. We will simply say that the platinum wire must be annealed and its purity must be such that the resistance ratio for the temperature interval  $R_{100}/R_0$  must be not less than 1.3925. It should be virtually strain-free during manufacturing and operation. The wire must be drawn from a melted ingot and annealed up to a temperature above the maximum operating temperature, and in any case, above 450°C.

Engine manufacturers usually purchase these sensing elements ready for installation in probes. The only thing to do is to secure the elements and to fit the output leads with 3 or 4 extension lines in order to eliminate line resistances. It should be noted that the resistance element output leads should not be trimmed, as their length is considered when the resistance is set by the manufacturer.

### 6.3.1.6 Checks during operation

Thermocouples are not easily checked when they are operating on components or in complete engines, chiefly in hot section components.

In actual fact, these thermocouples deteriorate and may become sensitive to thermal gradients. Due to this effect, calibrations will be meaningless, since the same temperature gradients cannot be reproduced.

Therefore, when defective operation not due to the acquisition channels (see paragraph 6.3.5) is detected in service, the best method consists in replacing the affected probe or rake by a new one, and in comparing the

measurements, after taking care to maintain reference rakes in the same measurement plane.

RTDs being installed, in general, in engine inlets, defective measurements may be detected either by comparing the readings obtained from several probes, or by referring to known engine operating points.

#### 6.3.1.7 Special case of type K thermocouples (Ref. 6.3-3)

This type of thermocouple, widely used by engine manufacturers, incorporates features which, if ignored, may lead to measurement errors. When used above about 400°C to 600°C, the signals delivered from these thermocouples are affected by positive drifts from the reference curve. This phenomenon is called "aging". These drifts stabilize after some operating time and, after this stage is reached, the fidelity of measurements becomes very high. To avoid this problem, these thermocouples may be artificially aged by holding for 15–20 hours at a temperature 30°C above the maximum operating temperature. Obviously, calibration must follow this aging treatment.

It should be noted that a previously aged thermocouple heated to above about 400°C will regain its initial characteristic curve when coming back to a lower temperature. This means that the aging effect will have disappeared and that the thermocouple may drift again.

Another instability factor affecting these thermocouples is the surface oxidation of leads at high temperature, chiefly on alumel leads. In this case, the thermocouples will tend to indicate a temperature that is higher than the actual temperature. These errors, due to a change of the chemical composition will be greater as the lead diameter decreases and the temperature increases. It has been observed that removing the oxide layer from bare leads tends to bring the readings back close to initial levels.

Finally, as recalled by Moffat (Ref. 6.3-8), type K thermocouples are sensitive to stresses. For example, when these thermocouples are secured to vibrating components, reading fluctuations may occur (up to 30°C).

To conclude, the use of the following sensors is recommended to obtain accurate readings in the above critical cases:

- Type E thermocouples at temperatures varying from –40°C to 700°C.

It should be pointed out that, compared to type K, this type of thermocouple has a high sensitivity (60 µV/°C compared to 40 µV/°C) and is not subject to drift when maintained at temperature, as opposed to type K. With these advantages, these thermocouples can be used at any location in the compressors of current engines.

- Beyond 700°C and up to about 1200°C, more stable thermocouples such as Platinel or Nicrosil-Nisil with a sensitivity close to that of type K thermocouples. However, it should be noted that, for the time being, Nicrosil-Nisil thermocouples are not widely used by engine manufacturers.

#### 6.3.1.8 Precious metal thermocouples (Ref. 6.3-3 and 6.3-9)

The various platinum alloy thermocouples are used to measure very high temperatures. In general, type B thermocouples (Platinum – 6% Rhodium/Platinum – 30% Rhodium) are preferred by engine manufacturers because of their better stability in combustion gas. Their emissivity is

of the order of 0,2 when new, reaching 0,5 depending on the duration of exposure to combustion gas. It should be noted that platinum (ref. 6.1-2) may be contaminated by various materials such as lead, cadmium, bismuth, germanium, zinc, tin, iron, antimony and sulphur. Beyond the operating limit of platinum base thermocouples, the only remaining possibility in oxidizing atmosphere is the Iridium/Iridium – 40% Rhodium thermocouple. The life of these thermocouples can be improved by using a ceramic coating providing a protection against the effects of the environment. When these two types of thermocouples (Platinum or Iridium base) are used after combustors in zones where reactions are not complete, they may play a "flame stabilizer" role and catalyse the reactions. Local phenomena produced will lead to errors in the measurements which cannot be corrected.

Catalytic effects may be eliminated by means of ceramic coatings deposited on thermocouples (and on probe components made of noble metal). However, the "flame stabilizer" effect will still remain. To solve this problem, the only solution will be to locate the probe in a zone where the combustion reaction is complete.

It is interesting to note the possibility to obtain now type B thermocouples sheathed with Platinum – 10% Rhodium (available diameters 0.6 mm; 0.75 mm; 1 mm; ...).

#### 6.3.2 Signal transmission and conditioning

For both types of sensing elements, the various functions of the measurement and acquisition channel are described in accordance with the diagrams shown in paragraph 6.1.2.1.

##### 6.3.2.1 Thermocouples

The signal shall be transmitted through extension lines made of the same metal as the sensing element to avoid temperature gradient effect.

The "sensing element – extension lead" junction shall be made in a cold zone (i.e. at a temperature below 100°C).

To avoid the effect of electromagnetic interference (noise, etc) on the measurements, the lines shall be shielded by means of a metal braid up to a location as near the hot junction as possible.

Two alternatives may be used for the cold junction:

*The 0°C cold junction box* (cooling by Peltier effect) which, by using a 0°C bath is the simplest, the most reliable and the cheapest equipment. In particular, this 0°C reference requires no correction of the acquired measurement.

Some precautions must be observed:

- The number of junctions remains limited by the box capacity.
- The bath temperature must be uniform.
- The bath temperature must be permanently monitored by means of a high precision resistance probe.
- The ambient temperature range where this box can be used must not be exceeded.

*The uniform temperature junction box (UTR):* in this case, the cold junction is made in a "cold" zone (temperature below 100°C) maintained at a known, but not necessarily constant temperature.

*Advantages of UTR:*

- Connections can be made as near the tested machine as possible, which allows the use of copper leads between

the tested machine and the control room (use of any type of thermocouple).

- Inert element: no risk of failure.

*Disadvantages:*

- Sensitivity to temperature gradients (in the box these gradients should be nil or very low).
- The temperature of interest must be calculated after determining the reference temperature in the UTR.

#### 6.3.2.2 RTDs

The resistance is measured through any one of the three basic 2-, 3- or 4-wire systems illustrated in figures 6.3-3, 6.3-4 and 6.3-5.

With the 2-wires system (fig. 6.3-3), when the bridge is balanced:

$$R_p = \frac{R_1}{R_2} \times R_3$$

The disadvantage of this system is that the line resistance must be known.

With the 3-wires arrangement (fig. 6.3-4), the line effect may be disregarded provided wires a, b and c are identical (same resistance).

For high accuracy measurements, the 4-wire arrangement is used (fig. 6.3-5). In fact, this is a double 3-wire measurement which eliminates line and contact resistance.

In a first step (see the arrangements in figure 6.3-5), when the bridge is balanced,  $R_3 + R_b = R_p + R_c$ .

In a second step, wires a and d and b and c are interchanged respectively, and we obtain

$$R'_3 + R_c = R_p + R_b$$

By summing up these two relations we obtain

$$R_p = \frac{R_3 + R'_3}{2}$$

Whatever the selected arrangement, the following rules shall be complied with:

- Use a very high input impedance precision voltmeter (to avoid disturbing the resistance measurement).
- Comply with the manufacturer's operating instructions as far as the measurement environment (possible insulation problems) and the specified temperature range (type of wiring used) are concerned.
- Comply with the instructions related to the supply current to avoid problems of probe heating.
- Use a stabilized power supply (no current variation or drift).
- The 2, 3 or 4 wires must be within a shielded cable.

#### 6.3.3 Signal Processing

##### *Filtering (Ref. 6.3-11)*

Disturbing signals, both low and high frequency, may be superimposed to the thermocouple or RTDs output signal. Therefore, before amplification, the signal is always filtered to eliminate these noise signals as much as possible by limiting the amplifier bandwidth.

##### *Amplification*

As the sensing element output signal is a very low voltage

(few microvolts in the case of a thermocouple) this signal must be amplified. Whatever the type of sensor (resistance probe or thermocouple) differential amplifiers with a high rate of common mode voltage rejection eliminate the problems associated with parasitic voltages.

##### *Switching*

The above type of amplifier is, in general, an expensive piece of equipment. Therefore, it may prove advantageous to use an electronic switching process similar to pneumatic switching sometimes used in pressure instrumentation systems. In this process, an electronic switching device successively connects several instrumentation channels to the same amplifier. In this manner, a single amplifier is required to acquire 12 or 14 temperature measurements, which provides a considerable cost saving.

This process can be used for the acquisition of steady data only. Its application to the measurement of transients is not recommended. In this case, each measurement channel must be amplified individually.

##### *Sampling — Multiplexing — Analog/digital conversion*

For a given parameter, an acquisition frequency and a measurement time must be selected. As such selection is governed by the type of the investigated physical process (rate of parameter variation, duration of the process, etc...), the first step consists of analysing the evolution of the measured parameter with time. When the process is not well known, the highest frequency and longest acquisition time, compatible with the acquisition system performance, will be selected in a first step. This selection is dependent on the required type of measurement. In general, in the case of a stabilized measurement (steady process), a low frequency (few Hertz) and a short measurement time will be adequate, and will provide the mean value of the parameter. In the case of a transient or dynamic process, the selected frequency will be higher (several tens of Hertz) and the time will be sufficiently long to be representative of the process.

Note that the signal must be filtered at a frequency twice less than the acquisition frequency.

The sampling rate is also limited by the performance of the multiplexer used before digitalising. A fast, high level multiplexer should allow the acquisition of several thousands of data channels per second; then, the maximum acquisition frequency of one channel is equal to the ratio of the multiplexer frequency to the number of acquired channels.

Computer recording requires analog/digital conversion. In general, such conversion is made by the multiplexer as and when channels are acquired. When fine correlations between channels are required, all acquisitions must be synchronized: in this case, an expensive sample and hold system freezing at a given time all acquired parameters in an analog memory before conversion must be used. Due to its cost and complexity of use, this system is not widely used today.

#### 6.3.4 Conversion into Engineering Units

For resistance probes, the temperature-output voltage relationship of the sensing element is generally described by a second order curve. When a high accuracy is required, several polynomials with different coefficients within a given measurement interval are used to describe this relationship within the complete range of measurement.

For thermocouples, the thermoelectric reference tables (Ref.

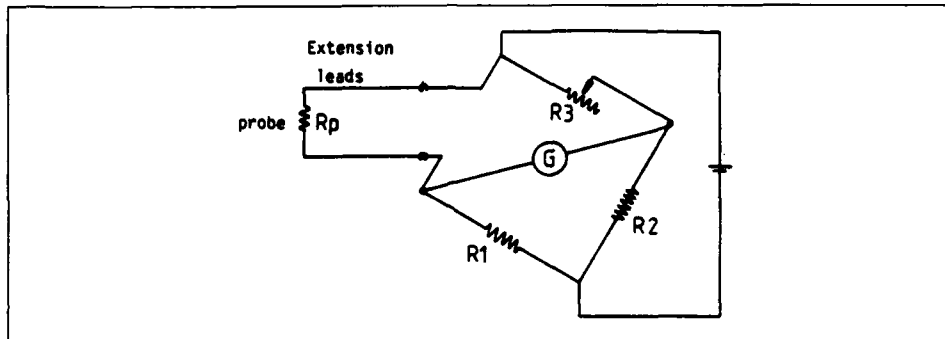


Fig. 6.3-3 Resistance measurement with Wheatstone bridge circuit: 2-wires system

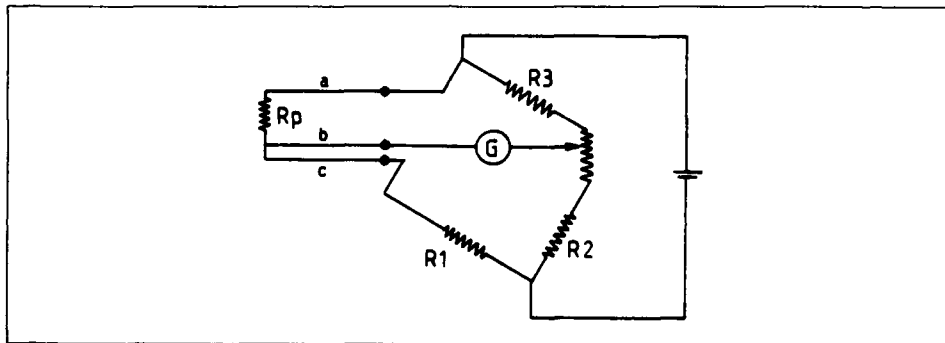


Fig. 6.3-4 Resistance measurement with Wheatstone bridge circuit: 3-wires system

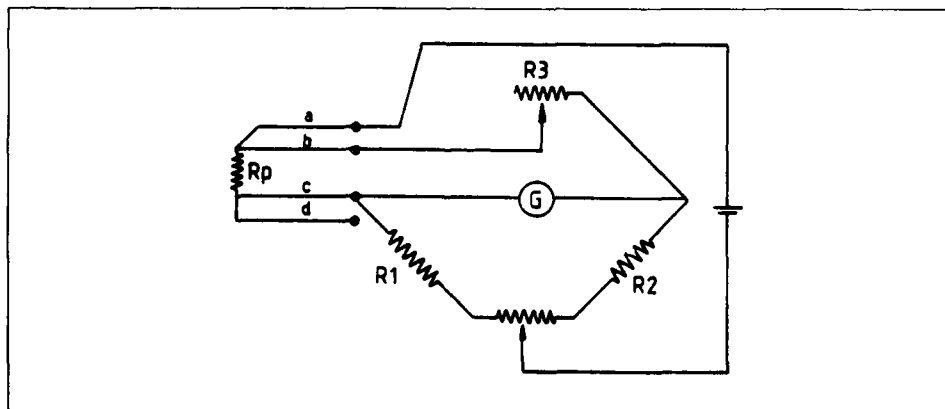


Fig. 6.3-5 Resistance measurement with Wheatstone bridge circuit: 4-wires system

6.3-4) are represented either by high order polynomials over the range of measurement, or by tables of values between which an interpolation is made.

Some thermocouple characteristics are sufficiently complex to require a large number of points to accurately define the calibrations; for example type K may require 30 or more. Use is frequently made of a difference curve to reduce the number of calibration points required. A difference curve defines the difference in electrical output between a given sample of wire and the standard tables published for that type of wire over a temperature range. Difference curves are normally very smooth in character. As few as three or four data points are often adequate to define one to the limits of accuracy required for this application.

### 6.3.5 Functional Checks on the Acquisition Channel

In general, two types of check are recommended:

*Routine checks* before and after each test: a known electrical signal from standard voltage sources is applied to the input of each amplifier to simulate the output voltage of a sensing element. An acquisition is launched by the computer and the measurement conformity with the known signal is checked. In general, these checks are made using an automatic control system in order to minimize their duration.

*Periodic check* (before adjustment) of each measurement channel used in the test facility, with a portable, high precision digital voltmeter under the control of a specialist approved by a national laboratory.

Note that for repeated tests on the same type of product it may be advantageous to define operation test-points as references stored in the computer memory. During a test run, passing through these test points will allow the detection of any measuring anomaly by direct comparison of the measured data with the references.

Finally, when several values of the same parameters are averaged, the comparison of each acquired value with the calculated average will allow for detection and elimination of any inconsistent value.

In general, as functional checks during the operation of the signal acquisition and processing system are simple and straightforward, these checks will be made first as soon as an anomaly is suspected in measurements. When the measurement channel is not involved, the investigation must cover the sensing elements (see paragraph 6.3.1.6).

*On line check:* for high precision measurements, a permanent check during testing can be considered in order to be able to correct any drift of the various instrumentation system components. For this purpose, signals supplied by sample thermocouples, from the same batch as the thermocouples installed in probes, and immersed in reference baths (e.g. triple point of water, fixed points of metals) are acquired each time the various engine temperatures are being measured.

## 6.4 Temperature Measurement Uncertainty Analysis

### 6.4.1 Reference model

The uncertainty affecting a temperature measurement will be determined using the general methodology developed in Section 3 "Uncertainty analysis".

Recall that this model is based on a breakdown of the error into systematic error, the upper limit of which is the bias, and random error. The uncertainty itself is a limit of the

error which has a given probability (in general 95%) of not being exceeded.

In general, the random error is a Gaussian random variable, the standard deviation of which can be evaluated from the result of  $n$  measurements.

Usually, the distribution function of the systematic error is unknown. The error upper limit, or bias, will be estimated from an exhaustive analysis of the measurement process.

The total bias and precision can be determined by adding the elemental contributions. If these are unrelated the best estimate is by Root-Sum-Square (RSS) addition in each category. An overall estimate of the Uncertainty of a single test can be given by combining bias and precision error. Usually, however, precision is based on statistics of calibrations or of previous test results, while bias errors have an element of engineering judgement. Therefore it is not strictly correct to add both contributions into a single Uncertainty value with a statistical confidence level.

Generally, two values are given, with the following effective confidence levels, i.e.

Additive uncertainty:  $U_{ADD} = B + t_{95}S$  (approx. 99% coverage).

Root Sum Square uncertainty:

$$U_{RSS} = \sqrt{B^2 + (t_{95}S)^2} \text{ (appr. 95\% coverage)}$$

in which the Student's factor  $t_{95} = 2$  for more than 30 degrees of freedom.

Finally, it should be noted that the distinction between systematic error and random error is essential when trying to reduce the uncertainty of a measurement:

- the short term precision error can be reduced by increasing the number of measurements,
- the bias can be reduced only by modifying the instrumentation system (calibration, acquisition and data reduction system).

### 6.4.2 Elemental errors

For error prediction a complete exhaustive list must be made of every possible error for all measurements that affect the end test result. These can be grouped in categories as follows:

1. Calibration Hierarchy; i.e. relation to a standard
2. Data acquisition due to outside influences on data transmission, transducer, signal conditioning and recording.
3. Data reduction, e.g. resolution and curve fit errors.
4. Non-Instrument or Sensor System errors, for example probe errors.

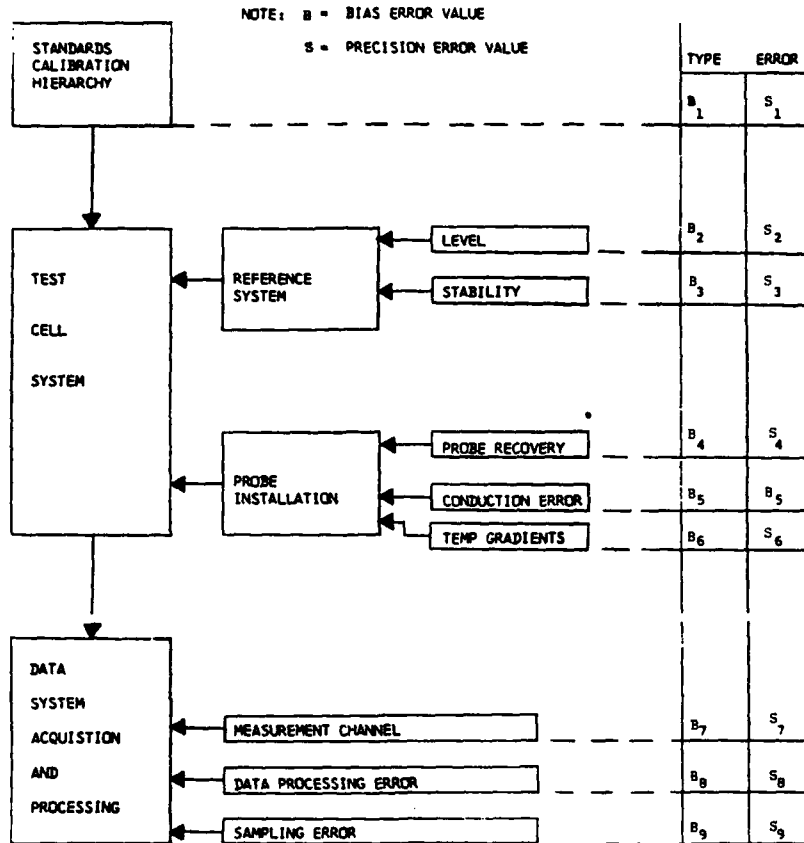
The table 6.4-1 shows a description of error sources in a temperature measurement system (thermocouple type).

### 6.4.3 Numerical Example

#### 6.4.3.1 Accuracy assessment

The uncertainty analysis described hereafter is based upon the following assumptions:

TABLE 6.4-1 Temperature measurement system (thermocouple type)



TEMPERATURE MEASUREMENT ERROR SOURCE DIAGRAM

B	S	DESCRIPTION OF ERROR SOURCE
B <sub>1</sub>	S <sub>1</sub>	Error due to manufacturer specification of wire or standard lab calibration, whichever is used.
B <sub>2</sub>	S <sub>2</sub>	Error due to reference temperature level.
B <sub>3</sub>	S <sub>3</sub>	Error due to reference temperature stability.
B <sub>4</sub>	S <sub>4</sub>	Error due to probe design caused by radiation, friction, etc., when measuring gas temperatures.
B <sub>5</sub>	S <sub>5</sub>	Error due to heat conduction.
B <sub>6</sub>	S <sub>6</sub>	Error due to temperature gradients along nonhomogeneous thermocouple wire.
B <sub>7</sub>	S <sub>7</sub>	Error from signal conditioning, millivolt calibration source and digital system.
B <sub>8</sub>	S <sub>8</sub>	Error from curve fit of thermocouple tables furnished by national standards laboratory.
B <sub>9</sub>	S <sub>9</sub>	Error associated with the ability to determine a representative value over a specified time interval for the data variations due to plant or engine instability.

- Measurements are achieved using type K thermocouples, at a level of about 150°C and at a Mach number of about 0.4.
- Cold junction box is used.
- Moisture effects are assumed to be negligible.
- Errors due to temperature profile or measurement locations in the stream are not considered.
- Error sources are only given for a single measuring chain, including:
  - Sensor.
  - Signal transmission, conditioning and processing.
  - Conversion into engineering units.

They are detailed in Table 6.4-2 for each process or part of the measurement system.

#### 6.4.3.2 Comments

Uncertainty may be reduced by:

*Individual calibration of thermocouples.* Therefore the error source "wire homogeneity" no longer has to be considered since each thermocouple is calibrated.

*Individual probes calibrations:* the error source "probes deviation" goes out. In this case, accuracy improvement may be significant but increase of work has to be considered.

*Use of direct connections from probes to cold junction instead of extension leads:*

- The junction error decreases from 0,3°C to 0,1°C.
- By combining the two previous improvements, then bias decreases to

TABLE 6.4-2

ERROR SOURCE		Type of Error	
		B	S
CALIBRATION  HIERARCHY	WIRE HOMOGENEITY	0,1 °C	—
	THERMOCOUPLES CALIBRATION (SAMPLES)	0,1 °C	—
	PROBE CALIBRATION (SAMPLING)	0,2 °C	—
	PROBES DEVIATION	0,2 °C	—
TEST CELL  SYSTEM	EXTENSION LEADS	0,3 °C	—
	COLD JUNCTION BOX	0,2 °C	—
DATA SYSTEM ACQUISITION AND PROCESSING	MEASUREMENT CHANNEL (OVERALL CHECK)	0,2 °C	0,1 °C
	DATA PROCESSING	0,1 °C	—

Final bias:

$$B = \pm \sqrt{0.1^2 + 0.1^2 + 0.2^2 + 0.2^2 + 0.3^2 + 0.2^2 + 0.2^2 + 0.1^2}$$

$$B = \pm 0.53^\circ\text{C}$$

$$\text{Precision error: } S = \pm 0.1^\circ\text{C}$$

Then:

$$U_{\text{ADD}} = 0.53^\circ\text{C} + 2 \times 0.1^\circ\text{C} = 0.73^\circ\text{C}$$

(99% coverage)

$$U_{\text{RSS}} = \sqrt{0.53^2 + (0.2)^2} = 0.57^\circ\text{C}$$

(95% coverage)

$$B = \sqrt{0.1^2 + 0.2^2 + 0.1^2 + 0.2^2 + 0.2^2 + 0.1^2} = 0.4^\circ\text{C}$$

$$\text{Therefore: } U_{\text{ADD}} = \pm 0.4^\circ\text{C} \pm 2 \times 0.1^\circ\text{C} = \pm 0.6^\circ\text{C}$$

$$U_{\text{RSS}} = \pm \sqrt{(0.4)^2 + (0.2)^2} = \pm 0.45^\circ\text{C}$$

Note

If we compare with the use of UTR mentioned in paragraph 6.3.2.1, from the uncertainty assessment point of view, we have to assume that thermocouple wires are directly connected to the box (no extension leads):

Errors due to a cold junction box:

- Bath temperature control system:  $\pm 0.2^\circ\text{C}$

- Input junction:  $\pm 0,1^{\circ}\text{C}$ .

Errors due to a UTR junction box:

- Temperature gradients inside the box:  $\pm 0,1^{\circ}\text{C}$  to  $\pm 0,2^{\circ}\text{C}$ .
- Resistance probe used for inside temperature measurement:  $\pm 0,2^{\circ}\text{C}$ .

Therefore it is clear that, from an uncertainty assessment point of view, both measurement systems are equivalent.

However, the use of UTR offers other advantages:

- Any type of thermocouple can be connected.
- A UTR is an inert element, from an operating point of view.

#### 6.4.3.3 Recommended practices

As a conclusion, temperature measurement uncertainties may be reduced if the recommended practices below are used (as mentioned in paragraph 6.3.1.3):

##### Conformity checks

- wire homogeneity.

- Wire samples calibration at some reference points typical of the intended measurements.

- Spools identification.

##### Manufacturing

- Thermocouples calibration (sampling, exceptionally individual calibration if necessary).

- Probes calibration in a wind tunnel (sampling, exceptionally individual calibration).

##### Mounting and testing (in the facility)

- Use shielded cables and proper grounding procedures.
- If possible, do not use extension leads. It would be better to bring wires from the probe up to the cold junction.
- Check the acquisition channel at least once before and after each test and if possible during testing, in order to find any anomalies.
- When converting into engineering units, consider the calibration results for the thermocouples wire and the probes recovery factor.

## 7. SPECIAL FACTORS IN SMALL ENGINES

### 7.1 Introduction

Measurement goals relative to determination of accurate component performance information are similar in most gas turbine engine or component development programmes, regardless of unit size. However, the size of the unit may influence the practices used to achieve these goals.

There are often conflicting requirements for instrumentation which are aggravated in the small gas turbine unit. For example, for certain types of tests, some unique characteristics of the small unit may dictate the need for a more extensive array of flow path pressure and temperature rakes at a component's rating stations than that required in a larger unit, but flow blockage limits may restrict the instrumentation to less than that allowable in the larger unit. An example of this is in inlet distortion testing, which is discussed in paragraph 7.4.

This section discusses some typical problems and example solutions encountered in small gas turbine components. The term "small" is relative and, as used herein, refers to components applicable to engines with core or gas generator mass flows below approximately 15 kg (30 pounds) per second.

### 7.2 Blockage Effects

Flow path blockage by pressure and temperature rakes has a direct effect on the measured performance of the component being tested. For example, the effect of the pressure loss from the flow across the component inlet instrumentation shows up downstream and directly causes a decrease in that component's measured performance. Another effect of the inlet instrumentation is that it may affect the relative angle of the inlet flow. On a rig, the pressure losses from the flow across the component discharge instrumentation may not directly affect the measured performance of the component being tested but the blockage may cause an effect that is similar to that caused by a reduction in the component's discharge flow area or a change in geometry.

In an engine test, the discharge instrumentation of one component will often represent the inlet instrumentation of the next downstream component. In a case such as this, the flow path pressure loss caused by the discharge instrumentation of one component will represent a loss to the downstream component performance.

General rules of thumb developed from experience restrict flow path instrumentation blockage to the order of 2 to 5 percent of the flow path area, depending on the flow path Mach number at a given rotating station. Less blockage can be tolerated when the flow path Mach number is relatively high. It is advisable to calculate the pressure loss caused by the instrumentation to ensure that this loss does not have a significant effect on the measured performance of the component being tested.

In component rigs, a common practice is to use an inlet plenum section upstream of the component being tested, which results in a low inlet flow path Mach number and a resulting low-inlet pressure loss, even with the existence of several inlet pressure and temperature rakes across the flow path. Sometimes inlet traversing instead of fixed rakes is used to survey the inlet condition (see paragraph 7.5), with a flow path blockage that is typically lower than that with fixed rakes. In the case of discharge instrumentation, the rakes may be located several blade chord lengths downstream to

minimize any adverse effects of the instrumentation on the measured component performance.

One technique that has been used to minimize instrumentation blockage has been to design pressure or temperature probes into the leading edges of component stator vanes. This is especially advantageous for determining interstage pressures and temperatures without significantly disrupting the normal flow characteristics. However, care must be exercised to define the probe geometry such that effects of flow disturbances from the mounting structure on pressure measurements or heat transfer effects on temperature measurements are minimized.

### 7.3 Instrumentation Scaling

The small flow passages, sometimes unusual flow path configurations, and higher rotational speeds associated with small gas turbine components require instrumentation practices which are compatible with their small size. The influences of measuring probes and their supports on the flow to be measured are more pronounced in test articles of small scale relative to those in larger ones because there is a limit to how small the probes can be scaled. In order to minimize flow disturbance, standard rake and probe designs call for streamlined supports to minimize drag coefficients and low frontal areas to minimize the blockage of the flow passage. These standard designs cannot always be completely scaled down directly proportional to flow size because minimum instrumentation sizes for mechanical integrity considerations are quickly reached. Furthermore, since component flow path Mach numbers are generally similar for large and small gas turbine engines, flow sensitivity to blockage is not reduced with reduced engine size. Probe-to-probe performance variations are also compounded in small scale designs because build tolerance and positioning errors represent larger percentages of the basic dimensions.

In addition to the problem of pressure losses by instrumentation flow blockage directly degrading the measured performance of an aerodynamic component, there are also some unique problems in pressure and temperature measurements which are aggravated in small units. For example, it is well known that a pressure measurement is influenced by the proximity of a measuring probe to an external flow disturbance (references 7-1 and 7-2). This disturbance could be caused by the support for the instrument itself, other instruments nearby, struts, or the confining walls of the flow path. The solution to this problem is to put as much distance as possible between the measuring probe and these disturbances, but this is more difficult to accomplish in a small unit with its limited space.

It is believed that the miniaturization of probes affects their performance, but not much information is available in the literature on this subject. Reference 7-3 states that "Reducing the size of probes does affect their performance. For example, the effect of boundary layer growth in small thermocouple probes has different effects than in large probes. This effect prohibits simple scaling of the ratio between probe entrance to vent hole area in miniature probes." Miniaturized probes are also more susceptible to contamination due to the presence of oil, dirt, or carbon and thus require more frequent inspection and cleaning than do larger scale instruments. Miniature probes and leads may also adversely affect stabilization time.

#### 7.4 Inlet Distortion Testing

Inlet distortion testing of small gas turbine engines normally requires a greater number of inlet total pressure distortion rakes than those required for large engines to accurately define mechanical distortion descriptors. This is because the critical vibration frequencies of fan and compressor blades in small engines are generally higher. In large engines, the critical blade vibratory frequencies are typically two or three times the maximum rotor speed of the engine (2 or 3 per rev). The 2 or 3 per rev content can be accurately measured using eight multi-element rakes.

Small engines have higher critical blade vibration frequencies, typically 4 per rev. In order to accurately measure the 4 per rev harmonic content, it is typically necessary to use ten rakes.

The increased number of inlet distortion rakes required for small engines leads to increased blockage at the aerodynamic interface plane. This problem is compounded when peak instantaneous distortion levels are measured because the high response pressure transducers must be located in the flow path.

Blockage effects are also of major concern when attempting to determine compressor interstage or exit conditions. The flow path areas can be quite small in small, high pressure ratio gas turbine components. This makes it difficult to install enough instrumentation to obtain adequate circumferential definition of the distortion patterns (pressure and temperature) as they are attenuated by the compression system. Since the inlet instrumentation may require 10 or more rakes, a similar number of circumferential measurements are desired in flowpath

locations downstream from the aerodynamic interface plane. Solutions to this problem have included use of multiple inlet distortion screen rotations or instrumentation rotations to effectively double or triple the downstream instrumentation, without the need for excessive blockage.

#### 7.5 Use of Traversing Probes

Traversing probe survey systems can be used to obtain data traditionally obtained with fixed radial and wake rakes without the associated blockage and flow disturbances. Sensor-to-sensor performance variations and limited spatial sampling problems are reduced or eliminated. Traversing probe survey data can also be used to define the required locations of fixed rakes and probes so that average flow properties can be measured with a minimum amount of instrumentation in the flow path.

Figures 7-1 and 7-2 (from Reference 7-4) show an example of a two-dimensional, high speed preprogrammed traversing probe system initially developed to support fan rig testing. In this system, a single sensor or group of sensors is stepped through a predetermined spatial matrix to obtain the desired performance and diagnostic measurements. The single matrix, preprogramming panel consists of 180 x 100 positions representing a 22.9 by 12.7 cm (9 by 5 inch) sampling area. The X-Y actuator system moves the probe in 0.127 cm (0.050 inch) increments with repeatability errors on the order of 0.0025 cm (0.001 inch). Interchangeable probe configurations allow a variety of tests to be performed through a simplified rig-actuator instrumentation interface. The flexibility of this system, both in selection of the positioning matrix and adaptability to a variety of probe configurations, has enabled its use in compressor and turbine test rigs, as well as in engine tests of components.

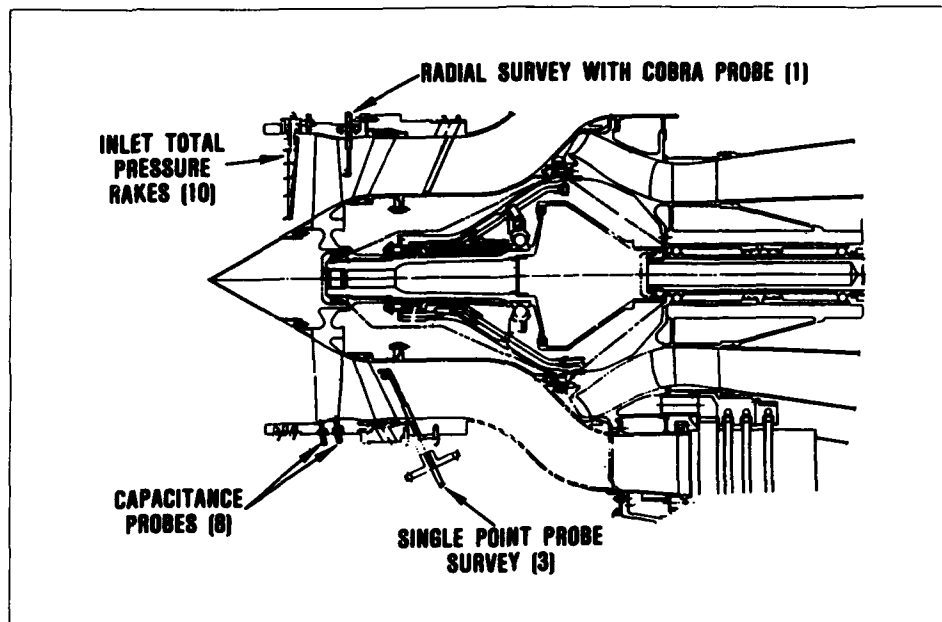


Fig. 7-1 Cross section of a fan rig



Fig. 7-2 Single probe actuator assembly in a fan rig

## 8. SPECIMEN CASES

### 8.1 Exhaust Nozzle Calibration

This section, 8.1, presents a specimen case for an exhaust nozzle component test. This example illustrates the process of instrumentation definition and uncertainty analysis for testing of an exhaust nozzle installed on an engine and is presented to illustrate use of the methods and principles described in the preceding sections of this document. Please bear in mind that, while this example illustrates the general process, the specific procedure to be followed in a particular case will require some engineering judgement and will depend on the specific type of test, the objectives of the test, and the particular measurement systems involved.

#### 8.1.1 Objective

This example involves the pre-test definition of flowpath pressure and temperature instrumentation required to determine the flow and thrust performance characteristics of a compound exhaust nozzle in a turbofan engine. The type of exhaust system for the example is a convergent nozzle for a turbofan engine, illustrated schematically in Figure 8.1-1.

The objective is to define exhaust nozzle instrumentation for an engine test from which flow and thrust coefficients can be determined. This objective is to be accomplished with use of fixed instrumentation rakes installed at the nozzle rating stations that are sufficient to obtain average values for the flow path temperatures and pressures in both the core and bypass streams without incurring excessive pressure losses due to blockage. Flow coefficients are to be determined for the mixing plane stations 7 and 17, and for the final nozzle exit station 8. The overall nozzle thrust coefficient will also be determined.

#### 8.1.2 Approach

The free pursuit of the objective was constrained by other objectives or limitations of the engine and test equipment. For example, one limitation was that the nozzle hardware could be modified to receive instrumentation, but not the engine hardware. This required that the core rakes be mounted from the outer nozzle skin, thus eliminating the need for modification of the engine hardware.

For the same reason, it was decided to mount the core elements and the bypass elements on a common rake. A dual element design for each probe, having both temperature and pressure elements in a common Kielhead, was also selected, in accordance with the recommendations of Section 2.10.

The general approach used for definition of the instrumentation described herein is as follows:

- A preliminary definition of radial and circumferential probe and rake positions is made, based on the results of analysing typical pressure and temperature profiles from previous tests of similar exhaust nozzles.
- The preliminary instrumentation design is checked for blockage and flowpath pressure losses.
- An uncertainty analysis of the nozzle coefficients, based on the preliminary instrumentation definition, and previous typical pressure and temperature profiles, is conducted.
- If the results of the uncertainty analysis indicate a satisfactory uncertainty level for the nozzle coefficients, then the preliminary instrumentation definition becomes the final one.

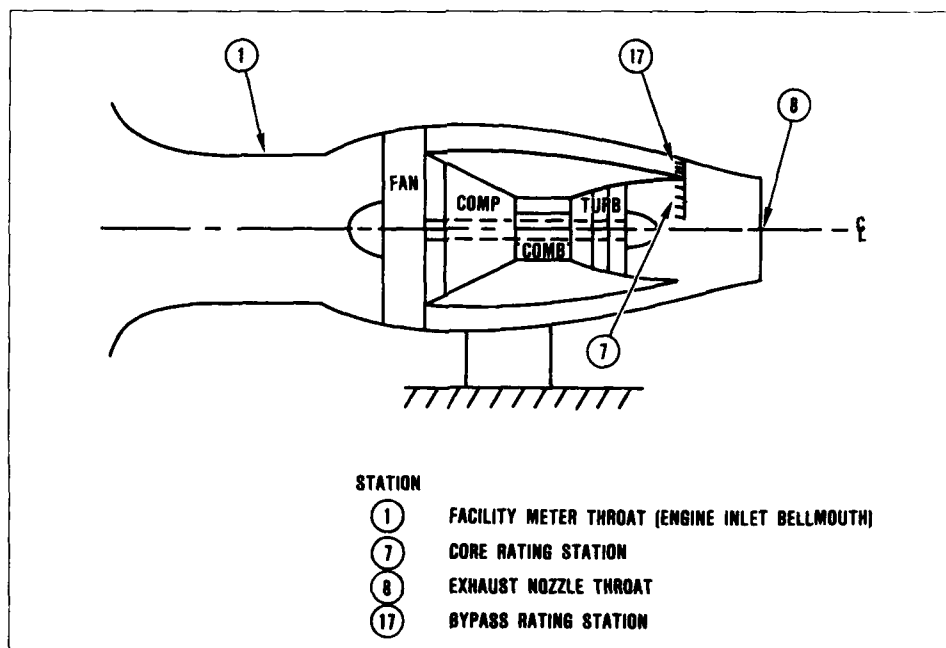


Fig. 8.1-1 Station notation for nozzle component in engine for specimen case

- e. If the results of the uncertainty analysis indicate an unsatisfactory uncertainty level for the nozzle coefficients, the individual elements of the uncertainty analysis are examined to determine what changes could be made to improve the uncertainty level. These might involve, for example, changes in any of the following: (1) the types and quantity of instrumentation, (2) the calibration and test procedures, (3) data acquisition equipment, and (4) the methods of data reduction and analysis. Tables showing the sensitivity of the nozzle parameters to various measurement variations will help to pin-point the fruitful areas for improvement.

Rather than set an uncertainty goal for each individual coefficient, the goal was established as one for the combined effect of the individual uncertainties of the nozzle flow and thrust coefficients on the predicted engine net thrust. This goal was established as an uncertainty of  $\pm 2.5$  percent in predicted net thrust at a 99 percent confidence level when the individual uncertainties of  $C_{w7}$ ,  $C_{w17}$ ,  $C_{w8}$ , and  $C_F$  are combined in an engine performance model at flight conditions of sea level static, standard day and 40,000 feet, Mach 0.8, standard atmosphere.

### 8.1.3 Mathematical Model

The uncertainty within which the objectives are met must be calculated from the uncertainties of the measurable quantities. The following equations represent the mathematical model which forms the basis for these uncertainty calculations:

Thrust coefficient:

$$C_t = \frac{F_G}{F_{GI}} = \frac{\text{Actual Gross Thrust}}{\text{Ideal Gross Thrust}}$$

Where:

$$F_{GI} = W_A \sqrt{\frac{2\gamma RT_i}{(\gamma - 1)g_c}} \left[ 1 - \left( \frac{P_i}{P_{AMB}} \right)^{\frac{1}{1-\gamma}} \right]$$

Flow Coefficient:

$$C_w = \frac{W_A}{W_{AI}} = \frac{\text{Actual Mass Flow}}{\text{Ideal Mass Flow}}$$

Where:

$$W_{AI} = \frac{P_i A}{(P_i/P_s)^{1/\gamma}} \sqrt{\frac{2\gamma g_c}{RT_i(\gamma - 1)}} \left[ 1 - \left( \frac{P_i}{P_s} \right)^{\frac{1}{1-\gamma}} \right] \quad \text{for unchoked flow}$$

$$W_{AI} = P_i A \sqrt{\frac{\gamma g_c}{RT_i}} \left( \frac{2}{\gamma + 1} \right)^{\frac{\gamma}{\gamma + 1}} \quad \text{for choked flow}$$

Notation and equations are consistent with section 2.10 (in consistent SI units,  $g_c$  in the above equations equals 1.0). The ideal flow equation applies to each stream at the stream confluence to evaluate the bypass and core flow coefficients at this location and to the "mixed" stream at the final nozzle exit to determine the flow coefficient at the nozzle throat. The average values of total pressure and total temperature are to be used in conjunction with the static pressure to calculate the ideal flows. The static pressure at the nozzle mixing plane has been previously surveyed in similar tests

and found to be uniform across the flow path. Therefore, static pressure across the flow path at the mixing plane is assumed to be constant and equal to the wall static measurement. Typical profiles for the total pressures, temperatures, and flow angles across the flow path are also known for similar exhaust systems from previous engine testing. These total pressures and total temperatures will be integrated across the flow path to determine their average values using mass-flow weighting for temperatures and momentum weighting for total pressures (Dzung method of Reference 2.10-1).

Total mass flow will be provided from a calibrated bellmouth at the engine inlet. The flow split between core and bypass will be determined by the data reduction system through an energy balance method. The sum of core and bypass flow must equal total flow. The uncertainties of all these measurements and calculations will be included in the evaluation of the uncertainty of flow and thrust coefficients.

At each test point, the engine will be controlled to maintain a constant power setting which will, at the same time, maintain essentially a constant exhaust nozzle pressure ratio. Ten complete surveys will be taken at each test point where each survey will include a complete sampling of all channels. The ten sets of data will be averaged to minimize effects of data scatter. Surveys will be typically 0.01 second apart.

### 8.1.4 Instrumentation Definition

An initial step in making a pre-test prediction of uncertainty of the nozzle coefficients to be determined from the test data is to describe the complete measurement systems. The measurement system models should show how the instrumentation is used, recorded, and calibrated, and form the basis for tracing the accumulation of errors. This section describes the temperature and pressure measurement systems, as well as typical temperature and pressure profiles from previous tests that form the basis for the pre-test uncertainty analysis.

#### 8.1.4.1 Temperature Measurement Model

The temperature measurement model is shown in Figure 8.1-2 and is described below. The gas path total temperature probes are made from Type K thermocouple wire.

When a wire roll is received from a manufacturer, some samples are taken from the roll and checked to ensure conformance to the initial calibration tolerances for special limits of error thermocouple wire, as called out in the American National Standards Institute (ANSI) MC96.1 report. This initial calibration tolerance is  $\pm 1.1^\circ\text{C}$  ( $\pm 2^\circ\text{F}$ ) from  $0^\circ\text{C}$  to  $276.7^\circ\text{C}$  ( $32^\circ\text{F}$  to  $530^\circ\text{F}$ ). Above  $276.7^\circ\text{C}$  ( $530^\circ\text{F}$ ), the tolerance is equal to  $0.004 (T - T_{\text{FREEZE PT}})$ . The calibration for the temperature range of  $65.6^\circ\text{C} < T < 204.4^\circ\text{C}$  ( $150^\circ\text{F} < T < 400^\circ\text{F}$ ) is performed with the measurement junction in a stirred oil bath and a transition from thermocouple wire to copper wire in a stirred ice bath. The voltages are converted to temperatures via a polynomial curve fit, based on the International Practical Temperature Scale (IPTS -68). These temperatures are then compared to temperature measurements made with a Standard Platinum Resistance Temperature Device (SPRTD) (the allowable deviation of the wire output from the SPRTD is generally the largest single error source of a gas path temperature measurement). For checks above  $204.4^\circ\text{C}$  ( $400^\circ\text{F}$ ), use is made of pure metal freeze points or an oven.

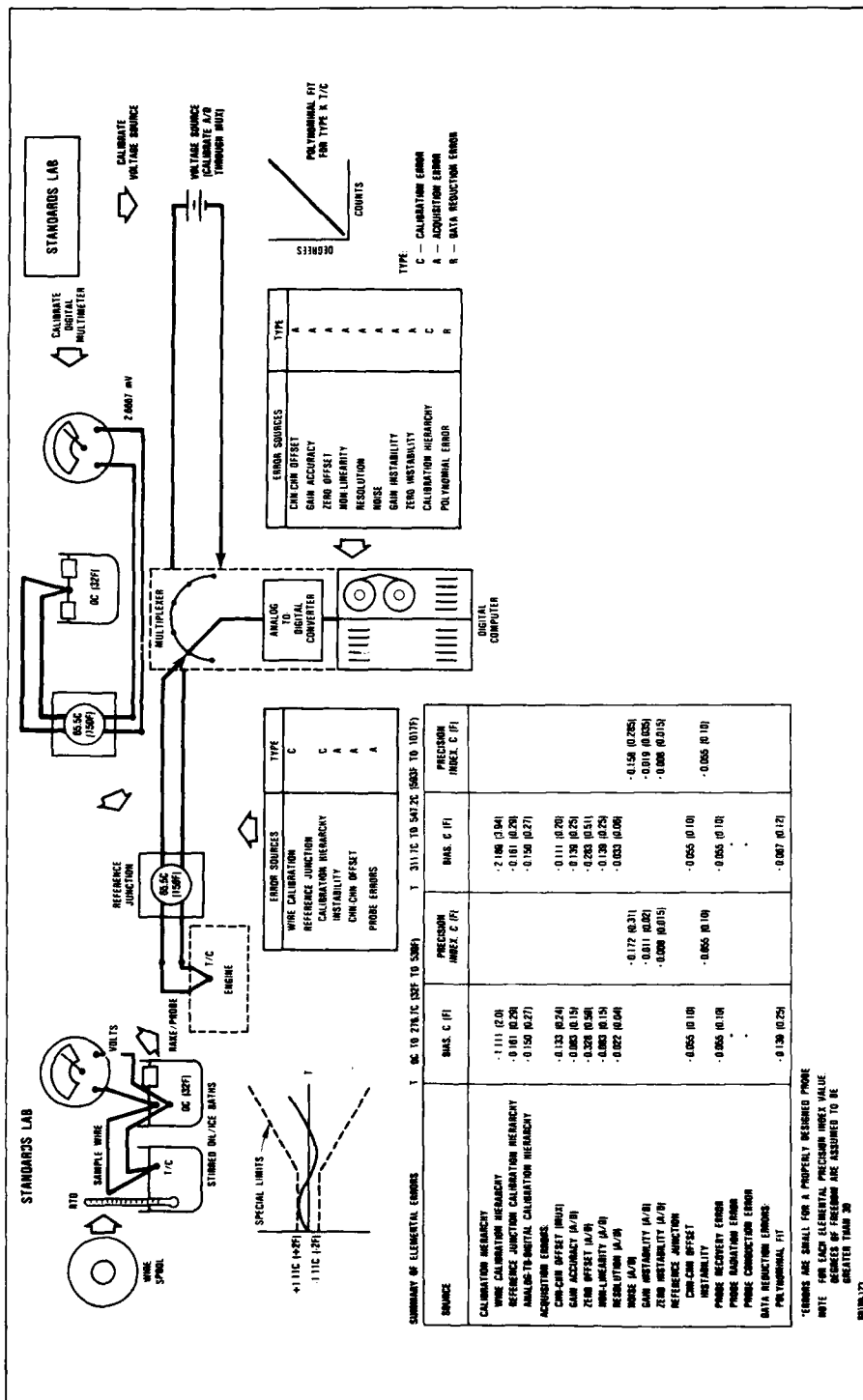


Fig. 8.1-2 Temperature measurement model elemental error sources

Once the roll has been declared acceptable, probes are made and installed in an engine. The probes are designed to minimize recovery, radiation, and conduction errors. To further reduce the recovery error, a probe of a particular design may be calibrated over a range of flow rates in a flow facility.

Extension wires are connected to the probe wires, and are plugged into a constant temperature (65.6°C, or 150°F) reference oven. This oven provides an accurate reference temperature and has been calibrated with a stirred ice bath and a high-precision voltmeter.

The signals from the thermocouple circuits are passed through an electronic switching arrangement, or a time-division multiplexer (MUX). The MUX sends the signals, one at a time, to the Analog to Digital (A-D) converter. The signal is then digitized and sent to the digital computer, where temperatures are computed from three voltages, using a polynomial curve fit based on the NBS Monograph 125 tables, using a 65.6°C (150°F) reference junction in place of the 0°C (32°F) reference junction.

The elemental error sources for temperature measurement fall into four categories: (1) Calibration Hierarchy, (2) Data Acquisition, (3) Data Reduction, and (4) Errors of Method. The first three error sources and their contribution to the uncertainty in the temperature measurement are listed in the table shown in Figure 8.1-2. The elemental errors shown are for a single sampling. The errors of method due to sampling uncertainty are discussed in section 8.1.4.4.

#### 8.1.4.2 Pressure Measurement Model

The steady state pressure measurement model illustrated in Figure 8.1-3 is for a electronic pressure scanning system.

This system includes a vibrating quartz reference standard and its own digital acquisition computer. In this system there is an individual pressure transducer for each measurement to be made in the engine (as opposed to rotary scanning systems that time-share a single pressure transducer). Up to 1024 pressures can be measured by a single system, and each transducer can be scanned up to 20,000 times per second.

The system shown is used with a host computer, but it can also operate as a stand-alone system. The components are housed in a cabinet that is normally placed in the control room to maintain a stable temperature.

An NBS-calibrated air piston gauge (dead weight tester) is used to calibrate the bourdon tube (sometimes referred to as a quartz manometer). The bourdon tube is then used to calibrate the vibrating quartz transfer standard, which is used to perform on-line calibrations of the pressure transducers. The transducers are calibrated by applying nitrogen through appropriate regulators, to the transfer standard quartz pressure transducer. Nitrogen is used because of its purity; plant or instrument air may contain contaminants or water and oil vapour. The output of the quartz pressure transducer is then compared to the output of a quartz manometer, and a third-order polynomial curve fit of (1/frequency) versus pressure is generated.

The system can operate in either of two modes, calibrate or operate. The transfer standard is used to recalibrate the individual pressure transducers during the test. This is done with another nitrogen source and appropriately sized regulators. The output of the transducers is compared to that of the transfer standard, and a pressure versus voltage second-order polynomial curve fit is generated for each transducer.

Once the calibrations have been performed, control valves isolate the calibration system and then allow the transducers to measure the pressures of interest.

The outputs from the pressure transducers are passed through an electronic switching arrangement, or a time-division multiplexer (MUX). The MUX sends the signals, one at a time, to the Analog to Digital (A-D) converter. The signal is then digitized and sent to the computer. Pressures are computed from the counts, using the polynomial curve fit generated during the calibrate mode. The gauge pressures must be corrected for ambient pressure. The ambient pressure is provided by a barometer that has been calibrated against a quartz manometer, with a nitrogen pressure source.

The elemental error sources for pressure measurement fall into the same four categories previously given for temperature measurement: (1) Calibration Hierarchy, (2) Data Acquisition, (3) Data Reduction, and (4) Errors of Method. The first three of these error sources and their contribution to the uncertainty in the pressure measurement are listed in the table shown in Figure 8.1-3. The elemental errors shown are based on current practice with this relatively new system. The errors of method due to sampling uncertainty are discussed in section 8.1.4.4.

#### 8.1.4.3 Pressure and Temperature Profiles

For use in the pre-test uncertainty analysis, pressure and temperature profiles were obtained from surveys of the exhaust streams of a similar exhaust system in previous engine tests. Plots of radial total pressure and temperature profiles at one circumferential location each are presented for the bypass stream in Figures 8.1-4 and 8.1-5. Plots of circumferential total pressure and temperature variation at one radial location each are presented for the bypass stream in Figures 8.1-6 and 8.1-7. Representative profiles for the core stream are not presented here, but the method for evaluation is the same as that to be described for the bypass stream.

#### 8.1.4.4 Spatial Sampling

##### 8.1.4.4.1 Radial Sampling

The bypass nozzle rating station total pressure and total temperature radial profiles obtained from previous tests of a nozzle similar to the one used in this example (and presented in Figures 8.1-4 and 8.1-5) will be used to illustrate the effect of the number of probes per rake on the calculated average radial values.

Table 8.1-1 shows the effect of the number of probes per rake selected on the average total pressure and the average total temperature obtained at one circumferential location. Probes are located at radial positions representing centres of equal areas.

TABLE 8.1-1 Effect of Number of Probes per Rake on Average Measured Values

No. Probes Centers of Equal Areas	Relative Momentum Weighted Total Pressure	Relative Mass Weighted Total Temperature
1	1.005	1.000
2	1.0028	1.0016
3	1.0018	1.0006
4	1.0012	1.0006
5	1.0008	1.0008
10	1.0003	1.0003

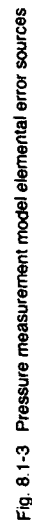


**Fig. 8.1-3 Pressure measurement model elemental error sources**

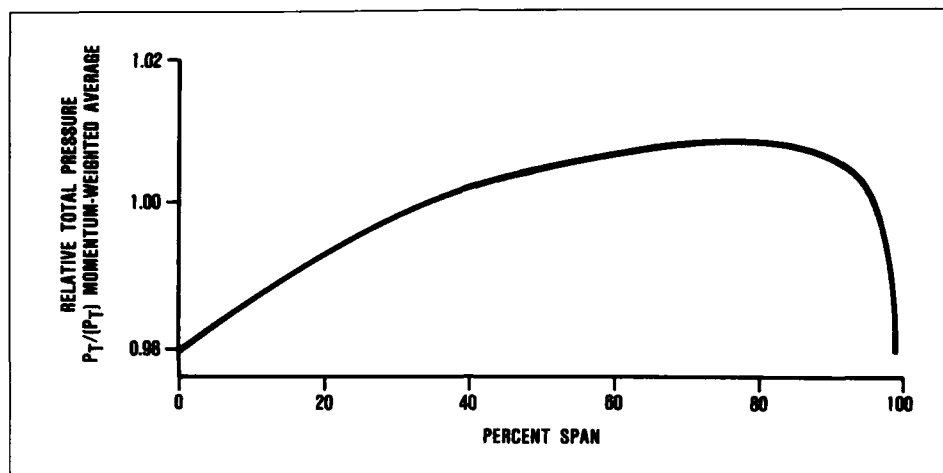


Fig. 8.1-4 Bypass total pressure profile at one circumferential location

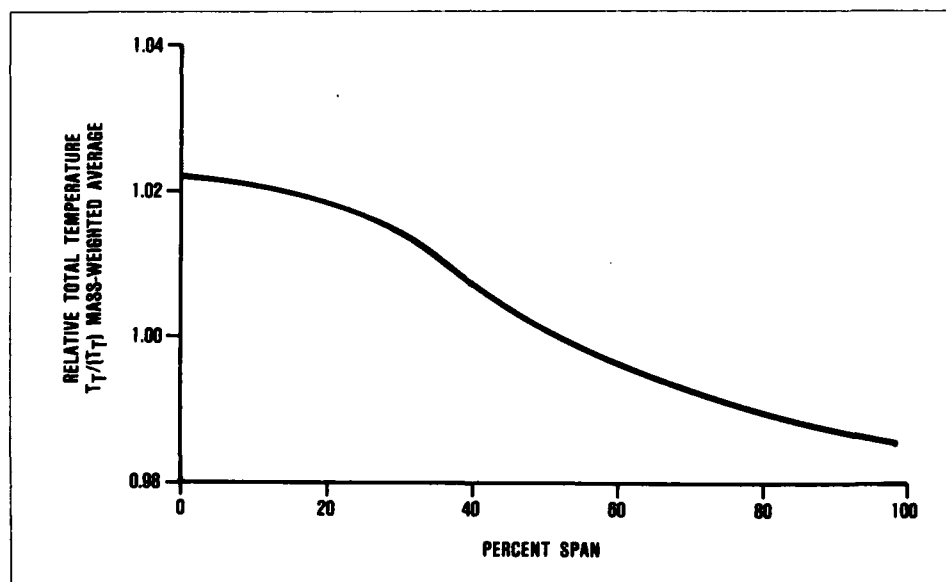


Fig. 8.1-5 Bypass total temperature radial profile at one circumferential location

As the number of probes increases, a point is reached where the average slowly approaches the value for an infinite number of radial locations. By chance, one probe at one centre of equal area happens to give a perfect average for temperature for the assumed profile, but this cannot be relied on because the actual profile can vary from engine-to-engine. With only 2 probes at this one circumferential location, the sampling error is approximately 0.3 percent in total pressure and 0.2 percent in total temperature. With 5 dual element probes, the sampling errors in both total temperature and total pressure become less than 0.1 percent. A rake configuration requiring 5 dual element temperature and pressure probes located on centres of equal areas was selected to provide good sampling accuracy, as well as redundancy in measurements in the event of probe failures.

There is some uncertainty that the probes are actually located at centres of equal areas when installed. If the probes are mislocated by one percent of span, the additional uncertainties evaluated from the radial profiles are:

0.025% (of reading) in Total Pressure  
0.05% (of reading) in Total Temperature

#### 8.1.4.4.2 Circumferential Sampling

The bypass nozzle rating station total pressure and total temperature circumferential variation at one radial location obtained from previous testing and shown in Figures 8.1-6 and 8.1-7 will be used to illustrate the effect of the number of circumferential locations selected on the calculated average circumferential values. Rakes will be equally spaced circumferentially. The pattern may not be precisely the same for all engines and test situations; i.e. the patterns may rotate from those shown. This probability precludes the elimination of some sources of error by judiciously placing the rakes at the exact average locations of the profiles, which in practice cannot be achieved with certainty. Also, since there are four pronounced peaks in the circumferential pressure profile, four rakes would probably not represent a good choice.

Figure 8.1-8 shows the effect of the number of circumferential locations selected on the average total pressure obtained at one radial location. Figure 8.1-9 shows similar information on total temperature. A total of 5 equally spaced circumferential positions was chosen for this example. The same 5 circumferential positions also will apply to the core instrumentation since both core and bypass probes are to be mounted on a common rake.

#### 8.1.4.4.3 Sampling Uncertainty

With selection of five 5-element rakes, the predicted uncertainties in total temperature and total pressure due to sampling errors to be used in the uncertainty analysis of Section 8.1.5 are summarized in Table 8.1-2.

TABLE 8.1-2 Sampling Error Uncertainties

Error Source	Total (%) Pressure	Total (%) Temperature
Radial Sampling	±0.08	±0.08
Circumferential Sampling	±0.1	±0.2
Probe Mislocation	±0.025	±0.05

These errors are presumed to be frozen at the time of testing, and will thus appear as bias errors in the uncertainty

analysis. For this example, sampling uncertainty is categorized as an error of method.

#### 8.1.4.5 Probe Configuration

Swirl in both the core and bypass flow streams has been previously surveyed in similar nozzle systems with the same engine model and found to be less than 10 degrees for each stream. Therefore simple dual element rakes using total pressure probes with 30 degrees of probe inlet chamfer were selected. These total pressure probes have an acceptance angle of 20 or more degrees (see section 5.2). A sketch of the selected rake design is shown in Figure 8.1-10.

#### 8.1.4.6 Rake Blockage and Pressure Loss

The instrumentation rake system having five radial and five circumferential positions for both fan bypass and core streams was analysed for flow blockage and pressure loss. The pressure loss is estimated by calculating the aerodynamic drag across the rakes and dividing by the flow area. The results of the study of the blockage and flowpath pressure losses indicated the design to be acceptable from this standpoint. Table 8.1-3 shows the percent blockage, flowpath Mach number, and estimated pressure loss for each rake assembly.

TABLE 8.1-3 Estimated Pressure Loss Across Instrumentation Rakes

Nozzle Rating Station	Flowpath Blockage Percent	Flow Mach No.	Estimated Pressure Loss Percent of Upstream Total Pressure
Bypass	2.0	0.2	0.03
Core	2.1	0.3	0.08

#### 8.1.5 Uncertainty Analysis

This section presents an uncertainty analysis of nozzle coefficients for the example exhaust system. The uncertainty analysis for this example case follows the procedure outlined on page 10 of Reference 2.10.1. Presented is an uncertainty analysis for the following nozzle coefficients:

Flow coefficient of the core mixing plane area,  $C_{w7}$   
Flow coefficient of the bypass mixing plane area  $C_{w17}$   
Flow coefficient of the final nozzle exit area  $C_{w8}$   
Overall nozzle thrust coefficient  $C_F$

To evaluate the uncertainties in these calculated parameters, information about the uncertainties for each measured parameter is required. Following the procedures outlined in Section 3, the uncertainty in any parameter is split into bias component B and precision component  $t_{95} S(\bar{x})$ . The total uncertainty is then given by:

$$U = \pm [B + t_{95} S(\bar{x})]$$

where:  $t_{95}$  is the Student t value for a 95% confidence level and  $S(\bar{x})$  is the standard error of the mean. Refer to section 3 for further explanation of these terms.

The measurement uncertainties for each measured parameter will be discussed in the following sections. Details of the calculation of  $t_{95}$  may be found in Reference 2.10-2.

In the general case,  $t_{95}$  would be calculated with use of the Welch-Satterthwaite method which may also be found in Reference 2.10-2. For this example, it is assumed that each

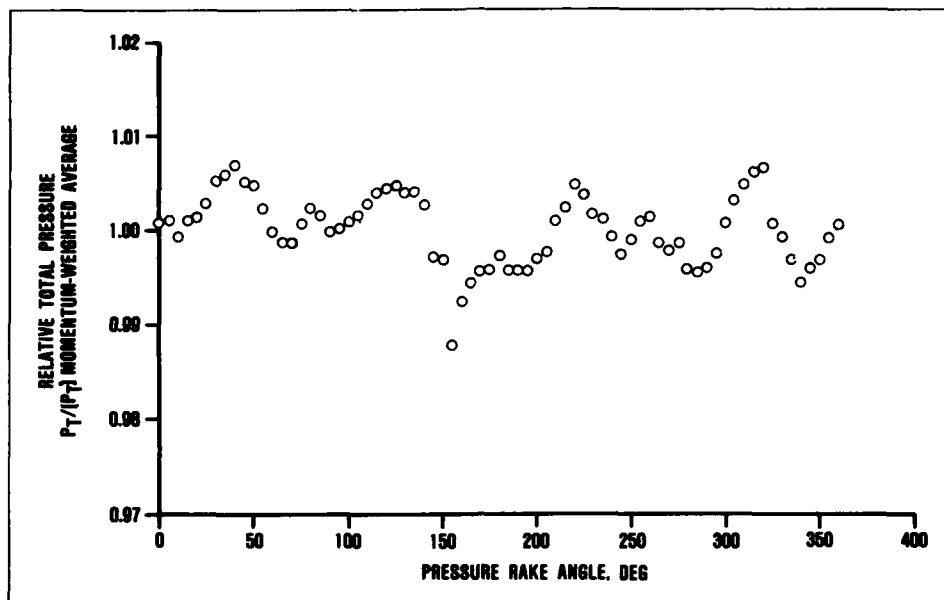


Fig. 8.1-6 Bypass total pressure circumferential variation at one radial position

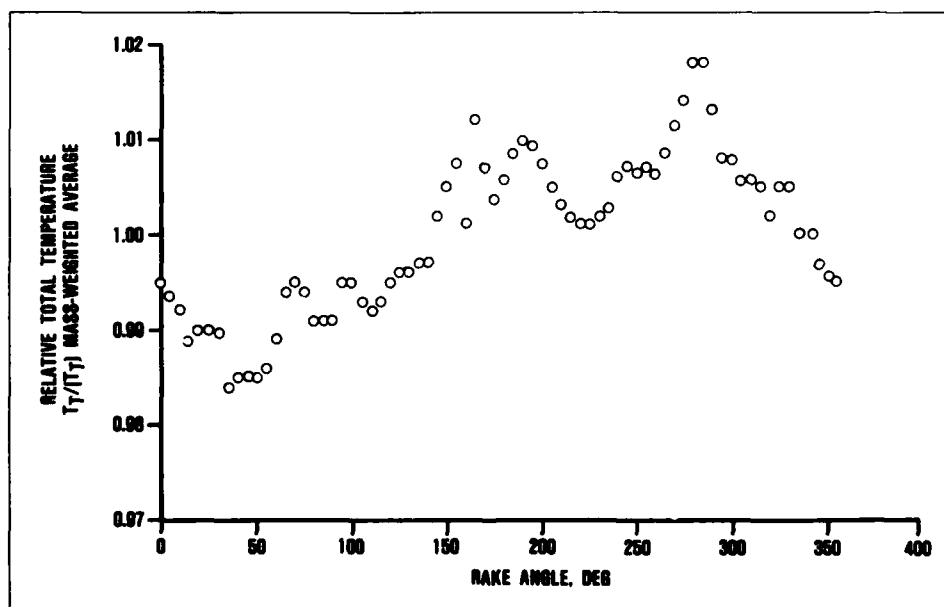


Fig. 8.1-7 Bypass total temperature circumferential variation at one radial position

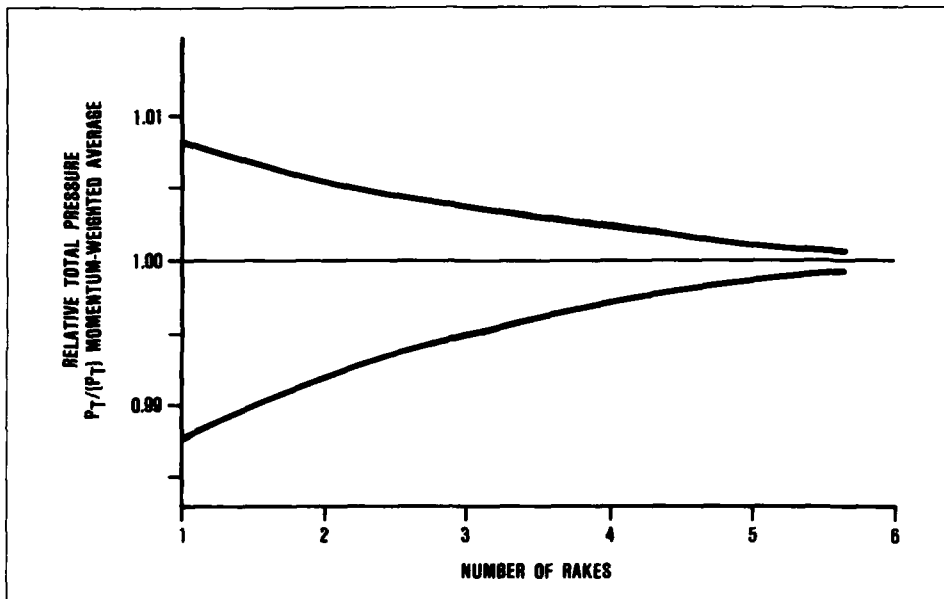


Fig. 8.1-8 Effect of number of circumferential positions on average total pressure at one radial position

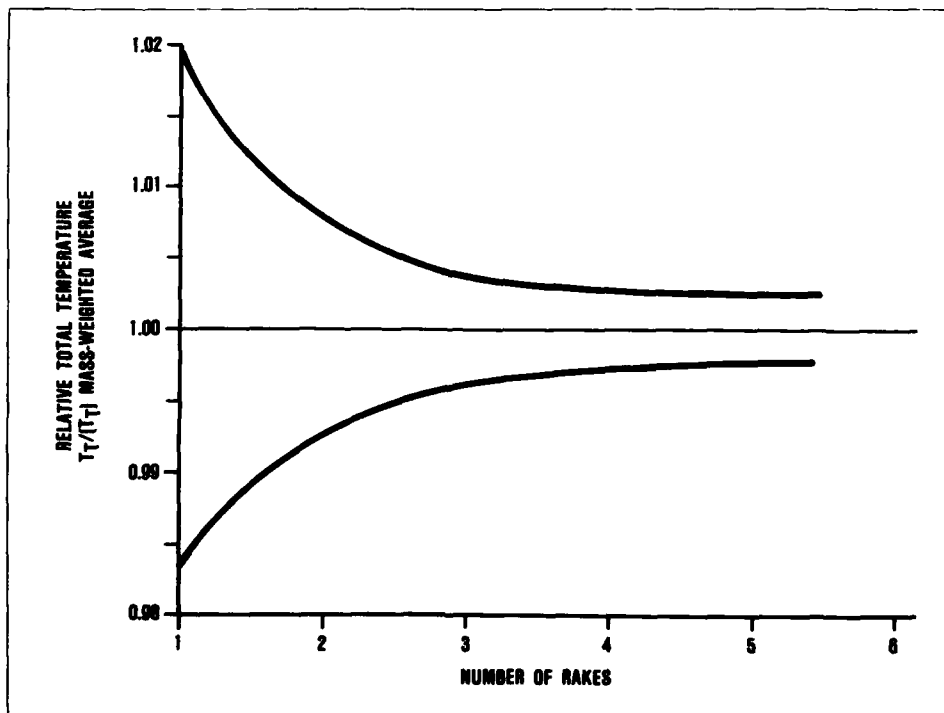


Fig. 8.1-9 Effect of number of circumferential positions on average total temperature at one radial position

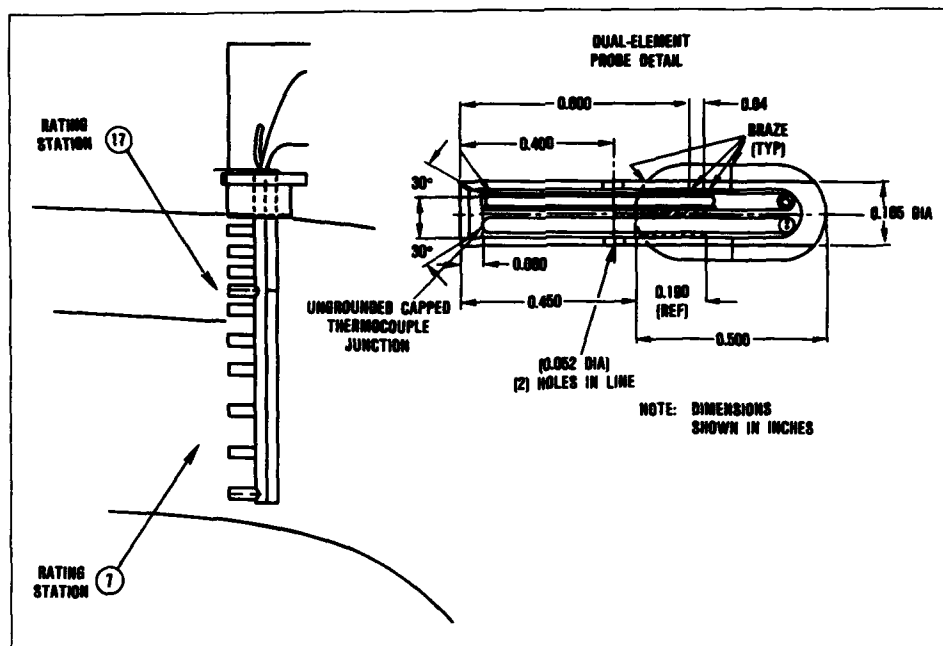


Fig. 8.1-10 Sketch of rake and probe

individual uncertainty is obtained from a large sample (i.e.  $N > 30$ ) in which case,  $t_{95}$  can be set equal to 2.0. Please note that a key assumption required to justify the above method of combining uncertainties is that all error sources are independent of one another.

The basic information used in the uncertainty analysis that follows includes the measurement uncertainty levels shown in Figures 8.1-2 and 8.1-3, Table 8.1-2, and the measured parameter values shown in Table 8.1-4. The individual uncertainties of the measurements in a common category such as, for example, the individual calibration errors, are combined by the process of "root-sum-squaring (RSS)". Other techniques are applied in the uncertainty analysis as described in the text.

The uncertainty numbers used in the analysis are initially in absolute SI units, but are converted from absolute units to percentages by dividing each RSS value of bias or precision by the appropriate parameter value shown in Table 8.1-4 and multiplying by 100. This is done as a convenience to the reader who may not be used to working in a particular type of units (British versus SI units, for example).

#### 8.1.5.1 Total Temperature Measurement Uncertainties

The value for total temperature used in this calculation is the mass-weighted average total temperature as recommended in Section 2.10.

Sources of temperature measurement uncertainty are grouped into the following four categories as recommended in Section 3.

- Calibration error ( $U_c$ )
- Data acquisition error ( $U_A$ )
- Data reduction error ( $U_R$ )
- Errors of method ( $U_M$ )

TABLE 8.1-4 Measurement Parameters Used in Uncertainty Analysis

Parameter	Value Used in Analysis
$T_{T7}$	750 K (1350°R)
$P_{T7}$	$1.0342 \times 10^5 \text{ N/m}^2$ (15.0 psia)
$P_{S7}$	$0.9722 \times 10^5 \text{ N/m}^2$ (14.1 psia)
$A_7$	$1483.9 \text{ cm}^2$ (230 in <sup>2</sup> )
$T_{T17}$	350 K (630°R)
$P_{T17}$	$0.9929 \times 10^5 \text{ N/m}^2$ (14.4 psia)
$P_{S17}$	$0.9722 \times 10^5 \text{ N/m}^2$ (14.1 psia)
$A_{17}$	$709.7 \text{ cm}^2$ (110 in <sup>2</sup> )
$A_R$	$987.1 \text{ cm}^2$ (153 in <sup>2</sup> )
$T_{T1}$	227.8 K (410°R)
$P_{AMB}$	$0.3034 \times 10^5 \text{ N/m}^2$ (4.4 psia)
$W_F$	0.15 kg/s (0.33 lbm/s)
$W_{AK}$	15.9 kg/s (35.08 lbm/s)
$F_G$	9497 N (2135 lbf)
LHV	42 795 KJ/Kg (18 400 Btu/lbm)

Figures 8.1-2 and 8.1-3 show those elemental uncertainties for temperature and pressure measurement which fall into the first three categories. Precision elemental errors are divided by the square root of the assumed number of data scans ( $\sqrt{10}$ ) and by the square root of the number of probes ( $\sqrt{25}$ ) when the precision error varies during the data scans. For example, random noise would be expected to vary over the relatively short time taken for the scans. Gain instability of the A-D converter, however, is due to temperature changes over a time period much longer than that of the scans; therefore its contribution should not be similarly reduced. In addition, bias components due to the

Multiplexer (MUX) channel-to-channel offset and the reference junction channel-to-channel offset are divided by the square root of the number of  $T_{T17}$  probes ( $\sqrt{25}$ ). This is valid because the channel-to-channel offsets are randomly distributed.

For calibration error, the uncertainties for  $T_{T17}$  are calculated from Figure 8.1-2 to be:

$$\frac{U_C}{T_{T17}} = \pm \left( \frac{B_C}{T_{T17}} + t_{95} \frac{S(\bar{x})_C}{T_{T17}} \right)$$

$$\frac{B_C}{T_{T17}} = \pm \frac{[(1.111)^2 + (0.161)^2 + (0.150)^2]^{1/2}}{350} \times 100 = \pm 0.324\%$$

$$\frac{t_{95} S(\bar{x})_C}{T_{T17}} = \pm \frac{2 \times 0}{350} = 0$$

$$\frac{U_C}{T_{T17}} = \pm (0.324\% + 0.0\%)$$

For this example, the uncertainties in  $T_{T17}$  due to acquisition errors are calculated to be:

$$\frac{U_A}{T_{T17}} = \pm \left( \frac{B_A}{T_{T17}} + t_{95} \frac{S(\bar{x})_A}{T_{T17}} \right)$$

$$\frac{B_A}{T_{T17}} = \pm \frac{[(0.133/\sqrt{25})^2 + (0.003)^2 + (0.328)^2 + (0.083)^2 + (0.022)^2 + (0.055/\sqrt{25})^2 + (0.055)^2]^{1/2}}{350} \times 100 = \pm 0.101\%$$

$$\frac{t_{95} S(\bar{x})_A}{T_{T17}} = \pm \frac{2[(0.172/\sqrt{25 \times 10})^2 + (0.011)^2 + (0.008)^2 + (0.055)^2]^{1/2}}{350} \times 100 = \pm 0.033\%$$

$$\frac{U_A}{T_{T17}} = \pm (0.101\% + 0.033\%)$$

The uncertainties due to data reduction errors (see Figure 8.1-2) are:

$$\frac{U_R}{T_{T17}} = \pm \left( \frac{B_R}{T_{T17}} + t_{95} \frac{S(\bar{x})_R}{T_{T17}} \right)$$

$$\frac{B_R}{T_{T17}} = \pm \frac{0.139}{350} \times 100 = \pm 0.040\%$$

$$\frac{t_{95} S(\bar{x})_R}{T_{T17}} = \pm \frac{2 \times 0}{350} = 0$$

$$\frac{U_R}{T_{T17}} = \pm (0.040\% + 0.0\%)$$

Finally, uncertainties due to errors of method must be considered. In the present example, these errors are due mostly to the fact that a flow with a strong temperature profile is being sampled at a small number of points. Section 8.1.4.4 covers the bias contributions to the error of method (see Table 8.1-2 in Section 8.1.4.4.3). There is no information available in the pre-test situation to estimate how the error of method changes with time variations of the profile. Using the RSS value of the individual contributions shown in Table 8.1-2 the following estimate is made for errors of method:

$$\frac{U_M}{T_{T17}} = \pm \left( \frac{B_M}{T_{T17}} + t_{95} \frac{S(\bar{x})_M}{T_{T17}} \right)$$

$$\frac{B_M}{T_{T17}} = \pm [(0.08\%)^2 + (0.2\%)^2 + (0.05\%)^2]^{1/2} = \pm 0.221\%$$

$$\frac{t_{95} S(\bar{x})_M}{T_{T17}} = \pm \frac{2 \times 0}{350} = 0$$

$$\frac{U_M}{T_{T17}} = \pm (0.221\% + 0.0\%)$$

Table 8.1-5 summarises the uncertainty information for  $T_{T17}$ :

TABLE 8.1-5 Total Temperature Uncertainties ( $T_{T17}$ )

Error Source	$\frac{B}{T_{T17}}$ (%)	$t_{95}$	$t_{95} \frac{S(\bar{x})}{T_{T17}}$ (%)
Calibration	$\pm 0.324$	2.0	$\pm 0.0$
Data Acquisition	$\pm 0.101$	2.0	$\pm 0.033$
Data Reduction	$\pm 0.040$	2.0	$\pm 0.0$
Errors of Method	$\pm 0.221$	2.0	$\pm 0.0$

To obtain the overall uncertainties in  $T_{T17}$ , the bias error uncertainties are first combined using the "Root-Sum-Square" (RSS) method as follows:

$$\frac{B_{T_{T17}}}{T_{T17}} = \pm \left[ \left( \frac{B_C}{T_{T17}} \right)^2 + \left( \frac{B_A}{T_{T17}} \right)^2 + \left( \frac{B_R}{T_{T17}} \right)^2 + \left( \frac{B_M}{T_{T17}} \right)^2 \right]^{1/2}$$

$$= \pm [(0.324)^2 + (0.101)^2 + (0.040)^2 + (0.221)^2]^{1/2}$$

$$= \pm 0.407\%$$

The uncertainties in  $T_{T17}$  due to precision error are found by combining the precision indices using RSS and multiplying by the overall  $t_{95}$  as follows:

$$t_{95} \frac{S_{T_{T17}}}{T_{T17}} = \pm t_{95} \left[ \left( \frac{S(\bar{x})_C}{T_{T17}} \right)^2 + \left( \frac{S(\bar{x})_A}{T_{T17}} \right)^2 + \left( \frac{S(\bar{x})_R}{T_{T17}} \right)^2 + \left( \frac{S(\bar{x})_M}{T_{T17}} \right)^2 \right]^{1/2}$$

$$= \pm 2[(0.0)^2 + (0.0165)^2 + (0.0)^2 + (0.0)^2]^{1/2}$$

$$= \pm 0.033\%$$

Thus the uncertainty in the  $T_{T17}$  total temperature measurement is given by:

$$\frac{U_{T_{T17}}}{T_{T17}} = \pm \left( \frac{B_{T_{T17}}}{T_{T17}} + t_{95} \frac{S(\bar{x})_{T_{T17}}}{T_{T17}} \right)$$

$$= \pm (0.407\% + 0.033\%)$$

#### 8.1.5.2 Total Pressure Measurement Uncertainties

The approach to calculating uncertainties in total pressures is the same as that for total temperatures except that bias limits cannot be reduced by the square root of the number of probes, since there are no channel-to-channel offsets. However, precision errors for non-repeatability are divided by the square root of the number of data scans since these vary during the data scans. The estimated contributions to the uncertainty in  $P_{T17}$  from the various error sources shown in Figure 8.1-3 and Table 8.1-2 are summarized in Table 8.1-6 below:

TABLE 8.1-6 Total Pressure Uncertainties ( $P_{T17}$ )

Error Source	$\frac{B}{P_{T17}}$ (%)	$t_{95}$	$t_{95} \frac{S(\bar{x})}{P_{T17}}$ (%)
Calibration	$\pm 0.048$	2.0	$\pm 0.0$
Data Acquisition	$\pm 0.056$	2.0	$\pm 0.001$
Data Reduction	$\pm 0.0$	2.0	$\pm 0.0$
Errors of Method	$\pm 0.130$	2.0	$\pm 0.0$

Combining the bias error and precision error uncertainties using the RSS method gives:

$$\frac{U_{P_{T17}}}{P_{T17}} = \left( \frac{B_{P_{T17}}}{P_{T17}} + t_{95} \frac{S(\bar{x})_{P_{T17}}}{P_{T17}} \right) = \pm (0.149\% + 0.001\%)$$

for the uncertainty in the total pressure measurement.

### 8.1.5.3 Static Pressure Measurement Uncertainties

For this example, the static pressure was assumed to be uniform across the measuring plane, and so measurements are taken using only wall static pressure taps. Uncertainties due to errors of method will, in this case, reduce to zero. Otherwise the calculation of uncertainty is identical to that for total pressure. Table 8.1-7 summarizes the error sources and uncertainties for the  $P_{S7}$  and  $P_{S17}$  static pressure measurements.

TABLE 8.1-7 Static Pressure Uncertainties

Error Source	$\frac{B}{P_{S17}}$ (%)	$t_{95}$	$t_{95} \frac{S(\bar{x})}{P_{S17}}$ (%)
Calibration	$\pm 0.049$	2.0	$\pm 0.0$
Data Acquisition	$\pm 0.053$	2.0	$\pm 0.001$
Data Reduction	$\pm 0.0$	2.0	$\pm 0.0$
Errors of Method	$\pm 0.0$	2.0	$\pm 0.0$

The overall relative uncertainty in the static pressure measurement is then given by:

$$\frac{U_{P_S}}{P_S} = \left( \frac{B_{P_S}}{P_S} + t_{95} \frac{S(\bar{x})_{P_S}}{P_S} \right) = \pm (0.072\% + 0.001\%)$$

### 8.1.5.4 Area Measurement Uncertainties

For the purposes of this calculation, the relative uncertainties in nozzle areas are estimated to be as shown in Table 8.1-8.

TABLE 8.1-8 Area Measurement Uncertainties

Flow Stream	$\frac{B}{A}$ (%)	$t_{95}$	$t_{95} \frac{S(\bar{x})}{A}$ (%)
Core Nozzle ( $A_7$ )	$\pm 1.0$	2.0	$\pm 0.0$
Bypass Nozzle ( $A_{17}$ )	$\pm 1.5$	2.0	$\pm 0.0$
Exit Nozzle ( $A_8$ )	$\pm 0.3$	2.0	$\pm 0.0$

These values are based on experience with the multiple measurements of similar exhaust systems by technicians. They include the ability to read the measuring tape, as well as calculation errors made because the walls are not round or concentric.

### 8.1.5.5 Uncertainty in Measurement of Total Mass Flow, $W_{AMB}$ , Fuel Flow, $W_F$ , Fuel Lower Heating Value, LHV, and Gross Thrust, $F_G$

The total mass flow,  $W_{AMB}$ , is based on measured airflow at the inlet to the engine adjusted for estimated external leakage and fuel addition. A separate uncertainty analysis performed for the air flow measurement gives the results shown in Table 8.1-9. This analysis was performed in accordance with Reference 8.1-1. A similar analysis has been performed for the fuel flow, gross thrust, and fuel

lower heating value measurements, and these results are also summarized in Table 8.1-9.

TABLE 8.1-9 Air Flow, Fuel Flow, and Thrust Uncertainties

Measurement	B (%)	$t_{95}$	$t_{95} S(\bar{x})$ (%)
Fuel Flow, $W_F$	$\pm 0.54$	2.0	$\pm 0.1$
Air Flow, $W_{AMB}$	$\pm 1.0$	2.0	$\pm 0.3$
Gross Thrust, $F_G$	$\pm 0.5$	2.0	$\pm 0.4$
Fuel Lower Heating Value, LHV	$\pm 0.15$	2.0	$\pm 0.0$

### 8.1.5.6 Parameters to be Calculated

The station nomenclature for the compound nozzle being considered is shown in Figure 8.1-1.

The measurements available for this analysis are as follows:

- (a) Core stream:  $T_{T7}$ ,  $P_{T7}$ ,  $P_{S7}$ ,  $A_7$
- (b) Bypass stream:  $T_{T17}$ ,  $P_{T17}$ ,  $P_{S17}$ ,  $A_{17}$
- (c) Engine nozzle:  $A_8$ ,  $P_{AMB}$
- (d) Engine overall:  $T_{T1}$   
 $W_F$  (fuel flow)  
 $W_{AMB}$  (total air flow)  
 $F_G$  (gross thrust)  
LHV (fuel lower heating value)

These measurements will be used to calculate the following parameters of interest:

- (a) Flow coefficient of core mixing plane area:  
 $C_{W7} = \frac{W_{A7}}{W_{A71}}$
- (b) Flow coefficient of bypass mixing plane area:  
 $C_{W17} = \frac{W_{A17}}{W_{A171}}$
- (c) Flow coefficient of exit nozzle area:  
 $C_{W8} = \frac{W_{A8}}{W_{A81}}$
- (d) Thrust coefficient of exhaust nozzle:  
 $C_F = \frac{F_G}{F_{G1}}$

Ideal values are signified above by the subscript 1. The objective of the current analysis is to determine the expected uncertainties in each of these flow and thrust coefficients.

### 8.1.5.7 Calculation of Ideal Flows

The core and bypass flow streams are known to be unchoked at the mixing plane, and so the following equation applies (from Section 2.10):

$$W_{A1} = \frac{P_1 A}{(P_1/P_S)^{1/\gamma}} \sqrt{\frac{2\gamma g_c}{RT_1(\gamma-1)}} \left[ 1 - \left( \frac{P_1}{P_S} \right)^{(1-\gamma)/\gamma} \right]$$

From this equation, the bias component is found to be given by:

$$\frac{B_{W_{A1}}}{W_{A1}} = \pm \left[ \left( \frac{1}{W_{A1}} \frac{\partial W_{A1}}{\partial T_1} B_{T_1} \right)^2 + \left( \frac{1}{W_{A1}} \frac{\partial W_{A1}}{\partial P_1} B_{P_1} \right)^2 + \left( \frac{1}{W_{A1}} \frac{\partial W_{A1}}{\partial P_S} B_{P_S} \right)^2 + \left( \frac{1}{W_{A1}} \frac{\partial W_{A1}}{\partial A} B_A \right)^2 \right]^{1/2}$$

Similarly, the combined precision component can be found using:

$$\frac{S_{W_{A1}}}{W_{A1}} = \pm \left[ \left( \frac{1}{W_{A1}} \frac{\partial W_{A1}}{\partial T_T} S(\bar{x})_{T_T} \right)^2 + \left( \frac{1}{W_{A1}} \frac{\partial W_{A1}}{\partial P_T} S(\bar{x})_{P_T} \right)^2 + \left( \frac{1}{W_{A1}} \frac{\partial W_{A1}}{\partial P_5} S(\bar{x})_{P_5} \right)^2 + \left( \frac{1}{W_{A1}} \frac{\partial W_{A1}}{\partial A} S(\bar{x})_A \right)^2 \right]^{1/2}$$

where:

$$\frac{1}{W_{A1}} \frac{\partial W_{A1}}{\partial T_T} = -\frac{1}{2} \frac{1}{T_T}$$

$$\frac{1}{W_{A1}} \frac{\partial W_{A1}}{\partial P_T} = C_1 \frac{1}{P_T}$$

$$\frac{1}{W_{A1}} \frac{\partial W_{A1}}{\partial P_5} = (1 - C_1) \frac{1}{P_5}$$

$$\frac{1}{W_{A1}} \frac{\partial W_{A1}}{\partial A} = \frac{1}{A}$$

and where:

$$C_1 = \left[ \frac{\gamma - 1}{\gamma} \right] \left[ 1 + \frac{1}{2} \left\{ \left( \frac{P_T}{P_5} \right)^{(\gamma-1)/\gamma} - 1 \right\} \right]^{-1}$$

These equations apply to either station 7 or 17, with use of measured parameters in the applicable stream.

The exit nozzle operates at a high pressure ratio and is thus choked. In this case, the following equation for choked convergent nozzles applies (see Section 2.10).

$$W_{A8} = P_{T8} A_8 \sqrt{\frac{\gamma g_c}{RT_{T8}}} \left( \frac{2}{\gamma + 1} \right)^{(\gamma+1)/(\gamma-1)}$$

For this equation, the relative bias component uncertainties are given by:

$$\frac{B_{W_{A8}}}{W_{A8}} = \pm \left[ \left( \frac{1}{W_{A8}} \frac{\partial W_{A8}}{\partial T_{T8}} B_{T_{T8}} \right)^2 + \left( \frac{1}{W_{A8}} \frac{\partial W_{A8}}{\partial P_{T8}} B_{P_{T8}} \right)^2 + \left( \frac{1}{W_{A8}} \frac{\partial W_{A8}}{\partial A_8} B_{A_8} \right)^2 \right]^{1/2}$$

Similarly, the combined relative precision component can be found using:

$$\frac{S_{W_{A8}}}{W_{A8}} = \pm \left[ \left( \frac{1}{W_{A8}} \frac{\partial W_{A8}}{\partial T_{T8}} S(\bar{x})_{T_{T8}} \right)^2 + \left( \frac{1}{W_{A8}} \frac{\partial W_{A8}}{\partial P_{T8}} S(\bar{x})_{P_{T8}} \right)^2 + \left( \frac{1}{W_{A8}} \frac{\partial W_{A8}}{\partial A_8} S(\bar{x})_{A_8} \right)^2 \right]^{1/2}$$

where:

$$\frac{1}{W_{A8}} \frac{\partial W_{A8}}{\partial T_{T8}} = -\frac{1}{2} \frac{1}{T_{T8}}$$

$$\frac{1}{W_{A8}} \frac{\partial W_{A8}}{\partial P_{T8}} = \frac{1}{P_{T8}}$$

$$\frac{1}{W_{A8}} \frac{\partial W_{A8}}{\partial A_8} = \frac{1}{A_8}$$

For ideal flow, the uncertainties due to bias and precision can be combined as follows:

$$\frac{U_{W_{A1}}}{W_{A1}} = \pm \left( \frac{B_{W_{A1}}}{W_{A1}} + t_{0.5} \frac{S(\bar{x})_{W_{A1}}}{W_{A1}} \right)$$

### 8.1.5.8 Calculations of Core and Bypass Flows

The core and bypass nozzle flows will not be measured directly in this test, but will be calculated using the energy balance method previously discussed in Section 2.10.5.

The energy balance method is based on application of the conservation of mass equation and on the first law of thermodynamics.

The conservation of mass equation defines that:  
total flow in = total flow out

The first law of thermodynamics defines that:  
total energy in = total energy out

The following quantities must be known: (1) The flow rates and temperatures of all flows entering and leaving the engine, including the flow rates and temperatures of all leakages and bleed flows, (2) the heating value of the fuel, and (3) any power or heat transfer input to or extracted from the engine.

By combining the conservation of mass and energy balance equations, a direct solution of core and bypass flows is obtained that satisfies both the flow continuity and energy balance relationships.

The values of the derivatives used in the calculation of uncertainties were generated by perturbing the measured values used by the data reduction program. Note that values obtained in this way are valid only for the test point being considered.

Measured values of  $T_{T7}$ ,  $T_{T17}$ ,  $T_{T1}$ ,  $W_F$ , LHV, and  $W_{A8}$  are required to calculate the bypass and core flows. Table 8.1-10 summarizes the results of this calculation:

TABLE 8.1-10 Bypass and Core Flows

Parameter	Value
$W_{A7}$ (core)	11.08 Kg/s (24.43 lbm/s)
$W_{A17}$ (bypass)	4.83 Kg/s (10.65 lbm/s)

Bias component uncertainties for calculated core flow are given by:

$$\frac{B_{W_{A7}}}{W_{A7}} = \pm \left[ \left( \frac{1}{W_{A7}} \frac{\partial W_{A7}}{\partial T_{T7}} B_{T_{T7}} \right)^2 + \left( \frac{1}{W_{A7}} \frac{\partial W_{A7}}{\partial T_{T17}} B_{T_{T17}} \right)^2 + \left( \frac{1}{W_{A7}} \frac{\partial W_{A7}}{\partial T_{T1}} B_{T_{T1}} \right)^2 + \left( \frac{1}{W_{A7}} \frac{\partial W_{A7}}{\partial W_F} B_{W_F} \right)^2 + \left( \frac{1}{W_{A7}} \frac{\partial W_{A7}}{\partial LHV} B_{LHV} \right)^2 + \left( \frac{1}{W_{A7}} \frac{\partial W_{A7}}{\partial W_{A8}} B_{W_{A8}} \right)^2 \right]^{1/2}$$

Similarly, the combined precision component for calculated core flow is given by:

$$\frac{S_{W_{A7}}}{W_{A7}} = \pm \left[ \left( \frac{1}{W_{A7}} \frac{\partial W_{A7}}{\partial T_{T7}} S(\bar{x})_{T_{T7}} \right)^2 + \left( \frac{1}{W_{A7}} \frac{\partial W_{A7}}{\partial T_{T17}} S(\bar{x})_{T_{T17}} \right)^2 + \left( \frac{1}{W_{A7}} \frac{\partial W_{A7}}{\partial T_{T1}} S(\bar{x})_{T_{T1}} \right)^2 + \left( \frac{1}{W_{A7}} \frac{\partial W_{A7}}{\partial W_F} S(\bar{x})_{W_F} \right)^2 + \left( \frac{1}{W_{A7}} \frac{\partial W_{A7}}{\partial LHV} S(\bar{x})_{LHV} \right)^2 + \left( \frac{1}{W_{A7}} \frac{\partial W_{A7}}{\partial W_{A8}} S(\bar{x})_{W_{A8}} \right)^2 \right]^{1/2}$$

where, from perturbing the appropriate measured parameters with use of the data reduction program:

$$\frac{1}{W_{A7}} \frac{\partial W_{A7}}{\partial T_{T7}} = \frac{-1.8346}{T_{T7}}$$

$$\frac{1}{W_{A7}} \frac{\partial W_{A7}}{\partial T_{T17}} = \frac{-0.4436}{T_{T17}}$$

$$\frac{1}{W_{A7}} \frac{\partial W_{A7}}{\partial T_{T1}} = \frac{0.7888}{T_{T1}}$$

$$\frac{1}{W_{A7}} \frac{\partial W_{A7}}{\partial W_F} = \frac{1.3567}{W_F}$$

$$\frac{1}{W_{A7}} \frac{\partial W_{A7}}{\partial LHV} = \frac{1.3567}{LHV}$$

$$\frac{1}{W_{A7}} \frac{\partial W_{A7}}{\partial W_{A8}} = \frac{-0.4222}{W_{A8}}$$

For the calculated bypass flow, the bias component uncertainties are given by:

$$\begin{aligned} \frac{B_{W_{A17}}}{W_{A17}} = \pm & \left[ \left( \frac{1}{W_{A17}} \frac{\partial W_{A17}}{\partial T_{T7}} B_{T_{T7}} \right)^2 + \left( \frac{1}{W_{A17}} \frac{\partial W_{A17}}{\partial T_{T17}} B_{T_{T17}} \right)^2 \right. \\ & + \left( \frac{1}{W_{A17}} \frac{\partial W_{A17}}{\partial T_{T1}} B_{T_{T1}} \right)^2 + \left( \frac{1}{W_{A17}} \frac{\partial W_{A17}}{\partial W_F} B_{W_F} \right)^2 \\ & \left. + \left( \frac{1}{W_{A17}} \frac{\partial W_{A17}}{\partial LHV} B_{LHV} \right)^2 + \left( \frac{1}{W_{A17}} \frac{\partial W_{A17}}{\partial W_{A8}} B_{W_{A8}} \right)^2 \right]^{1/2} \end{aligned}$$

The combined precision index for the bypass flow is given by:

$$\begin{aligned} \frac{S_{W_{A17}}}{W_{A17}} = \pm & \left[ \left( \frac{1}{W_{A17}} \frac{\partial W_{A17}}{\partial T_{T7}} S(\bar{x})_{T_{T7}} \right)^2 + \left( \frac{1}{W_{A17}} \frac{\partial W_{A17}}{\partial T_{T17}} S(\bar{x})_{T_{T17}} \right)^2 \right. \\ & + \left( \frac{1}{W_{A17}} \frac{\partial W_{A17}}{\partial T_{T1}} S(\bar{x})_{T_{T1}} \right)^2 + \left( \frac{1}{W_{A17}} \frac{\partial W_{A17}}{\partial W_F} S(\bar{x})_{W_F} \right)^2 \\ & + \left( \frac{1}{W_{A17}} \frac{\partial W_{A17}}{\partial LHV} S(\bar{x})_{LHV} \right)^2 \\ & \left. + \left( \frac{1}{W_{A17}} \frac{\partial W_{A17}}{\partial W_{A8}} S(\bar{x})_{W_{A8}} \right)^2 \right]^{1/2} \end{aligned}$$

where, from perturbing the appropriate measured parameter with use of the data reduction program:

$$\frac{1}{W_{A17}} \frac{\partial W_{A17}}{\partial T_{T7}} = \frac{4.2085}{T_{T7}}$$

$$\frac{1}{W_{A17}} \frac{\partial W_{A17}}{\partial T_{T17}} = \frac{1.0175}{T_{T17}}$$

$$\frac{1}{W_{A17}} \frac{\partial W_{A17}}{\partial T_{T1}} = \frac{-1.8094}{T_{T1}}$$

$$\frac{1}{W_{A17}} \frac{\partial W_{A17}}{\partial W_F} = \frac{-3.0788}{W_F}$$

$$\frac{1}{W_{A17}} \frac{\partial W_{A17}}{\partial LHV} = \frac{-3.0788}{LHV}$$

$$\frac{1}{W_{A17}} \frac{\partial W_{A17}}{\partial W_{A8}} = \frac{4.2623}{W_{A8}}$$

Once the individual values of the biases and precision indices are substituted, the overall uncertainties in  $W_{A7}$  and  $W_{A17}$  are given by:

$$\frac{U_{W_{A7}}}{W_{A7}} = \pm \left( \frac{B_{W_{A7}}}{W_{A7}} + t_{95} \frac{S(\bar{x})_{W_{A7}}}{W_{A7}} \right)$$

$$\frac{U_{W_{A17}}}{W_{A17}} = \pm \left( \frac{B_{W_{A17}}}{W_{A17}} + t_{95} \frac{S(\bar{x})_{W_{A17}}}{W_{A17}} \right)$$

#### 8.1.5.9 Calculation of Total Temperature at Nozzle Exit

A mass averaged total temperature is calculated at the nozzle exit. This average temperature will be used in the calculation of exit nozzle ideal flow and flow coefficient only.

The bias error for  $T_{T8}$  is:

$$\begin{aligned} \frac{B_{T_{T8}}}{T_{T8}} = \pm & \left[ \left( \frac{1}{T_{T8}} \frac{\partial T_{T8}}{\partial W_F} B_{W_F} \right)^2 + \left( \frac{1}{T_{T8}} \frac{\partial T_{T8}}{\partial LHV} B_{LHV} \right)^2 \right. \\ & + \left( \frac{1}{T_{T8}} \frac{\partial T_{T8}}{\partial W_{A8}} B_{W_{A8}} \right)^2 + \left( \frac{1}{T_{T8}} \frac{\partial T_{T8}}{\partial T_{T7}} B_{T_{T7}} \right)^2 \\ & \left. + \left( \frac{1}{T_{T8}} \frac{\partial T_{T8}}{\partial T_{T17}} B_{T_{T17}} \right)^2 + \left( \frac{1}{T_{T8}} \frac{\partial T_{T8}}{\partial T_{T1}} B_{T_{T1}} \right)^2 \right]^{1/2} \end{aligned}$$

Similarly, the combined precision index is given by:

$$\begin{aligned} \frac{S_{T_{T8}}}{T_{T8}} = \pm & \left[ \left( \frac{1}{T_{T8}} \frac{\partial T_{T8}}{\partial W_F} S(\bar{x})_{W_F} \right)^2 + \left( \frac{1}{T_{T8}} \frac{\partial T_{T8}}{\partial LHV} S(\bar{x})_{LHV} \right)^2 \right. \\ & + \left( \frac{1}{T_{T8}} \frac{\partial T_{T8}}{\partial W_{A8}} S(\bar{x})_{W_{A8}} \right)^2 + \left( \frac{1}{T_{T8}} \frac{\partial T_{T8}}{\partial T_{T7}} S(\bar{x})_{T_{T7}} \right)^2 \\ & \left. + \left( \frac{1}{T_{T8}} \frac{\partial T_{T8}}{\partial T_{T17}} S(\bar{x})_{T_{T17}} \right)^2 + \left( \frac{1}{T_{T8}} \frac{\partial T_{T8}}{\partial T_{T1}} S(\bar{x})_{T_{T1}} \right)^2 \right]^{1/2} \end{aligned}$$

where, from perturbing the appropriate measured parameters with use of the data reduction program:

$$\frac{1}{T_{T8}} \frac{\partial T_{T8}}{\partial W_F} = \frac{0.5918}{W_F}$$

$$\frac{1}{T_{T8}} \frac{\partial T_{T8}}{\partial LHV} = \frac{0.5918}{LHV}$$

$$\frac{1}{T_{T8}} \frac{\partial T_{T8}}{\partial W_{A8}} = \frac{-0.5835}{W_{A8}}$$

$$\frac{1}{T_{T8}} \frac{\partial T_{T8}}{\partial T_{T7}} = \frac{0.0502}{T_{T7}}$$

$$\frac{1}{T_{T8}} \frac{\partial T_{T8}}{\partial T_{T17}} = \frac{0.0067}{T_{T17}}$$

$$\frac{1}{T_{T8}} \frac{\partial T_{T8}}{\partial T_{T1}} = \frac{0.3468}{T_{T1}}$$

#### 8.1.5.10 Calculation of Average total Pressure at Nozzle Inlet Mixing Plane

Following the practice recommended in Section 2.10, Dzung's method is used to calculate an average total pressure at the nozzle inlet mixing plane. This average pressure will be used in the calculation of exit nozzle ideal

flow and flow coefficient only. The overall uncertainty in the average pressure is given by:

$$\frac{U_{P_{12}}}{P_{12}} = \pm \left( \frac{B_{P_{12}}}{P_{12}} + t_{0.95} \frac{S(\bar{x})_{P_{12}}}{P_{12}} \right) = \pm (0.149\% + 0.001\%).$$

#### 8.1.5.11 Calculation of Ideal Gross Thrust

The ideal gross thrust is calculated by adding the ideal gross thrusts calculated for each flow stream separately, as follows:

$$F_{GI} = F_{GI1} + F_{GI17}$$

where (from Section 2.10):

$$F_{GI1} = W_{A17} \left[ \frac{2\gamma RT_{17}}{(\gamma - 1)g_c} \left\{ 1 - \left( \frac{P_{17}}{P_{AMB}} \right)^{1/\gamma} \right\} \right]^{1/2}$$

and

$$F_{GI17} = W_{A17} \left[ \frac{2\gamma RT_{17}}{(\gamma - 1)g_c} \left\{ 1 - \left( \frac{P_{17}}{P_{AMB}} \right)^{1/\gamma} \right\} \right]^{1/2}$$

Since the values and uncertainties of the parameters in both equations are interrelated through the energy balance, the uncertainty sensitivities for the total ideal gross thrust were determined through use of the data reduction program. The uncertainty of ideal gross thrust is affected by the uncertainties of the measured parameters in the above equations, as well as by those of the additional parameters of  $W_{AB}$ ,  $W_F$ , LHV, and  $T_{T1}$  that are used in the energy balance equations.

The bias determination for ideal gross thrust is given by:

$$\begin{aligned} \frac{B_{F_{GI}}}{F_{GI}} = & \pm \left[ \left( \frac{1}{F_{GI}} \frac{\partial F_{GI}}{\partial T_{17}} B_{T_{17}} \right)^2 + \left( \frac{1}{F_{GI}} \frac{\partial F_{GI}}{\partial T_{17}} B_{T_{17}} \right)^2 \right. \\ & + \left( \frac{1}{F_{GI}} \frac{\partial F_{GI}}{\partial W_F} B_{W_F} \right)^2 + \left( \frac{1}{F_{GI}} \frac{\partial F_{GI}}{\partial LHV} B_{LHV} \right)^2 \\ & + \left( \frac{1}{F_{GI}} \frac{\partial F_{GI}}{\partial P_{17}} B_{P_{17}} \right)^2 + \left( \frac{1}{F_{GI}} \frac{\partial F_{GI}}{\partial P_{17}} B_{P_{17}} \right)^2 + \left( \frac{1}{F_{GI}} \frac{\partial F_{GI}}{\partial W_{AB}} B_{W_{AB}} \right)^2 \\ & \left. + \left( \frac{1}{F_{GI}} \frac{\partial F_{GI}}{\partial P_{AMB}} B_{P_{AMB}} \right)^2 + \left( \frac{1}{F_{GI}} \frac{\partial F_{GI}}{\partial T_{T1}} B_{T_{T1}} \right)^2 \right]^{1/2} \end{aligned}$$

and similarly the combined precision index is given by:

$$\begin{aligned} \frac{S_{F_{GI}}}{F_{GI}} = & \pm \left[ \left( \frac{1}{F_{GI}} \frac{\partial F_{GI}}{\partial T_{17}} S(\bar{x})_{T_{17}} \right)^2 + \left( \frac{1}{F_{GI}} \frac{\partial F_{GI}}{\partial T_{17}} S(\bar{x})_{T_{17}} \right)^2 \right. \\ & + \left( \frac{1}{F_{GI}} \frac{\partial F_{GI}}{\partial W_F} S(\bar{x})_{W_F} \right)^2 + \left( \frac{1}{F_{GI}} \frac{\partial F_{GI}}{\partial LHV} S(\bar{x})_{LHV} \right)^2 \\ & + \left( \frac{1}{F_{GI}} \frac{\partial F_{GI}}{\partial P_{17}} S(\bar{x})_{P_{17}} \right)^2 + \left( \frac{1}{F_{GI}} \frac{\partial F_{GI}}{\partial P_{17}} S(\bar{x})_{P_{17}} \right)^2 \\ & + \left( \frac{1}{F_{GI}} \frac{\partial F_{GI}}{\partial W_{AB}} S(\bar{x})_{W_{AB}} \right)^2 \\ & + \left( \frac{1}{F_{GI}} \frac{\partial F_{GI}}{\partial P_{AMB}} S(\bar{x})_{P_{AMB}} \right)^2 \\ & \left. + \left( \frac{1}{F_{GI}} \frac{\partial F_{GI}}{\partial T_{T1}} S(\bar{x})_{T_{T1}} \right)^2 \right]^{1/2} \end{aligned}$$

where, from perturbing the appropriate measured parameters with use of the data reduction program:

$$\frac{1}{F_{GI}} \frac{\partial F_{GI}}{\partial T_{17}} = \frac{0.025}{T_{17}}$$

$$\frac{1}{F_{GI}} \frac{\partial F_{GI}}{\partial T_{17}} = \frac{-0.1072}{T_{17}}$$

$$\frac{1}{F_{GI}} \frac{\partial F_{GI}}{\partial P_{17}} = \frac{0.2483}{P_{17}}$$

$$\frac{1}{F_{GI}} \frac{\partial F_{GI}}{\partial P_{17}} = \frac{0.0952}{P_{17}}$$

$$\frac{1}{F_{GI}} \frac{\partial F_{GI}}{\partial W_{AB}} = \frac{0.6385}{W_{AB}}$$

$$\frac{1}{F_{GI}} \frac{\partial F_{GI}}{\partial W_F} = \frac{0.3542}{W_F}$$

$$\frac{1}{F_{GI}} \frac{\partial F_{GI}}{\partial LHV} = \frac{0.3542}{LHV}$$

$$\frac{1}{F_{GI}} \frac{\partial F_{GI}}{\partial P_{AMB}} = \frac{-0.3387}{P_{AMB}}$$

$$\frac{1}{F_{GI}} \frac{\partial F_{GI}}{\partial T_{T1}} = \frac{0.2036}{T_{T1}}$$

The combined uncertainties in ideal gross thrust are then given by:

$$\frac{U_{F_{GI}}}{F_{GI}} = \pm \left( \frac{B_{F_{GI}}}{F_{GI}} + t_{0.95} \frac{S(\bar{x})_{F_{GI}}}{F_{GI}} \right)$$

#### 8.1.5.12 Calculation of Uncertainties in Flow Coefficients

For the core stream, for the bypass stream, and for the exit nozzle, the flow coefficient is defined as:

$$C_w = \frac{W}{W_i}$$

where  $W$  is the measured or calculated flow and  $W_i$  is the corresponding ideal flow.

The relative uncertainties due to bias component are then found using:

$$\frac{B_{C_w}}{C_w} = \pm \left[ \left( \frac{B_w}{W} \right)^2 + \left( \frac{B_{W_i}}{W_i} \right)^2 \right]^{1/2}$$

while the precision component is given by:

$$\frac{S_{C_w}}{C_w} = \pm \left[ \left( \frac{S(\bar{x})_w}{W} \right)^2 + \left( \frac{S(\bar{x})_{W_i}}{W_i} \right)^2 \right]^{1/2}$$

These are then combined to give the overall uncertainty using:

$$\frac{U_{C_w}}{C_w} = \pm \left( \frac{B_{C_w}}{C_w} + t_{0.95} \frac{S(\bar{x})_{C_w}}{C_w} \right)$$

#### 8.1.5.13 Calculation of Uncertainties in Nozzle Thrust Coefficient

The nozzle thrust coefficient is defined as:

$$C_F = \frac{F_G}{F_{GI}}$$

where  $F_G$  is the gross thrust and  $F_{GI}$  is the ideal gross thrust.

The relative uncertainties due to bias component are given by:

$$\frac{B_{CF}}{C_F} = \pm \left[ \left( \frac{B_{F_G}}{F_G} \right)^2 + \left( \frac{B_{F_{G1}}}{F_{G1}} \right)^2 \right]^{1/2}$$

with the precision component given by:

$$\frac{S_{CF}}{C_F} = \pm \left[ \left( \frac{S(\bar{x})_{F_G}}{F_G} \right)^2 + \left( \frac{S(\bar{x})_{F_{G1}}}{F_{G1}} \right)^2 \right]^{1/2}$$

These are combined to give the overall uncertainty using:

$$\frac{U_{CF}}{C_F} = \pm \left( \frac{B_{CF}}{C_F} + t_{95} \frac{S(\bar{x})_{CF}}{C_F} \right)$$

$$\frac{U_{CF}}{CF} = \pm \left( \frac{B_{CF}}{CF} + t_{95} \frac{S(\bar{x})_{CF}}{CF} \right) = \pm 1.31\%$$

$$\frac{U_{C_{W8}}}{C_{W8}} = \pm \left( \frac{B_{C_{W8}}}{C_{W8}} + t_{95} \frac{S(\bar{x})_{C_{W8}}}{C_{W8}} \right) = \pm 1.43\%$$

$$\frac{U_{C_{W7}}}{C_{W7}} = \pm \left( \frac{B_{C_{W7}}}{C_{W7}} + t_{95} \frac{S(\bar{x})_{C_{W7}}}{C_{W7}} \right) = \pm 2.36\%$$

$$\frac{U_{C_{W17}}}{C_{W17}} = \pm \left( \frac{B_{C_{W17}}}{C_{W17}} + t_{95} \frac{S(\bar{x})_{C_{W17}}}{C_{W17}} \right) = \pm 8.01\%$$

#### 8.1.5.14 Predicted Magnitudes of Measured and Calculated Parameters

The magnitudes and predicted uncertainties for all directly measured parameters are summarized in Table 8.1-11.

A probable initial reaction to the above results is that the uncertainty in  $C_{W17}$  is unacceptably large. This large uncertainty in  $C_{W17}$  is basically caused by a combination of a

TABLE 8.1-11 Magnitudes and Uncertainties of Measured Parameters

Measured Parameter	Magnitude	Bias, B(%)	Precision $t_{95} S(\bar{x})$ (%)
$T_{T7}$	750 K (1350°R)	0.370	0.014
$P_{T7}$	$1.0342 \times 10^5$ N/m <sup>2</sup> (15.0 psia)	0.149	0.001
$P_{S7}$	$0.9722 \times 10^5$ N/m <sup>2</sup> (14.1 psia)	0.072	0.001
$A_7$	1483.9 cm <sup>2</sup> (230 in <sup>2</sup> )	1.0	0.0
$T_{T17}$	350 K (630°R)	0.407	0.033
$P_{T17}$	$0.9929 \times 10^5$ N/m <sup>2</sup> (14.4 psia)	0.149	0.001
$P_{S17}$	$0.9722 \times 10^5$ N/m <sup>2</sup> (14.1 psia)	0.072	0.001
$A_{17}$	709.7 cm <sup>2</sup> (110 in <sup>2</sup> )	1.5	0.0
$A_R$	987.1 cm <sup>2</sup> (153 in <sup>2</sup> )	0.30	0.0
$T_{T1}$	227.8 K (410°R)	0.996	0.050
$P_{AMB}$	$0.3034 \times 10^5$ N/m <sup>2</sup> (4.4 psia)	0.074	0.001
$W_F$	0.15 kg/s (0.33 lbm/s)	0.5	.1
$W_{AR}$	15.9 kg/s (35.08 lbm/s)	1.0	0.3
$F_G$	9497 N (2135 lbf)	0.5	0.4
LHV	42 795 KJ/Kg (18 400 Btu/lbm)	0.15	0.0

Table 8.1-12 summarizes the magnitudes and uncertainties of the parameters calculated from the measured parameters in Table 8.1-11.

large sensitivity of  $W_{A17}$  uncertainty to the uncertainty of  $W_{AR}$  (through the energy balance determination of the flow split) and the low flowpath Mach number at Station 17.

TABLE 8.1-12 Magnitudes and Uncertainties of Calculated Parameters

Calculated Parameter	Magnitude	Bias, B(%)	Precision $t_{95} S$ (%)
$W_{A7}$	11.08 kg/s (24.43 lbm/s)	1.366	0.193
$W_{A71}$	11.34 kg/s (25.00 lbm/s)	1.68	0.014
$C_{W7}$	0.9772	2.167	0.193
$W_{A17}$	4.83 kg/s (10.65 lbm/s)	5.195	1.320
$W_{A171}$	4.91 kg/s (10.83 lbm/s)	4.21	0.037
$C_{W17}$	0.9816	6.689	1.320
$T_{T8}$	627.9 K (1130°R)	0.755	0.186
$P_{T8}$	$1.0204 \times 10^5$ N/m <sup>2</sup> (14.8 psia)	0.149	0.001
$W_{AR1}$	16.25 kg/s (35.82 lbm/s)	0.505	0.093
$C_{W8}$	0.9820	1.120	0.314
$F_{G1}$	9639 N (2166.9 lbf)	0.701	0.195
$C_F$	0.985	0.861	0.445

#### 8.1.5.15 Uncertainties of Nozzle Coefficients and Impact on Net Thrust Prediction

The calculated uncertainties of the nozzle coefficients are:

resulting in a small difference between measured  $P_{S17}$  and  $P_{T17}$ . Since the ideal flow is determined as a function of the ratio  $P_{S17}/P_{T17}$ , the individual uncertainties in  $P_{S17}$  and  $P_{T17}$  tend to multiply the effect on the ideal flow used to calculate  $C_{W17}$ . If a primary goal of this test were to obtain an accurate

determination of  $C_{w17}$  some other means of determining the flow split such as use of a calibrated turbine flow function or direct measurement in the bypass or core streams might be in order. However, to determine whether the above uncertainties are acceptable or unacceptable with regard to meeting the goals of this particular example, one must consider how the coefficients will be used. In this example, maps of the flow and thrust coefficients are to be incorporated into an engine model which will then be used to predict engine performance at various operating conditions.

As an example, the engine model is often used to produce curves of net thrust versus fan speed. The critical acceptance criterion is then whether the uncertainties induced in the net thrust calculation are acceptable. For the engine to be tested, the following derivatives were determined with use of the engine analytical model for the more sensitive of the two operating conditions being considered, that is, Mach 0.8, 40,000 feet, standard atmosphere:

$$\frac{1}{F_N} \frac{\partial F_N}{\partial C_F} = \frac{1.49}{C_F}$$

$$\frac{1}{F_N} \frac{\partial F_N}{\partial C_{w8}} = \frac{1.38}{C_{w8}}$$

$$\frac{1}{F_N} \frac{\partial F_N}{\partial C_{w7}} = \frac{0.06}{C_{w7}}$$

$$\frac{1}{F_N} \frac{\partial F_N}{\partial C_{w17}} = \frac{0.01}{C_{w17}}$$

The contribution of the flow and thrust coefficient uncertainties to the overall uncertainty in the net thrust as predicted by the engine model can then be calculated. The bias components are given by:

$$\frac{B_{FN}}{F_N} = \pm \left[ \left( 1.49 \times \frac{B_{CF}}{C_F} \right)^2 + \left( 1.38 \times \frac{B_{Cw8}}{C_{w8}} \right)^2 + \left( 0.06 \times \frac{B_{Cw7}}{C_{w7}} \right)^2 + \left( 0.01 \times \frac{B_{Cw17}}{C_{w17}} \right)^2 \right]^{1/2}$$

while the precision components are given by:

$$\frac{S_{FN}}{F_N} = \pm \left[ \left( 1.49 \times \frac{S(\bar{x})_{CF}}{C_F} \right)^2 + \left( 1.38 \times \frac{S(\bar{x})_{Cw8}}{C_{w8}} \right)^2 + \left( 0.06 \times \frac{S(\bar{x})_{Cw7}}{C_{w7}} \right)^2 + \left( 0.01 \times \frac{S(\bar{x})_{Cw17}}{C_{w17}} \right)^2 \right]^{1/2}$$

Table 8.1-13 summarizes the associated numerical values. It is interesting to note that  $C_{w7}$  and  $C_{w17}$ , which showed the largest degree of uncertainty of the nozzle coefficients, have the least impact on predicted net thrust. Taking the RSS of each row of the table gives the following result:

$$\frac{U_{FN}}{F_N} = \pm \left( \frac{B_{FN}}{F_N} + t_{95} \frac{S(\bar{x})_{FN}}{F_N} \right) = \pm (2.01\% + 0.79\%)$$

$$\frac{U_{FN}}{F_N} = \pm 2.8\% \quad \text{uncertainty in engine model calculated thrust due to flow and thrust coefficient uncertainties only.}$$

This level of uncertainty does not meet the stated goal of  $\pm 2.5\%$  uncertainty on net thrust. In order to reduce this level of uncertainty, it is necessary to concentrate on

improving those measurements which contribute most to the final uncertainty in net thrust. Refer now to Table 8.1-13 which shows the individual contributions of the uncertainties of  $C_F$ ,  $C_{w8}$ ,  $C_{w7}$ , and  $C_{w17}$  to calculated net thrust uncertainty and to Table 8.1-14 which shows the individual contributions of each measured parameter to the uncertainties of  $C_F$ ,  $C_{w8}$ ,  $C_{w7}$ , and  $C_{w17}$ .

Table 8.1-13 shows quite clearly that the  $C_F$  and  $C_{w8}$  uncertainties are the dominant contributors to calculated net thrust uncertainty. Similarly, Table 8.1-14 shows the uncertainties in measured  $W_{A8}$  and  $F_G$  to be the dominant contributors to the uncertainty in  $C_F$ . For  $C_{w8}$ , the uncertainty in  $W_{A8}$  is the dominant contributor.

These results indicate that the inlet air flow and gross thrust measurements are the main ones in need of improvement. Further improvements in the temperature and pressure measurements would not have a major impact and so the temperature and pressure measurement instrumentation defined herein is considered to be satisfactory. Since thrust and air flow measurements are not the subject of this document the details of how the uncertainty of these measurements could be improved will not be discussed. However, if the uncertainty of the inlet airflow measurement alone could be reduced by one-fifth, the uncertainty of the net thrust prediction would be within the stated goal of  $\pm 2.5\%$ .

## 8.2 Compressor Efficiency Measurement

### 8.2.1 Introduction

The case chosen in this section is the measurement of the efficiency of a compressor stage. This case is one that is presented in very brief form in ANSI/ASME PTC 19.1, "Measurement Uncertainty", Performance Test Codes Supplement, 1985 (Reference 8.2-1). In that document, a recommended step-by-step procedure for performing uncertainty estimates is given which is described and expanded in Section 3 of this document. In the sample case described here, the procedure is applied to a hypothetical but typical compressor test with sufficient detail given to show one way in which the bias and precision estimates can be determined from various specific kinds of calibration data and prior test experience. The measurement systems used and the details of the uncertainty analysis, are by no means the only ones that can be employed in this kind of a test. Any systems and calibration methods that are used, however, must be scrutinized in comparable detail in order to generate the uncertainty analysis.

This sample case illustrates the considerable complexity which is involved in actual testing of turbomachinery and includes discussion of many of the instrumentation effects such as flow blockage which must be properly evaluated if a truly useful uncertainty analysis is to be done. It also contains a discussion of predicted and measured flow profiles which have a large influence on data interpretation. Related references on turbomachinery uncertainty analysis are, 8.2-2 and 8.2-3.

### 8.2.2 Measurement Objectives

The general requirements for measurement of the performance of compressors and turbines are described in Sections 2.6 and 2.8 of this document.

In this specimen case, the objective will be to measure the isentropic efficiency of a research compressor run as an isolated component and leaving out all the problems

TABLE 8.1-13 Individual contributions to the uncertainty in engine model calculated thrust

	$C_F$	$C_{MB}$	$C_{W7}$	$C_{W17}$	$F_N$
$F_N$ bias, %	1.283	1.546	0.130	0.067	2.01
$F_N$ precision, %	0.663	0.433	0.012	0.013	0.79
$F_N$ uncertainty, %	1.946	1.979	0.142	0.080	2.80

TABLE 8.1-14 Individual contributions to the uncertainty,  $U = \pm(B + t_{95} S(\hat{x}))$ , of the calculated nozzle coefficients

	$T_{17}$	$P_{17}$	$P_{S7}$ or $P_{S17}$	$A_7$	$T_{117}$	$P_{117}$	$A_{17}$	$A_8$	$T_{11}$	$P_{AMB}$	$W_F$	$U_{17}$	$W_{AS}$	$F_6$
$C_F$	0.0417	0.0372			0.0108	0.0141			0.2132	0.0253	0.2264	0.053	0.8306	0.90
$C_{MB}$	0.0097	0.1061			0.0015	0.1061		0.30			0.1898	0.044	1.355	
$C_{W7}$	0.7340	1.241	0.531	1.00	0.1951				0.8250		0.8683	0.203	0.5489	
$C_{W17}$	1.6245		1.675		0.4988	3.592	1.50		1.8927		1.9705	0.462	5.541	

described in the preceding sections concerning simulation of engine conditions and correction of the ideal model to the real engine. This allows the uncertainty due to lack of precise knowledge of inlet swirl, inflow distortion, etc. to be set aside and a more idealized uncertainty analysis carried out illustrating the effects of pressure and temperature error and their relation to other error sources in the given test.

The tests were conducted on a single stage compressor having the design parameters shown in Table 8.2-1. The test section included an inlet duct representative of an engine transition duct between fan and compressor and also included variable inlet guide vanes and stator vanes. The purpose of the test was to determine aerodynamic performance and demonstrate that use of low aspect ratio blading can permit high levels of blade loading to be achieved at an acceptable level of efficiency. This is a typical type of compressor test and, for this specimen case, is a practical example of a case in which one primary objective is the measurement of overall efficiency.

TABLE 8.2-1 Design Parameters

Referred Speed, rpm	12 210
Rotor Tip Speed, m./sec. (ft./sec.)	442.0 (1450)
Referred Flow, kg/sec. (lbm/sec.)	47.28 (104.2)
Referred Weight Flow Per Unit Annulus Area, kg/m <sup>2</sup> -sec (lbm/ft <sup>2</sup> -sec.)	195.3 (40.0)
Rotor Pressure Ratio	1.845
Stage Pressure Ratio	1.805
Rotor Adiabatic Efficiency, %	92.1
Stage Adiabatic Efficiency, %	88.5

The sequence of tests carried out lead to the generation of a performance map for the test vehicle as shown in Figure 8.2-1. In this specimen case, we will concentrate on the pretest estimate of the uncertainty of one point on the efficiency vs.

mass flow curve with the understanding that the test sequence overall would involve the measurement of a series of such points at each of several constant speed lines. The initial step in estimating the uncertainty of the line which is ultimately fit to the array of points is to estimate the uncertainty of one point, and that is the objective of this specimen case.

In summary, the objective of the test was to measure absolute isentropic efficiency (often called adiabatic efficiency) at a preset mass flow referred to a fixed condition at a fixed referred rotor speed. The uncertainty in the efficiency measurement as well as in the flow and speed setting is discussed in sections below.

**8.2.3 The Defined Measurement Process and Math Models**  
The elements of the defined measurement process are shown in Figure 8.2-2. Each of these is described in the paragraphs below.

#### Fundamentals of the Measurement

The principle of the measurement is based on comparing the actual and the ideal enthalpy transferred to the fluid by the compressor which in turn is determined by measuring the temperature and pressure of the fluid at the inlet and discharge of the compressor as described in more detail in Section 2.6 of this document.

The instrumentation we will concentrate on for the analysis of uncertainty in overall efficiency measurement is the instrumentation at the rotor inlet, Station 2, and at the stator exit, Station 3. At Station 2, two rakes with 9 Kielhead probes (sensors) were employed for total pressure measurement. Two 9-probe rakes were also employed for temperature measurement. At Station 3, four rakes were employed for pressure and four for temperature again with 9 probes each. In addition, 4 wall static pressure taps were used on the inner and the outer walls in the same planes to facilitate estimation of mass and momentum flow distributions and blockage. All of the above instrumentation was circumferentially traversable so that a large number of

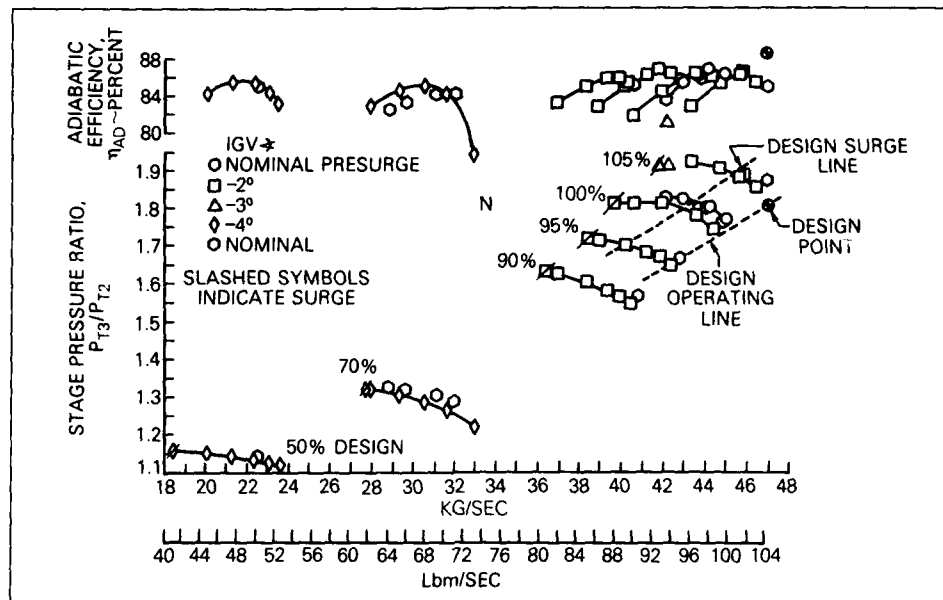


Fig. 8.2-1 Stage pressure ratio and adiabatic efficiency

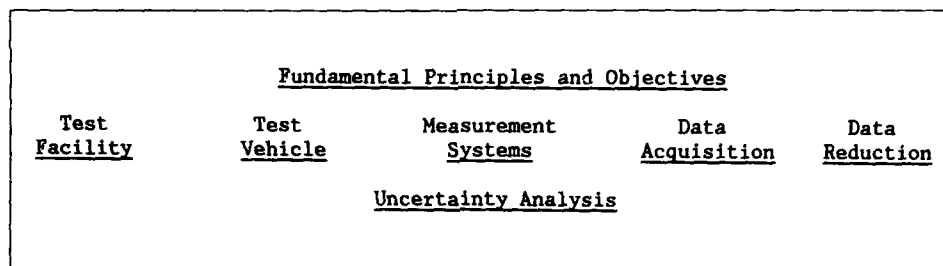


Fig. 8.2-2 The defined measurement process

circumferential samples could be acquired. This was necessary because of the large departures from axial symmetry caused by vanes and Stators. As shown in Figure 8.2-3, 100 samples were used to obtain circumferential averages at each station. This is sufficiently dense so that error due to circumferential sampling was assumed to be negligible compared to other error sources.

In addition to the above, traversing wedge probes were used at each station to determine air angle which was used in through-flow calculations and, where necessary, to correct for yaw effects on the probes.

The data for a single point on the compressor map comes from a series of data acquisitions at fixed referred operating conditions — that is, flow and speed. To obtain overall performance the data reduction is done in the following steps:

1. The raw pressure and temperature data was converted

into engineering units using thermocouple wire and transducer calibration information. Temperature data was corrected further for total temperature recovery which is obtained from calibration of the rakes and is a function of both Mach No. and pressure.

2. Circumferentially, mass-flow averaged total temperature and momentum averaged pressures were calculated for each radial position using the measured circumferential distributions of total pressure and temperature.
3. Station average values of total pressure and temperature were calculated from the circumferentially averaged values obtained in Step 2 above. Weighting of the radial profiles was carried out with an axisymmetric through-flow analysis using the test data as boundary conditions.
4. Overall isentropic efficiency was calculated from the station average total pressure and temperature using the following equation:

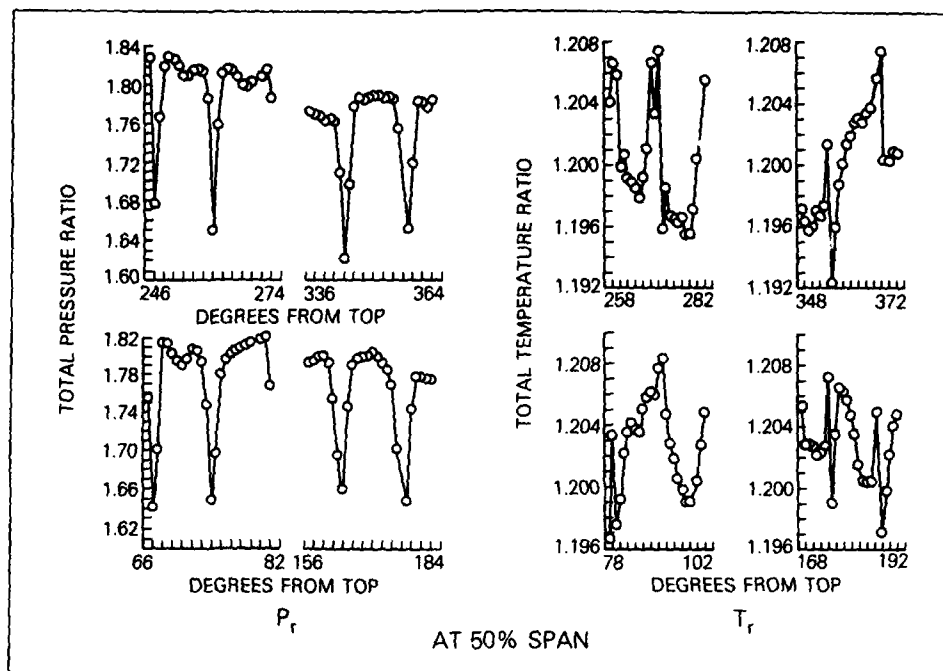


Fig. 8.2-3 Circumferential profiles at exit

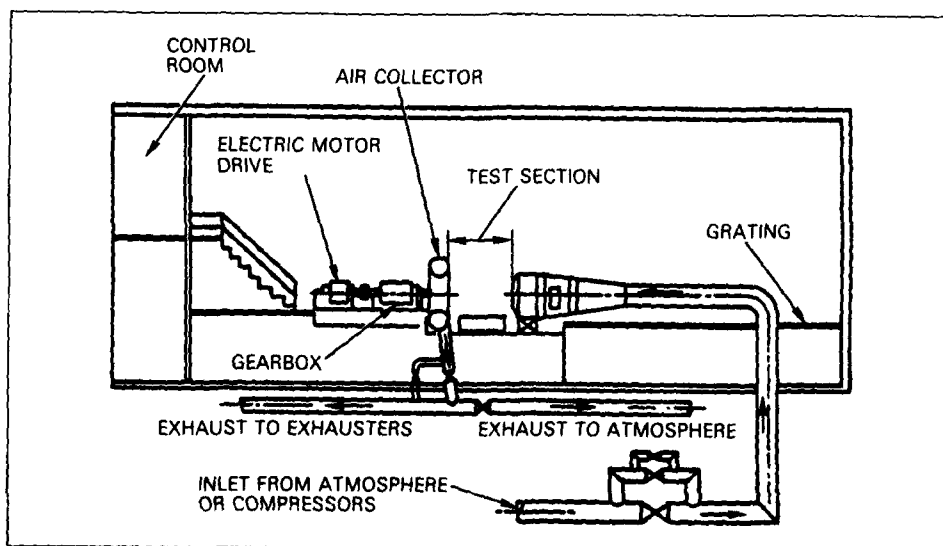


Fig. 8.2-4 Test facility

$$\eta = \frac{\Delta H_{\text{ideal}}}{\Delta H_{\text{actual}}} = \frac{(\bar{P}_{T3}/\bar{P}_{T2})^{1/\gamma} - 1}{(\bar{T}_{T3}/\bar{T}_{T2}) - 1}$$

### 8.2.3.2 The Test Facility

The test program was conducted in a versatile compressor test facility shown in Figure 8.2-4. This test facility is equipped with a synchronous motor with a multi-ratio gearbox to provide speed range capability. The inlet airflow is drawn through filters prior to a flatplate orifice then through an inlet plenum to provide a uniform total pressure and temperature profile to the test rig. The air flow is exhausted from the rig into a toroidal collector through a set of various size valves providing coarse and fine adjustment of backpressure or throttling for the test compressor and then through exhausters. The low pressure provided by the exhausters was also used to vent the rotor front cavity.

In order for the measurement to be meaningful, all parameters which affect the result must be controlled and their uncertainties estimated. The two most important facility-related parameters are: airflow, controlled by the coarse and fine throttle valves, and speed, controlled by the motor and gearbox.

The estimation of the uncertainty of the mass flow measurement, which is determined from pressure and temperature measurements at the metering orifice, is described in detail in Reference 8.2-1.

Airflow to the stage was measured by means of a flatplate orifice designed to the specifications defined by the International Standards Organization (ISO 5167). All orifice-related instrumentation was installed in accordance with Power Test Code 19.5, 4-1959. This system provided a flow rate measurement uncertainty of  $\pm 0.7\%$  (2S) estimated from cross calibrations with choked flow venturis.

The rotor speed was measured using an impulse-type pickup through a frequency-to-DC converter. The measurement uncertainty was within  $\pm 0.1$  percent of the indicated speed.

### 8.2.3.3 Test Vehicle Definition

Obviously the physical dimensions, airfoil shapes, stagger angles, flow areas, etc. of the test compressor must be well defined by the design, construction, and assembly process. Most of these dimensional quantities are given and not controllable by the test operator and, therefore, are not normally considered in the uncertainty analysis. It must be emphasized, however, that errors can arise due to the fact that the compressor being tested may not be the nominal one shown in design drawings because of the build-up of the fabrication tolerances within allowed limits. A sketch of the test vehicle used in this test is shown in Figure 8.2-5.

From the point of view of uncertainty analysis, the secondary parameters which are under the test operator's control and do affect the resulting measurement must be defined. The parameters of importance in this test case are:

- **Rotor Blade Tip Clearance**

The effect of clearance on compressor efficiency is shown in Figure 2.6-5 of Section 2.6 in this document. The cold static clearances are set on assembly, and, during running the clearance is established essentially by the metal temperatures of the rotor and case or alternatively by direct measurement. Prior test information can be used to assess repeatability of the clearance for this specimen case. For example, if the tip

clearance uncertainty is,  $e/h$  (percent) =  $\pm 0.2$  percent (2 S), where  $e$  = tip clearance error and  $h$  = blade height. Then from Figure 2.6-5, 0.2 percent  $e/h$  is equivalent to 0.34 percent in efficiency.

- **Stator Vane Angles**

In compressor development, one of the most important experimental tasks is stator vane angle optimization. To carry out the tests required, some means for manually or remotely setting vane angles is required, and the performance measurement of the compressor will depend somewhat on the accuracy with which the vane angles are set. From other tests, a typical sensitivity of efficiency vs. vane angle for this compressor is estimated to be;  $1^\circ$  in vane angle  $\approx 0.5$  percent in efficiency. This can be used to estimate the uncertainty associated with vane angle setting. The angle uncertainty estimated from shaft angle resolver calibration data for this case was  $\pm 0.2^\circ$  (2 S); therefore, the uncertainty in efficiency from this source is 0.10 percent.

- **Air Angle and Flow Profiles**

A fundamental prerequisite to the design of temperature and pressure probe rakes is a knowledge, acquired either via prior testing or via calculation, of the most probable pressure and temperature profiles at the measuring stations and the range of variation which these profiles might be expected to have around the mean. Both the radial and circumferential profiles must be known as well as the anticipated thickness and profile in the wall boundary layers. Finally, the airflow angles at the measuring station and the variability over the full range of operating conditions must be estimated.

Figure 8.2-6 shows this data for the specimen compressor running in the planned test facility. Both the design intent as well as the post-test results are shown.

### 8.2.3.4 Measurement Systems

The primary measurement systems used in this test case are the systems for the measurement of pressure and temperature. All secondary measurement systems which affect the uncertainty analysis, namely, rotor speed, airflow, clearance, and vane angles have already been addressed above. The pressure and temperature measurement systems used in this specimen case are typical of those covered as recommended practices in the text of this document. Each type of measurement is described below.

#### 8.2.3.4.1 Pressure Measurement System

The pressure measurement systems are shown schematically in Figure 8.2-7. All pressure sensors, both those on rakes and wall taps, are connected via pneumatic tubing to scanning valves which contain the transducers. Each of the scanning valves has 48 ports, 3 of which are used for in-scan calibration. That is, two scan valve ports are connected to calibrated pressure sources in the form of deadweight pressure transfer standards which provide on-line real time calibration at 60 and 80 percent of the transducer range. The third port is supplied with ambient barometric pressure. The port at 60 percent full scale is called the confidence channel. The detailed calibration curve of the transducer, as obtained using the local primary pressure standard (a series of working standard deadweight testers traceable to national and to international standards)

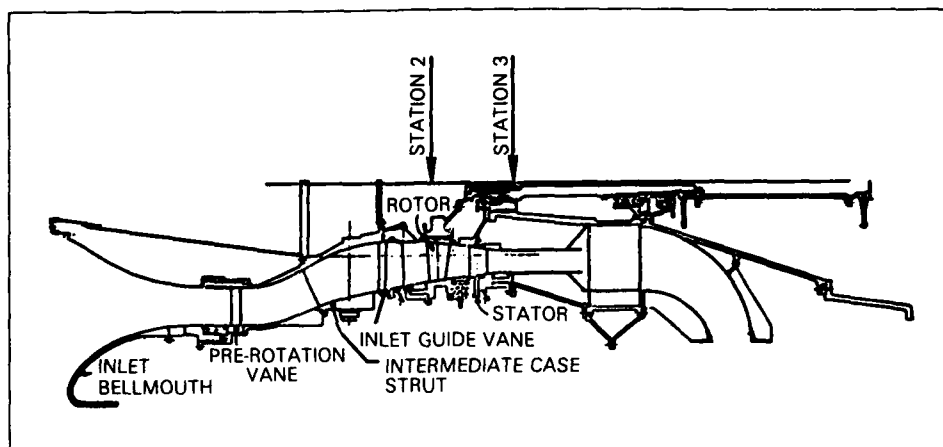


Fig. 8.2-5 Test vehicle

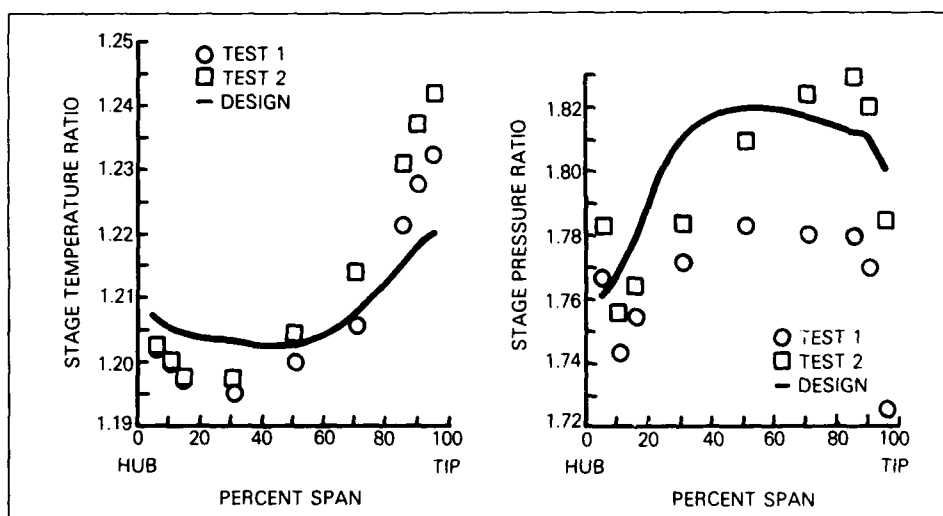


Fig. 8.2-6 Stage temperature and pressure ratios

is then adjusted on each data acquisition. The reference barometric pressure transducer is also calibrated with a deadweight gage. The rationale for and the accuracy achievable with this approach is described in Reference 8.2-4.

The calibration hierarchy for this pressure measurement system is shown in Figure 8.2-8.

The explanation of this calibration hierarchy is as follows:

1. The laboratory primary calibration standards, consisting of dead weight pressure standards traceable to the national standards lab, are used to calibrate the transfer calibration standards, the on-line secondary standard, the confidence pressure standards, and the

reference ambient pressure transducer. The uncertainty in the primary standards obtained from records of checks performed on returning to NBS is  $\pm 0.015$  percent of reading. Since the primary lab standards are used to check the secondary standards, the secondary standards have somewhat reduced accuracy estimated from the above checks to be  $\pm 0.025$  percent of reading.

2. The laboratory standards are used to calibrate each scanivalve transducer at six-month intervals or on indication of a problem disclosed by the secondary calibration procedure (see 4 below). This calibration is six point for mono-directional and eleven point for bi-directional transducers. The results of these periodic "as-is" calibrations are recorded and used to estimate a

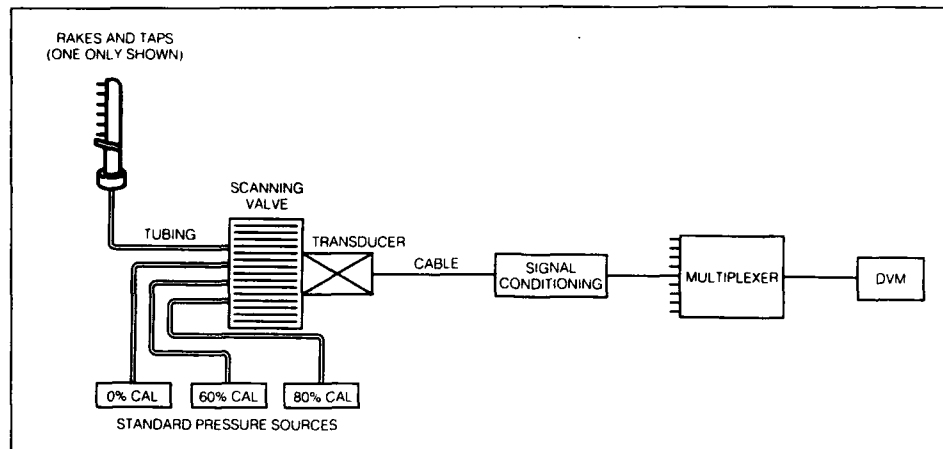


Fig. 8.2-7 Pressure measurement system

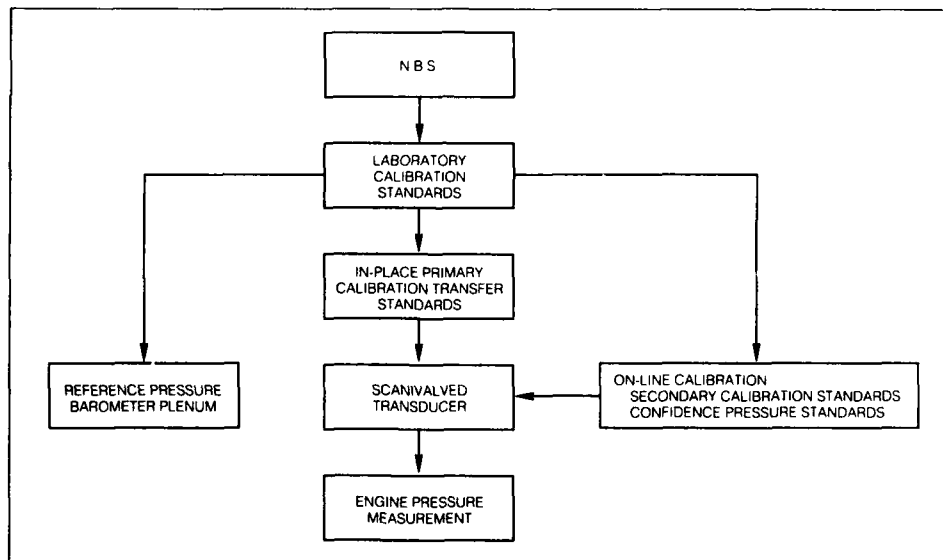


Fig. 8.2-8 Pressure calibration hierarchy

- portion of the uncertainty as explained in Reference 8.2-2. A second order polynomial calibration curve is used and the dispersion of data around this curve as determined from many calibrations is:  $2SE = \pm 0.03$  percent.
3. The scanivalve transducers are referenced to the barometric pressure transducer. The barometer calibration history produces another component of the uncertainty estimate. Records of these calibrations yield a bias of 0.030 percent and a precision of  $\pm 0.06$  percent.
  4. During each data scan, calibration pressures are applied to the scanivalve transducer using the on-line standards via three of the scanivalve ports. Two of these pressures, at ambient and 80 percent of full scale, are used to adjust the average slope and intercept of the calibration curve. A third port provides a calibrated confidence pressure at 60 percent of full scale which is used as a check on the adjusted calibration curve. The confidence channel must read within 0.1 percent of the confidence pressure. If it does not, the data acquisition computer flags that particular data scan and recalibration or replacement of the transducer or

perhaps other troubleshooting is required. This procedure is based on the work reported in Reference 8.2-4 where it is shown that the shape of a transducer calibration curve is more stable than the zero and slope. The uncertainty due to this process is estimated from the confidence channel results. The secondary standard used as a confidence check has an uncertainty of 0.025 percent which would appear as a bias. The record of the standard deviation of this confidence check yields  $2S = 0.06$  percent, and this is a precision error.

The uncertainty resulting from this calibration process is summarized in the table of elemental error sources presented in Section 8.2.4.

#### *Errors of Method*

The "errors of method" or "installation" effects for this pressure measurement system consist of the following:

##### *Yaw and Pitch Effects*

Because the Kiel head sensor designs used in this probe (like those described in Section 5) could tolerate changes of  $\pm 20^\circ$  in air angle with negligible errors, contributions to error are negligible from this source near the compressor design point.

##### *Blockage and Streamline Distortion*

The size of probe supports and spacing between each probe were designed to conform to standards like those presented in Section 5 to minimize errors associated with blockage. The size of the probes was ultimately constrained by structural design considerations.

The total area of the rakes and support was 3 percent of the total flow area and at Station 2 and 5 percent at Station 3. Probe supports employed low drag coefficient cross sections. The separation distance between adjacent sensors and the between end sensors to wall were larger than the minimum distances consistent with having negligible interaction (Section 5.2.1.3).

The blockage effects from these probes were in fact significant as determined from the measurements obtained from wall statics and rakes placed upstream of Station 2. Thus, a total pressure and flow loss of 0.8 percent was estimated for the rakes of Station 2. Since, however, the rakes of Station 3 used for the efficiency measurement were placed so as to be out of the wakes of the upstream rakes, they will only see a small fraction of this pressure loss. Very little data has been published on these effects so it is difficult to include well-defined terms for this in the uncertainty analysis. The uncertainty due to this blockage would be categorized as an "error of method". Its effect on the efficiency measurement is considered to be small and not quantifiable from the data available.

A much more significant effect of probe blockage was the choking of the rig exit which prevented the rig from operating at the design operating line at high speed. While this does not directly effect the efficiency measurement, it does need to be accounted for in the interpretation of results.

##### *Effect of Unsteady Flow*

At the location of the stator exit rakes, the wakes of the rotor were estimated to have attenuated to the point that pressure fluctuations were less than 20 percent. Since the probes and tubing were designed so as to produce negligible bias for this condition (Reference 8.2-5), the effects of fluctuation are assumed to be negligible.

#### *Pressure Measurement System Data Acquisition Errors*

The data acquisition system for this test is shown in Figure 8.2-9. The procedure used in this test at each data acquisition point consisted of the following: a multipoint circumferential traverse that covered 1 inlet guide vane gap at the rotor inlet and 2 stator vane gaps at the stator exit measuring total pressure and total temperature. During this time, consisting of approximately 15 minutes, the test vehicle is held at constant referred conditions to within the limits described above. The time between each data scan after movement to the next circumferential position was set at 10 seconds to ensure that transient response of the 100 foot pressure lines from the test vehicle to the scanivalve had died out.

The data acquisition system errors normally listed for pressure systems (Reference 8.2-1) are as follows:

- Excitation Voltage
- Signal Conditioning
- Recording Device
- Pressure Transducer
- Probe Errors
- Environmental Effects

Since this system employs on-line calibration, the excitation voltage and signal conditioning errors are observable in the repeatability of the on-line calibration process as determined from the confidence channel checks. The recording device error is essentially the precision of the voltmeter and the least count of the A/D converter. These are also observable in the on-line calibration.

Probe errors in this specimen case are not assigned to the data acquisition system but are put in the "errors of method" category under probe design error sources as discussed in Section 3.

Environmental effects such as drift in transducer sensitivity with temperature are also eliminated by the secondary calibration process. In this data system, which employs scanning valves, another data acquisition error source is port-to-port precision. As part of the system check-out in this test, a common pressure source was applied to all ports of each scanivalve through the installed system of tubing and connector panels to be used in the test. Any ports which deviate by more than 0.030 percent of reading are flagged for service. Historic records of this check indicate that the port-to-port precision is 0.020 percent,  $2S$ , in a single data scan. This is without evacuating every other port to eliminate hysteresis.

In summary, all data acquisition error sources in the pressure measurement system with the exception of "probe errors" and port to-port-precision are estimated from the pressure transducer primary and secondary calibration process yielding in this case a bias of  $\pm 0.025$  percent and a precision  $2S$  of  $\pm 0.060$  percent. The port-to-port precision error is 0.020 percent, and the probe errors are assumed negligible.

#### *Pressure Measurement System Data Reduction Errors*

The data reduction errors in this case arise from the following sources:

1. Conversion of the digitized millivolt signal to pressure units using the calibration curve adjusted by the secondary calibration process.
2. Computation of the flow weighted average pressure at

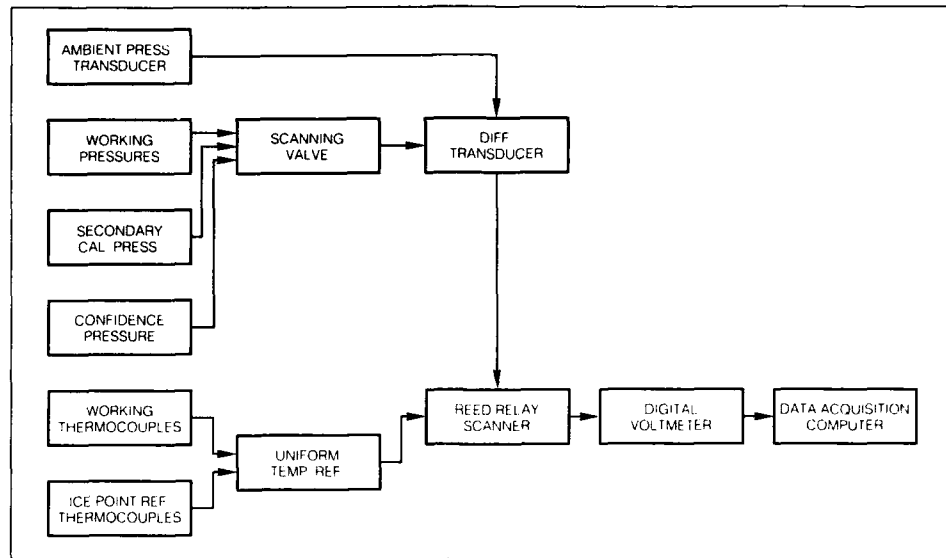


Fig. 8.2-9 Data acquisition system

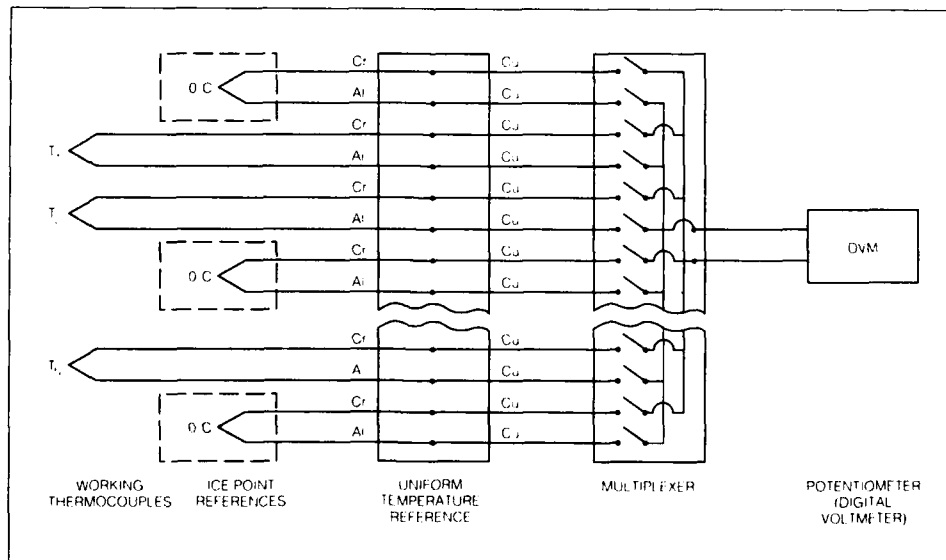


Fig. 8.2-10 Temperature measurement system

each station including sampling error (See Section 8.2.3.6).

#### 8.2.3.4.2 Temperature Measurement System

The temperature measurement system used in this test is depicted schematically in Figure 8.2-10.

The potentiometer used to read out both the reference thermocouples and the working thermocouples (probes) is calibrated using a voltage source which is itself calibrated against a set of NBS traceable standard cells. The calibration-to-calibration precision of this intercomparison against the standard cells is:

$$2S = \pm 2 \sqrt{\frac{\sum (V_i - \bar{V})^2}{N - 1}}$$

where  $V_i$  is the voltage observed in the  $i$ th calculation.

The standard cells are calibrated against the national standard such that their magnitude is defined to  $\pm 0.09$   $\mu$ volts, ( $2S$ ) also based on successive calibrations.

Used with type K thermocouples with a slope of 40  $\mu$ volts/K, the potentiometer calibration precision is equivalent to  $\pm 0.04$ K with a bias from the standard cells of  $\pm 0.02$ K. It has the same precision in use that it has in calibration,  $\pm 0.04$ K verified using analysis of variance in the intercomparisons discussed below.

#### Temperature References

The probe thermocouples are referenced to uniform temperature references (UTRs) consisting of copper plates each with a provision for 32 thermocouple connections. Three of the 32 connections are attached to ice point cells in such a way that at least 2 ice point cells are referenced by each UTR and each ice point references several UTRs. The performance of the system is checked by intercomparing the UTRs and the ice point cells each time a data point is acquired.

The hypothesis that all the reference thermocouples on the UTR are at the same temperature is checked by intercomparing them. One thermocouple is selected as a reference. The other 2 are compared to that thermocouple which results in 2 deviations per UTR. Since the references are common,  $2S$  can be calculated over all the UTRs.

The UTR precision is

$$2S_{UTR} = \pm 2 \sqrt{\frac{\sum (T_i - TR)^2}{N}}$$

where  $TR$  is the temperature indicated by the selected reference thermocouple. This is a measure of the uncontrollable small temperature gradients in the UTR. Note that  $N$  is used rather than  $N-1$  because  $TR$  is not calculated from the  $T_i$ .

In properly installed UTRs, bias is usually negligible. If not, it can be added to the uncertainty terms or subtracted from the data post-test.

The reference thermocouples are scanned on every data point so sample sizes substantially greater than 20 build up very quickly.

For the test stand in which this test was run, records of the temperature difference observed yielded.

$$2S_{UTR} = \pm 0.31 \text{ K}$$

#### Ice Points

The ice points are calibrated compared to a primary laboratory standard ice point cell using platinum resistance thermometers referenced against a master platinum resistance thermometer calibrated by the national standards laboratory.

The calibration-to-calibration precision is calculated from the calibration records for the ice point cell where each  $T_i$  is the calibration value of an "as-is" calibration taken just prior to recalibration.

$$2S_{IP} = \pm 2 \sqrt{\frac{\sum (T_i - \bar{T})^2}{N - 1}} = \pm 0.05 \text{ K}$$

The primary ice point is calibrated against the national standard to  $\pm 0.04$ K.

The intercomparison of the ice points and the UTRs can also be used to calculate a standard deviation for the ice points using analysis of variance techniques. The result confirms the calibration-to-calibration precision of  $\pm 0.05$ K. The ice point precision  $2S$  is  $\pm 0.05$ K. The bias is  $\pm 0.04$ K. In use, the ice point precision is the same as its working calibration  $\pm 0.05$ K.

#### The Reference Thermocouples

Type K thermocouples are delivered with accuracy specifications of  $\pm 1.1$ K\* in the operating temperature range of the UTR which is near room temperature. This accuracy is unsuitable for gas turbine performance testing; therefore, the thermocouple wire must be calibrated relative to the international practical temperature scale, IPTS 68.

The thermocouples are calibrated using a differential voltage method employing standard thermocouples that have been calibrated against a platinum resistance thermometer (Reference 8.2-6). For the temperature range below 500°F, the thermocouples to be calibrated are immersed with the standard thermocouples in a well-stirred oil bath.

The differences between the reference thermocouples and the standard thermocouples are measured on a potentiometer. Since the differences between the thermocouples change little with the absolute temperature level, the oil bath temperature level is not critical. However, it must be isothermal. The precision error of the calibration is monitored by observing the difference between 2 standard thermocouples periodically relocated in the oil bath. If the differences are  $\Delta T_i$ , the precision is calculated from:

$$2S_{RT} = \pm 2 \sqrt{\frac{\sum (\Delta T_i - \bar{\Delta T})^2}{N - 1}} = \pm 0.05 \text{ K}$$

Since many thermocouples are calibrated,  $N$  exceeds 30.

The precision is confirmed by periodically rotating a full set of thermocouples in the bath, testing each thermocouple at each position. The standard deviation calculated position to position and  $2S_{RT}$  above should be equal. The precisions determined either way range between  $\pm 0.049$ K and  $\pm 0.053$ K. The reference thermocouple calibration precision can be rounded off to  $\pm 0.05$ K.

The precision error of the potentiometer used in the thermocouple calibration laboratory when calibrated against standard cells is equivalent to a temperature error of

\* ANSINC 96:1 (Special Grade)

$\pm .03K$ , 2S calibration to calibration, and the bias relative to the NBS of the standard cells is  $\pm .02K$  quoted by the NBS. (Note that this potentiometer has somewhat better accuracy than those mentioned earlier which are in the data acquisition system). The precision is calculated from successive calibrations.

The standard thermocouples are calibrated against platinum resistance thermometers. The platinum resistance thermometers are calibrated relative to the NBS to  $\pm .006K$  (NBS quote). The precision (2S calibration to calibration of the reference thermocouples) is  $\pm .03K$ .

#### *The Working Thermocouples*

The working thermocouples used in the temperature rakes are calibrated the same way as the reference thermocouples described above. In the operating temperature range of this test, the precision and bias of the working thermocouples is the same as the reference thermocouples. To achieve the accuracy indicated, each length of thermocouple wire used for each probe is separately calibrated, and the appropriate calibration for each probe is stored in the database.

#### *Curve Fitting*

The thermocouple calibration data is recorded as differences vs. a standard type K thermocouple as defined for example in NBS Monograph 1225. The calibration points are fitted to a polynomial curve which is then used for volts-to-temperature conversion in the data system. The curve fit error is estimated to be  $\pm .006K$ . Detailed description of the methods for comparison and interpolation are described in Reference 8.2-6.

#### *Temperature Probe Recovery Ratio*

By definition, total temperature is the temperature the air would reach if it were brought to a complete rest isentropically. Total temperature probes are commonly designed with some form of stagnation shield that reduces the velocity at the sensor, but in practice, probe designs do not recover all of the freestream total temperature. The recovery error can be determined by using standard designs and their associated recovery factors described in Section 5.2 and in the various reports referenced in that section. For high accuracy measurements, this approach is not always adequate. It may not be possible to use a standard design, and the recovery ratio is very sensitive to the mechanical and aerodynamic configuration of the probe so small differences in manufacturing tolerances have appreciable effects on recovery ratio especially at high Mach number. In this specimen case of efficiency measurement, probe recovery was determined by calibration.

In practice, a free air jet is used to calibrate recovery ratios. In a properly designed free air jet operating adiabatically, the true total temperature in the jet is equal to the static temperature in the plenum upstream of the jet where the gas velocity is very low.

The recovery ratio ( $R$ ) of a temperature probe is expressed as the ratio of the probe temperature to the true total temperature.

$$R = \frac{T_j}{T_T} = \frac{T_T - \Delta T}{T_T}$$

where  $\Delta T = T_T - T_j$

and  $T_T$  = total temperature as measured in the plenum

$T_j$  = junction temperature

The error equation is:

$$\frac{dR}{R} = \sqrt{\left(\frac{dT_T}{T_T - \Delta T}\right)^2 + \left[\left(\frac{\Delta T}{T_T - \Delta T}\right)\left(\frac{dT_T}{T_T}\right)\right]^2}$$

There are two error terms to address: the measurement error in the probe to be compared against the plenum total temperature probe,  $\Delta T$ , and the uncertainty in the total temperature itself.

Recovery ratio is calculated using the temperature difference between the plenum thermocouple and the probe being calibrated. The recovery ratio changes slowly with absolute temperature level so the actual level of temperature in the plenum is not critical. The plenum thermocouple is calibrated as described above and has a calibration bias of  $\pm .04K$  and a precision of  $\pm .05K$ .

The working precision of the plenum thermocouple is calculated from the repeatability of the difference between the plenum thermocouple and a reference probe. From the records of calibration, it is found that two standard deviations from calibration to calibration are  $\pm .03K$ .

The precision of the working probe recovery calibration is periodically checked by repeat calibrations of selected probes.

The results of typical repeat tests as a function of Mach number for yaw and pitch angles up to  $15^\circ$  at 290K show that the precision of the recovery ratio determination expressed in temperature units is  $\pm .08K$  which is consistent with the precision of the plenum and working thermocouples used in the measurement.

The precision error increases if all the sensors are not individually calibrated because probes of the same design vary more from one to another than any one probe varies over time. Two standard deviations from one probe to another varies with the type of probe and the quality control in fabrication.

The uncertainty in total temperature is not traceable to the NBS since there is no standard for total temperature.

In the absence of any heat transfer effects, an adiabatic expansion defines the recovery ratio in terms of the plenum total temperature, but there are often heat transfer effects. In general, heat transfer effects can be diagnosed by checking for relationships between the measured recovery ratio and temperature differentials between the plenum and nozzle walls and the surrounding environment. For an adiabatic expansion, recovery ratio would not be a function of such temperature differentials but for non-adiabatic expansions it would be. Such relationships can be defined by a regression analysis of the recovery ratio on the difference between the plenum temperature and temperatures in the environment around the jet. Heat transfer effects in this free jet calibration facility added on additional  $\pm 0.1K$  bias to the recovery corrections.

As an additional check, the recovery ratios of selected probes can be tested in other facilities. A reference standard probe can be developed from such cross checks and used as a calibration standard.

#### **8.2.3.5 The Data Acquisition System**

The data acquisition system used in this test is depicted in Figure 8.2-9 and some of its features are described under measurement systems in the last section.

All low level signals in this system are carried on 3 wire shielded, twisted pair cables, single point grounds, and shields carried through all connectors and the scanner to the voltmeter. Consequently, error sources due to common mode voltage, ground loops, or inductively and capacitatively coupled electrical noise are small.

The system includes a 16-bit digital voltmeter so that least count errors are negligible when the transducers are operating above 10 percent of their full scale range.

The electrical measurements are checked by using three precise NBS traceable voltage source connected through the multiplexer to the voltmeter so that the sources are read on each data scan. Any differences exceeding  $\pm 0.005$  mv are flagged for corrective maintenance. The records of this check yield a precision estimate of 1.5  $\mu$ volts which is equivalent to .04K and a bias of 2.5  $\mu$ volts of .07K.

In this test, a total of 90 temperatures and 245 pressure channels constituted each data scan along with rotor speed vane angles and various operational quantities like oil pressure, bearing temperature, etc.

A system reliability display is generated after each data scan which includes the following:

- Calibrated voltage source readings.
- Results of secondary calibration and confidence pressure check for each transducer.
- Identification of transducers which exceed  $\pm 0.1$  percent full scale limit at the 60 percent confidence pressure.
- List of test parameters affected by out of limit transducers.

To ensure the entire system is operating properly, a pretest verification is carried consisting of a leak check of all pressure systems and checkout of ambient readings of all data channels.

#### 8.2.3.6 Data Reduction

Conversion of Millivolts to Engineering Units.

The on-line secondary calibration process described above for pressure yields a corrected calibration curve the accuracy of which is estimated from the accumulated record of zero, 80 percent full scale, and 60 percent full scale calibrations as previously described.

Computation of Flow Weighted Averages — Spatial Sampling Error

The accuracy of the station average depends not only on the accuracy of the individual sensors but also on the number of points sampled and how these points are distributed in space. Experience in previous tests had shown that a large number of circumferential samples were required. Because of the large number (100) of circumferential samples, the assumption was made that the sampling error due to circumferential sampling density was negligible compared to other errors.

The nine-sensor temperature and pressure rakes, however, sample only nine radial points and as it is necessary to estimate the magnitude of the error which might arise due to the limited sampling density.

The strategy used to estimate this error is as follows:

1. Starting with the design radial profiles, calculate the

station average value by numerical integration using a successively increasing number of sampling points and see how the result converges. From this determine how many sample points are required to ensure that the result with a finite sample is within a prescribed limit of the true value. The result of these calculations are shown in Table 8.2-2 for an increasing number of sample points and for rakes designed with either sensors at centres of equal area or on an unequal spacing with higher density near the walls. The centres of equal area spacing is a common rake design standard; however in this test, the rakes were designed with a higher density of sensors near the inner and outer walls in order to better define the profiles in those regions. In this rake design, one sensor was placed close to the outer wall and one close to the inner wall. The remainder was equally spaced between the walls.

The results in Table 8.2-2 show the pressure ratios  $\langle Pr \rangle$ , temperature ratios  $\langle Tr \rangle$  and efficiency  $\eta$  using both area weighting and mass/momentum flow weighting. In these tables, the 21-probe integration was considered to be almost fully converged. As can be seen for the rake design used in this test, 9 probes produce a mass/momentum weighted efficiency that is 0.001 or 0.1 percent different from the converged value.

2. While the above analysis shows how the sampling density affects the station average for a specific given profile, it does not show what uncertainty might arise if the actual profile differs significantly from the design profile. To estimate this, it is necessary to postulate the range of possible variation which might occur around the design profile. In a pretest estimate, this could be obtained by calculation using a range of boundary condition assumptions or by comparing design vs. actual profiles achieved in prior tests. Figure 8.2-11 shows design and actual profiles obtained in a similar test.

Carrying out numerical integrations to obtain area and mass weighted averages for various sampling densities as in 1 above yields the results in Table 8.2-3. This shows that the nine sampling point rakes, which produced an uncertainty of .01 percent in efficiency for the design distribution, give a comparable error for the actual distribution. The difference between the nine point and the 21 point result was  $0.8732 - 0.8739$  or .0007 indicating a possible sampling uncertainty of  $\pm 0.07$  percent.

In conclusion, the measurement uncertainty due to sampling error is estimated to be the sum of the above results for this test — that is,  $\pm(0.10 + 0.07) = \pm 0.17$  percent in efficiency. This is included as a separate category in the overall uncertainty (Section 8.2-5). These tables incidentally also show the difference between the design and actual efficiency and the difference between area weighting and mass momentum weighting.

#### Computation of Overall Isentropic Efficiency

In estimating the uncertainty of the overall isentropic efficiency measurement, the expression for adiabatic efficiency is employed using the station average values of pressure and temperature.

TABLE 8.2-2  
Sensing at centers of equal areas — design flow profiles

N Probes	<PR>area	<TR>area	< $\eta$ >area	<PR>mass	<TR>mass	< $\eta$ >mass
3	1.8080	1.2078	.8871	1.8072	1.2075	.8880
5	1.8061	1.2081	.8846	1.8052	1.2077	.8867
7	1.8056	1.2082	.8838	1.8048	1.2077	.8850
9	1.8055	1.2083	.8835	1.8046	1.2078	.8847
11	1.8054	1.2083	.8834	1.8045	1.2078	.8846
21 pts.	1.8053	1.2083	.8831	1.8044	1.2080	.8844

Sensors Concentrated Near Walls - Design Flow Profiles

N Probes	<PR>area	<TR>area	< $\eta$ >area	<PR>mass	<TR>mass	< $\eta$ >mass
3	1.7971	1.2105	.8696	1.7963	1.2096	.8704
5	1.8034	1.2049	.8801	1.8029	1.2081	.8818
7	1.8049	1.2084	.8827	1.8042	1.2079	.8840
9	1.8055	1.2083	.8837	1.8047	1.2078	.8848
11	1.8057	1.2082	.8841	1.8049	1.2077	.8852
21	1.8081	1.2081	.8848	1.8053	1.2097	.8858

<PR>area = average pressure ratio, area weighted  
 <TR>area = average temperature ratio, area weighted  
 < $\eta$ >area = average efficiency area weight  
 < $\eta$ >mass = above quantities mass flow weighted

TABLE 8.2-3  
Sensors at centers of equal areas — actual profiles

N Probes	<PR>area	<TR>area	< $\eta$ >area	<PR>mass	<TR>mass	< $\eta$ >mass
3	1.8012	1.2097	.8745	1.8011	1.2096	.8748
5	1.8006	1.2107	.8707	1.8006	1.2104	.8718
7	1.8008	1.2110	.8701	1.8008	1.2106	.8715
9	1.8009	1.2111	.8699	1.8009	1.2107	.8715
11	1.8010	1.2111	.8698	1.8010	1.2107	.8714
21 pts.	1.8011	1.2112	.8697	1.8012	1.2108	.8715

Sensors Concentrated Near Walls - Actual Profiles

N Probes	<PR>area	<TR>area	< $\eta$ >area	<PR>mass	<TR>mass	< $\eta$ >mass
3	1.8000	1.2183	.8459	1.8010	1.2166	.8530
5	1.8012	1.2127	.8657	1.8016	1.2117	.8697
7	1.8016	1.2115	.8697	1.8020	1.2108	.8724
9	1.8018	1.2111	.8710	1.8020	1.2105	.8732
11	1.8018	1.2109	.8716	1.8020	1.2104	.8736
21	1.8018	1.2106	.8723	1.8019	1.2102	.8739

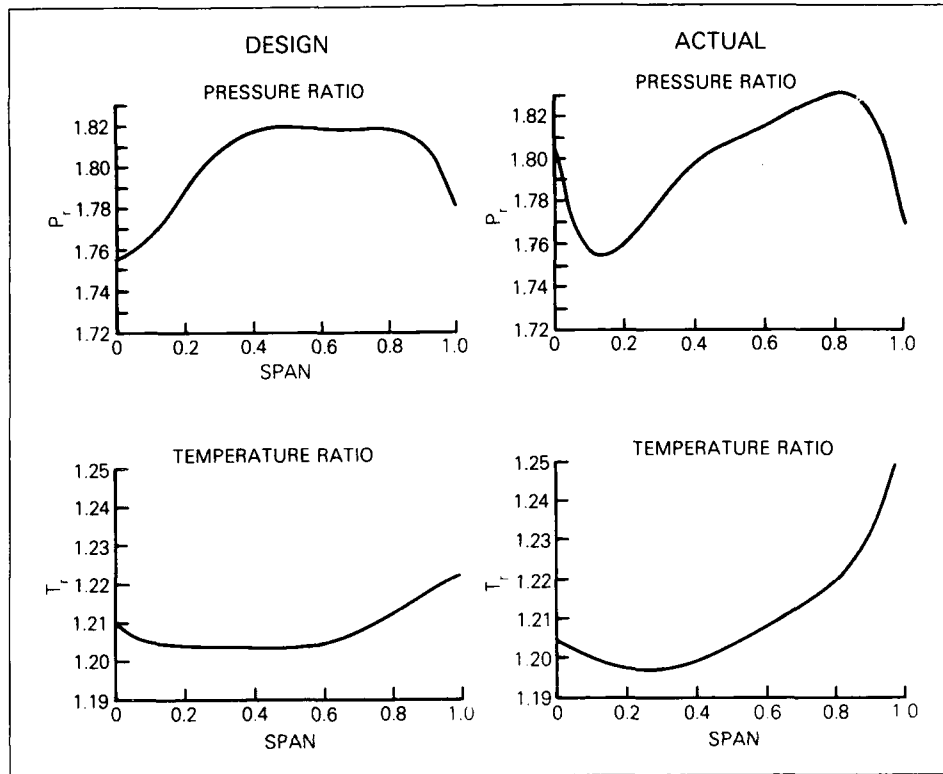


Fig. 8.2-11 Design and actual profiles

In this example, it is assumed that the uncertainty due to the term  $\gamma$  in the expression for adiabatic efficiency is negligible. Various options are available as discussed in Section 2; but for this single stage test, use of an average  $\gamma$  produces negligible error.

Therefore, the expression for adiabatic efficiency:

$$\eta = \frac{(\bar{P}_{13}/\bar{P}_{12})^{\gamma} - 1}{(\bar{T}_{13}/\bar{T}_{12}) - 1} \quad (8.2-1)$$

$$G = \frac{\gamma - 1}{\gamma}$$

$$\gamma = C_p/C_v$$

can be expanded in a Taylor Series keeping the lowest order terms as is described in detail in Reference 8.2-1 and expressions for the bias and precision of the efficiency can be expressed in terms of the differentials of the pressure and temperature and the coefficients of the Taylor expansion called influence coefficients. The results are as follows:

$$d\eta = \sqrt{\left(\frac{dP_{13}/P_{13}}{T_{13}/T_{12} - 1}\right)^2 \left(\frac{dT_{13}}{T_{13}}\right)^2 + \left(\frac{dP_{12}}{P_{12}}\right)^2 \left(\frac{dT_{12}}{T_{12}}\right)^2 + \left(\frac{dT_{12}}{T_{12}}\right)^2 \left(\frac{dT_{13}}{T_{13}}\right)^2} \quad (8.2-2)$$

In this expression, the quantities  $dP$  and  $dT$  are interpreted as the uncertainty in pressure and temperature and  $dP/P$

and  $dT/T$  are relative uncertainties in pressure and temperature.

We are now ready to summarize the uncertainty model, list all error sources, and estimate total uncertainty for this specimen case.

#### 8.2.4 Elemental Uncertainty Models

##### 8.2.4.1 Pressure Measurement System Elemental Error Sources

Calibration Error Sources	% of Reading	
	Bias (B)	Precision (2S)
Laboratory calibration standards (Deadweight Piston Gauges) used for defining transducer curve shape	±.015	
In-place transfer standards (Deadweight Piston Gauges) used for secondary calibration	±.025	
Dispersion around 2nd order cal curve (2SEE)		±.030
Repeatability as observed in confidence channel	±.025	±.060

	% of Reading	
	Bias (B)	Precision (2S)
Reference barometric pressure transducer	±0.030	±0.060
<i>Data Acquisition Errors</i>		
Port-to-port Precision		±0.030
Excitation voltage, signal conditioning, least count, etc.	±0.025	±0.060
<i>Data Reduction Errors</i>		
Sampling Error		See 8.2.5
Unit conversion via cal. curve		±0.06
<i>Errors of Method</i>		Negligible
<i>Total Pressure Uncertainty (RSS)</i>		
$B_p = \pm 0.057\%$ $2S_p = \pm 0.127\%$		
$B_p = \sqrt{\Sigma B^2}$ , $2S_p = \sqrt{\Sigma (2S)^2}$		

#### 8.2.4.2 Temperature Measurement System — Elemental Error Sources

The temperature measurement uncertainty model is summarized in the following table.

	% Reading	
	Bias (B)	Precision (2S)
<i>Calibration Error Sources</i>		
Data System Potentiometer		
Primary Calibration	±0.02	
Secondary Calibration	±0.04	
Working Repeatability		±0.04
Ice Point Calibration		
Primary	±0.04	
Secondary	±0.05	
Working Repeatability		±0.03
T/C Wire Calibration		
Cal. Lab Potential Primary	±0.02	
Secondary	±0.03	
Pt Resistance Primary		
Thermometer	±0.01	
Secondary Standard		
Thermometer	±0.03	
Oil Bath Thermocouple Bias	±0.04	
Oil Bath Thermocouple Precision		±0.05
Working Thermocouple Bias	±0.04	
Working Thermocouple Precision		±0.05
Probe Recover Calibration		
Plenum Thermocouple Bias	±0.04	
Plenum Thermocouple Precision		±0.05
Free Jet Heat Transfer	±0.10	
<i>Data Acquisition Errors</i>		
A/D Least Count Error		Negligible
Voltmeter/Multiplexer error	±0.07	±0.04
<i>Data Reduction Errors</i>		
Curve Fitting Error		±0.01
Sampling Error		(see 8.2.5)
<i>Error of Method</i>		
UTR Gradient Errors (2S UTR)		±0.31
UTR Ref. T/C Precision		±0.05
<i>Total Temperature Uncertainty (RSS)</i>		
$B_T = \pm 0.21\text{K}$ $2S_T = \pm 0.36\text{K}$		
$B_T = \sqrt{\Sigma B^2}$ , $2S_T = \sqrt{\Sigma (2S)^2}$		

#### 8.2.5 Overall Uncertainty Model for Efficiency Measurement

##### 8.2.5.1 Test Vehicle Related Errors

	Bias	Precision
Tip Clearance Control	0.34%	
Vane Angle Setting		0.10%

Tip clearance is counted as bias because it would remain constant during any given test provided case temperatures were approximately constant and no rubs or erosion occurred. Vane angle setting, on the other hand, varies during the test since many changes in vane angle setting were made to investigate the effect on efficiency.

##### 8.2.5.2 Uncertainty in Efficiency Due to Pressure and Temperature Measurement Uncertainty

The overall uncertainty in efficiency is estimated using Equation 8.2-2. The estimate is done in two steps: first, calculating bias error and second, precision error. The elemental errors from the last section are:

	% Reading	
	Bias $B_p$	Precision $2S_p$
Pressure Error	±0.057	±0.125
	K	
	Bias $B_T$	Precision $2S_T$
Temperature Error	±0.21	±0.36

In the calculation of total error, the errors in PT3 and PT2 are essentially the same as are the errors in TT3 and TT2. The error terms in Equation 8.2-2 can be equated with the bias and precision errors as follows:

For Bias Error:

$$B_p = \frac{d\bar{P}_{T2}}{\bar{P}_{T2}} \approx \frac{d\bar{P}_{T3}}{\bar{P}_{T3}} = \pm 0.057\%$$

$$B_T = \frac{d\bar{T}_{T2}}{\bar{T}_{T2}} \approx \frac{d\bar{T}_{T3}}{\bar{T}_{T3}} = \pm \frac{0.21 \text{ K}}{\left( \frac{288 \text{ K} + 344 \text{ K}}{2} \right)} = \pm 0.060\%$$

For Precision Error:

$$2S_p = \frac{d\bar{P}_{T2}}{\bar{P}_{T2}} \approx \frac{d\bar{P}_{T3}}{\bar{P}_{T3}} = \pm 0.127\%$$

$$2S_T = \frac{d\bar{T}_{T2}}{\bar{T}_{T2}} \approx \frac{d\bar{T}_{T3}}{\bar{T}_{T3}} = \pm \frac{0.36 \text{ K}}{\left( \frac{288 \text{ K} + 344 \text{ K}}{2} \right)} = \pm 0.11\%$$

The other quantities required in Equation 8.2-2 for this specimen case are:

$$\text{For Air } G = \frac{\gamma - 1}{\gamma} = \frac{1.4 - 1.0}{1.4} = 0.29$$

$$\text{Pressure Ratio } (\bar{P}_{T3}/\bar{P}_{T2}) = 1.8$$

$$\text{Temperature Ratio } (\bar{T}_{T3}/\bar{T}_{T2}) = 1.2$$

$$\text{Efficiency } \eta = 0.885$$

$$\text{Pressure Influence Coefficient: } \frac{G(\bar{P}_{T3}/\bar{P}_{T2})^G - 1}{(\bar{T}_{T3}/\bar{T}_{T2} - 1)} = 1.69$$

Temperature Influence Coefficient:  $\frac{\eta(\bar{T}_{13}/\bar{T}_{12})}{(\bar{T}_{13}/\bar{T}_{12} - 1)} = 5.31$

Propagating the errors we get

For Bias Pressure Error Temperature Error

$$B\eta = d\eta_{\text{bias}} = \sqrt{I_p(Bp^2 + Bp^2) + I_T(B_T^2 + B_T^2)}$$

$$B\eta = \pm 0.22\%$$

For Precision Pressure Error Temperature Error

$$2S\eta = d\eta_{\text{precision}} = \sqrt{I_p[(2Sp)^2 + (2Sp)^2] + I_T[(2S_{T1})^2 + (2S_{T1})^2]}$$

$$2S\eta = \pm 0.43\%$$

The total uncertainty is then (See Section 3)

$$U_{\text{RSS}} = \sqrt{B\eta^2 + (2S\eta)^2} = \pm 0.48\%$$

$$U_{\text{ADD}} = (B\eta + 2S\eta) = \pm 0.65\%$$

This is the uncertainty in the compressor efficiency measurement which results from the uncertainty in the pressure and temperature measurements alone.

#### 8.2.5.3 Overall Uncertainty

The overall uncertainty of the measurement is then as follows:

%

Bias Precision

Test Vehicle Uncertainty  $\pm 0.34$   $\pm 0.010$

Pressure and Temperature Measurement Uncertainty  $\pm 0.22$   $\pm 0.43$

Sampling Uncertainty  $\pm 0.15$  —

Root Sum Square  $\pm 0.43\%$   $\pm 0.43\%$

$$U_{\text{RSS}} = \sqrt{(0.43)^2 + (0.43)^2} = \pm 0.61\%$$

$$U_{\text{ADD}} = (0.43) + (0.43) = \pm 0.86\%$$

The conclusion of this uncertainty analysis is that the efficiency of the compressor stage can be determined by the defined measurement process to  $\pm 0.61$  percent in efficiency at the 95 percent confidence level and to  $\pm 0.86$  percent in efficiency at the 99 percent confidence level. The observed difference between the measured efficiency and the design efficiency (Figure 8.2-1) is well in excess of the experimental uncertainty.

## 9. REFERENCES

## Section 1

- 1.2.1 Ashwood, P.F. *The Uniform Engine Test Programme*, AGARD Advisory Report No.248, 1988.

## Section 2

- 2.4-1 Rayle, R.E. Jr *An Investigation of the Influence of Orifice Geometry on Static Pressure Measurement*, Thesis, 1949. MIT. Cambridge, Massachusetts.
- 2.4-2 Shaw, R. *The Influence of hole dimensions on static pressure measurement*, J. Fluid Mech., Vol.7, Part 4, April 1960.
- 2.5-1 Martin, R.J.  
Mellick, H.C. *A Feasibility Study for Definition of Inlet Flow Quality and Development Criteria*, AIAA 72 — 1098
- 2.5-2 Fart, A.P. *Evaluation of F-15 Inlet Distortion*, AIAA 73 — 784
- 2.5-3 Hercock, R.G.  
Williams, D.D. *Distortion-induced Engine Instability. Aerodynamic Response*, AGARD LS72 Paper No.3, November 1974
- 2.5-4 SAE  
Committee S-16 *Gas Turbine Engine Inlet Flow Distortion Guidelines*, ARP 1420, March 1978.
- 2.5-5 SAE  
Committee S-16 *Inlet Total Pressure Considerations for Gas Turbine Engines*, AIR 1419, June 1981.
- 2.6-1 Wassell, A.B. *Reynolds Number Effects in Axial Compressors*, ASME Journal of Engineering for Power, April 1968.
- 2.6-2 Schaffler, A. *Experimental and Analytical Investigation of the Effects of Reynolds Number and Blade Surface Roughness on Multi-stage Axial Flow Compressors*, ASME Journal of Engineering for Power 1979 Vol.2.
- 2.6-3 Miller, D.C. *The Performance Prediction of Scaled Axial Compressors from Model Tests*, Institution of Mechanical Engineers, C181/77, Sept. 1977.
- 2.7-1 *Suitable Averaging Techniques in Non-Uniform Internal Flows*, AGARD-AR-182, June 1983.
- 2.7-2 *Modern Methods of Testing Rotating Components of Turbomachines (Instrumentation)*, AGARD-AG-207, April 1975.
- 2.10-1 Pianko, M.  
Wazelt, F. *Suitable Averaging Techniques in Non-Uniform Internal Flows*, AGARD-AR-182, June 1983.
- 2.10-2 Abernethy, R.B., et.al.  
Thompson, J.W., Jr. *Handbook: Uncertainty in Gas Turbine Measurements*, USAF AEDC-TR73-5 (AD755356), February 1973 (Revised January 1980)

## Section 3

- 3-1 Abernethy, R.B.  
Ringhiser, B. *The History and Statistical Development of the New ASME-SAE-AIAA-150 Measurement Uncertainty Methodology*, AIAA-85-1403, 1985.
- 3-2 *Fluid Flow Measurement Uncertainty*, ISO/DIS 5168. ISO Committee, TC30 SC9, Draft 1985.
- 3-3 *Measurement Uncertainty*, ANSI/ASME Power Test Code 19.1, Part 1.
- 3-4 Poti, N.D.  
Rabe, D.C. *Verification of Compressor Data Accuracy by Uncertainty Analysis and Testing Methods*, ASME 8703273, 1987.
- 3-5 Adams, G.R. et al. *Uncertainty Methodology for In-Flight Thrust Determination*, SAE 831438, 1983.
- 3-6 Adams, G.R. et al. *Application of In-Flight Thrust Measurement Uncertainty*, SAE 831434, 1983
- 3-7 Roberts, J.R. *Uncertainty of In-Flight Thrust Determination*, SAE AIR 1678
- 3-8 Rasney, E.C.  
Wilt, C.E. *Development of In-Flight Thrust Measurement Procedures for Afterburning Turbofan Engine*, AIAA 85-1405, 1985.
- 3-9 Cohen, H.  
Rogers, G.F.C.  
Saravanamuttoo, H. *Gas Turbine Theory*, 3rd Edition, Longman, 1987.
- 3-10 Benedict, R.P. *Fundamentals of Temperature, Pressure and Flow Measurements*, (Chapter 17), John Wiley & Sons, 3rd Edition, 1984.
- 3-11 Doebelin, E.O. *Measurement Systems*, McGraw Hill, Revised Edition, 1975.

- 3-12 Chatfield, C. *Statistics for Technology*, Chapman & Hall, Second Edition, 1978.
- 3-13 Abernethy, R.B. Thompson, J.W. Jr. *The Measurement Uncertainty Handbook*, Revised Edition, Instrument Society of America, 1980.
- 3-14 Ascough, J.C. *UETP Post-test Random Uncertainty Analysis*, RAE Tech Memo, p.1067, September 1985.
- 3-15 Smith, R.E., Jr Wehofer, S. *From Measurement Uncertainty to Measurement Communications, Credibility and Cost Control in Propulsion Ground Test Facilities*, J. Fluids Eng. June 1985.
- 3-16 Powell, B.D. *On-line Data Validation, An Application of Measurement Uncertainty Statistics*, ISA 1984.
- 3-17 Boedecker, C.A. *A Unique Rapid Uncertainty Analysis for Turbine Engine Testing*, ASME 86-GT-280, 1986.
- 3-18 Roberts, J.H. *Engine Thrust Measurement Uncertainty*, AIAA-85-1404, 1985.
- 3-19 *Precision of Test Methods, Determination of Repeatability and Reproducibility*, ISO 5725
- 3-20 Kelton, W.O. Law, A.M. *Simulation, Modeling and Analysis*, McGraw Hill (1982)

#### Section 4

- 4-1 *Suitable Averaging Techniques in Non-Uniform Internal Flows*, AGARD-AR-182, June 1983.

#### Section 5

- 5.1-1 Benedict, R.P. *Fundamentals of Temperature, Pressure and Flow Measurement*, John Wiley and Sons, 1984.
- 5.1-2 Doebelin, E.O. *Measurement Systems — Application and Design*, McGraw-Hill, 1975.
- 5.1-3 Merritt, R. *Keeping Up with Pressure Sensors*, Instrumentation and Control Systems, April 1982.
- 5.1-4 Gross, C. Juanerena, D.B. *A Miniature 48-Channel Pressure Sensor Module Capable of In-Site Calibration*, ISA ISBN 87664-362-4, 1977.
- 5.1-5 *High-sampling-Rate Pressure Transducer Has In-Site Calibration*, NASA Tech Briefs, Winter 1978.
- 5.1-6 Wuest, W. *Pressure and Flow Measurement*, AGARD-AG-160, Volume 11, 1980
- 5.2-1 Dudzinski, T.J. Krause, L.N. *Effect of inlet geometry on flow-angle characteristics of miniature total pressure tubes*, NASA Technical Note NASA-TN-D-6406
- 5.2-2 Kiel, G. *Gesamtdruckgerät mit großer Unempfindlichkeit gegen Schräganströmung*, Bericht 35/03 der Deutschen Versuchsanstalt für Luftfahrt e.V., Berlin Adlershof.
- 5.2-3 Gracey, W. Letko, W. Russel, W.P. *Wind Tunnel Investigation of a Number of Total Pressure Tubes at High Angle of Attack*, Langley Aeronautical Laboratory, Langley Field, Va., NASA Technical Note 2331.
- 5.2-4 Wust, W. *Strömungs sonden Teil 1. Gesamtdrucksonden* Aerodynamische Versuchsanstalt Göttingen, V 116-9, 1960
- 5.2.5 Gettelman, C.C. Krause, L.N. *Considerations entering into Selection of Probes for Pressure Measurement in Jet Engines*, Aeronautical Instrumentation, Session II, Paper No. 52-12-1.
- 5.2-6 Millan, F.A. *Experiments on Pitot Tubes in Shear Flow*, Great Britain ARC Rep Mem. 3028, 1957.
- 5.2-7 Krause, L.N. Gettelman, C.C. *Effect of Interaction among Probes, Supports, Duct Walls and Jet Boundaries on Pressure Measurements in Ducts and Jets*, Aeronautic Instrumentation Session II, Paper No. 52-12-2.
- 5.2-8 Fransson, T.M. *Aerodynamic Probe Calibrations 7th Symposium on Measuring Techniques in Transonic and Supersonic Flows Report Nr. LTA-TM-9-83*.
- 5.2-9 Rayle, R.E. *Influence of Orifice Geometry on Static Pressure Measurements* ASME Paper 59-A-234, December 1959.
- 5.2-10 Kuwano, M., Wu, J.M. Moulden, T.H. *An Experimental Study of Orifice Size on Static Pressure Measurements*, International Symposium on space technology and science proceedings Tokyo 1977
- 5.2-11 Boehm-Raffay, H. Fassol, H.K. *Versuche über die Ausbildung von Druckmeßbohrungen* Maschinenbau und Warmewirtschaft 10 (1955) 7.
- 5.2-12 Hubbard, C.W. *Investigation of Errors of Pitot Tubes*, Transactions ASME Vol. 61, 1939 pp 477-492

- 5.2-13 Ower E.  
Johansen, F.C. *The Design of Pitot Static Tubes*. Great Britain, ARC, Rand M 981, 1925, 12p + 11p of fig.
- 5.2-14 Falsom, R.G. *Reviews of the Pitot Tubes*. Transaction ASME Vol.78 pp 1447-1460 Oct. 1956.
- 5.2-15 Bohn, D.  
Simon, H. *Mehrparametrische Approximation der Eichräume und Eichflächen von Unterschall- bzw. Überschall-5-Loch-Sonden* ATM März 1975 — Lieferung 470
- 5.2-16 Bryer, D.W.  
Walshe, D.E.  
Garner, H.C. *Pressure Probes Selected for Three Dimensional Flow Measurement*. R & M No.3037. A.R.C. Technical Report.
- 5.2-17 Glawe, G.E.  
Krause, L.N. *Miniature Probes for Use in Gas Turbine Testing*. Lewis Research Center, National Aeronautics & Space Administration. SAE 750094 Febr. 1975,
- 5.2-18 Glawe, G.E.  
Krause, L.N.  
Dudzinsky, T.J. *A Small Combination Sensing Probe for Measurement of Temperature, Pressure and Flow Direction*. NASA Technical Note NASA-TN-D-4816.
- 5.2-19 Couch, L.M. *Geometric Optimization of the Supersonic Stagnation Pressure Probe*. ISA ASI 75L42 (2511-2557) (1975).
- 5.2-20 Sieverding, C.  
Maretto, L.  
Lehthaus, F.  
Lawaczek, O. *Design and Calibration of Four Probes for Use in Transonic Turbine Cascade Testing*. Von Karman Institute for Fluid Dynamics.
- 5.2-21 *Modern Methods of Testing Rotating Components of Turbomachines (Instrumentation)*. AGARDOGRAPH No. 207, April 1975.
- 5.3-1 *Pneumatic Instrumentation Lines and Their Use in Measuring Rocket Nozzle Pressure*. Aerojet General Report No. RN-DR-0124.
- 5.3-2 Hougen, J.O.,  
Martin, J.R.  
Walsh, R.A. *Dynamics of Pneumatic Transmission Lines*, Control Engineering, September 1963, p.114.
- 5.3-3 Grant, H.P. *Measuring Time-Averaged Stagnation Pressure in a Pulsatile Airflow*. ISA 23rd International Symposium, May 1977.
- 5.3-4 Weyer, H.  
Schodl, R. *Methods for Measuring Fluctuating Quantities in Turbomachinery, Experimental Techniques in Turbomachinery*, Milan, October 1973.
- 5.3-5 Wennerstrom, A. *Steady State Aerodynamic Measurements*, ASME Lecture Series, 1984.
- 5.3-6 *Pressure Transducers*, Electronic Products Magazine, November 1981.
- 5.3-7 Abernethy, R.B.  
Ringhiser, B. *The History and Statistical Development of the New ASME-SAE-AIAA-ISO Measurement Uncertainty Methodology*, AIAA-85-1403.
- 5.3-8 Gorton, R.E.  
Sanders, D.G. *Real Time Calibration of Multiplexed Pressure Measuring Systems*, ISA ASI 74214 (57-62), 1974.
- Section 6**
- 6.1-1 Echelle Internationale Pratique de Température de 1968 + édition amendée de 1975. (IPTS-688)
- 6.1-2 Miller, F. *La Mesure des Températures de l'Ambiante à 2500 K* PYC Edition.
- 6.1-3 Bert, J. *Physique des Capteurs I — Capteurs de Températures*, Collection DIA, Editeur Belin.
- 6.1-4 Benedict, R.P. *Fundamentals of Temperature, Pressure and Flows Measurements*, P.E. 3e Edition, A Wiley Interscience Publication.
- 6.2-1 Moffat, J. *Gas Temperature Measurements, Applied Methods and Instruments*. Charles R. Herzfeld, gen. ed. 4 vols. New York: Reinhold Publishing Corp., 1962. Vol. 3, Part 2. A.I.Dahl, ed.
- 6.2-2 King, W.J. *Measurement of High Temperature in High Velocity Gas Streams*, Transactions ASME 65 (July 1943): pp 421-31.
- 6.2-3 Moffat, E.M. *Multiple Shielded High Temperature Probes*, Comparison of experimental and calculated errors. SAET-13 (January 1952)
- 6.2-4 Simmons, F.S. *Recovery Corrections for Butt-Welded, Straight-Wire Thermocouples in High-Velocity, High-Temperature Gas Streams*. Washington, D.C.: NACA Research Memorandum E54G22a, September 1954.

- 6.2-5 Stickney, T.M. *Recovery and Time-Response Characteristics of Six Thermocouple Probes in Subsonic and Supersonic Flow*, Washington D.C.: NACA Technical Note 3455, July 1955.
- 6.2-6 Glaw, G.E.  
Simmons, F.S.  
Stickney, T.M. *Radiation and Recovery Corrections and Time Constants of Several Chromel-Alumel Thermocouple Probes in High-Temperature, High-Velocity Gas Streams*, Washington, D.C.: NACA Technical Note 3766, October 1956.
- 6.2-7 Glawe, G.E.  
Krause, L.N. *Miniature Probes for Use in Gas Turbine Testing*, NASA Technical Memorandum X-71738, February 1974.
- 6.2-8 Glawe, G.E.  
Holanda, R.  
Krause, L.N. *Recovery and Radiation Corrections and Time Constants of Several Sizes of Shielded and Unshielded Thermocouple Probes for measuring Gas Temperature*, Washington D.C.: NASA Technical Paper 1099, January 1978.
- 6.2-9 Haig, B. *A Design Procedure for Thermocouple Probes*, Preprint 158C, Society of Automotive Engineers (SAE), April 1960.
- 6.2-10 Hottel, H.C.  
Kalitinsky, A. *Temperature Measurements in High Velocity Air Streams*, Journal of Applied Mechanics Transaction ASME 67 (March 1945); pp A-25 to A-32.
- 6.2-11 Kirschey, G.  
Wagner, R. *Full Annular Combustor Test Facility for High Temperature High Pressure Testing*, MTU, 8000 München, Dachauer Str. 665.
- 6.3-1 *American National Standard for Temperature Measurement Thermocouples*, MC. 96-1 1975.
- 6.3-2 *Standard Recommended Practice for Preparation and Use of Freezing Point Reference Baths*, ASTM E. 563-76 (Reapproved 1980), American National Standard.
- 6.3-3 Fleeger, D.W.  
Seyb, N.J. *Aerodynamic Measurements in Turbomachines*, AGARDograph No. 207 — Section II, April 1975.
- 6.3-4 Norme Française NFC 42-3221 (Novembre 1978) — Tables de références des couples thermoélectriques.
- 6.3-5 Norme Française NFC 42-323 (Février 1985) — Identification des couples thermoélectriques.
- 6.3-6 Norme Française NFC 42-322 (Mars 1982) — Tolérances des couples thermoélectriques.
- 6.3-7 Norme DIN No. 43-760 (R.T.D's).
- 6.3-8 Moffat, R.J. Notes concerning temperature measurement for I.S.A. 28th International Instrumentation Symposium.
- 6.3-9 Alwang, W.G. Lecture série 1981-7, von Kármán Institute, "Measurement Technique in Turbomachines".
- 6.3-10 Agnew, B.  
Elder, R.L.  
Terrel, M. *An Investigation of the Response of Temperature Sensing Probes to an Unsteady Flow Field*, ASME-85-GT-223, Gas Turbine Conference, March 18-21, 1985 Houston, Texas.
- 6.3-11 Gardenhire, L.W. AGARDograph No.160 Vol. I, AGARD Flight Test Instrumentation Series, Chap. 6 — Sampling and Filtering, (1974).

#### Section 7

- 7-1 Krause, L.N.  
Gettelman, C.C. *Considerations Entering into the Selection of Probes for Pressure Measurements in Jet Engines*, ISA Paper No. 52-12-1, 1952.
- 7-2 Krause, L.N.  
Gettelman, C.C. *Effects of Interaction Among Probes, Supports, Duct Walls, and Jet Boundaries on Pressure Measurements in Ducts and Jets*, ISA Paper No. 52-12-2, 1952.
- 7-3 Fleeger, D.W.  
Seyb, N.J. *Aerodynamic Measurements in Turbomachines*, Section II of AGARDograph No.207 on Modern Methods of Testing Rotating Components of Turbomachines (Instrumentation), 1975.
- 7-4 Allan III, J. *Instrumentation Problems in Small Gas Turbine Engines*, AIAA Paper 88333-1293, June 1983.

#### Section 8

- 8.1-1 *Fluid Flow Measurement Uncertainty*, ISO TC30 SC9, Draft of January, 1985 (Revision to ISO/DIS 5/68).
- 8.2-1 *Measurement Uncertainty*, ANSI/ASME, PTC 19.1
- 8.2-2 Boedicker, C.A. *A Unique, Rapid Analysis for Turbine Engine Testing*, ASME-86-GT-280 (1986).

- 8.2-3 Poti, N.B.  
Rabe, D.C. *Verification of Compressor Data Accuracy by Uncertainty Analysis and Testing Methods*, ASME 8703273 (1987).
- 8.2-4 Gorton, R.E.  
Sanders, D.G. *Real-Time Calibration of Multiplexed Pressure Measuring Systems*, ISA, ASI 74214 pp. 57-62 (1974).
- 8.2-5 Grant, H.P. *Measuring Time-Averaged Stagnation Pressure in Pulsatile Airflow*, ISA 23rd International Symposium, May 1977.
- 8.2-6 Sanders, D.G. *Accuracy of Type K Thermocouple Wire Below 500°: A Statistical Analysis*, ISA Transactions, Volume 13, No.3, pp. 202-211, (1974).

REPORT DOCUMENTATION PAGE			
1. Recipient's Reference	2. Originator's Reference	3. Further Reference	4. Security Classification of Document
	AGARD—AR-245	ISBN 92-835-0499-2	UNCLASSIFIED
5. Originator	Advisory Group for Aerospace Research and Development North Atlantic Treaty Organization 7 rue Ancelle, 92200 Neuilly sur Seine, France		
6. Title	RECOMMENDED PRACTICES FOR MEASUREMENT OF GAS PATH PRESSURES AND TEMPERATURES FOR PERFORMANCE ASSESSMENT OF AIRCRAFT TURBINE ENGINES AND COMPONENTS		
7. Presented at			
8. Author(s)/Editor(s)	Edited by H.I.H.Saravanamuttoo		9. Date June 1990
10. Author's/Editor's Address	Various		11. Pages 160
12. Distribution Statement	This document is distributed in accordance with AGARD policies and regulations, which are outlined on the Outside Back Covers of all AGARD publications.		
13. Keywords/Descriptors	<div style="display: flex; justify-content: space-between;"> <div> <input checked="" type="checkbox"/> Components of gas turbines  Component testing  Instrumentation  Measurement of uncertainty  Performance of gas turbines </div> <div> Pressure measurement  Temperature measurement  Sensor design  Turbine engines  <i>French translation. (JS)</i> </div> </div>		
14. Abstract	<input checked="" type="checkbox"/> The Advisory Report summarizes the results of the Propulsion and Energetics Panel Working Group 19. It is of interest to engineers concerned with steady state testing of aircraft turbine engines and their components, and provides information on gas path pressure and temperature measurement techniques and instrumentation.  Manufacturers and research institutions throughout the world have developed their own practices for measurement techniques and instrumentation. These practices vary significantly, leading to confusion and misunderstanding between researchers, development organizations, contract agencies and customers. The trend towards multi-company and multi-national engine projects increases these difficulties. The goal of this report is to recommend practices, the application of which will generate confidence through a common understanding, which will increase the quality of the data obtained. The recommended practices described address components and instrumentation, and the problems of interpreting the information obtained in terms of spatial and temporal resolution. Measurement uncertainties are discussed in detail. <i>Keywords.</i>		

<p>AGARD Advisory Report No.245 Advisory Group for Aerospace Research and Development, NATO</p> <p><b>RECOMMENDED PRACTICES FOR MEASUREMENT OF GAS PATH PRESSURES AND TEMPERATURES FOR PERFORMANCE ASSESSMENT OF AIRCRAFT TURBINE ENGINES AND COMPONENTS</b></p> <p>Edited by H.L.H.Saravanamuttoo Published June 1990 160 pages</p> <p>The Advisory Report summarizes the results of the Propulsion and Energetics Panel Working Group 19. It is of interest to engineers concerned with steady state testing of aircraft turbine engines and their components, and</p> <p>P.T.O.</p>	<p>AGARD-AR-245</p> <p>Components of gas turbines Component testing Instrumentation Measurement of uncertainty Performance of gas turbines Pressure measurement Temperature measurement Sensor design Turbine engines</p>	<p>AGARD Advisory Report No.245 Advisory Group for Aerospace Research and Development, NATO</p> <p><b>RECOMMENDED PRACTICES FOR MEASUREMENT OF GAS PATH PRESSURES AND TEMPERATURES FOR PERFORMANCE ASSESSMENT OF AIRCRAFT TURBINE ENGINES AND COMPONENTS</b></p> <p>Edited by H.L.H.Saravanamuttoo Published June 1990 160 pages</p> <p>The Advisory Report summarizes the results of the Propulsion and Energetics Panel Working Group 19. It is of interest to engineers concerned with steady state testing of aircraft turbine engines and their components, and</p> <p>P.T.O.</p>	<p>AGARD-AR-245</p> <p>Components of gas turbines Component testing Instrumentation Measurement of uncertainty Performance of gas turbines Pressure measurement Temperature measurement Sensor design Turbine engines</p>
<p>AGARD Advisory Report No.245 Advisory Group for Aerospace Research and Development, NATO</p> <p><b>RECOMMENDED PRACTICES FOR MEASUREMENT OF GAS PATH PRESSURES AND TEMPERATURES FOR PERFORMANCE ASSESSMENT OF AIRCRAFT TURBINE ENGINES AND COMPONENTS</b></p> <p>Edited by H.L.H.Saravanamuttoo Published June 1990 160 pages</p> <p>The Advisory Report summarizes the results of the Propulsion and Energetics Panel Working Group 19. It is of interest to engineers concerned with steady state testing of aircraft turbine engines and their components, and</p> <p>P.T.O.</p>	<p>AGARD-AR-245</p> <p>Components of gas turbines Component testing Instrumentation Measurement of uncertainty Performance of gas turbines Pressure measurement Temperature measurement Sensor design Turbine engines</p>	<p>AGARD Advisory Report No.245 Advisory Group for Aerospace Research and Development, NATO</p> <p><b>RECOMMENDED PRACTICES FOR MEASUREMENT OF GAS PATH PRESSURES AND TEMPERATURES FOR PERFORMANCE ASSESSMENT OF AIRCRAFT TURBINE ENGINES AND COMPONENTS</b></p> <p>Edited by H.L.H.Saravanamuttoo Published June 1990 160 pages</p> <p>The Advisory Report summarizes the results of the Propulsion and Energetics Panel Working Group 19. It is of interest to engineers concerned with steady state testing of aircraft turbine engines and their components, and</p> <p>P.T.O.</p>	<p>AGARD-AR-245</p> <p>Components of gas turbines Component testing Instrumentation Measurement of uncertainty Performance of gas turbines Pressure measurement Temperature measurement Sensor design Turbine engines</p>

<p>provides information on gas path pressure and temperature measurement techniques and instrumentation.</p> <p>Manufacturers and research institutions throughout the world have developed their own practices for measurement techniques and instrumentation. These practices vary significantly, leading to confusion and misunderstanding between researchers, development organizations, contract agencies and customers. The trend towards multi-company and multi-national engine projects increases these difficulties. The goal of this report is to recommend practices, the application of which will generate confidence through a common understanding, which will increase the quality of the data obtained. The recommended practices described address components and instrumentation, and the problems of interpreting the information obtained in terms of spatial and temporal resolution. Measurement uncertainties are discussed in detail.</p> <p>ISBN 92-835-0499-2</p>	<p>provides information on gas path pressure and temperature measurement techniques and instrumentation.</p> <p>Manufacturers and research institutions throughout the world have developed their own practices for measurement techniques and instrumentation. These practices vary significantly, leading to confusion and misunderstanding between researchers, development organizations, contract agencies and customers. The trend towards multi-company and multi-national engine projects increases these difficulties. The goal of this report is to recommend practices, the application of which will generate confidence through a common understanding, which will increase the quality of the data obtained. The recommended practices described address components and instrumentation, and the problems of interpreting the information obtained in terms of spatial and temporal resolution. Measurement uncertainties are discussed in detail.</p> <p>ISBN 92-835-0499-2</p>
<p>provides information on gas path pressure and temperature measurement techniques and instrumentation.</p> <p>Manufacturers and research institutions throughout the world have developed their own practices for measurement techniques and instrumentation. These practices vary significantly, leading to confusion and misunderstanding between researchers, development organizations, contract agencies and customers. The trend towards multi-company and multi-national engine projects increases these difficulties. The goal of this report is to recommend practices, the application of which will generate confidence through a common understanding, which will increase the quality of the data obtained. The recommended practices described address components and instrumentation, and the problems of interpreting the information obtained in terms of spatial and temporal resolution. Measurement uncertainties are discussed in detail.</p> <p>ISBN 92-835-0499-2</p>	<p>provides information on gas path pressure and temperature measurement techniques and instrumentation.</p> <p>Manufacturers and research institutions throughout the world have developed their own practices for measurement techniques and instrumentation. These practices vary significantly, leading to confusion and misunderstanding between researchers, development organizations, contract agencies and customers. The trend towards multi-company and multi-national engine projects increases these difficulties. The goal of this report is to recommend practices, the application of which will generate confidence through a common understanding, which will increase the quality of the data obtained. The recommended practices described address components and instrumentation, and the problems of interpreting the information obtained in terms of spatial and temporal resolution. Measurement uncertainties are discussed in detail.</p> <p>ISBN 92-835-0499-2</p>

AGARD

NATO  OTAN

7 rue Ancelle • 92200 NEUILLY-SUR-SEINE

FRANCE

Telephone (1)47.38.57.00 • Telex 610 176

**DISTRIBUTION OF UNCLASSIFIED  
AGARD PUBLICATIONS**

AGARD does NOT hold stocks of AGARD publications at the above address for general distribution. Initial distribution of AGARD publications is made to AGARD Member Nations through the following National Distribution Centres. Further copies are sometimes available from these Centres, but if not may be purchased in Microfiche or Photocopy form from the Sales Agencies listed below.

**NATIONAL DISTRIBUTION CENTRES**

**BELGIUM**

Coordonnateur AGARD — VSL  
Etat-Major de la Force Aérienne  
Quartier Reine Elisabeth  
Rue d'Evere, 1140 Bruxelles

**LUXEMBOURG**

See Belgium

**CANADA**

Director Scientific Information Services  
Dept of National Defence  
Ottawa, Ontario K1A 0K2

**NETHERLANDS**

Netherlands Delegation to AGARD  
National Aerospace Laboratory, NLR  
Kluyverweg 1  
2629 HS Delft

QWAV

**DENMARK**

Danish Defence Res  
Ved Idrætsparken 4  
2100 Copenhagen C

**NASA**

Aeronautics and  
Administration

as Paid  
Articles and  
Non



**FRANCE**

O.N.E.R.A. (Directi  
29 Avenue de la Div  
92320 Châtillon

**SPECIAL FOURTH CLASS MAIL  
BOOK**

**GERMANY**

Fachinformationszei  
Karlsruhe  
D-7514 Eggenstein

AGARDAR245900905S002672

DEFENSE  
TECHNICAL INFORMATION CE  
-FDAC

**GREECE**

Hellenic Air Force  
Air War College  
Scientific and Techni  
Dekelia Air Force Base  
Dekelia, Athens TGA 1016

RON STATION BLDG 5  
ANDRIA VA 223046145

**ICELAND**

Director of Aviation  
c/o Flugrad  
Reykjavik

Renugern House  
65 Brown Street  
Glasgow G2 8EX

**ITALY**

Aeronautica Militare  
Ufficio del Delegato Nazionale all'AGARD  
3 Piazzale Adenauer  
00144 Roma/EUR

**UNITED STATES**

National Aeronautics and Space Administration (NASA)  
Langley Research Center  
M/S 180  
Hampton, Virginia 23665

THE UNITED STATES NATIONAL DISTRIBUTION CENTRE (NASA) DOES NOT HOLD  
STOCKS OF AGARD PUBLICATIONS, AND APPLICATIONS FOR COPIES SHOULD BE MADE  
DIRECT TO THE NATIONAL TECHNICAL INFORMATION SERVICE (NTIS) AT THE ADDRESS BELOW.

**SALES AGENCIES**

National Technical  
Information Service (NTIS)  
5285 Port Royal Road  
Springfield  
Virginia 22161, USA

ESA/Information Retrieval Service  
European Space Agency  
10, rue Mario Nikis  
75015 Paris, France

The British Library  
Document Supply Centre  
Boston Spa, Wetherby  
West Yorkshire LS23 7BQ  
England

Requests for microfiche or photocopies of AGARD documents should include the AGARD serial number, title, author or editor, and publication date. Requests to NTIS should include the NASA accession report number. Full bibliographical references and abstracts of AGARD publications are given in the following journals:

Scientific and Technical Aerospace Reports (STAR)  
published by NASA Scientific and Technical  
Information Branch  
NASA Headquarters (NIT-40)  
Washington D.C. 20546, USA

Government Reports Announcements (GRA)  
published by the National Technical  
Information Services, Springfield  
Virginia 22161, USA



Printed by Specialised Printing Services Limited  
40 Chigwell Lane, Loughton, Essex IG10 3TZ

ISBN 92-835-0499-2